

**INTERPRETABILITY AND FAIRNESS IN MACHINE LEARNING: A
FORMAL METHODS APPROACH**

by

BISHWAMITTRA GHOSH

**A THESIS SUBMITTED FOR THE DEGREE OF
DOCTOR OF PHILOSOPHY**

in

COMPUTER SCIENCE

in the

GRADUATE DIVISION

of the

NATIONAL UNIVERSITY OF SINGAPORE

2023

Supervisor:

Dr Kuldeep S. Meel

Examiners:

Dr Harold Soh Soon Hong

Dr Reza Shokri

Declaration

I hereby declare that this thesis is my original work and it has been written by me in its entirety. I have duly acknowledged all the sources of information which have been used in the thesis.

This thesis has also not been submitted for any degree in any university previously.



Bishwamittra Ghosh

August 25, 2023

Acknowledgments

I would like to express my sincere gratitude to everyone who has supported me throughout my PhD. This has been a journey of self-discovery, patience, and continuous effort to surpass myself day by day. I am fortunate to have met amazing researchers around the world, communicating ideas and learning from them. Reflecting on Socrates' famous words, "Know Thyself", my PhD has been a journey of understanding my limitations and fostering a mindset of overcoming shortcomings while enjoying the pursuit of knowledge. At this moment, I truly understand that the outcome of my PhD goes beyond the thesis itself; it encompasses my personal growth and development.

I come from a humble background in Bangladesh, where my passion for math, science, and computer science has always been a driving force. Today, I am immensely grateful to announce that my dream of pursuing a PhD in computer science has become a reality. I am deeply thankful to the brilliant minds I have had the privilege to encounter throughout my doctoral journey.

I am immensely grateful to my advisor, Dr. Kuldeep S. Meel, for playing a crucial role in my PhD journey. Under his guidance, I have learned the importance of being an independent researcher and have been provided with numerous opportunities to achieve this goal. I owe my confidence as a researcher to Kuldeep's unwavering support in connecting me with exceptional researchers through conferences, workshops, internships, and research visits. His leadership, passion, and dedication have truly inspired me. I consider myself privileged to have been a part of his research lab and to have experienced the vibrant research culture it offers. I vividly recall the early semesters in NUS, where Kuldeep would spend hours discussing with the research group, creating an environment that fostered growth and learning. As a new PhD student, his supervision boosted my confidence and enabled me to flourish in the doctoral program. Kuldeep's sharp intellect and innovative thinking have not only made me enjoy graduate school but have also facilitated my personal growth. I am grateful for his relentless guidance, which has not only enhanced my skills as a researcher but also shaped me into a better person.

I feel incredibly fortunate to have had the opportunity to collaborate with exceptional individuals throughout my research journey. Debabrota Basu, Dmitry

Malioutov, Krisnha P. Gummadi, Daniel Neider, Arijit Khan, Jonathan Scarlet, Chandrika Bhardwaj, Vijay Saraswat, Naheed Anjum Arafat, and Lorenzo Ciampiconi are among the remarkable collaborators who have generously shared their knowledge and experience with me. I come to understand that finding a meaningful research problem is a crucial step and I am grateful to have had the opportunity to collaborate and brainstorm with such insightful collaborators. In addition, I thank Harold Soh and Reza Shokri, who examine my thesis with utmost attention. Their feedback has been a driving force for me to reflect positively on my thesis, building a mindset for a broader view on research in general.

I would like to express my sincere appreciation to my friends in Singapore who have provided invaluable support throughout my journey. Neamul Kabir, Sanjay Saha, Amlan Saha, Rafiul Islam, Zubair Faruqui, Mohimenul Mahi, Ramzan Miah, Muhim Muktadir Zim, and Shayok Ghosh have been pillars of support and encouragement. I am also grateful for the exceptional colleagues who have made a significant impact on my professional growth. Priyanka Golia, Teodora Baluta, Yash Pote, Arijit Shaw, Suwei Yang, Jiong Yang, Mate Soos, Tim van Bremen, Anna Latour, Yacine Izza, Gunjan Kumar, Paulius Dilkas, Shubham Sharma, Rahul Gupta, and Zhanzhong Pang have been sources of inspiration and collaboration. Additionally, I would like to extend a special thank you to my childhood friends, Kalyan Roy, Sukanto Kundu, Nayem Ul Haque, and Niranjan Chandra Roy. I am fortunate to have such a supportive community. I extend my thanks to all the staff members in SOC, NUS for their exceptional efficiency in addressing out needs.

I would like to express my heartfelt gratitude to my family for their support and encouragement. My parents, sister, brother-in-law, and uncle have been constant pillars of strength throughout my journey. While I deeply regret that my father is not here with me today, I find solace in the belief that his blessings will always guide me. I am also immensely grateful to my wife, Dola Ghosh, who has been my unwavering source of support and companionship throughout this challenging journey. Her presence has made the road to completion much smoother, and I am grateful for her love and encouragement.

Bishwamittra Ghosh

Contents

Acknowledgments	i
Abstract	viii
List of Publications	x
List of Algorithms	xi
List of Figures	xii
List of Tables	xiv
I Prologue	1
1 Introduction	2
1.1 Interpretable Rule-based Machine Learning	3
1.1.1 Scalability via Incremental Learning	4
1.1.2 Expressiveness via Logical Relaxation	5
1.2 Fairness in Machine Learning	5
1.2.1 Probabilistic Fairness Verification	6
1.2.2 Interpreting Fairness: Identifying Sources of Bias	8
1.3 Thesis Outline	8
2 Preliminaries	10
2.1 Formal Methods	10
2.1.1 Propositional Satisfiability (SAT)	10
2.1.2 Relaxation of Logical Formulas	11
2.1.3 Inner Product	11

2.1.4	Maximum Satisfiability (MaxSAT)	12
2.1.5	Stochastic Boolean Satisfiability (SSAT)	13
2.1.6	Stochastic Subset Sum Problem	14
2.2	Interpretable Machine Learning	14
2.2.1	Rule-based Classification	15
2.2.2	Decision Lists	15
2.2.3	Decision sets	16
2.3	Fairness in Machine Learning	16
2.3.1	Dataset and Distribution	16
2.3.2	Fairness Metrics	17
2.4	Bayesian Network	19
2.5	Global Sensitivity Analysis (GSA): Variance Decomposition	20

II Interpretable Rule-based Machine Learning 22

3 Scalability via Incremental Learning 24

3.1	Related Work	26
3.2	Problem Formulation	28
3.3	Interpretable Classification Rule Learning via MaxSAT	29
3.3.1	Description of Variables	29
3.3.2	MaxSAT Encoding	30
3.3.3	Learning with Non-binary Features	34
3.3.4	Flexible Interpretability Objectives	34
3.4	Incremental Learning of Interpretable Classification Rules	35
3.4.1	Mini-batch Learning	35
3.4.2	Iterative Learning	38
3.5	Learning Other Interpretable Classifiers	40
3.5.1	Learning DNF classifiers	40
3.5.2	Learning Decision Lists	41
3.5.3	Learning Decision Sets	42
3.6	Empirical Performance Analysis	43
3.6.1	Experimental Setup	43
3.6.2	Experimental Results	46

3.7	Chapter Summary	56
4	Expressiveness via Logical Relaxation	58
4.1	Problem Formulation	61
4.2	Classification Rules in Relaxed Logical Form	62
4.2.1	Description of Variables	62
4.2.2	Construction of the ILP Query	63
4.2.3	Incremental Mini-batch Learning	65
4.2.4	Learning with Non-binary Features	67
4.2.5	Learning Rules in Other Logical Forms	68
4.3	Empirical Performance Analysis	68
4.3.1	Experimental Setup	68
4.3.2	Experimental Results	69
4.4	Chapter Summary	75
 III Fairness in Machine Learning		 77
5	Fairness Verification using SSAT	79
5.1	An SSAT-based Fairness Verifier	80
5.1.1	Enumeration Approach using RE-SSAT encoding	81
5.1.2	Inference Approach using ER-SSAT Encoding	85
5.1.3	Practical Settings	89
5.2	Empirical Performance Analysis	90
5.2.1	Experimental Setup	91
5.2.2	Experimental Analysis	92
5.3	Chapter Summary	97
6	Handling Feature Correlations in Fairness Verification	98
6.1	Fairness Verification with Graphical Models	99
6.1.1	Stochastic Subset Sum Problem	100
6.1.2	A Dynamic Programming Solution	102
6.1.3	Stochastic Subset Sum Problem with Correlated Variables	106
6.1.4	Fairness Verification using Probability of Positive Prediction	108

6.1.5	Extension to Practical Settings	108
6.2	Empirical Performance Analysis	109
6.2.1	Scalability Analysis	110
6.2.2	Accuracy Analysis	110
6.3	Chapter Summary	112
IV Epilogue		113
7	Interpreting Fairness: Identifying Sources of Bias	115
7.1	Related Work	119
7.2	Fairness Influence Functions: Formulation and Properties	119
7.2.1	Fairness Metrics as the Variance of Prediction	120
7.2.2	Formulation of FIF	121
7.3	An Algorithm to Estimate Fairness Influence Functions	125
7.4	Empirical Performance Analysis	127
7.4.1	Performance and Functionality in Estimating FIFs	129
7.4.2	Explainability and Applicability of FIFs	133
7.5	Chapter Summary	134
8	Conclusion And Future Work	136
Bibliography		141
A	Interpretable Classification Rules	160
A.1	Performance Comparison: Incremental vs. Non-incremental Encoding	160
A.2	Representative Interpretable Classifiers	161
B	Fairness Verification with Feature Correlation	171
B.1	Extended Experimental Results	171
B.1.1	Accuracy Comparison Among Different Verifiers	171
B.1.2	Scalability Comparison Among Different Verifiers	173
B.1.3	Verifying Fairness Algorithms on Multiple Fairness Metrics	173
B.1.4	Performance Analysis of Bayesian Network	175
C	Feature Correlations in SSAT-based Fairness Verifier	178

D	Fairness Influence Functions	181
D.1	Proofs of Properties and Implications of FIF	181
D.2	A Smoothing Operator: Cubic Splines	183
D.3	Computing FIFs for Equalized Odds and Predictive Parity	185
	D.3.1 FIFs of Equalized Odds	185
	D.3.2 FIFs of Predictive Parity	185
D.4	Experimental Evaluations	186
	D.4.1 Experimental Setup	186
	D.4.2 Accuracy: Equalized Odds & Predictive Parity via FIFs.	186
	D.4.3 Execution Time: Equalized Odds & Predictive Parity via FIFs	186
	D.4.4 Ablation Study: Effect of Spline Intervals	189
	D.4.5 Ablation Study: Effect of Maximum Order of Intersectionality	189
	D.4.6 FIF of Different Datasets	190

Abstract

Interpretability and Fairness in Machine Learning: A Formal Methods Approach

by

Bishwamittra Ghosh

Doctor of Philosophy in Computer Science

National University of Singapore

The significant success of machine learning in past decades has led to a host of applications of algorithmic decision-making in different safety-critical domains. The high-stake predictions of machine learning in medical, law, education, transportation and so on have far-reaching consequences on the end-users. Consequently, there has been a call for the regulation of machine learning by defining and improving the interpretability, fairness, robustness, and privacy of predictions. In this thesis, we focus on the interpretability and fairness aspects of machine learning, particularly on *learning interpretable rule-based classifiers*, *verifying fairness*, and *interpreting sources of unfairness*. Prior studies aimed for these problems are limited by either scalability or accuracy or both. To alleviate these limitations, we integrate formal methods and automated reasoning with interpretability and fairness in machine learning and provide scalable and accurate solutions to the underlying problems.

In interpretable machine learning, rule-based classifiers are particularly effective in representing the decision boundary using a set of rules. The interpretability of rule-based classifiers is generally related to the size of the rules, where smaller rules with higher accuracy are preferable in practice. As such, interpretable classification learning becomes a combinatorial optimization problem suffering from poor scalability in large datasets. To this end, we discuss an incremental learning framework, called IMLI, which applies an iterative solving of maximum satisfiability (MaxSAT) queries in mini-batch learning and enables classification on million-size datasets. Although being interpretable, rule-based classifiers often suffer from limited expressiveness, for example, classifiers based on propositional logic. To learn more expressible yet interpretable classification rules, we discuss a relaxation of classifiers based on logical formulas. For learning relaxed rule-based classifiers, we discuss an efficient learning

framework, called **CRR**, building on incremental learning and mixed integer linear programming (MILP). **CRR** obtains higher accuracy yet less rule size than existing interpretable classifiers.

Fairness in machine learning centers on quantifying and mitigating the bias or unfairness of machine learning classifiers. In the presence of multiple fairness metrics for quantifying bias, we discuss a probabilistic fairness verifier, called **Justicia**, with the goal of formally verifying the bias of a classifier given the probability distribution of features. Building on stochastic satisfiability (SSAT), **Justicia** improves the scalability of verification; and unlike prior approaches, **Justicia** verifies compound sensitive groups combining multiple sensitive features. For a more accurate fairness verification, we extend **Justicia** to consider feature correlations represented as a Bayesian Network, resulting in an accurate verification of fairness.

Fairness metrics globally quantify bias, but do not detect or interpret its sources. To interpret group-based fairness metrics, we discuss fairness influence function (FIF) with an aim of quantifying the influence of individual features and the intersection of multiple features on the bias of a classifier. FIF interprets fairness by revealing potential individual or intersectional features attributing highly to the bias. Building on global sensitivity analysis, we discuss an algorithm, called **FairXplainer**, for estimating the FIFs of features, resulting in a better approximation of bias based on FIFs and a higher correlation of FIFs with fairness interventions.

List of Publications

This thesis is based on the following publications.

1. [“How Biased are Your Features?": Computing Fairness Influence Functions with Global Sensitivity Analysis](#)
Bishwamittra Ghosh, Debabrota Basu, Kuldeep S. Meel
In Proceedings of FAccT, 2023
2. [Efficient Learning of Interpretable Classification Rules](#)
Bishwamittra Ghosh, Dmitry Malioutov, Kuldeep S. Meel
In Proceedings of JAIR, 2022
3. [Algorithmic Fairness Verification with Graphical Models](#)
Bishwamittra Ghosh, Debabrota Basu, Kuldeep S. Meel
In Proceedings of AAI, 2022
4. [Justicia: A Stochastic SAT Approach to Formally Verify Fairness](#)
Bishwamittra Ghosh, Debabrota Basu, Kuldeep S. Meel
In Proceedings of AAI, 2021
5. [Classification Rules in Relaxed Logical Form](#)
Bishwamittra Ghosh, Dmitry Malioutov, Kuldeep S. Meel
In Proceedings of ECAI, 2020
6. [IMLI: An Incremental Framework for MaxSAT-Based Learning of Interpretable Classification Rules](#)
Bishwamittra Ghosh, Kuldeep S. Meel
In Proceedings of AIES, 2019

List of Algorithms

1	MaxSAT-based Mini-batch Learning	38
2	Iterative CNF Classifier Learning	39
3	Iterative Learning of Decision Lists	41
4	Iterative Learning of Decision Sets	42
5	Justicia: An SSAT-based Fairness Verifier	85
6	FairXplainer: An algorithm for estimating FIFs	126

List of Figures

3.1	Scalability of Interpretable Classifiers	50
3.2	Training time, test error, and rule size of different formulations in IMLI	52
3.3	Effect of the number of clauses in IMLI	54
3.4	Effect of regularization λ in IMLI	56
3.5	Effect of batch-size in IMLI	57
4.1	Illustration of a relaxed-CNF classification rule	60
4.2	Effect of data-fidelity λ in CRR	73
4.3	Effect of the number of clause k in CRR	74
4.4	Effect of mini-batch size in CRR	75
4.5	Effect of the number of iterations in CRR	76
5.1	A decision tree classifier on sensitive and non-sensitive features	81
5.2	Fairness verification on compound sensitive groups	93
5.3	Robustness of fairness verification	96
5.4	Runtime of different encodings in Justicia	96
6.1	Simulation of stochastic subset-sum problem	105
6.2	Scalability of FVGM	109
6.3	Accuracy of FVGM	111
7.1	Demonstration of FIF in health insurance	117
7.2	Execution time of FIFs in SP	130
7.3	FIFs under fairness intervention	131
7.4	FIFs for COMPAS dataset	132
7.5	FIFs under fairness affirmative/punitive actions	134
A.1	Scalability: incremental vs. non-incremental encoding	161

A.2	Performance comparison between non-incremental vs. incremental encoding	162
B.1	Accuracy of FVGM on logistic regression classifier	172
B.2	Accuracy of FVGM on SVM classifier	173
B.3	Ablation study: effect of the number of features	174
B.4	Verifying fairness poisoning attack using FVGM	175
B.5	Verifying compound sensitive groups using FVGM	176
B.6	Ablation study: effect of Bayesian network on FVGM	177
D.1	Execution time of FIFs	188
D.2	Ablation study on FIFs: effect of spline intervals	188
D.3	Ablation study on FIFs: effect of maximum order of intersectionality .	189
D.4	FIFs for Adult dataset	190
D.5	FIFs for Titanic dataset	191

List of Tables

3.1	Accuracy and rule-size of interpretable classifiers	47
3.2	Accuracy of IMLI and non-interpretable classifiers	51
3.3	Accuracy and rule-size of different classification rules learned using IMLI	53
4.1	Accuracy, rule-size, and training time of rule-based classifiers	70
4.2	Accuracy of CRR and non-rule-based classifiers	72
5.1	Accuracy of <i>Justicia</i>	92
5.2	Scalability of <i>Justicia</i>	93
5.3	Fairness verification of fairness metrics and algorithms	95
7.1	Approximation error of SP using FIFs	129
D.1	Approximation error of EO and PP using FIFs	187

Part I

Prologue

Chapter 1

Introduction

The last decades have witnessed significant progress in machine learning with a host of applications of algorithmic decision-making in different safety-critical domains, such as medical [50, 84, 91], law [92, 176], education [109], and transportation [139, 195]. In high-stake domains, machine learning predictions have far-reaching consequences on the end-users [51]. With the aim of applying machine learning for societal goods, there have been increasing efforts to regulate machine learning by imposing interpretability [157], fairness [14], robustness [150], and privacy [135] in predictions. In this thesis, we focus on the interpretability and fairness aspects of machine learning. We establish a close integration of formal methods and automated reasoning with machine learning and discuss efficient algorithmic solutions for problems arising in interpretability and fairness in machine learning.

Towards responsible and trustworthy machine learning, we discuss two research themes in this thesis: interpretability and fairness of machine learning classifiers. *In interpretable machine learning*, rule-based classifiers effectively represent the decision boundary using a set of rules comprising input features. Interpretable rule-based classifiers not only interpret the decision function but also are applied to explain the prediction of black-box classifiers [63, 112, 124, 151, 170], a fundamental research question in explainable artificial intelligence (XAI). In this thesis, we discuss efficient algorithms based on incremental learning for interpretable rule-based classifiers. In another research theme of *fairness in machine learning*, unregulated classifiers tend to exhibit bias/unfairness to certain demographic groups in the data unless classifiers are trained with a fairness objective. Consequently, research on fairness centers on quantifying bias using multiple fairness definitions and mitigating bias based on multiple fairness algorithms. In this thesis, we study probabilistic fairness verification problem, where we formally verify the bias of a classifier given the

probability distribution of input features. Finally, we combine both research themes: interpretability and fairness and discuss a framework to interpret the sources of bias. In particular, we formalize and compute fairness influence functions, a way to quantify the influence of individual and the intersection of multiple features on the bias of a classifier. To summarize our thesis on interpretability and fairness in machine learning, we prioritize on improving the *scalability* and the *accuracy* of solutions—either or both of which are absent in prior works.

1.1 Interpretable Rule-based Machine Learning

The problem in interpretable machine learning is to learn a classifier making interpretable predictions to the end-users. To achieve the interpretability of predictions, decision functions in the form of classification rules such as decision trees, decision lists, decision sets, etc. are particularly effective [23, 40, 76, 80, 94, 93, 101, 129, 153, 186, 192]. At this point, it is important to acknowledge that interpretability is an informal notion, and formalizing it in full generality is challenging. In our context of rule-based classifiers, we use *sparsity of rules* (that is, fewer rules each having fewer Boolean literals), which has been considered a proxy of interpretability in various domains, specifically in the medical domain [58, 95, 101, 116, 126].

In the thesis, we study two interpretable rule-based classifiers, characterized by their expressiveness. At first, we study classifiers represented as formulas in propositional logic. In propositional logic, Conjunctive Normal Form (CNF) and Disjunctive Normal Form (DNF) are useful representations of Boolean formulas. Popular interpretable rule-based classifiers such as decision tree, decision lists, and decision sets share the logical structure of CNF/DNF in their representation of the decision function. Thereby, we discuss a learning framework for interpretable CNF classifiers, wherein the interpretability of the classification rule is defined by the number of Boolean literals in the CNF formula. Compared to CNF, Boolean cardinality constraints are more expressive as they allow numerical bounds on Boolean literals [169]. Relying on the concept of cardinality constraints to increase expressiveness, our second interpretable rule-based classifier is a logical relaxation of CNF/DNF classifiers, namely *relaxed-CNF*.

The problem of learning rule-based classifiers is known to be computationally

intractable. The earliest tractable approaches for classifiers such as decision trees and decision lists relied on heuristically chosen objective functions and greedy algorithmic techniques [36, 37, 146]. In these approaches, the size of rules is controlled by early stopping, ad-hoc rule pruning, etc. In recent approaches, the interpretable classification problem is reduced to an optimization problem, where the accuracy and sparsity of rules are optimized jointly [93, 129]. Different optimization solvers such as linear programming [116], sub-modular optimizations [93], Bayesian optimizations [101], and MaxSAT [115] are then deployed to find the best classifier with maximum accuracy and minimum rule-size. The discrete combinatorial nature of learning rule-based classifiers leads to the intractability of the problem and suffers from scalability issues in large datasets. Therefore, we discuss an incremental learning approach by wrapping traditional optimization solvers such as MaxSAT and MILP to efficiently learn rule-based classifiers in a mini-batch learning setting. Here we summarize the contributions of the thesis on interpretable rule-based machine learning¹.

1.1.1 Scalability via Incremental Learning

We discuss an incremental learning framework, called IMLI, based on MaxSAT for learning interpretable classification rules expressed in CNF. IMLI considers a joint objective function to optimize the accuracy and sparsity of classification rules and learns a rule-based classifier by solving an appropriately designed MaxSAT query. Despite the progress of MaxSAT solving in the last decade, the straightforward MaxSAT-based solution cannot scale to real-world classification datasets of thousands to millions of samples. Therefore, we incorporate an efficient incremental learning technique inside the MaxSAT formulation by integrating mini-batch learning and iterative rule-learning. The resulting framework learns a classifier by iteratively covering the training data, wherein in each iteration, it solves a sequence of smaller MaxSAT queries corresponding to each mini-batch. In our experiments, IMLI achieves the best balance among prediction accuracy, interpretability, and scalability. For instance, IMLI attains a competitive prediction accuracy and interpretability with respect to existing interpretable classifiers and demonstrates impressive scalability

¹Corresponding Python library is at <https://github.com/meelgroup/mlc>.

on large datasets where both interpretable and non-interpretable classifiers fail. As an application, we deploy IMLI in learning other interpretable representations: DNF classifiers, decision lists, and decision sets.

1.1.2 Expressiveness via Logical Relaxation

We extend our incremental learning framework to learn a more relaxed representation of classification rules with higher expressiveness. Elaborately, we consider relaxed definitions of standard OR/AND operators in propositional logic by allowing exceptions in the construction of a clause and also in the selection of clauses in a rule. Building on these relaxed definitions, we introduce relaxed-CNF classification rules motivated by the popular usage of checklists in the medical domain and the higher expressiveness of Boolean cardinality constraints. Relaxed-CNF generalizes widely employed rule representations including CNF, DNF, and decision sets. While the combinatorial structure of relaxed-CNF rules offers exponential succinctness, the naïve learning techniques are computationally expensive. To this end, we discuss an incremental mini-batch learning procedure, called CRR, that employs advances in MILP solvers to efficiently learn relaxed-CNF rules. Our experimental analysis demonstrates that CRR can generate relaxed-CNF rules, which are more accurate and sparser compared to the alternative rule-based models.

1.2 Fairness in Machine Learning

As a technology machine learning is oblivious to societal good or bad. The success of machine learning as an accurate predictor, however, finds applications in high-stake decision-making, such as college admission [118], recidivism prediction [178], job applications [3] etc. In such applications, the deployed classifier often demonstrates bias towards certain *sensitive demographic groups* involved in the data [47]. For example, a classifier deciding the eligibility of college admission may offer more admission to White-male candidates than to Black-female candidates—possibly because of the historical bias in the admission data, or the accuracy-centric learning objective of the classifier, or a combination of both [21, 96, 202]. Following such phenomena, multiple fairness metrics, such as *statistical parity*, *equalized odds*, *predictive parity* etc, have been proposed to quantify the bias of the classifier. For

example, if the classifier in college admission demonstrates a statistical parity of 0.6, it means that White-male candidates are offered admission 60% more frequently than Black-female candidates [22, 54, 60]. To this end, different fairness enhancing algorithms have been devised to improve fairness with respect to one or multiple fairness metrics. These algorithms try to rectify and mitigate bias in three ways: *pre-processing* the data [85, 196, 28], *in-processing* the classifier [197], and *post-processing* the outcomes of a classifier [86, 69]. There is also study on fairness attack algorithms to worsen the fairness of a classifier, such as by adding poisoned data samples [174]. In the presence of multiple fairness metrics and algorithms, in this thesis, we contribute to two fundamental problems in fairness: (i) probabilistic verification of fairness² and (ii) interpreting sources of unfairness³.

1.2.1 Probabilistic Fairness Verification

The problem in probabilistic fairness verification is to verify the bias of a classifier given the distribution of input features. The early works on fairness verification focused on measuring fairness metrics of a classifier for a given dataset [17]. Naturally, such techniques were limited in enhancing confidence of users for wide deployment. Consequently, recent verifiers seek to achieve verification beyond finite dataset and in turn focus on the probability distribution of features [4, 15]. More specifically, the input to the verifier is a classifier and the probability distribution of features, and the output is an estimate of fairness metrics that the classifier obtains given the distribution.

In order to solve the fairness verification problem, existing works have proposed two principled approaches. Firstly, [4] propose a formal method approach to reduce the verification problem into the weighted volume computation of an SMT formula. Secondly, [15] propose a sampling approach that relies on extensively enumerating the conditional probabilities of prediction given different sensitive features and thus, incurs high computational cost. Additionally, existing works assume feature independence of non-sensitive features and consider correlated features within a limited scope, such as conditional probabilities of non-sensitive features w.r.t. sensitive features and ignore correlations among non-sensitive features. As a result, the

²Corresponding Python library is at <https://github.com/meelgroup/justicia>.

³Corresponding Python library is at <https://github.com/ReAILE/bias-explainer>.

scalability and *accuracy* of existing verifiers remain major challenges.

1.2.1.1 Formal Fairness Verification

We discuss an efficient fairness verification framework, starting with a general approach for finite classifiers by encoding them as Boolean formulas, and later a special case of linear classifiers. Based on stochastic satisfiability (SSAT) [106], *Justicia* verifies the fairness of Boolean classifiers such as decision tree by solving appropriately designed SSAT formulas. *Justicia* also extends verification to compound sensitive groups, which are a combination of multiple categorical sensitive features such as $\text{race} \in \{\text{White}, \text{Black}\}$ and $\text{gender} \in \{\text{male}, \text{female}\}$. SSAT encoding, by construction, allows separate quantification to each sensitive feature without any restriction on the number of features, thereby it is natural in SSAT-based formulation to extend the verification problem to multiple sensitive features unlike earlier methods. In experiments, *Justicia* is more scalable than the existing probabilistic verifiers [4, 15] because of the efficient SSAT encoding.

1.2.1.2 Tractable Fairness Verification with Feature Correlation

Linear classifiers have attracted significant attention from researchers in the context of designing and testing prototype fairness enhancing and attack algorithms [143, 194, 45, 82]. In the context of verifying the bias of linear classifiers, existing fairness verifiers suffer from two-fold limitations: (i) poor scalability due to applying SSAT/SMT or sampling based techniques and (ii) inaccuracy due to ignoring feature correlations. To alleviate these limitations, we discuss a fairness verification framework for linear classifiers, namely *FVGM*, for an accurate and scalable fairness verification. *FVGM* relies on a novel *stochastic subset-sum* encoding for linear classifiers obtaining an efficient pseudo-polynomial solution using dynamic programming. To address feature-correlations, *FVGM* considers a graphical model, particularly a Bayesian Network to represent the conditional dependence (and independence) among features in the form of a Directed Acyclic Graph (DAG). Experimentally, *FVGM* is more accurate and scalable than existing fairness verifiers; *FVGM* can verify group and causal fairness metrics. We also demonstrate two novel applications of *FVGM* as a fairness verifier: (a) detecting fairness attacks, and (b) computing fairness influences of a subset of features on shifting the incurred bias of

the classifiers from the original bias.

1.2.2 Interpreting Fairness: Identifying Sources of Bias

Fairness metrics measure global bias, but do not detect or interpret its sources [16, 110, 133]. In order to diagnose the emergence of bias in the predictions of classifier, it is important to compute explanations, such as how different features attribute to the global bias. Motivated by the GDPR’s “right to explanation”, research on interpreting model predictions [151, 112, 111] has surged, but interpreting prediction bias has received less attention [16, 110]. In order to identify and interpret the sources of bias and also the impact of affirmative/punitive actions to alleviate/deteriorate bias, it is important to understand *which features contribute how much to the bias of a classifier* applied on a dataset. To this end, we follow a global feature-attribution approach to interpret the sources of bias, where we relate the *influences* of input features towards the resulting bias of the classifier. In this context, existing bias attributing methods [16, 110] are variants of local function approximation [171], whereas bias is a global statistical property of a classifier. Thus, *we aim to design a bias attribution method that is global by construction*. In addition, existing methods only attribute the individual influence of features on bias while neglecting the *intersectionality* among features. Quantifying intersectionality allows us to interpret bias induced by the higher-order interactions among features; hence accounting for intersectionality is important to understand bias as suggested by recent literature [27, 185].

We discuss an algorithm, called **FairXplainer**, based on global sensitivity analysis to estimate the fairness influence function (FIF) of individual and intersectional features. In experiments, **FairXplainer** approximates bias based on FIFs more accurately than existing methods. We also demonstrate higher correlation of FIFs with fairness interventions, thereby demonstrating the importance of FIFs in designing improved fairness algorithms in future.

1.3 Thesis Outline

We organize the thesis as follows. In **part I**, we discuss preliminaries in Chapter 2. In **part II** on interpretable rule-based machine learning, we discuss an incremental

learning framework based on MaxSAT for learning interpretable rule-based classifiers with higher scalability. We conclude this part by applying incremental learning on a more expressible yet interpretable rule-based classifier in Chapter 4. In **part III** on fairness in machine learning, we discuss probabilistic fairness verification based on SSAT for classifiers represented as Boolean formulas in Chapter 5. In Chapter 6, we accommodate feature correlations in fairness verification and discuss a tractable verification algorithm for linear classifiers. In **part IV**, we combine both interpretability and fairness in machine learning by interpreting group fairness metrics in Chapter 7. We conclude the thesis in Chapter 8.

Chapter 2

Preliminaries

We represent sets/vectors by bold letters, and the corresponding distributions by calligraphic letters. We express random variables in uppercase, and the valuation or an assignment of a random variable in lowercase. For example, $\mathbf{X} = \{X_i\}$ is a set of random variables. The distribution of a random variable is $X \in \mathcal{X}$ and its valuation is $X = x$.

2.1 Formal Methods

2.1.1 Propositional Satisfiability (SAT)

Let ϕ be a Boolean formula defined over a set of Boolean variables $\mathbf{B} = \{B_1, B_2, \dots, B_m\}$. A literal V is a variable B or its complement $\neg B$, and a clause C is a disjunction (\vee) or a conjunction (\wedge) of literals.¹ ϕ is in Conjunctive Normal Form (CNF) if $\phi \triangleq \bigwedge_i C_i$ is a conjunction of clauses where each clause $C_i \triangleq \bigvee_j V_j$ is a disjunction of literals. In contrast, ϕ is in Disjunctive Normal Form (DNF) if $\phi \triangleq \bigvee_i C_i$ is a disjunction of clauses where each clause $C_i \triangleq \bigwedge_j V_j$ is a conjunction of literals. We use σ to denote an assignment of variables in \mathbf{B} where $\sigma(B_i) \in \{\text{true}, \text{false}\}$. A *satisfying assignment* σ^* of ϕ is an assignment that evaluates ϕ to true and is denoted by $\sigma^* \models \phi$. The propositional satisfiability (SAT) problem finds a satisfying assignment σ^* to a CNF formula ϕ such that $\forall i, \sigma^* \models C_i$, wherein $\sigma^* \models C_i$ if and only if $\exists V_j \in C_i, \sigma^*(V_j) = \text{true}$. Informally, σ^* satisfies at least one literal in each clause of a CNF.

¹While *term* is reserved to denote disjunction of literals, we use clause for both disjunction and conjunction.

2.1.2 Relaxation of Logical Formulas

A hard-OR or a soft-AND clause is a tuple (C, η) with an extra parameter η , where η is the threshold on the literals in C . Let $\mathbb{1}[\text{true}] = 1$ and $\mathbb{1}[\text{false}] = 0$. Motivated by Boolean cardinality constraints, we introduce relaxed-CNF formulas, where in addition to ϕ , we have two more parameters η_c and η_l . We say that (ϕ, η_c, η_l) is in relaxed-CNF and σ^* is its satisfying assignment if and only if $\sigma^* \models (\phi, \eta_c, \eta_l)$ whenever $\sum_{i=1}^k \mathbb{1}[\sigma^* \models (C_i, \eta_l)] \geq \eta_c$, where $\sigma^* \models (C_i, \eta_l)$ if and only if $\sum_{V \in C_i} \mathbb{1}[\sigma^* \models V] \geq \eta_l$. Informally, σ^* satisfies a clause (C_i, η_l) if at least η_l literals in C_i are set to true by σ^* and σ^* satisfies (ϕ, η_c, η_l) if at least η_c clauses out of all $\{(C_i, \eta_l)\}_{i=1}^k$ clauses are true.

Theorem 1 ([19]). Let (C, η) be a clause in a relaxed-CNF where C has m literals and $\eta \in \{1, \dots, m\}$ is the threshold on literals. An equivalent compact encoding of (C, η) into a CNF formula $\phi = \bigwedge_i C_i$ requires $\binom{m}{m-\eta+1}$ clauses where each clause is distinct and has $m - \eta + 1$ literals of (C, η) . Therefore, the total number of literals in ϕ is $(m - \eta + 1) \binom{m}{m-\eta+1} = m$ (equal succinctness) when $\eta = 1$, otherwise $(m - \eta + 1) \binom{m}{m-\eta+1} > m$ (exponential succinctness).

2.1.3 Inner Product

In the thesis, we use true as 1 and false as 0 interchangeably. Between two vectors \mathbf{U} and \mathbf{V} of the same length defined over Boolean variables or constants (such as 0 and 1), we define $\mathbf{U} \circ \mathbf{V}$ to refer to their inner product. Formally, $\mathbf{U} \circ \mathbf{V} \triangleq \bigvee_i (U_i \wedge V_i)$ is a disjunction of element-wise conjunction where U_i and V_i denote the i^{th} variable/constant of \mathbf{U} and \mathbf{V} , respectively. In this context, the conjunction “ \wedge ” between a variable and a constant follows the standard interpretation: $B \wedge 0 = 0$ and $B \wedge 1 = B$.

For example, let us consider a vector of variables $\mathbf{U} = [U_1, U_2, U_3]$ and a vector of constants of the same length $\mathbf{v} = [0, 1, 1]$. Then, $\mathbf{U} \circ \mathbf{v} = U_2 \vee U_3$. Applying numerical interpretation, the inner product can also be expressed as $\mathbf{U} \circ \mathbf{v} \triangleq \sum_i (U_i \cdot V_i)$. Hence, for the running example $\mathbf{U} = [U_1, U_2, U_3]$ and $\mathbf{v} = [0, 1, 1]$, we derive $\mathbf{U} \circ \mathbf{v} = u_2 + u_3$. In the thesis, we use Boolean interpretation of the inner product for learning CNF

classification rules in Chapter 3 and numerical interpretation for learning relaxed-CNF classification rules in Chapter 4.

2.1.4 Maximum Satisfiability (MaxSAT)

The MaxSAT problem is an optimization analog to the satisfiability (SAT) problem, which is complete for the class FP^{NP} . Although the MaxSAT problem is NP-hard, dramatic progress has been made in designing solvers that can handle large-scale problems arising in practice. This has encouraged researchers to reduce several optimization problems into MaxSAT such as optimal planning [154], automotive configuration [184], group-testing [35], data analysis in machine learning [20], and automatic test pattern generation for cancer therapy [105].

The MaxSAT problem finds an optimal assignment satisfying the maximum number of clauses in a CNF. In interpretable machine learning, we consider a *weighted* variant of the MaxSAT problem—more specifically, a weighted-partial MaxSAT problem—that optimizes over a set of hard and soft constraints in the form of a weighted-CNF formula. In a weighted-CNF formula, a weight $W(C_i) \in \mathbb{R}^+ \cup \{\infty\}$ is defined over each clause C_i , wherein C_i is called a *hard* clause if $W(C_i) = \infty$, and C_i is a *soft* clause, otherwise. To avoid notational clutter, we overload $W(\cdot)$ to denote the weight of an assignment σ . In particular, we define $W(\sigma)$ as the sum of the weights of *unsatisfied clauses* in a CNF, formally,

$$W(\sigma) = \sum_{i|\sigma \neq C_i} W(C_i).$$

Given a weighted-CNF formula $\phi \triangleq \bigvee_i C_i$ with weight $W(C_i)$, the weighted-partial MaxSAT problem finds an optimal assignment σ^* that achieves the minimum weight. Formally, $\sigma^* = \text{MAXSAT}(\phi, W(\cdot))$ if $\forall \sigma \neq \sigma^*, W(\sigma^*) \leq W(\sigma)$. The optimal weight of the MaxSAT problem $W(\sigma^*)$ is infinity (∞) when at least one hard clause becomes unsatisfied. Therefore, the weighted-partial MaxSAT problem finds σ^* that satisfies all hard clauses² and as many soft clauses as possible such that the total weight of unsatisfied soft clauses is minimum. In Chapter 3, we reduce the classification problem to the solution of a weighted-partial MaxSAT problem. The knowledge of the inner workings of MaxSAT solvers is not required for this chapter.

²In our formulation, we assume that there is a satisfying assignment to a CNF formula containing all hard clauses.

2.1.5 Stochastic Boolean Satisfiability (SSAT)

Stochastic Boolean satisfiability (SSAT) was originally introduced by [134] to model *games against nature*. SSAT is a conceptual framework that has been employed to capture several fundamental problems in artificial intelligence such as the computation of maximum a posteriori (MAP) hypothesis [56], propositional probabilistic planning [113], and circuit verification [97].

SSAT problem [106] is a counting analog of the SAT problem concerning with the probability of satisfaction of the formula. SSAT problem computes the probability of satisfaction of a CNF formula ϕ defined on the ordered set of *quantified* Boolean variables \mathbf{B} . An SSAT formula is of the form

$$\Phi = Q_1 B_1, \dots, Q_m B_m, \phi, \quad (2.1)$$

where $Q_i \in \{\exists, \forall, \mathfrak{P}^{p_i}\}$ is either of the existential (\exists), universal (\forall), or randomized (\mathfrak{P}^{p_i}) quantifiers on B_i and ϕ is a quantifier-free CNF formula. In case of a randomized quantifier \mathfrak{P}^{p_i} , $p_i \triangleq \Pr[B_i = 1] \in [0, 1]$ is the probability of B_i being assigned to 1. In the SSAT formula Φ , the quantifier part $Q_1 B_1, \dots, Q_m B_m$ is known as the *prefix* of the formula ϕ . Let B be the outermost variable in the prefix. The semantics of SSAT formulas are defined recursively in the following.

1. $\Pr[\text{true}] = 1, \Pr[\text{false}] = 0,$
2. $\Pr[\Phi] = \max_B \{\Pr[\Phi|_B], \Pr[\Phi|_{\neg B}]\}$ if B is existentially quantified (\exists),
3. $\Pr[\Phi] = \min_B \{\Pr[\Phi|_B], \Pr[\Phi|_{\neg B}]\}$ if B is universally quantified (\forall),
4. $\Pr[\Phi] = p \Pr[\Phi|_B] + (1 - p) \Pr[\Phi|_{\neg B}]$ if B is randomized quantified (\mathfrak{P}^p) with probability p of being true,

where $\Phi|_B$ and $\Phi|_{\neg B}$ denote the SSAT formulas derived by eliminating the outermost quantifier of B by substituting the value of B in the CNF ϕ with 1 and 0, respectively. In this thesis, we focus on two specific types of SSAT formulas: *random-exist* (RE) SSAT and *exist-random* (ER) SSAT. In the ER-SSAT (resp. RE-SSAT) formula, all existentially (resp. randomized) quantified variables are followed by randomized (resp. existentially) quantified variables in the prefix.

Remark. The decision problem of ER-SSAT is NP^{PP} whereas RE-SSAT problem is PP^{NP} -complete [106].

The problem of SSAT and its variants have been pursued by theoreticians and practitioners for over three decades [114, 56, 73]. We refer the reader to [98, 99] for a detailed survey. It is worth remarking that the past decade has witnessed a significant performance improvements of SSAT solving, thanks to the close integration of techniques from SAT solving with advances in weighted model counting [162, 31, 30].

2.1.6 Stochastic Subset Sum Problem

Let $\mathbf{B} \triangleq \{B_i\}_{i=1}^{|\mathbf{B}|}$ be a set of Boolean variables and $W_i \in \mathbb{Z}$ be the weight of B_i . Given a constraint of the form $\sum_{i=1}^{|\mathbf{B}|} W_i B_i = \tau$, for a constant threshold $\tau \in \mathbb{Z}$, the subset-sum problem seeks to compute an assignment $\mathbf{B} \in \{0, 1\}^{|\mathbf{B}|}$ such that the constraint evaluates to true when \mathbf{B} is substituted with \mathbf{b} . Subset sum problem is known to be a NP-complete problem and well-studied in theoretical computer science [87]. The *counting* version of the subset-sum problem counts all \mathbf{b} 's for which the above constraint holds. In this thesis, we consider the constraint $\sum_{i=1}^{|\mathbf{B}|} W_i B_i \geq \tau$ where variables B_i 's are stochastic. While the counting problem of $\sum_{i=1}^{|\mathbf{B}|} W_i B_i = \tau$ is NP-hard to approximate, there is a FPRAS solution for approximately counting the solutions of $\sum_{i=1}^{|\mathbf{B}|} W_i B_i \geq \tau$ [48]. We, in particular, are interested in computing the probability $\Pr[\sum_{i=1}^{|\mathbf{B}|} W_i B_i \geq \tau]$, referred to as *stochastic subset-sum* problem (S3P). Details of S3P are in Chapter 6.1.1.

2.2 Interpretable Machine Learning

We consider a binary classification problem where the dataset \mathbf{D} is a collection of n samples $\{(\mathbf{x}^{(i)}, y^{(i)})\}_{i=1}^n$ generated from an underlying distribution \mathcal{D} . Here, the feature valuation vector $\mathbf{x} = [x_1, \dots, x_m] \in \{0, 1\}^m$ is a vector of m Boolean features with $y \in \{0, 1\}$ being the binary class label. Thus, (\mathbf{x}, y) is called a positive sample if $y = 1$, and a negative sample otherwise. We use (\mathbf{X}, Y) to denote the random variables corresponding to (\mathbf{x}, y) . Hence, each feature $X_j \in \mathbf{X}$ is sampled from a Bernoulli distribution \mathcal{X}_j , and $\mathcal{D} = \prod_{j=1}^m \mathcal{X}_j$ is the product distribution of all

features.

2.2.1 Rule-based Classification

A classifier $\mathcal{R} : \mathbf{X} \rightarrow \hat{Y} \in \{0, 1\}$ is a function that takes a feature vector as input and outputs the predicted class label \hat{Y} . In a rule-based classifier such as a CNF formula, we view \mathcal{R} as a propositional formula defined over Boolean features \mathbf{X} such that, if \mathcal{R} becomes true for an input, the prediction $\hat{Y} = 1$ and $\hat{Y} = 0$, otherwise. The goal is to design \mathcal{R} not only to approximate the training data, but also to generalize to unseen samples arising from the same distribution. Additionally, we prefer to learn a *sparse* \mathcal{R} in order to favor interpretability. We define the structural complexity of \mathcal{R} , referred to as *rule size*, in terms of the number of literals it contains. Let $\text{clause}(\mathcal{R}, i)$ denote the i^{th} clause of \mathcal{R} and $|\text{clause}(\mathcal{R}, i)|$ be the number of literals in $\text{clause}(\mathcal{R}, i)$. Thus, the size of the classifier is $|\mathcal{R}| = \sum_i |\text{clause}(\mathcal{R}, i)|$, which is the sum of literals in all clauses in \mathcal{R} .

Example 2.2.1. Let $\mathcal{R} \triangleq (X_1 \vee X_3) \wedge (\neg X_2 \vee X_3)$ be a CNF classifier defined over three Boolean features $[X_1, X_2, X_3]$. For an input $[0, 1, 1]$, the prediction of \mathcal{R} is 1, whereas for an input $[1, 1, 0]$, the prediction is 0 because \mathcal{R} is true and false in these two cases, respectively. Moreover, $|\mathcal{R}| = 2 + 2 = 4$ is the size of \mathcal{R} .

2.2.2 Decision Lists

A decision list is a rule-based classifier consisting of “if-then-else” rules. Formally, a decision list [153] is an ordered list \mathcal{R}_L pairs $(C_1, V_1), \dots, (C_k, V_k)$ where the rule C_i is a conjunction of literals (alternately, a single clause in a DNF formula) and $V_i \in \{0, 1\}$ is a Boolean class label³. Additionally, the last clause $C_k \triangleq \text{true}$, thereby V_k is the default class. A decision list is defined as a classifier with the following interpretation: for an input feature vector \mathbf{x} , $\mathcal{R}_L(\mathbf{x})$ is equal to V_i where i is the least index such that the feature vector satisfies the rule, $\mathbf{x} \models C_i$. Since the last clause is true, $\mathcal{R}_L(\mathbf{x})$ always exists. Intuitively, whichever clause (starting from the first) in \mathcal{R}_L is satisfied for an input, the associated class-label is considered as its prediction.

³In a more practical setting, $V_i \in \{0, \dots, N\}$ can be multi-class for $N \geq 1$.

2.2.3 Decision sets

A decision set is a set of *independent* “if-then” rules. Formally, a decision set \mathcal{R}_S is a set of pairs $\{(C_1, V_1), \dots, (C_{k-1}, V_{k-1})\}$ and a default pair (C_k, V_k) , where C_i is—similar to a decision list—a conjunction of literals and $V_i \in \{0, 1\}$ is a Boolean class label. In addition, the last clause $C_k \triangleq \text{true}$ and V_k is the default class. For a decision set, if an input \mathbf{x} satisfies one clause, say C_i , then the prediction is V_i . If \mathbf{x} satisfies no clause, then the prediction is the default class V_k . Finally, if \mathbf{x} satisfies ≥ 2 clauses, \mathbf{x} is assigned a class using a tie-breaking [93].

2.3 Fairness in Machine Learning

In this section, we discuss preliminaries in fairness in machine learning, followed by methods to verify fairness and interpret unfairness.

2.3.1 Dataset and Distribution

In the fairness literature, features are categorized into two types: non-sensitive and sensitive features. Hence, we consider a dataset \mathbf{D} as a collection of n triples $\{(\mathbf{x}^{(i)}, \mathbf{a}^{(i)}, y^{(i)})\}_{i=1}^n$ generated from an underlying distribution \mathcal{D} . The feature vector $\mathbf{z}^{(i)} \triangleq (\mathbf{x}^{(i)}, \mathbf{a}^{(i)})$ is a concatenation of non-sensitive features $\mathbf{x}^{(i)}$ and sensitive features $\mathbf{a}^{(i)}$. Each non-sensitive data point $\mathbf{x}^{(i)}$ consists of m_1 features $[x_1^{(i)}, \dots, x_{m_1}^{(i)}] \in \mathbb{R}^{m_1}$. Each sensitive data point $\mathbf{a}^{(i)}$ consists of m_2 categorical features $[a_1^{(i)}, \dots, a_{m_2}^{(i)}] \in \mathbb{N}^{m_2}$. Thus, the cardinality of feature vector $\mathbf{z}^{(i)}$ is denoted by m , formally $|\mathbf{z}^{(i)}| \triangleq m = m_1 + m_2$. The binary class corresponding to $(\mathbf{x}^{(i)}, \mathbf{a}^{(i)})$ is $y^{(i)} \in \{0, 1\}$. We refer to $y^{(i)}$ as the true class.

We denote the random variables corresponding to $(\mathbf{z}, \mathbf{x}, \mathbf{a}, y)$ with $(\mathbf{Z}, \mathbf{X}, \mathbf{A}, Y)$. Each non-sensitive feature $X_i \in \mathbf{X}$ is sampled from a continuous probability distribution \mathcal{X}_i , and each categorical sensitive feature $A_j \in \mathbf{A}$ is sampled from a discrete probability distribution \mathcal{A}_j . Thus, \mathcal{D} is the product distribution of all features, $\mathcal{D} \triangleq \prod_{i=1}^{m_1} \mathcal{X}_i \prod_{j=1}^{m_2} \mathcal{A}_j$. For sensitive features, a valuation vector $\mathbf{a} = [a_1, \dots, a_{m_2}]$ is called a *compound sensitive group*. For example, consider $\mathbf{A} = [\text{race}, \text{sex}]$ where $\text{race} \in \{\text{Asian}, \text{Color}, \text{White}\}$ and $\text{sex} \in \{\text{female}, \text{male}\}$. Thus $\mathbf{a} = [\text{Asian}, \text{female}]$ is a compound sensitive group. We represent a binary classifier trained on the dataset \mathbf{D}

as $\mathcal{M} : (\mathbf{X}, \mathbf{A}) \rightarrow \hat{Y}$. Here, $\hat{Y} \in \{0, 1\}$ is the class predicted for (\mathbf{X}, \mathbf{A}) . Given this setup, we discuss different fairness metrics to compute the bias in the prediction of a classifier [54, 69, 127].

2.3.2 Fairness Metrics

A classifier \mathcal{M} that solely optimizes accuracy, i.e. the average number of times $\hat{Y} = Y$, may discriminate certain compound sensitive groups over others [34]. In the following, we describe two well-known fairness definitions: group fairness and causal fairness. To this end, we denote $f(\mathcal{M}, \mathcal{D})$ to quantify the fairness of the classifier \mathcal{M} given the distribution of features \mathcal{D} . Alternatively, a fairness metric can be computed on a finite dataset instead of on the distribution. In that case, we use the notation $f(\mathcal{M}, \mathbf{D})$, which is the bias of the classifier \mathcal{M} on a dataset \mathbf{D} .

Statistical Parity (SP). Statistical parity belongs to *independence* measuring group fairness metrics, where the prediction \hat{Y} is statistically independent of sensitive features \mathbf{A} [54]. The statistical parity of a classifier is measured as

$$f_{\text{SP}}(\mathcal{M}, \mathcal{D}) \triangleq \max_{\mathbf{a}} \Pr[\hat{Y} = 1 | \mathbf{A} = \mathbf{a}] - \min_{\mathbf{a}} \Pr[\hat{Y} = 1 | \mathbf{A} = \mathbf{a}],$$

which is the difference between the maximum and minimum conditional probability of positive prediction the classifier for different sensitive groups.

Disparate impact (DI). Disparate impact also belongs to independence measuring group fairness metrics. Disparate impact measures the ratio between the minimum and the maximum conditional probability of positive prediction of the classifier over all sensitive groups, and prescribe the ratio to be close to 1 [54]. Formally, the disparate impact of a classifier is

$$f_{\text{DI}}(\mathcal{M}, \mathcal{D}) \triangleq \frac{\min_{\mathbf{a}} \Pr[\hat{Y} = 1 | \mathbf{A} = \mathbf{a}]}{\max_{\mathbf{a}} \Pr[\hat{Y} = 1 | \mathbf{A} = \mathbf{a}]}.$$

Equalized Odds (EO). *Separation* measuring group fairness metrics such as equalized odds [69] constrain that the predicted class \hat{Y} is independent of \mathbf{A} given the true class Y . Formally, for $Y \in \{0, 1\}$, equalized odds is defined as

$$f_{\text{EO}}(\mathcal{M}, \mathbf{D}) \triangleq \max_y \left(\max_{\mathbf{a}} \Pr[\hat{Y} = 1 | \mathbf{A} = \mathbf{a}, Y = y] - \min_{\mathbf{a}} \Pr[\hat{Y} = 1 | \mathbf{A} = \mathbf{a}, Y = y] \right).$$

Equalized odds intuitively implies the maximum statistical parity conditioned on Y .

Predictive Parity (PP). *Sufficiency* measuring group fairness metrics such as Predictive Parity (PP) constrain that the ground class Y is independent of \mathbf{A} given the prediction \hat{Y} . Formally,

$$f_{\text{PP}}(\mathcal{M}, \mathcal{D}) \triangleq \max_y \left(\max_{\mathbf{a}} \Pr[Y = 1 \mid \mathbf{A} = \mathbf{a}, \hat{Y} = y] - \min_{\mathbf{a}} \Pr[Y = 1 \mid \mathbf{A} = \mathbf{a}, \hat{Y} = y] \right).$$

Path-specific Causal Fairness (PCF). Let $\mathbf{a}_{\text{max}} \triangleq \arg \max_{\mathbf{a}} \Pr[\hat{Y} = 1 \mid \mathbf{A} = \mathbf{a}]$. We consider mediator features $\mathbf{Z} \subseteq \mathbf{X}$ sampled from the conditional distribution $\mathcal{Z}_{\mid \mathbf{A}=\mathbf{a}_{\text{max}}}$. This emulates the fact that mediator variables have the same sensitive features \mathbf{a}_{max} . To this end, the path-specific causal fairness, abbreviated as PCF, of a classifier is

$$f_{\text{PCF}}(\mathcal{M}, \mathcal{D}) \triangleq \max_{\mathbf{a}} \Pr[\hat{Y} = 1 \mid \mathbf{A} = \mathbf{a}, \mathbf{Z}] - \min_{\mathbf{a}} \Pr[\hat{Y} = 1 \mid \mathbf{A} = \mathbf{a}, \mathbf{Z}].$$

Therefore, path-specific causal fairness constrains that the prediction \hat{Y} is not directly dependent of sensitive features \mathbf{A} while \mathbf{A} may indirectly affects \hat{Y} only through mediator features \mathbf{Z} . Hence, path-specific causal fairness is a variation of counterfactual fairness and causal fairness without mediator features [15].

Example 2.3.1. Following [15], we consider a classifier that decides the hiring of employees based on three features: gender (sensitive), years of experience (non-sensitive), and college-participation (mediator). It is practical to consider that $\text{gender} \in \{\text{male}, \text{female}\}$ can affect the college-participation of individuals, and all three features are determining factors for the hiring process. Let ‘male’ be the most favored group by the classifier, for instance. Path-specific causal fairness ensures that a female candidate should be given a job offer with similar probability as a male candidate. She, however, went to (participated in) college as if she were a male candidate while other non-mediator features such as ‘years of experience’ are the same. Therefore, path-specific causal fairness measures the effect of gender on job offer, but ignores the effect of gender on whether candidates went to college.

Fairness Verification. We verify the fairness of a classifier by comparing $f(\mathcal{M}, \mathcal{D})$ with a fairness threshold, denoted by $\epsilon \in [0, 1]$, that quantifies the desired level of fairness. In particular, a classifier is ϵ -fair with respect to statistical parity, equalized odds, predictive parity, and path-specific causal fairness if and only if $f(\mathcal{M}, \mathcal{D}) \leq \epsilon$. In contrast, a classifier achieves $(1 - \epsilon)$ -disparate impact if and only if $f(\mathcal{M}, \mathcal{D}) \geq 1 - \epsilon$. In all above fairness metrics, a lower value of ϵ refers to higher fairness of the classifier.

2.4 Bayesian Network

In general, a Probabilistic Graphical Model [88], and specifically a *Bayesian network* [137, 32], encodes the dependencies and conditional independence between a set of random variables. In fairness verification with correlated features, we leverage an access to a Bayesian network on sensitive and non-sensitive features $\mathbf{X} \cup \mathbf{A}$ that represents the joint distribution on them. A Bayesian network is denoted by a pair (G, θ) , where $G \triangleq (\mathbf{V}, \mathbf{E})$ is a DAG (Directed Acyclic Graph), and θ is a set of parameters encoding the conditional probabilities induced by the joint distribution under investigation. Each vertex $V_i \in \mathbf{V}$ corresponds to a random variable. Edges $\mathbf{E} \in \mathbf{V} \times \mathbf{V}$ imply conditional dependencies among variables. For each variable $V_i \in \mathbf{V}$, let $\text{Pa}(V_i) \subseteq \mathbf{V} \setminus \{V_i\}$ denote the set of parents of V_i . Given $\text{Pa}(V_i)$ and parameters θ , V_i is independent of its other non-descendant variables in G . Thus, for the assignment v_i of V_i and \mathbf{u} of $\text{Pa}(V_i)$, the aforementioned semantics of a Bayesian network encodes the joint distribution of \mathbf{V} as:

$$\Pr[V_1 = v_1, \dots, V_{|\mathbf{V}|} = v_{|\mathbf{V}|}] = \prod_{i=1}^{|\mathbf{V}|} \Pr[V_i = v_i | \text{Pa}(V_i) = \mathbf{u}; \theta]. \quad (2.2)$$

The complexity $C(G)$ of a Bayesian network (G, θ) with discrete random variables \mathbf{V} is defined as the number of independent parameters used to define the probability distribution of \mathbf{V} [125]. Let $\text{Card}(V)$ denote the number of distinct values that a random variable V can take. As such, for each conditional probability $\Pr[V_i = v_i | \text{Pa}(V_i) = \mathbf{u}; \theta]$, we need $\text{Card}(\text{Pa}(V_i))(\text{Card}(V_i) - 1)$ independent parameters. Thus, the total complexity of a Bayesian network is:

$$C(G) = \sum_{i=1}^{|\mathbf{V}|} \text{Card}(\text{Pa}(V_i))(\text{Card}(V_i) - 1) \quad (2.3)$$

2.5 Global Sensitivity Analysis (GSA): Variance Decomposition

Global sensitivity analysis is an active field of research that studies how the global uncertainty in the output of a function can be attributed to the different sources of uncertainties in the input variables [161]. Sensitivity analysis is an essential component for quality assurance and impact assessment of models in EU [52], USA [132], and research communities [160]. *Variance-based sensitivity analysis* is a form of global sensitivity analysis, where variance is considered as the measure of uncertainty [172, 173]. To illustrate, let us consider a real-valued function $g(\mathbf{Z})$, where \mathbf{Z} is a vector of m input variables $\{Z_1, \dots, Z_m\}$. Now, we decompose $g(\mathbf{Z})$ among the subsets of inputs, such that:

$$\begin{aligned} g(\mathbf{Z}) &= g_0 + \sum_{i=1}^m g_{\{i\}}(Z_i) + \sum_{i<j}^m g_{\{i,j\}}(Z_i, Z_j) + \dots + g_{\{1,2,\dots,m\}}(Z_1, Z_2, \dots, Z_m) \\ &= g_0 + \sum_{\mathbf{S} \subseteq [m]} g_{\mathbf{S}}(\mathbf{Z}_{\mathbf{S}}) \end{aligned} \quad (2.4)$$

The standard condition of this decomposition is the orthogonality of each term in the right-hand side of Eq. (2.4) [172]. In this decomposition, g_0 is a constant, $g_{\{i\}}$ is a function of Z_i , $g_{\{i,j\}}$ is a function of Z_i and Z_j , and so on. Adhering to the set-based notations, we denote by $g_{\mathbf{S}}$ a function of a non-empty subset of variables $\mathbf{Z}_{\mathbf{S}} \triangleq \{Z_i \mid i \in \mathbf{S}\} \subseteq \mathbf{Z}$, where $\mathbf{S} = \{S_i \mid 1 \leq |S_i| \leq m\} \subseteq [m]$ is a non-empty subset of indices with $[m] \triangleq \{1, 2, \dots, m\}$. Here, $|\mathbf{S}| = 1$ quantifies an individual variable's effect while $|\mathbf{S}| > 1$ quantifies the higher-order intersectional effect of variables.

Considering g as square integrable, we obtain the decomposition of the variance of $g(\mathbf{Z})$ expressed as the sum of variances of $g_{\mathbf{S}}$'s [172].

$$\text{Var}[g(\mathbf{Z})] = \sum_{i=1}^m V_{\{i\}} + \sum_{i<j}^m V_{\{i,j\}} + \dots + V_{\{1,2,\dots,m\}} = \sum_{\mathbf{S} \subseteq [m_1]} V_{\mathbf{S}} \quad (2.5)$$

where $V_{\{i\}}$ is the variance of $g_{\{i\}}$, $V_{\{i,j\}}$ is the variance of $g_{\{i,j\}}$ and so on. Formally,

$$V_{\mathbf{S}} \triangleq \text{Var}_{\mathbf{Z}_{\mathbf{S}}} \left[\mathbb{E}_{\mathbf{Z} \setminus \mathbf{Z}_{\mathbf{S}}} [g(\mathbf{Z}) \mid \mathbf{Z}_{\mathbf{S}}] \right] - \sum_{\mathbf{S}' \subset \mathbf{S}} V_{\mathbf{S}'}. \quad (2.6)$$

Here, \mathbf{S}' denotes all the non-empty and ordered proper subsets of \mathbf{S} . Thus, $V_{\mathbf{S}}$ is the variance w.r.t. $\mathbf{Z}_{\mathbf{S}}$ by subtracting the variances of all non-empty proper subsets of $\mathbf{Z}_{\mathbf{S}}$. As a result, Eq. (2.5) demonstrates how the variance of $g(\mathbf{Z})$ can be decomposed into terms attributable to each input feature, as well as the intersectional effects among them. Conversely, together all terms sum to the total variance of the model output.

Part II

Interpretable Rule-based Machine Learning

We discuss an incremental learning framework based on MaxSAT for interpretable classification rules in Chapter 3. This allows us to scale up classification on large datasets. In Chapter 4, we improve the expressiveness of rule-based classifiers and apply incremental solving for an efficient learning.

Chapter 3

Scalability via Incremental Learning

We discuss an efficient learning framework for interpretable rule-based classifiers with a particular emphasis on the scalability in learning. In rule-based classifiers, rules governing the prediction are explicit (by design) in contrast to black-box classifiers [157]. In particular, we study classifiers expressed as Boolean formulas, wherein we define interpretability in terms of the number of Boolean literals that the formula contains. Here, we illustrate an interpretable classifier that decides if a tumor cell is malignant or benign based on different features of tumors.

A tumor is malignant if
[(compactness SE < 0.1) **OR** $\neg(0.1 \leq \text{concave points} < 0.2)$] **AND**
[$\neg(0.2 \leq \text{area} < 0.3)$ **OR** $\neg(0.1 \leq \text{largest symmetry} < 0.2)$]

Example 3.0.1. We illustrate an interpretable classification rule in CNF for classifying a tumor cell. We consider WDBC (Wisconsin Diagnostic Breast Cancer) dataset [2] to learn a CNF formula with two *clauses* and four Boolean *literals*. In the formula, clauses are connected by Boolean ‘AND’, where each clause contains *literals* connected by Boolean ‘OR’. Informally, a tumor cell is malignant if at least one literal in each clause becomes true.

The problem of learning rule-based classifiers is known to be computationally intractable. The earliest tractable approaches for classifiers such as decision trees and decision lists relied on heuristically chosen objective functions and greedy algorithmic techniques [36, 37, 146]. In these approaches, the size of rules is controlled by early stopping, ad-hoc rule pruning, etc. In recent approaches, the interpretable

classification problem is reduced to an optimization problem, where the accuracy and the sparsity of rules are optimized jointly [93, 129]. Different optimization solvers such as linear programming [116], sub-modular optimizations [93], and Bayesian optimizations [101] are then deployed to find the best classifier with maximum accuracy and minimum rule size. In our study, we study an alternate optimization approach that fits particularly well to rule-learning problems. Particularly, we study and improve a *maximum satisfiability* (MaxSAT) solution for learning interpretable rule-based classifiers. Building on MaxSAT, [115] considers a learning framework to jointly optimize the accuracy and the size of classification rules. The said approach constructs and solves a MaxSAT query of $\mathcal{O}(kn)$ size (number of clauses) to learn a k -clause CNF formula on a dataset containing n samples (Chapter 3.3.2). Naturally, the naïve formulation cannot scale to large values of n and k . To scale learning to large datasets, we discuss an incremental learning technique along with the MaxSAT formulation.

Contributions. The contribution of this chapter is a MaxSAT-based formulation, called **IMLI** (**I**ncremental **M**axSAT-based **L**earning of **I**nterpretable classification rules), for learning interpretable classification rules expressible in propositional logic. For the simplicity of exposition, our initial focus is on learning classifiers expressible in CNF formulas; we later discuss how the CNF learning formulation can be extended to popular interpretable classifiers such as decision lists and decision sets. Our incremental learning is an integration of mini-batch learning and iterative rule-learning, which are studied separately in classical learning problems. In the presented incremental approach, **IMLI** learns a k -clause CNF formula using an iterative separate-and-conquer algorithm, where in each iteration, a single clause is learned by covering a part of the training data (Chapter 3.4). Furthermore, to efficiently learn a single clause in a CNF, **IMLI** relies on mini-batch learning, where it solves a sequence of smaller MaxSAT queries corresponding to each mini-batch.

In our experimental evaluations, **IMLI** demonstrates the best balance among prediction accuracy, interpretability, and scalability in learning classification rules. In particular, **IMLI** achieves competitive prediction accuracy and interpretability w.r.t. state-of-the-art interpretable classifiers. Besides, **IMLI** achieves impressive scalability by classifying datasets even with 1 million samples, wherein existing

classifiers, including those of the non-interpretable ones, either fail to scale or achieve poor prediction accuracy. Finally, as an application, we deploy IMLI in learning interpretable classifiers such as decision lists and decision sets.

We organize the rest of the chapter as follows. We discuss related literature in Chapter 3.1. In Chapter 3.2, we formally define interpretable rule-based classification problem and discuss a MaxSAT-based solution proposed by [115] in Chapter 3.3. In Chapter 3.4, we discuss the key technical contribution of this chapter, IMLI, an improved MaxSAT-based learning formulation based on incremental solving. In Chapter 3.5, we apply IMLI in learning different interpretable classifiers. We then discuss our experimental results in Chapter 3.6 and conclude in Chapter 3.7.

3.1 Related Work

The progress in designing interpretable rule-based classifiers finds its root in the development of decision trees [23, 144, 145], decision lists [153], classification rules [38] etc. In early works, the focus was to improve the efficiency and scalability of the model rather than designing models that are interpretable. For example, decision rule approaches such as C4.5 rules [146], CN2 [36], RIPPER [38], and SLIPPER [37] rely on heuristic-based branch pruning and ad-hoc local criteria e.g., maximizing information gain, coverage, etc.

Recently, several optimization frameworks have been proposed for interpretable classification, where both accuracy and rule size are optimized during training. For example, [116] proposed exact learning of rule-based classifiers based on Boolean compressed sensing using a linear programming formulation. [175] presented two-level Boolean rules, where the trade-off between classification accuracy and interpretability is studied. In their work, the Hamming loss is used to characterize prediction accuracy, and sparsity is used to characterize the interpretability of rules. [186] proposed a Bayesian optimization framework for learning falling rule lists, which is an ordered list of if-then rules. Other similar approaches based on Bayesian analysis for learning classification rules are [101, 188]. Building on custom discrete optimization techniques, [6] proposed an optimal learning technique for decision lists using a branch-and-bound algorithm. In a separate study, [93] highlighted the importance of decision sets over decision lists in terms of interpretability and

considered a sub-modular optimization problem for learning a near-optimal solution for decision sets. Our approach for interpretable classification, however, relies on the improvement in formal methods over the decades, particularly the efficient CDCL-based solution for satisfiability (SAT) problems [168].

Formal methods, particularly SAT and its variants, have been deployed in interpretable classification in recent years. In the context of learning decision trees, SAT and MaxSAT-based solutions are proposed by [5, 81, 129, 167]. In addition, researchers have applied SAT for learning explainable decision sets [79, 75, 164, 193]. In most cases, SAT/MaxSAT solutions are not sufficient in solving large-scale classification tasks because of the NP-hardness of the underlying problem. This observation motivates us in combining MaxSAT with more practical algorithms such as incremental learning.

Incremental learning has been studied in improving the scalability of learning problems, where data is processed in parts and results are combined to use lower computation overhead. In case of non-interpretable classifiers such as SVM, several solutions adopting incremental learning are available [177, 159]. For example, [29] proposed an online recursive algorithm for SVM that learns one support-vector at a time. Based on radial basis kernel function, [149] proposed a local incremental learning algorithm for SVM. In the context of deep neural networks, stochastic gradient descent is a well-known convex optimization technique—a variant of which includes computing the gradient on mini-batches [71, 103, 120]. Federated learning, on the other hand, decentralizes training on multiple local nodes based on local data samples with only exchanging learned parameters to construct a global model in a central node [89, 90]. Another notable technique is Lagrangian relaxation that decomposes the original problem into several sub-problems, assigns Lagrangian multipliers to make sure that sub-problems agree, and iterates by solving sub-problems and adjusting weights based on disagreements [55, 83, 100]. To the best of our knowledge, our method is the first method that unifies incremental learning with MaxSAT based formulation to improve the scalability of learning rule-based classifiers.

Classifiers that are interpretable by design can be applied to improve the explainability of complex black-box machine learning classifiers. There is rich literature on extracting decompositional and pedagogical rules from non-linear classifiers such

as support vector machines [12, 13, 43, 117, 130] and neural networks [10, 66, 166, 163, 201, 200]. In recent years, local model-agnostic approaches for explaining black-box classifiers are proposed by learning surrogate simpler classifiers such as rule-based classifiers [65, 136, 148, 152]. The core idea in local approaches is to use a rule-learner that can classify synthetically generated neighboring samples with class labels provided by the black-box classifier. To this end, our framework IMLI can be directly deployed as an efficient rule-learner and can explain the inner-working of black-box classifiers by generating interpretable rules.

3.2 Problem Formulation

We are given

1. a dataset $\mathbf{D} = \{(\mathbf{x}^{(i)}, y^{(i)})\}_{i=1}^n$ of n samples, where feature vector $\mathbf{x}^{(i)} \in \{0, 1\}^m$ contains m features and class label $y^{(i)} \in \{0, 1\}$,
2. a positive integer $k \geq 1$ denoting the number of clauses to be learned in the classification rule, and
3. a regularization parameter $\lambda \in \mathbb{R}^+$.

Our goal is to learn a rule-based classifier \mathcal{R} represented as a k -clause CNF formula separating samples of class 1 from class 0.

We learn classifiers that balance two goals: of being accurate but also interpretable. Various notions of interpretability have been discussed in the context of classification problems. A common proxy for interpretability in the context of decision rules is the sparsity of rule. For instance, a rule involving fewer literals is highly interpretable. In this chapter, we minimize the total number of literals in all clauses, which motivates us to find \mathcal{R} with minimum $|\mathcal{R}|$. Let \mathcal{R} classify all samples correctly during training. Among all the classification rules that classify all samples correctly, we choose the sparsest (most interpretable) such \mathcal{R} .

$$\min_{\mathcal{R}} |\mathcal{R}| \text{ such that } \forall i, y^{(i)} = \mathcal{R}(\mathbf{x}^{(i)})$$

In practical classification tasks, perfect classification is unlikely. Hence, we need to balance interpretability with classification error. Let $\mathcal{E}_{\mathbf{D}} = \{(\mathbf{x}^{(i)}, y^{(i)}) | y^{(i)} \neq \mathcal{R}(\mathbf{x}^{(i)})\}$

be the set of samples in \mathbf{D} that are misclassified by \mathcal{R} . Therefore, we balance between classification-accuracy and rule-sparsity and optimize the following function.¹

$$\min_{\mathcal{R}} |\mathcal{E}_{\mathbf{D}}| + \lambda|\mathcal{R}| \quad (3.1)$$

Higher values of λ generate a rule with a smaller rule size but of more training errors, and vice-versa. Thus, λ can be tuned to trade-off between accuracy and interpretability for a rule-based classifier, which we experiment extensively in Chapter 3.6.

3.3 Interpretable Classification Rule Learning via MaxSAT

In this section, we revisit [115] by discussing a MaxSAT-based learning framework for an interpretable rule-based classifier, particularly a CNF classifier \mathcal{R} . We first describe the decision variables in Chapter 3.3.1 and present the MaxSAT encoding in Chapter 3.3.2. The MaxSAT formulation assumes binary features as input. We conclude this section by learning \mathcal{R} with non-binary features in Chapter 3.3.3 and discussing more flexible interpretability constraints of \mathcal{R} in Chapter 3.3.4.

3.3.1 Description of Variables

We initially preprocess feature vector \mathbf{x} to account for the negation of Boolean features while learning a classifier.² In the preprocessing step, we negate each feature in \mathbf{x} to a new feature and append it to \mathbf{x} . For example, if “age ≥ 25 ” is a Boolean feature, we add another feature “age < 25 ” in \mathbf{x} by negating the feature “age ≥ 25 ”. Hence, in the rest of the chapter, we refer m as the modified number of features in \mathbf{x} . We next discuss the variables in the MaxSAT problem.

We consider two types of Boolean variables: (i) *feature* variables B corresponding to input features and (ii) *error* variables ξ corresponding to the classification error of samples. We define a Boolean variable B_j^i that becomes true if feature X_j appears in the i^{th} clause of \mathcal{R} , thereby contributing to an increase in the rule size of \mathcal{R} , and

¹In our formulation, it is straightforward to add class-conditional weights (e.g., to penalize false-alarms more than mis-detects), and to allow instance weights (per sample).

²This preprocessing is similarly applied in [116].

B_j^i is assigned false, otherwise. Moreover, we define an error variable ξ_l to attribute to whether the l^{th} sample $(\mathbf{x}^{(l)}, y^{(l)})$ is classified correctly or not. Specifically, ξ_l becomes true if $(\mathbf{x}^{(l)}, y^{(l)})$ is misclassified, and becomes false otherwise. We next discuss the MaxSAT encoding to solve the classification problem.

3.3.2 MaxSAT Encoding

We consider a partial-weighted MaxSAT formula, where we encode the objective function in Eq. (3.1) as soft clauses and the learning constraints as hard clauses. We next discuss the MaxSAT encoding in detail.

- **Soft clauses for maximizing training accuracy:** For each training sample, we construct a soft unit³ clause $\neg\xi_l$ to account for a penalty for misclassification. Since the penalty for misclassification of a sample is 1 in Eq. (3.1), the weight of this soft clause is also 1.

$$E_l := \neg\xi_l; \quad W(E_l) = 1 \quad (3.2)$$

Intuitively, if a sample is misclassified, the associated error variable becomes true, thereby dissatisfying the soft clause E_l .

- **Soft clauses for minimizing rule-sparsity:** To favor rule-sparsity, we learn a classifier with as few literals as possible. Hence, for each feature variable B_j^i , we construct a unit clause as $\neg B_j^i$. Similar to training accuracy, the weight for this clause is derived as λ from Eq. (3.1).

$$S_j^i := \neg B_j^i; \quad W(S_j^i) = \lambda \quad (3.3)$$

- **Hard clauses for encoding constraints:** In a MaxSAT problem, constraints that must be satisfied are encoded as hard clauses. In rule-based classification, we have a learning constraint that, if the error variable is false, the associated sample must be correctly classified, and vice-versa. Let $\mathbf{B}_i = \{B_j^i \mid j \in \{1, \dots, m\}\}$ be a vector of feature variables corresponding to the i^{th} clause in \mathcal{R} . Then, we define the following hard clause.

³A unit clause has a single literal.

$$H_l := \neg\xi_l \rightarrow \left(y^{(l)} \leftrightarrow \bigwedge_{i=1}^k \mathbf{x}^{(l)} \circ \mathbf{B}_i \right); \quad W(H_l) = \infty \quad (3.4)$$

In the hard clause, $\bigwedge_{i=1}^k \mathbf{x}^{(l)} \circ \mathbf{B}_i$ is a CNF formula including variables B_j^i for which the associated feature-value is 1 in $\mathbf{x}^{(l)}$. Since $y^{(l)} \in \{0, 1\}$ is a constant, the constraint to the right of the implication “ \rightarrow ” is either $\bigwedge_{i=1}^k \mathbf{x}^{(l)} \circ \mathbf{B}_i$ or its complement. Therefore, the hard clause enforces that if the sample is correctly classified (using $\neg\xi_l$), either $\bigwedge_{i=1}^k \mathbf{x}^{(l)} \circ \mathbf{B}_i$ or its complement is true depending on the class-label of the sample. We highlight that the single-implication “ \rightarrow ” in the hard clause H_l acts as a double-implication “ \leftrightarrow ” due to the soft clause E_l . Because, according to the definition of “ \rightarrow ”, the left constraint $\neg\xi_l$ can be false while the right constraint of “ \rightarrow ” is true. This, however, incurs unnecessarily dissatisfying the soft clause E_l , which is a sub-optimal solution and hence this solution is not returned by the MaxSAT solver.

We next discuss the translation of soft and hard clauses into a CNF formula, which can be invoked by any MaxSAT solver.

Translating E_l, S_j^i, H_l to a CNF formula. The soft clauses E_l and S_j^i are unit clauses and hence, no translation is required for them. In the hard clause, when $y^{(l)} = 1$, the simplification is $H_l := \neg\xi_l \rightarrow \bigwedge_{i=1}^k \mathbf{x}^{(l)} \circ \mathbf{B}_i$. In this case, we apply the equivalence rule in propositional logic $(A \rightarrow B) \equiv (\neg A \vee B)$ to encode H_l into CNF. In contrast, when $y_i = 0$, we simplify the hard clause as $H_l := \neg\xi_l \rightarrow \neg(\bigwedge_{i=1}^k \mathbf{x}^{(l)} \circ \mathbf{B}_i) \Rightarrow \neg\xi_l \rightarrow \bigvee_{i=1}^k \neg(\mathbf{x}^{(l)} \circ \mathbf{B}_i)$. Since $\mathbf{x}^{(l)} \circ \mathbf{B}_i$ constitutes a disjunction of literals, we apply Tseytin transformation to encode $\neg(\mathbf{x}^{(l)} \circ \mathbf{B}_i)$ into CNF. More specifically, we introduce an auxiliary variable $z_{l,i}$ corresponding to the clause $\neg(\mathbf{x}^{(l)} \circ \mathbf{B}_i)$. Formally, we replace $H_l := \neg\xi_l \rightarrow \bigvee_{i=1}^k \neg(\mathbf{x}^{(l)} \circ \mathbf{B}_i)$ with $\bigwedge_{i=0}^k H_{l,i}$, where $H_{l,0} := (\neg\xi_l \rightarrow \bigvee_{i=1}^k z_{l,i})$ and $H_{l,i} := z_{l,i} \rightarrow \neg(\mathbf{x}^{(l)} \circ \mathbf{B}_i)$ for $i = \{1, \dots, k\}$. Finally, we apply the equivalence of $(A \rightarrow B) \equiv (\neg A \vee B)$ on $H_{l,i}$ to translate them into CNF. For either value of $y^{(l)}$, the weight of each translated hard clause in the CNF formula is ∞ .

Once we translate all soft and hard clauses into CNF, the MaxSAT query Q is

the conjunction of all clauses.

$$Q := \bigwedge_{l=1}^n E_l \wedge \bigwedge_{i=1, j=1}^{i=k, j=m} S_j^i \wedge \bigwedge_{l=1}^n H_l$$

Any off-the-shelf MaxSAT solver can output an optimal assignment σ^* of the MaxSAT query $(Q, W(\cdot))$. We extract σ^* to construct the classifier \mathcal{R} and compute training errors as follows.

Construction 2. Let $\sigma^* = \text{MAXSAT}(Q, W(\cdot))$. Then $X_j \in \text{clause}(\mathcal{R}, i)$ if and only if $\sigma^*(B_j^i) = 1$. Additionally, $(\mathbf{x}^{(l)}, y^{(l)})$ is misclassified if and only if $\sigma^*(\xi_l) = 1$.

Complexity of the MaxSAT query. We analyze the complexity of the MaxSAT query in terms of the number of Boolean variables and clauses in the CNF formula Q .

Proposition 3. To learn a k -clause CNF classifier for a dataset of n samples over m boolean features, the MaxSAT query Q defines $km + n$ Boolean variables. Let n_{neg} be the number of negative samples in the training dataset. Then the number of auxiliary variables in Q is kn_{neg} .

Proposition 4. The MaxSAT query Q has $km + n$ unit clauses corresponding to the constraints E_l and S_j^i . For each positive sample, the hard clause H_l is translated into k clauses. For each negative sample, the CNF translation requires at most $km + 1$ clauses. Let n_{pos} and n_{neg} be the number of positive and negative samples in the training set. Therefore, the number of clauses in the MaxSAT Query Q is $km + n + kn_{pos} + (km + 1)n_{neg} \approx \mathcal{O}(kmn)$ when $n_{pos} = n_{neg} = \frac{n}{2}$.

Example 3.3.1. MaxSAT Encoding.

We illustrate the MaxSAT encoding for a toy example consisting of four samples and two binary features. Our goal is to learn a two clause CNF classifier that can

approximate the training data.

$$\mathbf{D}_{\text{orig}} = \begin{bmatrix} X_1 & X_2 & Y \\ 0 & 0 & 1 \\ 0 & 1 & 0 \\ 1 & 0 & 0 \\ 1 & 1 & 1 \end{bmatrix} \implies \mathbf{D} = \begin{bmatrix} X_1 & \neg X_1 & X_2 & \neg X_2 & Y \\ 0 & 1 & 0 & 1 & 1 \\ 0 & 1 & 1 & 0 & 0 \\ 1 & 0 & 0 & 1 & 0 \\ 1 & 0 & 1 & 0 & 1 \end{bmatrix}$$

In the preprocessing step, we negate the features $\{X_1, X_2\}$ in \mathbf{D}_{orig} and add complemented features $\{\neg X_1, \neg X_2\}$ in \mathbf{D} . In the MaxSAT encoding, we define 8 feature variables (4 features \times 2 clauses in the classifier) and 4 error variables. For example, for feature X_2 , introduced feature variables are $\{B_3^1, B_3^2\}$ and for feature $\neg X_2$, introduced variables are $\{B_4^1, B_4^2\}$. For four samples, error variables are $\{\xi_1, \xi_2, \xi_3, \xi_4\}$. We next show the soft and hard clauses in the MaxSAT encoding

$$\begin{aligned} E_1 &:= (\neg \xi_1); & E_2 &:= (\neg \xi_2); & E_3 &:= (\neg \xi_3); & E_4 &:= (\neg \xi_4) \\ S_1^1 &:= (\neg B_1^1); & S_2^1 &:= (\neg B_2^1); & S_3^1 &:= (\neg B_3^1); & S_4^1 &:= (\neg B_4^1); \\ S_1^2 &:= (\neg B_1^2); & S_2^2 &:= (\neg B_2^2); & S_3^2 &:= (\neg B_3^2); & S_4^2 &:= (\neg B_4^2); \\ H_1 &:= (\neg \xi_1 \rightarrow ((B_2^1 \vee B_4^1) \wedge (B_2^2 \vee B_4^2))); \\ H_2 &:= (\neg \xi_2 \rightarrow (\neg(B_2^1 \vee B_3^1) \vee \neg(B_2^2 \vee B_3^2))); \\ H_3 &:= (\neg \xi_3 \rightarrow (\neg(B_1^1 \vee B_4^1) \vee \neg(B_1^2 \vee B_4^2))); \\ H_4 &:= (\neg \xi_4 \rightarrow ((B_1^1 \vee B_3^1) \wedge (B_1^2 \vee B_3^2))); \end{aligned}$$

In this example, we consider regularizer $\lambda = 0.1$, thereby setting the weight on accuracy as $W(E_i) = 1$ and rule-sparsity weight as $W(S_j^i) = 0.1$. Intuitively, the penalty for misclassifying a sample is 10 times than the penalty for adding a feature in the classifier. For this MaxSAT query, the optimal solution classifies all samples correctly by assigning four feature variables $\{B_1^1, B_4^1, B_2^2, B_3^2\}$ to true. Therefore, by applying Construction 2, the classifier is $(X_1 \vee \neg X_2) \wedge (\neg X_1 \vee X_2)$.⁴

⁴The presented MaxSAT-based formulation does not learn a CNF classifier with both X_i and $\neg X_i$ in the same clause. The reason is that a clause with both X_i and $\neg X_i$ connected by OR (\vee) does not increase accuracy but increases rule size and hence, this is not an optimal classifier.

3.3.3 Learning with Non-binary Features

The presented MaxSAT encoding requires input samples to have binary features. Therefore, we discretize datasets with categorical and continuous features into binary features. For each continuous feature, we apply equal-width discretization that splits the feature into a fixed number of bins. For example, consider a continuous feature $X_c \in [a, b]$. In discretization, we split the domain $[a, b]$ into three bins with two split points $\{a', b'\}$ such that $a < a' < b' < b$. Therefore, the resulting three discretized features are $a \leq X_c < a'$, $a' \leq X_c < b'$, and $b' \leq X_c \leq b$. An alternate to this close-interval discretization is open-interval discretization, where we consider six discretized features with each feature being compared with one threshold. In that case, the discretized features are: $X_c \geq a$, $X_c \geq a'$, $X_c \geq b'$, $X_c < a'$, $X_c < b'$, $X_c \leq b$. Both open-interval and close-interval discretization techniques have their use-cases where one or the other is appropriate. For simplicity, we experiment with close-interval discretization in this chapter.

After applying discretization on continuous features, the dataset contains categorical features only, which we convert to binary features using one-hot encoding [95]. In one-hot encoding, a Boolean vector of features is introduced with cardinality equal to the number of distinct categories. For example, consider a categorical feature having three categories ‘red’, ‘green’, and ‘yellow’. In one hot encoding, samples with category-value ‘red’, ‘green’, and ‘yellow’ would be converted into binary features by taking values 100, 010, and 001, respectively.

3.3.4 Flexible Interpretability Objectives

In interpretable classification rules, we can consider more flexible interpretability objectives than the simplified one in Eq. (3.1). In Eq. (3.1), we prioritize all features equally by providing the same weight to the clause S_j^i for all values of i and j . In practice, users may prefer rules containing certain features. In the MaxSAT formulation, such an extension can be achieved by modifying the weight function and/or the definition of S_j^i . For example, to constrain the classifier to never include a feature, the weight of the clause $S_j^i := \neg B_j^i$ can be set to ∞ . In contrast, to always include a feature, we can define $S_j^i := B_j^i$ with weight ∞ . In both cases, we treat S_j^i as a hard clause.

Another use case may be to learn rules where clauses have disjoint set of features. To this end, we consider a pseudo-Boolean constraint $\sum_{i=1}^k B_j^i \leq 1$, which specifies that the feature X_j appears in at-most one of the k clauses. This constraint may be soft or hard depending on the priority in the application domain. In either case, we convert this constraint to CNF using pseudo-Boolean to CNF translation [141]. Thus, the MaxSAT formulation allows us to consider varied interpretability constraints by only modifying the MaxSAT query without requiring changes in the MaxSAT solving. Therefore, the *separation between modeling and solving* turns out to be the key strength of the presented MaxSAT formulation.

3.4 Incremental Learning of Interpretable Classification Rules

To facilitate a scalable learning, we discuss the key technical contribution of this chapter, IMLI, an incremental learning framework of interpretable classification rules based on MaxSAT. The complexity of the MaxSAT query in Chapter 3.3.2 increases with the number of samples n in the training dataset and the number of clauses k in the CNF classifier. To scale on large n and k , our incremental learning is built on two concepts: (i) mini-batch learning and (ii) iterative learning.

3.4.1 Mini-batch Learning

Our first improvement is to implement a mini-batch learning technique tailored for rule-based classifiers. Mini-batch learning has two-fold advantages. Firstly, instead of solving a large MaxSAT query for the whole training data, this approach solves a sequence of smaller MaxSAT queries derived from mini-batches of smaller size. Secondly, this approach extends to online learning, where the classifier can be updated incrementally with new samples while also generalizing to previously observed samples. In our context of rule-based classifiers, we consider the following heuristic in mini-batch learning.

A Heuristic for Mini-Batch Learning. Let \mathcal{R}' be a classifier learned on the previous batch. In mini-batch learning, we aim to learn a new classifier \mathcal{R} that can generalize to both the current batch and previously seen samples. For that, we

consider a soft constraint such that \mathcal{R} does not *differ much* from \mathcal{R}' while training on the current batch. Thus, we hypothesize that by constraining \mathcal{R} to be syntactically similar to \mathcal{R}' , it is possible to generalize well; because samples in all batches originate from the same distribution⁵. Since our study focuses on rule-based classifiers, we consider the Hamming distance between two classifiers as a notion of their syntactic dissimilarity. In the following, we define the Hamming distance between two CNF classifiers $\mathcal{R}, \mathcal{R}'$ with the same number of clauses as follows.

$$d_H(\mathcal{R}, \mathcal{R}') = \sum_{i=1}^k \left(\sum_{v \in C_i} \mathbb{1}(v \notin C'_i) + \sum_{v \in C'_i} \mathbb{1}(v \notin C_i) \right),$$

where C_i and C'_i are the i^{th} clause in \mathcal{R} and \mathcal{R}' , respectively and $\mathbb{1}$ is an indicator function that returns 1 if the input is true and returns 0 otherwise. Intuitively, $d_H(\mathcal{R}', \mathcal{R})$ calculates the total number of different literals in each (ordered) pair of clauses in \mathcal{R} and \mathcal{R}' . For example, consider $\mathcal{R} = (X_1 \vee X_2) \wedge (\neg X_1)$ and $\mathcal{R}' = (\neg X_1 \vee X_2) \wedge (\neg X_1)$. Then $d_H(\mathcal{R}, \mathcal{R}') = 2 + 0 = 2$, because in the first clause, the literals in $\{X_1, \neg X_1\}$ are absent in either formulas, and the second clause is identical for both \mathcal{R} and \mathcal{R}' . In the following, we discuss a modified objective function for mini-batch learning.

Objective Function. In mini-batch learning, we design an objective function to penalize both classification errors on the current batch and the Hamming distance between new and previous classifiers. Let $\mathbf{D}_b \subset \mathbf{D}$ be the current mini-batch, where $|\mathbf{D}_b| \ll |\mathbf{D}|$. The objective function in mini-batch learning is

$$\min_{\mathcal{R}} |\mathcal{E}_{\mathbf{D}_b}| + \lambda d_H(\mathcal{R}, \mathcal{R}'). \quad (3.5)$$

In the objective function, $\mathcal{E}_{\mathbf{D}_b}$ is the misclassified subset of samples in the current batch \mathbf{D}_b . Unlike controlling the rule-sparsity in the non-incremental approach in the earlier section, in Eq. (3.5), λ *controls the trade-off between classification errors*

⁵We apply Hamming distance heuristics in IMLI with the assumption that the probability distribution of features remains same across batches. One way to account for distribution shifts is to consider last p (> 1) batches instead of the (single) previous batch in the objective function in mini-batch learning. For a feature variable B_j^i , we consider its majority assignment in last p classification rules and encode as a soft clause to retain the majority assignment in the current batch. Moreover, we can reweigh the soft clause by prioritizing assignments of B_j^i in recent batches.

and the syntactic differences between consecutive classifiers. Next, we discuss how to encode the modified objective function as a MaxSAT query.

MaxSAT Encoding of Mini-batch Learning. In order to account for the modified objective function, we only modify the soft clause S_j^i in the MaxSAT query Q . In particular, we define S_j^i to penalize for the complemented assignment of the feature variable B_j^i in \mathcal{R} compared to \mathcal{R}' .

$$S_j^i := \begin{cases} B_j^i & \text{if } X_j \in \text{clause}(\mathcal{R}', i) \\ \neg B_j^i & \text{otherwise} \end{cases}; \quad W(S_j^i) = \lambda$$

S_j^i is either a unit clause B_j^i or $\neg B_j^i$ depending on whether the associated feature X_j appears in the previous classifier \mathcal{R}' or not. In this encoding, the Hamming distance of \mathcal{R} and \mathcal{R}' is minimized while attaining minimum classification errors on the current batch (using soft clause E_l in Eq. (3.2)) To this end, mini-batch learning starts with an empty CNF formula as \mathcal{R}' without any feature, and thus $S_j^i := \neg B_j^i$ for the first batch. We next analyze the complexity of the MaxSAT encoding for mini-batch learning.

Proposition 5. Let $n' \triangleq |\mathbf{D}_b| \ll |\mathbf{D}|$ be the size of a mini-batch, $n'_{neg} \leq n'$ be the number of negative samples in the batch, and m be the number of Boolean features. According to Proposition 3, to learn a k -clause CNF classifier in mini-batch learning, the MaxSAT encoding for each batch has $km + n'$ Boolean variables and kn'_{neg} auxiliary variables. Let $n'_{pos} = n' - n'_{neg}$ be the number of positive samples in the batch. Then, according to Proposition 4, the number of clauses in the MaxSAT query for each batch is $km + n' + kn'_{pos} + (km + 1)n'_{neg} \approx \mathcal{O}(kmn')$ when $n'_{pos} = n'_{neg} = \frac{n'}{2}$.

Assessing the Performance of \mathcal{R} . Since we apply a heuristic objective in mini-batch learning, \mathcal{R} may be optimized for the current batch while generalizing poorly on the full training data. To tackle this, after learning on each batch, we decide whether to keep \mathcal{R} or not by assessing the performance of \mathcal{R} on the training data and keep \mathcal{R} if it achieves higher performance. We measure the performance of \mathcal{R} on the full training data \mathbf{D} using a weighted combination of classification errors and rule size. In particular, we compute a combined loss function $\text{loss}(\mathcal{R}) \triangleq |\mathcal{E}_{\mathbf{D}}| + \lambda|\mathcal{R}|$

on the training data \mathbf{D} , which is indeed the value of the objective function that we minimize in the non-incremental learning in Chapter 3.2. Additionally, we discard the current classifier \mathcal{R} when the loss does not decrease ($\text{loss}(\mathcal{R}) > \text{loss}(\mathcal{R}')$).

We present the algorithm for mini-batch learning in Algorithm 1.

Algorithm 1 MaxSAT-based Mini-batch Learning

```

1: function MINIBATCHLEARNING( $\mathbf{D}, \lambda, k$ )
2:    $\mathcal{R} \leftarrow \bigwedge_{i=1}^k \text{false}$  ▷ Empty CNF formula
3:    $\text{loss}_{\max} \leftarrow \infty$ 
4:   for  $i \leftarrow 1, \dots, N$  do ▷  $N$  is the total batch-count
5:      $\mathbf{D}_b \leftarrow \text{GETBATCH}(\mathbf{D})$ 
6:      $Q, W(\cdot) \leftarrow \text{MAXSATENCODING}(\mathcal{R}, \mathbf{D}_b, \lambda, k)$  ▷ Returns a
       weighted-partial CNF
7:      $\sigma^* \leftarrow \text{MAXSAT}(Q, W(\cdot))$ 
8:      $\mathcal{R}_{\text{new}} \leftarrow \text{CONSTRUCTCLASSIFIER}(\sigma^*)$ 
9:      $\text{loss} \leftarrow |\mathcal{E}_{\mathbf{D}}| + \lambda |\mathcal{R}_{\text{new}}|$  ▷ Compute loss
10:    if  $\text{loss} < \text{loss}_{\max}$  then
11:       $\text{loss}_{\max} \leftarrow \text{loss}$ 
12:       $\mathcal{R} \leftarrow \mathcal{R}_{\text{new}}$ 
13:  return  $\mathcal{R}$ 

```

3.4.2 Iterative Learning

We now discuss an iterative learning algorithm for rule-based classifiers. The major advantage of iterative learning is that we solve a smaller MaxSAT query because of learning a *partial* classifier in each iteration. Our iterative approach is motivated by the set-covering algorithm—also known as separate-and-conquer algorithm—in symbolic rule learning [57]. In this approach, the core idea is to define the *coverage of a partial classifier* (for example, a clause in a CNF classifier). For a specific definition of coverage, this algorithm separates samples covered by the partial classifier and recursively conquers remaining samples in the training data by learning another partial classifier until no sample remains. The final classifier is an aggregation of all partial classifiers—the conjunction of clauses in a CNF formula, for example.

Iterative learning is different from mini-batch learning in several aspects. In mini-batch learning, we learn all clauses in a CNF formula together, while in iterative learning, we learn a single clause of a CNF in each iteration. Additionally, in mini-

batch learning, we improve scalability by reducing the number of samples in the training data using mini-batches, while in iterative learning, we improve scalability by reducing the number of clauses to learn at once. Therefore, an efficient integration of iterative learning and mini-batch learning would benefit scalability from both worlds. In the following, we discuss this integration by first stating iterative learning for CNF classifiers.

In iterative learning, we learn one clause of a CNF classifier in each iteration, where the clause refers to a partial classifier. The coverage of a clause in a CNF formula is the set of samples that *do not satisfy* the clause. The reason is that if a sample does not satisfy at least one clause in a CNF formula, the prediction of the sample by the full formula is class 0, because CNF is a conjunction of clauses. As a result, considering covered samples in the next iteration does not change their prediction regardless of whatever clause we learn in later iterations. To this end, a single clause learning can be performed efficiently by applying mini-batch learning discussed before. In Algorithm 2, we provide an algorithm for learning a CNF classifier iteratively by leveraging mini-batch learning. This algorithm is a double-loop algorithm, where in the outer loop we apply iterative learning and in the inner loop, we apply mini-batch learning.

Algorithm 2 Iterative CNF Classifier Learning

```

1: procedure ITERATIVECNFLEARNING( $\mathbf{X}, \mathbf{y}, \lambda, k$ )
2:    $\mathcal{R} \leftarrow \text{true}$  ▷ Initial formula
3:   for  $i \leftarrow 1, \dots, k$  and  $\mathbf{D} \neq \emptyset$  do
4:      $C_i \leftarrow \text{MINIBATCHLEARNING}(\mathbf{D}, \lambda, 1)$  ▷ Single clause learning,  $k = 1$ 
5:      $\mathbf{D}' \leftarrow \text{COVERAGE}(\mathbf{D}, C_i)$ 
6:     if  $\mathbf{D}' = \emptyset$  then ▷ Terminating conditions
7:       break
8:      $\mathcal{R} \leftarrow \mathcal{R} \wedge C_i$ 
9:      $\mathbf{D} \leftarrow \mathbf{D} \setminus \mathbf{D}'$  ▷ Removing covered samples
10:  return  $\mathcal{R}$ 

```

Terminating conditions. In Algorithm 2, we terminate iterative learning based on three conditions: (i) when \mathcal{R} contains all k clauses, (ii) the training data \mathbf{D} is empty (that is, no sample remains uncovered), and (iii) no new sample is covered by the current partial classifier. Since the first two conditions are trivial, we elaborate

on the third condition. When clause C_i cannot cover any new sample from the training dataset \mathbf{D} , the next iteration will result in the same clause C_i because the training data remains the same. In this case, we do not include clause C_i to classifier \mathcal{R} because of zero coverage.

3.5 Learning Other Interpretable Classifiers

In earlier sections, we discuss the learning of CNF classifiers using IMLI. IMLI can also be applied to learning other interpretable rule-based representations. In this section, we discuss how IMLI can be applied in learning DNF classifiers, decision lists, and decision sets.

3.5.1 Learning DNF classifiers

For learning DNF classifiers, we leverage De Morgan’s law where complementing a CNF formula results in a DNF formula. To learn a DNF classifier, say $\mathcal{R}'(\mathbf{X})$, we can trivially show that $Y = \mathcal{R}'(\mathbf{X}) \leftrightarrow \neg(Y = \neg\mathcal{R}'(\mathbf{X}))$ for the feature vector \mathbf{X} . Here $\neg\mathcal{R}'(\mathbf{X})$ is a CNF formula, by definition. Thus, we learn a DNF classifier by first complementing the class-label $y^{(i)}$ to $\neg y^{(i)}$ for each sample in the training dataset $\{(\mathbf{x}^{(i)}, y^{(i)})\}_{i=1}^n$, learning a CNF classifier on $\{(\mathbf{x}^{(i)}, \neg y^{(i)})\}_{i=1}^n$, and finally complementing the learned classifier to DNF. For example, the CNF classifier “(Male \vee Age $<$ 50) \wedge (Education = Graduate \vee Income \geq 1500)” is complemented to a DNF classifier as “(not Male \wedge Age \geq 50) \vee (Education \neq Graduate \wedge Income \leq 1500)”.

To learn a DNF classifier incrementally, such as through mini-batch and iterative learning, we adopt the following procedure. For learning a DNF classifier using mini-batch learning, we first learn a CNF classifier on dataset $\{(\mathbf{x}^{(i)}, \neg y^{(i)})\}_{i=1}^n$ and complement the classifier to a DNF classifier at the end of mini-batch learning. To learn a DNF classifier in the iterative approach, we learn a single clause of the DNF classifier in each iteration, remove covered samples, and continue till no training sample remains. In this context, the coverage of a clause in a DNF formula is the set of samples satisfying the clause.

3.5.2 Learning Decision Lists

In IMLI, we apply an iterative learning approach for efficiently learning a decision list. A decision list \mathcal{R}_L is a list of pairs $(C_1, V_1), \dots, (C_k, V_k)$, where we learn one pair in each iteration. We note that the clause C_i is a conjunction of literals—equivalently, a single clause DNF formula. Hence, our task is to deploy IMLI to efficiently learn a single clause DNF formula C_i . In particular, we opt to learn this clause for the majority class, say V_i , in the training dataset by setting the majority samples as class 1 and all other samples as class 0. As a result, even if the MaxSAT-based learning, presented in this chapter, is targeted for binary classification, we can learn a multi-class decision list in IMLI.

In Algorithm 3, we present the iterative algorithm for learning decision lists. In each iteration, the algorithm learns a pair (C_i, V_i) , separates the training set based on the coverage of (C_i, V_i) and conquers the remaining samples recursively. The coverage of (C_i, V_i) is the set of samples that satisfies clause C_i . Finally, we add a default rule $(C_k, V_{\text{default}})$ to \mathcal{R}_L where $C_k \triangleq \text{true}$ denoting that the clause is satisfied by all samples. We select the default class V_{default} in the following order: (i) if any class(s) is not in the predicted classes $\{V_i\}_{i=1}^{k-1}$ of the decision list, V_{default} is the majority class among missing classes, and (ii) V_{default} is the majority class of the original training set \mathbf{D} , otherwise.

Algorithm 3 Iterative Learning of Decision Lists

```

1: procedure DECISIONLISTLEARNING( $\mathbf{D}, \lambda, k$ )
2:    $\mathcal{R}_L \leftarrow \{\}$ 
3:   for  $i \leftarrow 1, \dots, k - 1$  and  $\mathbf{D} \neq \emptyset$  do
4:      $V_i \leftarrow \text{MAJORITYCLASS}(\{y^{(i)}\}_{i=1}^{|\mathbf{D}|})$   $\triangleright V_i$  specifies the target class given
      class label
5:      $C_i \leftarrow \text{MINIBATCHDNFLEARNING}(\mathbf{D}, \lambda, 1, V_i)$   $\triangleright$  Ref. Chapter 3.5.1
6:      $\mathbf{D}' \leftarrow \text{COVERAGE}(\mathbf{D}, C_i)$ 
7:     if  $\mathbf{D}' = \emptyset$  then
8:       break
9:      $\mathcal{R}_L \leftarrow \mathcal{R}_L \cup \{(C_i, V_i)\}$ 
10:     $\mathbf{D} \leftarrow \mathbf{D} \setminus \mathbf{D}'$ 
11:     $\mathcal{R}_L \leftarrow \mathcal{R}_L \cup \{(\text{true}, V_{\text{default}})\}$   $\triangleright$  Default rule
12:  return  $\mathcal{R}_L$ 

```

3.5.3 Learning Decision Sets

We now describe an iterative procedure for learning decision sets. A decision set comprises of an individual clause-class pair (C_i, V_i) where C_i denotes a single clause DNF formula similar to decision lists. In a decision set, a sample can satisfy multiple clauses simultaneously, which is attributed as an *overlapping between clauses* [93]. Concretely, the overlap between two clauses C_i and C_j with $i \neq j$ is the set of samples $\{\mathbf{x} | \mathbf{x} \models C_i \wedge \mathbf{x} \models C_j\}$ satisfying both clauses. One additional objective in learning a decision set is to minimize the overlap between clauses, as studied in [93]. Therefore, along with optimizing accuracy and rule-sparsity, we discuss an iterative procedure for decision sets that additionally minimizes the overlap between clauses.

Algorithm 4 Iterative Learning of Decision Sets

```

1: procedure DECISIONSETSLearning( $\mathbf{D}, \lambda, k$ )
2:    $\mathcal{R}_S = \{\}$ 
3:    $\mathbf{D}_{cc} = \{\}$  ▷ Contains correctly covered samples
4:   for  $i \leftarrow 1, \dots, k - 1$  and  $\mathbf{D} \neq \emptyset$  do
5:      $V_i \leftarrow \text{MAJORITYCLASS}(\{y^{(i)}\}_{i=1}^{|\mathbf{D}|})$ 
6:      $\mathbf{D}_w = \mathbf{D} \cup \{(\mathbf{x}, \neg V_i) | (\mathbf{x}, y) \in \mathbf{D}_{cc}\}$  ▷ Appending covered samples with
       complemented class
7:      $C_i \leftarrow \text{MINIBATCHDNFLearning}(\mathbf{D}_w, \lambda, 1, V_i)$ 
8:      $\mathbf{D}' \leftarrow \text{CORRECTCOVERAGE}(\mathbf{D}, C_i, V_i)$ 
9:     if  $(\mathbf{D}' = \emptyset)$  then
10:       break
11:      $\mathcal{R}_S \leftarrow \mathcal{R}_S \cup \{(C_i, V_i)\}$ 
12:      $\mathbf{D} \leftarrow \mathbf{D} \setminus \mathbf{D}'$ 
13:      $\mathbf{D}_{cc} = \mathbf{D}_{cc} \cup \mathbf{D}'$ 
14:    $\mathcal{R}_S \leftarrow \mathcal{R}_S \cup \{(\text{true}, V_{\text{default}})\}$ 
15:   return  $\mathcal{R}_S$ 

```

In Algorithm 4, we present an iterative algorithm for learning a decision set. The iterative algorithm is a modification of separate-and-conquer algorithm by additionally focusing on minimizing overlaps in a decision set. Given a training data $\mathbf{D} = \{(\mathbf{x}^{(i)}, y^{(i)})\}_{i=1}^n$, a regularization parameter λ , and the number of clauses k , the core idea of Algorithm 4 is to learn a pair (C_i, V_i) in each iteration, separate covered samples from \mathbf{D} , and conquer remaining samples recursively. In contrast to learning decision lists, we have following modifications in Algorithm 4.

- The first modification is with respect to the definition of coverage for decision

sets. Unlike decision lists, we separate samples that are *correctly covered* by (C_i, V_i) in each iteration. Given a dataset $\mathbf{D} = \{(\mathbf{x}^{(l)}, y^{(l)})\}$, the correctly covered samples of (C_i, V_i) is a dataset $\mathbf{D}_{cc} = \{(\mathbf{x}^{(l)}, y^{(l)}) \mid \mathbf{x}^{(l)} \models C_i \wedge y^{(l)} = V_i\}_{l=1}^{|\mathbf{D}|} \subseteq \mathbf{D}$ of samples that satisfy C_i and have matching class-label as V_i .

- The second modification is related to the training dataset considered in each iteration. Let \mathbf{D} denote *the remaining training dataset* in the current iteration and V_i be the majority class in \mathbf{D} . Hence, V_i is the target class in the current iteration. Also, let \mathbf{D}_{cc} denotes the set of samples *correctly covered in all previous iterations*. In Algorithm 4, we learn the current rule C_i on the working dataset $\mathbf{D}_w = \mathbf{D} \cup \{(\mathbf{x}, \neg V_i) \mid (\mathbf{x}, y) \in \mathbf{D}_{cc}\}$. Thus, \mathbf{D}_w is constructed by joining the remaining training samples with correctly covered samples in \mathbf{D}_{cc} with complemented class label to the target class V_i . Thus, by explicitly labeling covered samples as class $\neg V_i$, the new clause C_i learns to falsify already covered samples. This heuristic allows us to minimize the overlap of C_i compared to previously learned clauses $\{C_j\}_{j=1}^{i-1}$.

Finally, the default clause for decision sets is learned similarly as in decision lists.

3.6 Empirical Performance Analysis

In this section, we empirically evaluate the performance of IMLI. We first present the experimental setup and the objective of the experiments, followed by experimental results.

3.6.1 Experimental Setup

We implement a prototype of IMLI in Python to evaluate the performance of the MaxSAT-based formulation for learning classification rules. To implement IMLI, we deploy a state-of-the-art MaxSAT solver Open-WBO [119], which returns the current best solution upon reaching a timeout.

We compare IMLI with state-of-the-art interpretable and non-interpretable classifiers. Among interpretable classifiers, we compare with RIPPER [38], BRL [101], CORELS [6], and BRS [188]. Among non-interpretable classifiers, we compare with Random Forest (RF), Support Vector Machine with linear kernels (SVM), Logistic

Regression classifier (LR), and k-Nearest Neighbors classifier (kNN). We deploy the Scikit-learn library in Python for implementing non-interpretable classifiers.

We experiment with real-world binary classification datasets from UCI [46], Open-ML [181], and Kaggle repository (<https://www.kaggle.com/datasets>), as listed in Table 3.1. In these datasets, the number of samples vary from about 200 to 1,000,000. The datasets contain both real-valued and categorical features. We process them to binary features by setting the maximum number of bins as 10 during discretization. For non-interpretable classifiers such as RF, SVM, LR, and kNN that take real-valued features as inputs, we only convert categorical features to one-hot encoded binary features.

We perform ten-fold cross-validation on each dataset and evaluate the performance of different classifiers based on the median prediction accuracy on the test data. Additionally, we compare the median size of generated rules among rule-based interpretable classifiers. We consider a comparable combination (100) of hyper-parameters choices for all classifiers, that we fine-tune during cross-validation. For IMLI, we vary the number of clauses $k \in \{1, 2, \dots, 5\}$ and the regularization parameter λ in a logarithmic grid by choosing 5 values between 10^{-4} and 10^1 . For mini-batch learning in IMLI, we set the number of samples in each mini-batch, $n' \in \{50, 100, 200, 400\}$. Thus, we consider $\lceil n/n' \rceil$ mini-batches, where n denotes the size of training data. To construct mini-batches from a training dataset, we sequentially split the data into $\lceil n/n' \rceil$ batches with each batch having n' samples. Furthermore, to ignore the effect of batch-ordering, we perform mini-batch learning in two rounds such that each batch participates twice in the training.

For BRL algorithm, we vary four hyper-parameters: the maximum cardinality of rules in $\{2, 3, 4\}$, the minimum support of rules in $\{0.05, 0.175, 0.3\}$, and the prior on the expected length and width of rules in $\{2, 4, 6, 8\}$ and $\{2, 5, 8\}$, respectively. For CORELS algorithm, we vary three hyper-parameters: the maximum cardinality of rules in $\{2, , 5\}$, the minimum support of rules in $\{0.01, 0.17, 0.33, 0.5\}$, and the regularization parameter in $\{0.005, 0.01, 0.015, 0.02, 0.025, 0.03\}$. For BRS algorithm, we vary three hyper-parameters: the maximum length of rules in $\{1, 2, 3, 4\}$, the number of initial rules in $\{500, 1000, 1500, 2000, 2500, 3000\}$, and the minimum support of rules in $\{1, 4, 7, 10\}$. For RF and RIPPER classifiers, we vary the cut-off on the number of samples in the leaf node using a linear grid between 3 to 500 and

1 to 300, respectively. For SVM and LR classifiers, we discretize the regularization parameter on a logarithmic grid between 10^{-3} and 10^3 . For kNN, we vary the number of neighbors in a linear grid between 1 and 500. We conduct each experiment on an Intel Xeon E7 – 8857 v2 CPU using a single core with 16 GB of RAM running on a 64bit Linux distribution based on Debian. For all classifiers, we set the training timeout to 1000 seconds.

Objectives of Experiments. In the following, we present the objectives of our experimental study.

1. How are the accuracy and size of classification rules generated by IMLI compared to existing interpretable classifiers?
2. How is the scalability of IMLI in solving large-scale classification problems compared to existing interpretable classifiers?
3. How does IMLI perform in terms of accuracy and scalability compared to classifiers that are non-interpretable?
4. How does the incremental learning in IMLI perform compared to non-incremental MaxSAT-based learning in terms of accuracy, rule-sparsity, and scalability?
5. How do different interpretable classification rules learned using IMLI perform in terms of accuracy and rule size?
6. What are the effects of different hyper-parameters in IMLI?

Summary of Experimental Results. To summarize our experimental results, IMLI achieves the best balance among prediction accuracy, interpretability, and scalability compared to existing interpretable rule-based classifiers. Particularly, compared to the most accurate classifier RIPPER, IMLI demonstrates on average 1% lower prediction accuracy, wherein the accuracy of IMLI is higher than BRL, CORELS, and BRS in almost all datasets. In contrast, IMLI generates significantly smaller rules than RIPPER, specifically in large datasets. Moreover, BRL, CORELS, and BRS report comparatively smaller rule size than IMLI on average, but with a significant decrease in accuracy. In terms of scalability, IMLI achieves the best

performance compared to other interpretable and non-interpretable classifiers by classifying datasets with one million samples. While CORELS also scales to such large datasets, its accuracy is lower than that of IMLI by at least 2% on average. Therefore, IMLI is not only scalable but also accurate in practical classification problems while also being interpretable by design. We additionally analyze the comparative performance of different formulations presented in this chapter, where the incremental approach empirically proves its efficiency than the naïve MaxSAT formulation. Furthermore, we learn and compare the performance of different interpretable representations: decision lists, decision sets, CNF, and DNF formulas using IMLI and present the efficacy of IMLI in learning varied interpretable classifiers. Finally, we study the effect of different hyper-parameters in IMLI, where each hyper-parameter provides a precise control among training time, prediction accuracy, and rule-sparsity. In the following, we discuss our experimental results in detail.

3.6.2 Experimental Results

Comparing IMLI with interpretable classifiers. We compare IMLI with existing interpretable classifiers in three aspects: test accuracy, rule size, and scalability.

Test accuracy and rule size. We present the experimental results of test accuracy and rule size among interpretable classifiers in Table 3.1, where the first, second, and third columns represent the name of the dataset, the number of samples, and the number of features in the dataset, respectively. In each cell from the fourth to the eighth column in the table, the top value represents the median test accuracy and the bottom value represents the median size of rules measured through ten-fold cross-validation.

In Table 3.1, IMLI and CORELS generate interpretable classification rules in all 15 datasets in our experiments. In contrast, within a timeout of 1000 seconds, RIPPER, BRL, and BRS fail to generate any classification rule in three datasets, specifically in large datasets ($\geq 200,000$ samples).

We now compare IMLI with each interpretable classifier in detail. Compared to RIPPER, IMLI has lower accuracy in 9 out of 12 datasets. More specifically, the accuracy of IMLI is 1% lower on average than RIPPER. The improved accuracy of RIPPER, however, results in the generation of higher size classification rules than

Table 3.1: Comparison of accuracy and rule size among interpretable classifiers. Each cell from the fourth to the eighth column contains test accuracy (top) and rule size (bottom). ‘—’ represents a timeout. Numbers in bold represent the best performing results among different classifiers.

Dataset	Size	Features	RIPPER	BRL	CORELS	BRS	IMLI
Parkinsons	195	202	94.44	94.74	89.74	84.61	94.74
			7.0	11.5	2.0	5.0	7.5
WDBC	569	278	98.08	93.81	92.04	92.98	94.74
			13.0	22.0	2.0	7.0	11.5
Pima	768	83	77.14	68.18	75.32	75.32	78.43
			6.0	13.5	2.0	3.0	23.0
Titanic	1,043	38	78.72	62.98	81.9	80.86	81.82
			6.0	15.0	4.0	4.0	5.5
MAGIC	19,020	100	82.68	76.95	78.05	77.5	78.26
			102.0	81.0	4.0	3.0	8.5
Tom’s HW	28,179	946	85.91	—	83.27	83.13	85.24
			30.0	—	4.0	18.5	44.5
Credit	30,000	199	82.39	46.12	81.18	80.45	82.12
			32.5	26.5	2.0	7.0	17.5
Adult	32,561	94	84.37	72.08	79.78	70.75	81.2
			115.5	46.5	4.0	4.0	30.0
Bank Marketing	45,211	82	90.01	84.66	89.62	86.75	89.84
			36.5	13.0	2.0	2.0	24.5
Connect-4	67,557	126	76.72	65.83	68.68	70.49	75.36
			118.0	18.5	4.0	11.0	50.5
Weather AUS	107,696	169	84.22	43.26	83.67	—	83.78
			26.0	22.0	2.0	—	22.0
Vote	131,072	16	97.12	94.78	95.86	95.14	96.69
			132.0	41.5	3.5	1.0	15.0
Skin Seg	245,057	30	—	79.25	91.62	68.48	94.71
			—	6.0	9.0	5.0	30.0
BNG(labor)	1,000,000	89	—	—	88.56	—	90.91
			—	—	2.0	—	24.0
BNG(credit-g)	1,000,000	97	—	—	72.08	—	75.48
			—	—	2.0	—	27.5

IMLI in most datasets. In particular, IMLI generates sparser rules than RIPPER in 9 out of 12 datasets, wherein RIPPER times out in 3 datasets. Interestingly, the difference in rule size is more significant in larger datasets, such as in ‘Vote’ dataset, where RIPPER learns a classifier with 132 Boolean literals compared to 15 Boolean literals by IMLI. Therefore, IMLI is better than RIPPER in terms of rule-sparsity, but lags slightly in accuracy.

IMLI performs better than BRL both in terms of accuracy and rule-sparsity. In particular, IMLI has higher accuracy and lower rule size than BRL in 12 and 8 datasets, respectively, in a total of 12 datasets, wherein BRL times out in 3 datasets. While comparing with CORELS, IMLI achieves higher accuracy in almost all datasets (14 out of 15 datasets). A similar trend is observed in comparison with BRS, where IMLI achieves higher accuracy in all of 12 datasets and BRS times out in 3 datasets. CORELS and BRS, however, generates sparser rules than IMLI in most datasets, but by costing a significant decrease in accuracy. For example, in the largest dataset ‘BNG(credit-g)’ with 1 Million samples, BRS times out and CORELS generates a classifier with 72.08% accuracy with rule size 2. IMLI, in contrast, learns a classifier with 27.5 Boolean literals achieving 75.48% accuracy, which is 3% higher than CORELS. Therefore, IMLI makes a good balance between accuracy and rule size compared to existing interpretable classifiers while also being highly scalable. In the following, we discuss the results on the scalability of all interpretable classifiers in detail.

Scalability. We analyze the scalability among interpretable classifiers by comparing their training time. In Figure 3.1, we use cactus plots⁶ to represent the training time (in seconds) of all classifiers in 1000 instances (10 folds \times 100 choices of hyper-parameters) derived for each dataset. In the cactus plot, the number of solved instances (within 1000 seconds) is on the X -axis, whereas the training time is on the Y -axis. A point (x, y) on the plot implies that a classifier yields lower than or equal to y seconds of training in x many instances.

In Figure 3.1, we present results in an increasing number of samples in a dataset (from left to right). In WDBC and Adult datasets presented on the first two plots in Figure 3.1, CORELS solves lower than 600 instances within a timeout of 1000

⁶Cactus plots are often used in (Max)SAT community to present the scalability of different solvers/methods [9, 11].

seconds. The scalability performance of BRS is even worse, where it solves around 700 and 200 instances in WDBC and Adult datasets, respectively. The other three classifiers: IMLI, BRL, and RIPPER solve all 1000 instances, where BRL takes comparatively higher training time than the other two. The performance of IMLI and RIPPER is similar, with RIPPER being comparatively better in the two datasets. However, the efficiency of IMLI compared to other classifiers becomes significant as the number of samples in a dataset increases. In particular, in ‘Weather AUS’ dataset, BRS cannot solve a single instance, BRL and CORELS solves 400 instances, and RIPPER solves around 600 instances. IMLI, however, solves all 1000 instances in this dataset. Similarly, in ‘BNG(labor)’ dataset, all other classifiers except IMLI and CORELS cannot solve any instance. While IMLI mostly takes the maximum allowable time (1000 seconds) in solving all instances in this dataset, CORELS can solve lower than 400 instances. The improved performance of IMLI is due to incremental learning based on the novel integration of iterative learning and mini-batch learning. Contrary to our incremental learning, earlier approaches are based on heuristic rule-pruning (e.g., RIPPER) and rule-mining followed by Bayesian optimization (e.g., BRL, BRS) and branch and bounds algorithms (e.g., CORELS). Thus, owing to incremental learning, IMLI establishes itself as the most scalable classifier compared to other state-of-the-art interpretable classifiers.

Comparison with non-interpretable classifiers. We compare IMLI with state of the art non-interpretable classifiers such as LR, SVM, kNN, and RF in terms of their median test accuracy in Table 3.2. In the majority of the datasets, IMLI achieves comparatively lower test accuracy than the best performing non-interpretable classifier. The decrease in the test accuracy of IMLI is attributed to two factors. Firstly, while we train IMLI on discretized data, non-interpretable classifiers are trained on non-discretized data and thus IMLI incurs additional classification errors due to discretization. Secondly, IMLI learns a rule-based classifier, whereas non-interpretable classifiers can learn more flexible decision boundaries and thus fit data well. In Table 3.2, we also observe that IMLI achieves impressive scalability than competing classifiers by solving datasets with 1,000,000 samples where most of the non-interpretable classifiers fail to learn any decision boundary on such large datasets. Thus, IMLI, being an interpretable classifier, demonstrates lower accuracy

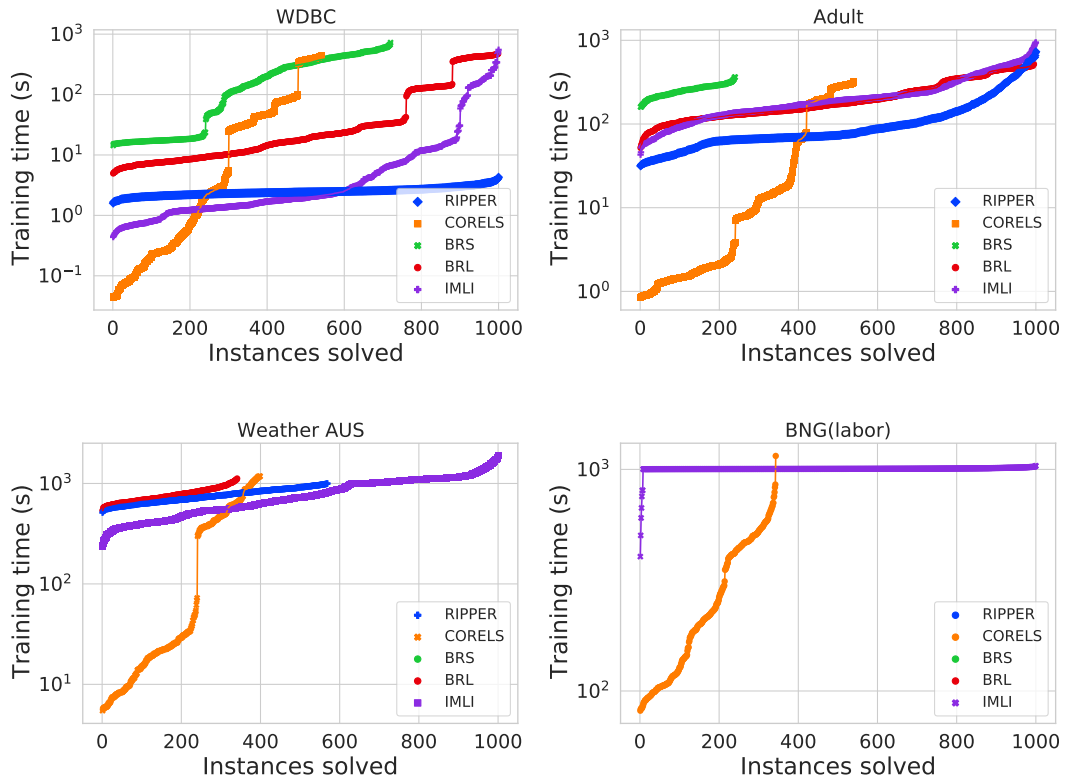


Figure 3.1: Comparison of scalability among interpretable classifiers. The plots are arranged in increasing sizes of datasets (from left to right). In each cactus plot, IMLI solves all 1000 instances for each dataset, while competitive classifiers often fail to scale, specially in larger datasets.

than competing non-interpretable classifiers, but higher scalability in practice.

Comparison among different formulations in IMLI. We compare the performance of different formulations for learning classification rules as presented in this chapter. In Figure 3.2, we show cactus plots for assessing training time (in seconds), test error (in percentage), and rule size among different formulations. In the cactus plot, a point (x, y) denotes that the formulation yields lower than or equal to y training time (similarly, test error and rule size) in x many instances in each dataset.

In Figure 3.2, we denote the baseline non-incremental MaxSAT-based formulation as IMLI-B⁷, incremental MaxSAT-based formulation with only mini-batch learning as IMLI-M, and incremental MaxSAT-based formulation with both mini-batch and

⁷Since IMLI-B is a non-incremental formulation and does not involve any mini-batch learning, we consider two hyper-parameters for IMLI-B: the number of clauses in $\{1, 2, \dots, 10\}$ and the regularization parameter λ as 10 values chosen from a logarithmic grid between 10^{-4} and 10^1 .

Table 3.2: Comparison of IMLI with non-interpretable classifiers in terms of test accuracy. In the table, ‘—’ represents a timeout. Numbers in bold represent the best performing results among different classifiers.

Dataset	Size	LR	SVM	kNN	RF	IMLI
Parkinsons	195	89.74	89.74	97.5	90.0	94.74
WDBC	569	98.25	98.25	98.23	96.49	94.74
Pima	768	78.43	79.08	74.5	79.22	78.43
Titanic	1,043	80.86	80.38	81.34	82.69	81.82
MAGIC	19,020	79.18	79.34	84.6	88.2	78.26
Tom’s HW	28,179	96.2	97.13	88.15	97.78	85.24
Credit	30,000	82.2	81.9	81.83	82.15	82.12
Adult	32,561	85.26	85.05	83.8	86.69	81.2
Bank Marketing	45,211	90.09	89.28	89.43	90.27	89.84
Connect-4	67,557	79.39	—	85.51	88.11	75.36
Weather AUS	107,696	85.64	—	78.59	86.26	83.78
Vote	131,072	96.43	96.37	97.05	97.38	96.69
Skin Seg	245,057	91.86	—	99.96	99.96	94.71
BNG(labor)	1,000,000	—	—	—	—	90.91
BNG(credit-g)	1,000,000	—	—	—	80.58	75.48

iterative learning as IMLI. We first observe the training time of different formulations in the left-most column in Figure 3.2, where IMLI-B soon times out and solves lower than 300 instances out of 1000 instances in each dataset. This result suggests that the non-incremental formulation cannot scale in practical classification task. Comparing between IMLI and IMLI-M, both formulations solve all 1000 instances in each dataset with IMLI-M undertaking significantly higher training time than IMLI. Therefore, IMLI achieves better scalability than IMLI-M indicating that an integration of mini-batch and iterative learning achieves a significant progress in terms of scalability than mini-batch learning alone.

We next focus on the test error of different formulations in the middle column in Figure 3.2. Firstly, IMLI-B has a higher test error than the other two formulations since IMLI-B times out in most instances and learns a sub-optimal classification rule with reduced prediction accuracy. In contrast, IMLI has the lowest test error compared to two formulations in all datasets. This result indicates the effectiveness of integrating both iterative and mini-batch learning with MaxSAT-based formulation in generating more accurate classification rules.

Moving focus on the rule size in the rightmost column in Figure 3.2, IMLI-B

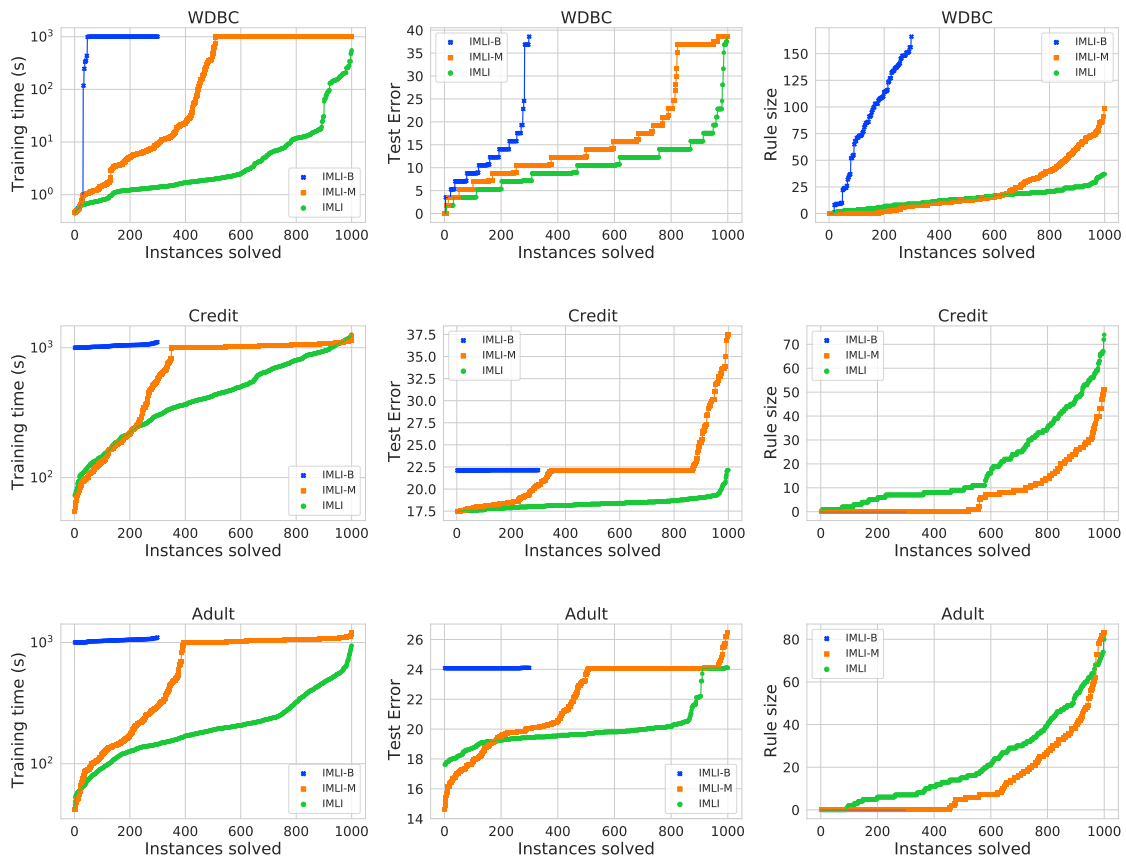


Figure 3.2: Comparison of training time, test error, and rule size among different formulations presented in the chapter. In each cactus plot, the incremental formulation IMLI with both mini-batch and iterative learning demonstrates the best performance in training time and test error than compared two formulations: non-incremental MaxSAT formulation IMLI-B and incremental formulation with only mini-batch learning IMLI-M. In terms of rule size, IMLI often generates higher size rules than IMLI-M.

achieves the highest rule size in WDBC dataset. In contrast, the rule size of IMLI-B is lowest (zero) in Credit and Adult datasets. In the last two datasets, IMLI-B times out during training and returns the default rule “true” by predicting all samples as class 1. The other two formulations IMLI and IMLI-M demonstrate a similar trend in rule size in all datasets with IMLI-M generating comparatively smaller size rules in Credit and Adult datasets. In this context, the improvement of rule-sparsity of IMLI-M is due to a comparatively higher test error (or lower accuracy) than IMLI as observed in all three datasets. Therefore, IMLI appears to be the best performing formulation w.r.t. training time, test error, and rule size by balancing between

Table 3.3: Comparison of test accuracy (top value) and rule size (bottom value) among different rule-based representations learned using IMLI. Numbers in bold denote the best performing results among different representations.

Dataset	CNF	DNF	Decision Sets	Decision Lists
Parkinsons	94.74	89.47	94.87	89.74
	7.5	6.0	15.0	6.5
WDBC	94.74	96.49	95.61	95.61
	11.5	15.0	15.5	10.0
Pima	78.43	77.13	76.97	76.97
	23.0	9.0	15.0	13.5
Titanic	81.82	82.29	81.82	82.3
	5.5	10.5	8.5	8.0
MAGIC	78.26	77.44	75.87	77.79
	8.5	41.5	10.0	14.0
Tom’s HW	85.24	85.15	85.72	85.95
	44.5	26.5	45.0	59.5
Credit	82.12	82.15	82.03	82.22
	17.5	14.0	9.5	21.5
Adult	81.2	84.28	80.07	80.96
	30.0	34.5	7.0	24.5
Bank Marketing	89.84	89.77	89.67	89.79
	24.5	7.5	6.0	10.5
Connect-4	75.36	70.63	68.09	69.83
	50.5	42.0	4.5	24.0
Weather AUS	83.78	84.23	83.69	83.85
	22.0	14.0	4.0	26.0
Skin Seg	94.71	93.68	87.92	91.17
	30.0	15.0	3.0	7.0

accuracy and rule size while being more scalable.

Performance evaluation of different interpretable representations in IMLI.

We deploy IMLI to learn different interpretable rule-based representations: CNF and DNF classifiers, decision lists, and decision sets and present their comparative performance w.r.t. test accuracy and rule size in Table 3.3. In each cell in this table, the top value represents the test accuracy and the bottom value represents the size of generated rules.

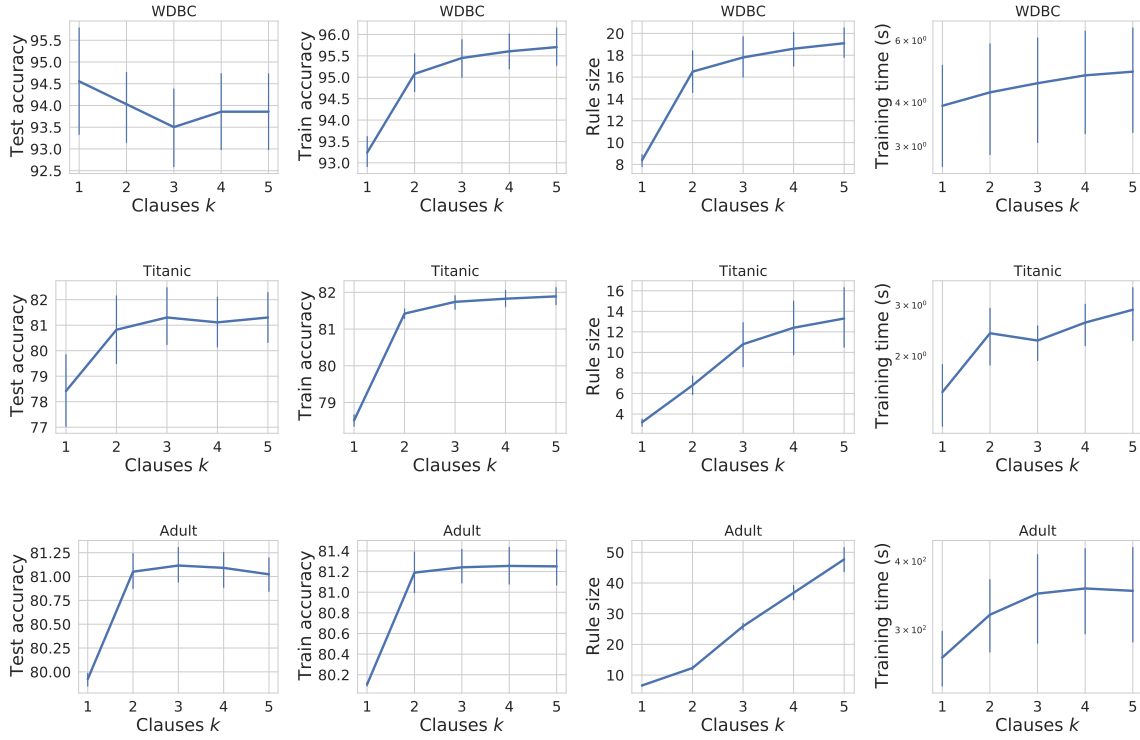


Figure 3.3: Effect of the number of clauses k on accuracy (test and train), rule size, and training time. As k increases, both train and test accuracy of IMLI increase while generating rules with higher size by incurring higher training time.

We learn all four interpretable representations on twelve datasets, where the CNF classifier appears to be the most accurate representation by achieving the highest accuracy in five datasets. In contrast, both DNF and decision lists achieve the highest accuracy in three datasets each; decision sets demonstrate the least performance in test accuracy by being more accurate in one dataset. To this end, the poor accuracy of decision sets is traded off by its rule size as decision sets generate the sparsest rules compared to other representations. More precisely, decision sets have the smallest rule size in six datasets, while CNF, DNF, and decision lists have the smallest rule size in two, three, and one dataset, respectively. These results suggest that CNF classifiers are more favored in applications where higher accuracy is preferred, while decision sets are preferred in applications where higher interpretability is desired. In both cases, one could deploy IMLI for learning varied representations of classification rules.

Ablation study. We experiment the effect of different hyper-parameters in IMLI on prediction accuracy, rule size, and training time in different datasets. In the following, we discuss the impact of the number of clauses, regularization parameter, and size of mini-batches in IMLI.

Effect of the number of clauses k . In Figure 3.3, we vary k while learning CNF classifiers in IMLI. As k increases, both training and test accuracy generally increase in different datasets (plots in the first and second columns). Similarly, the size of rules increases with k by incurring higher training time (plots in the third and fourth columns). The reason is that a higher value of k allows more flexibility in fitting the data well by incurring more training time and generating higher size classification rules. Therefore, the number of clauses in IMLI provides control on training-time vs accuracy and also on accuracy vs rule-sparsity.

Effect of regularizer λ . In Figure 3.4, we vary λ in a logarithmic grid between 10^{-4} and 10^1 . As stated in Eq. (3.5), a higher value of λ puts more priority on the minimal changes in rules between consecutive mini-batches in incremental learning while allowing higher mini-batch errors. Thus, in the first and second columns in Figure 3.4, as λ increases, both training and test accuracy gradually decrease. In addition, the size of rules (plots in the third column) also decreases. Finally, we observe that the training time generally decreases with λ . This observation indicates that higher λ puts lower computational load to the MaxSAT solver as a fraction of training examples is allowed to be misclassified. Thus, similar to the number of clauses, regularization parameter λ in IMLI allows to trade-off between accuracy and rule size in a precise manner.

Effect of the size of mini-batch. In Figure 3.5, we present the effect of mini-batch size in IMLI. As we consider more samples in a batch, both test and training accuracy increase in general as presented in the first and second columns in Figure 3.5. Similarly, the size of generated rules also increases with the number of samples. Due to solving higher size MaxSAT queries, the training time also increases in general with an increase in mini-batch size. Therefore, by varying the size of mini-batches, IMLI allows controlling on training time vs the prediction accuracy (and rule size) of generated rules.

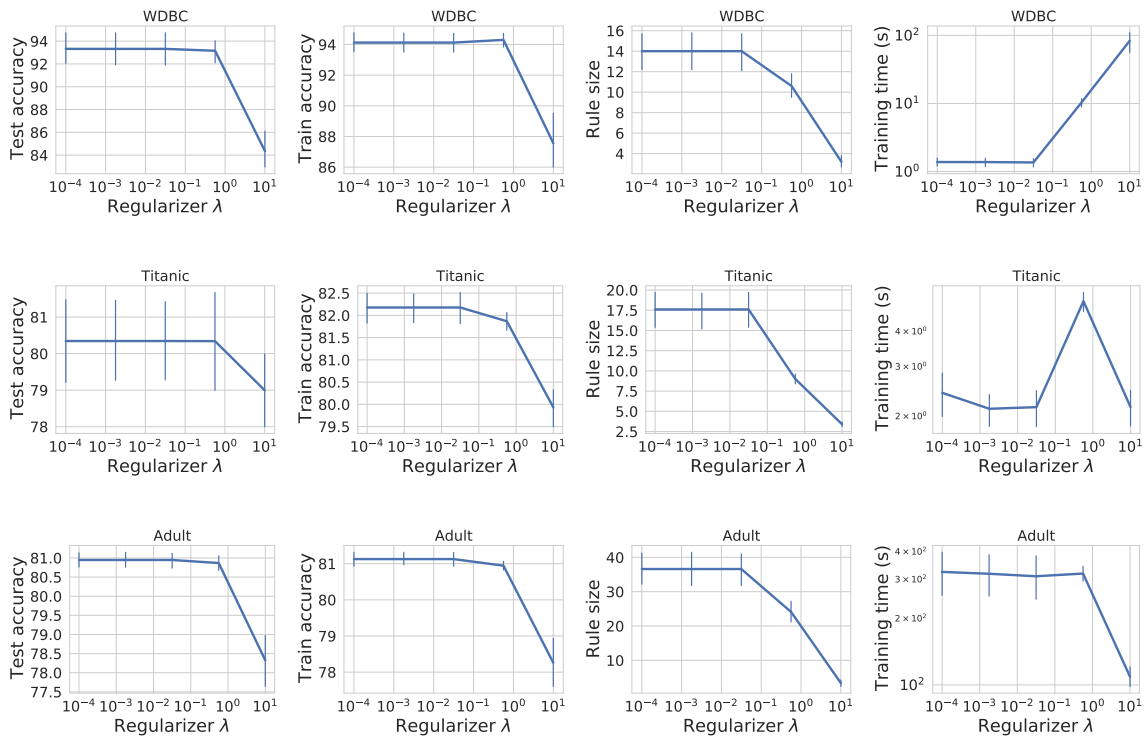


Figure 3.4: Effect of regularization λ on accuracy (test and train), rule size, and training time. As λ increases, lower priority is given to accuracy. As a result, both training and test accuracy decrease with λ by generating smaller rules.

3.7 Chapter Summary

Interpretable machine learning is gaining more focus with applications in many safety-critical domains. Considering the growing demand for interpretable models, it is challenging to design learning frameworks that satisfy all aspects: being accurate, interpretable, and scalable in practical classification tasks. In this chapter, we discuss a MaxSAT-based framework IMLI for learning interpretable rule-based classifiers expressible in CNF formulas. IMLI is built on efficient integration of incremental learning, specifically mini-batch and iterative learning, with MaxSAT-based formulation. In our empirical evaluation, IMLI achieves the best balance among prediction accuracy, interpretability, and scalability. In particular, IMLI demonstrates competitive prediction accuracy and rule size compared to existing interpretable rule-based classifiers. In addition, IMLI achieves impressive scalability than both interpretable and non-interpretable classifiers by learning interpretable rules on million-size datasets with higher accuracy. Finally, IMLI generates other

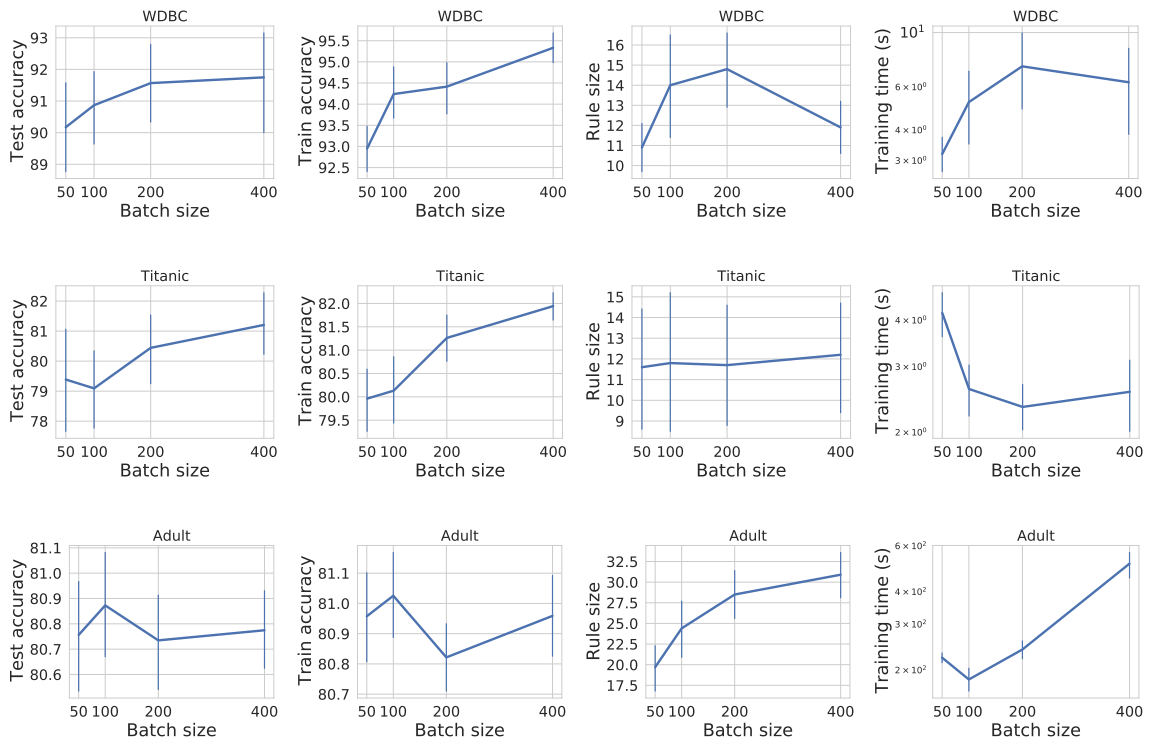


Figure 3.5: Effect of bath size on accuracy (test and train), rule size, and training time. As we consider more samples in a mini-batch, IMLI generates more accurate and larger size classification rules.

popular interpretable classifiers such as decision lists and decision sets using the same framework. In the next chapter, we leverage the incremental learning in IMLI to learn more expressible yet interpretable classification rules.

Chapter 4

Expressiveness via Logical Relaxation

In this chapter, we focus on improving the expressiveness of interpretable rule-based classifiers. As demonstrated in Chapter 3, CNF/DNF rules are considered interpretable, but they are less expressive compared to Boolean cardinality constraints. A Boolean cardinality constraint allows one to express numerical bounds on Boolean variables [169]. In this chapter, we introduce a novel formulation of interpretable classification rules, namely *relaxed-CNF*, which achieve benefits of both worlds: it is interpretable similar to CNF/DNF but more expressible by allowing cardinality constraints in the representation.

We find the motivation of relaxed-CNF rules from checklists. A checklist is a list of conditions that one needs to check, e.g., a list of items to take on a travel trip. Checklists have several applications in interpretable decision making [26, 58], particularly in the medical domain. For example, the CHADS2 score in medicine is a clinical prediction rule for estimating the risk of stroke [58]. Another example of checklists is a psychometric test, known as Myers–Briggs Type Indicator (MBTI) [26], which indicates differing psychological preferences in how people perceive the world around them and make decisions. An influential study on the importance of checklists [61] finds that highly complex and specialized problems can be handled smoothly by the development and consistent usage of checklists, which we formally call as relaxed-CNF rules.

Relaxed-CNF: An Informal Introduction. In interpretable rule-based classification, the simplest logical rules are single level-rules: ORs or ANDs of Boolean *literals*, where each literal denotes either a Boolean input feature or its negation. A

clause is a collection of N literals connected by OR/AND. To satisfy a clause, an OR operator requires 1 out of N literals to be assigned to 1 in the clause, while an AND operator requires all N out of N literals to be assigned to 1. A CNF formula is a conjunction (AND) of clauses where each clause is a disjunction (OR) of literals, and a DNF formula is a disjunction of clauses where each clause is a conjunction of literals. Therefore, CNF and DNF formulas can be viewed as two-level rules with several applications in interpretable decision-making. For example, a decision set is a DNF rule referring to a set of “if-else” conditions [79, 93]. In this chapter, we consider a richer set of logical formulas that capture the structure of checklists. To this end, we consider *hard-OR* clauses, where at least $M > 1$ out of N literals are assigned to 1, and we similarly define *soft-AND* clauses which allow some of the literals (at most $N - M$) to be 0. To be precise, the definitions of hard-OR and soft-AND overlap. Consequently, we use hard-OR when $M \leq N/2$ and soft-AND otherwise. To extend the standard definition of CNF (which is ANDs of ORs), we define *relaxed-CNF* to denote soft-ANDs of hard-ORs. Similarly, *relaxed-DNF* is hard-ORs of soft-ANDs. Since hard-OR and soft-AND are differentiated based on the value of M and N , relaxed-CNF and relaxed-DNF have the same structural representation. In early work, Craven and Shavlik [39] considered single level M -of- N rules to explain black-box neural-network classifiers. Recently, Emad et al. [49] have developed a semi-quantitative group testing approach for learning sparse single level M -of- N rules, which are quite restrictive in their ability to fit the data. In contrast, in this chapter, we study a much richer family of two-level relaxed-CNF rules.

Relaxed-CNF rules are more flexible than pure CNF rules, and they can accurately fit more complex classification boundaries. For example, relaxed-CNF clauses allow a compact encoding of the majority function¹ in Boolean logic, which would require exponentially many clauses in CNF, showing the exponential gap in the succinctness of the two representations. In addition, relaxed-CNF and CNF rules have the same functional form where a user has to compute the sum of true literals/clauses and then compare the sum to different thresholds (as in the example in Figure 4.1). From the computational perspective, the structural flexibility of relaxed-CNF compared to CNF/DNF makes it harder to learn. Therefore, in this chapter, we ask the following

¹The majority function is a Boolean function that evaluates to 0 when half or more arguments are false, and 1 otherwise [140].

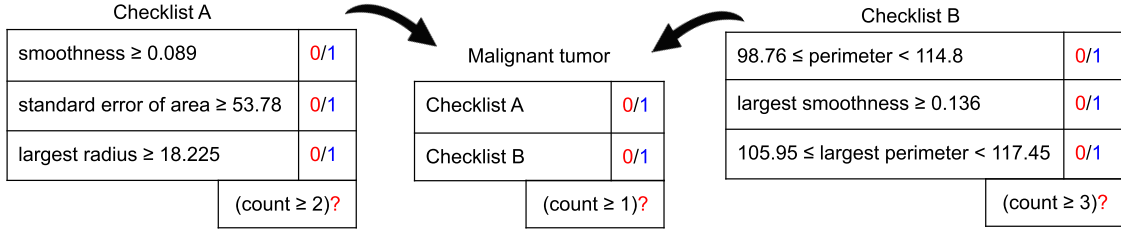


Figure 4.1: An illustrative example of a relaxed CNF classification rule, which describes the decision function in the form of a two-level checklist. This classifier is learned on the WDBC (Wisconsin diagnostic breast cancer) dataset and it predicts whether a tumor cell is malignant or not based on the characteristics of the tumor cell. The first column in each checklist contains Boolean literals. An entry in the second column is 1 if the corresponding literal is true by an observed tumor cell, and 0 otherwise. In the first level, checklist A (resp. B) is true if the count of true literals is at least 2 (resp. 3). In the second level, a tumor cell is predicted as malignant if the count of true checklists is at least 1.

research question: *can we design a combinatorial framework to efficiently learn relaxed-CNF rules?*

Contribution. The contribution of this chapter is an affirmative answer to the above question by proposing an efficient combinatorial learning framework for relaxed-CNF rules, namely CRR (Classification Rules in Relaxed form). In CRR, we construct a learning objective to maximize both the prediction accuracy and the rule-sparsity of the generated classification rule. To this end, we design a Mixed-Integer Linear Programming (MILP) formulation for learning the optimal relaxed-CNF rule from data. To learn a k -clause relaxed-CNF rule (say \mathcal{R}) using the naïve MILP formulation, the size of the MILP query expressed as the number of constraints is $\mathcal{O}(nk)$, where n is the number of training samples in the dataset. Consequently, this formulation fails to handle large datasets. To address the scalability of CRR, we discuss an efficient mini-batch training methodology as studied in Chapter 3, where we incrementally learn \mathcal{R} from data by iteratively solving smaller MILP queries corresponding to batches.

Through a comprehensive experimental evaluation over datasets from the UCI and Kaggle repository, we observe that CRR with relaxed-CNF rules achieves an improved trade-off between accuracy and rule sparsity and scales to datasets with

more than 10^5 samples. More significantly, CRR generates relaxed-CNF rules with higher accuracy than CNF rules generated by [62]. Furthermore, compared to decision lists generated by [38], relaxed-CNF rules are sparser in large datasets.

4.1 Problem Formulation

Given

1. a dataset $\mathbf{D} = \{(\mathbf{x}^{(i)}, y^{(i)})\}_{i=1}^n$ of n samples, where feature vector $\mathbf{x}^{(i)} \in \{0, 1\}^m$ contains m features and class label $y^{(i)} \in \{0, 1\}$,
2. a positive integer $k \geq 1$ denoting the number of clauses to be learned in the classification rule,
3. an integer threshold on literals $\eta_l \in \{0, \dots, m\}$ indicating the minimum number of literals required to be true to satisfy a clause,
4. an integer threshold on clauses $\eta_c \in \{0, \dots, k\}$ indicating the minimum number of clauses required to be true to satisfy a formula, and
5. a data-fidelity parameter $\lambda \in \mathbb{R}^+$,

we learn a classification rule \mathcal{R} expressed as a k clause relaxed-CNF formula separating samples of class 1 from class 0.

Our goal is to find rules that balance two goals: being accurate while also sparse to avoid over-fitting. To this end, we seek to minimize the total number of literals in all clauses, which motivates us to find \mathcal{R} with minimum $|\mathcal{R}|$. In particular, suppose \mathcal{R} classifies all samples correctly, i.e., $\forall i, y^{(i)} = \mathcal{R}(\mathbf{x}^{(i)})$. Among all the rules that classify all samples correctly, we choose the sparsest such \mathcal{R} :

$$\min_{\mathcal{R}} |\mathcal{R}| \text{ such that } \forall i, y^{(i)} = \mathcal{R}(\mathbf{x}^{(i)})$$

In practical classification tasks, perfect classification is very unusual. Hence, we need to balance rule-sparsity with prediction error. Let $\mathcal{E}_{\mathbf{D}}$ be the set of samples which are misclassified by \mathcal{R} on the dataset \mathbf{D} , i.e., $\mathcal{E}_{\mathbf{D}} = \{(\mathbf{x}^{(i)}, y^{(i)}) | y^{(i)} \neq \mathcal{R}(\mathbf{x}^{(i)})\}$. Hence we aim to find \mathcal{R} as follows:²

²In our formulation, it is straightforward to add class-conditional weights (e.g. to penalize false-alarms more than mis-detects), and to allow instance weights (per sample).

$$\min_{\mathcal{R}} \frac{\lambda}{n} |\mathcal{E}_{\mathbf{D}}| + \frac{1 - \lambda}{k \cdot m} |\mathcal{R}|,$$

where $|\mathcal{R}|$ denotes the size of rule, i.e., the number of literals in relaxed-CNF formula \mathcal{R} (ref. 2.2.1).

Each term in the objective function is normalized in $[0, 1]$. The data-fidelity parameter $\lambda \in [0, 1]$ serves to balance the trade-off between prediction accuracy and sparsity. Higher values of λ produce lower prediction errors by sacrificing the sparsity of \mathcal{R} , and vice versa. It can be viewed as an inverse of the regularization parameter.

4.2 Classification Rules in Relaxed Logical Form

In this section, we describe the main contribution of this chapter, CRR, a framework for learning relaxed-CNF rules. CRR converts the learning problem into an ILP-based formulation, learns the optimal assignment of variables and constructs rule \mathcal{R} based on the assignment. We organize the rest of this section as follows. We discuss the decision variables in Chapter 4.2.1, the constraints and the linear programming relaxation in Chapter 4.2.2, the incremental learning in Chapter 4.2.3, feature discretization in Chapter 4.2.4, and adaptation of CRR for learning other classification rules in Chapter 4.2.5.

4.2.1 Description of Variables

CRR considers two types of *decision* variables: (i) feature variables and (ii) noise or classification error variables. Since feature X_j can be present or not present in each of the k clauses, CRR considers k variables, each denoted by B_j^i corresponding to feature X_j to denote its participation in the i^{th} clause, i.e., $B_j^i = \mathbb{1}[j^{\text{th}} \text{ feature is selected in } i^{\text{th}} \text{ clause}]$. The q^{th} sample in the training dataset, however, can be misclassified by \mathcal{R} . Therefore, CRR introduces a noise variable $\xi_q \in \{0, 1\}$ corresponding to the q^{th} sample, so that the assignment of ξ_q can be interpreted whether $(\mathbf{x}^{(q)}, y^{(q)})$ is misclassified by \mathcal{R} or not, i.e., $\xi_q = \mathbb{1}[q^{\text{th}} \text{ sample is misclassified}]$. Hence, the key idea of CRR for learning \mathcal{R} is to define an ILP (Integer Linear Program) query over $k \cdot m + n$ decision variables,

denoted by $\{B_1^1, B_2^1, \dots, B_m^1, \dots, B_m^k, \xi_1, \dots, \xi_n\}$. In this context, we define $\mathbf{B}_i = \{B_j^i \mid j = 1, \dots, m\}$ as a *vector of feature variables* corresponding to the i^{th} clause.

4.2.2 Construction of the ILP Query

In Eq. (4.1), we discuss the ILP query Q for learning a k -clause relaxed-CNF rule \mathcal{R} . The objective function in Eq. (4.1a) takes care of both the rule-sparsity and the prediction accuracy of \mathcal{R} . Since CRR prefers a sparser rule with as few literals as possible, we construct the objective function by preferring B_j^i to be 0. Moreover, to encourage \mathcal{R} to predict the training samples accurately, we penalize the number of variables ξ_q that are different from 0. In this context, we utilize the parameter λ to trade off between sparsity and accuracy. Therefore, the objective function of the ILP query Q is to minimize the normalized sum of all noise variables ξ_q weighed by the data-fidelity parameter λ and feature variables B_j^i weighed by $1 - \lambda$.

We formulate the constraints of the ILP query Q as follows. Initially, we define the range of the decision variables and add constraints accordingly (Eq. 4.1b and 4.1c). For each sample, at first, we add constraints to mimic the behavior of hard-OR of literals in a clause, and then we add constraints to apply soft-AND of clauses in a formula (refer to Preliminaries in Chapter 2).

We first consider the case when the q^{th} sample has positive class label (Eq. 4.1d). $\mathbf{x}^{(q)} \circ \mathbf{B}_i \geq \eta_l$ resembles the hard-OR operation of literals in a clause. We introduce k *auxiliary* $\{0, 1\}$ variables $\{\xi_{q,1}, \dots, \xi_{q,k}\}$ to check whether at least η_c clauses are satisfied, i.e., $\xi_{q,i} = \mathbb{1}[i^{\text{th}} \text{ clause is dissatisfied for } q^{\text{th}} \text{ sample}]$, which let us impose the operation of soft-AND over clauses. We then add a constraint to make sure that at most $k - \eta_c$ clauses are allowed to be dissatisfied, otherwise the noise variable ξ_q is assigned to 1, i.e., the q^{th} sample is detected as aw noise.

A negative labeled sample has to dissatisfy more than $k - \eta_c$ clauses in \mathcal{R} so that the sample is predicted as 0, which is equivalent to satisfying more than $k - \eta_c$ constraints $\mathbf{x}^{(q)} \circ \mathbf{B}_i < \eta_l$. As mentioned earlier, we introduce $\{0, 1\}$ variable $\xi_{q,i}$ to specify if the constraint $\mathbf{x}^{(q)} \circ \mathbf{B}_i < \eta_l$ is dissatisfied or not and restrict the count of dissatisfied clauses $\sum_{i=1}^k \xi_{q,i}$ to be less than η_c .

$$\min \frac{\lambda}{n} \sum_{q=1}^n \xi_q + \frac{1-\lambda}{k \cdot m} \sum_{i=1}^k \sum_{j=1}^m B_j^i \quad (4.1a)$$

such that,

$$B_j^i \in \{0, 1\}, i = 1, \dots, k, j = 1, \dots, m \quad (4.1b)$$

$$\xi_q \in \{0, 1\}, q = 1, \dots, n \quad (4.1c)$$

$$\text{if } \forall q \in \{1, \dots, n\}, \text{ if } y^{(q)} = 1, \quad (4.1d)$$

$$\mathbf{x}^{(q)} \circ \mathbf{B}_i + m\xi_{q,i} \geq \eta_l, i = 1, \dots, k \quad (4.1e)$$

$$k\xi_q + k - \eta_c \geq \sum_{i=1}^k \xi_{q,i}$$

$$\xi_{q,i} \in \{0, 1\}, i = 1, \dots, k$$

$$\text{if } \forall q \in \{1, \dots, n\}, y^{(q)} = 0, \quad (4.1f)$$

$$\mathbf{x}^{(q)} \circ \mathbf{B}_i < \eta_l + m\xi_{q,i}, i = 1, \dots, k \quad (4.1g)$$

$$k\xi_q + \eta_c > \sum_{i=1}^k \xi_{q,i}$$

$$\xi_{q,i} \in \{0, 1\}, i = 1, \dots, k$$

In the following, we show the complexity of the ILP query in terms of the number of variables and constraints.

Proposition 6. Given a training dataset with n samples and m binary features, the ILP query Q for learning a binary classification rule in relaxed-CNF has $k \cdot m + n$ decision variables, $k \cdot n$ auxiliary variables, and $k \cdot m + n \cdot (k + 3)$ integer constraints.

An ILP solver takes query Q as input and returns the optimal assignment σ^* of the variables. We extract relaxed-CNF rule \mathcal{R} from the solution as follows.

Construction 7. Let $\sigma^* = \text{ILP}(Q)$, then $X_j \in \text{clause}(\mathcal{R}, i)$ if and only if $\sigma^*(B_j^i) = 1$.

Learning thresholds η_l and η_c : Given the training dataset \mathbf{D} and data-fidelity parameter λ , one could learn the optimum value of the thresholds η_c and η_l of the desired rule \mathcal{R} by specifying their range as constraints in the ILP query Q in Eq. 4.1. More precisely, we need to add two integer constraints $\eta_c \in \{0, \dots, k\}$ and $\eta_l \in \{0, \dots, m\}$ in the above query and then learn their values from the solution.

A more generalized version to CNF rules would be to learn different thresholds on literals for different clauses, i.e., $\eta_{l,i}$ for the i^{th} clause. This facilitates to capture the complex decision boundaries, while still producing rule-based decisions. In our ILP formulation, it is straight-forward to consider such generalization where we put constraints $\eta_{l,i} \in \{0, \dots, m\}, i = 1, \dots, k$ and replace η_l with $\eta_{l,i}$ in Eq. 4.1e and 4.1g.

Relaxing the ILP problem: The ILP query Q has binary integer constraints and the solution of this integer program is computationally intractable. A common approach that efficiently finds an approximate solution to such a problem extends to relax the integer constraints, solves the LP-relaxed (linear programming relaxation) problem, and then rounds the non-integer variables to get an integer solution as in [116]. In our case, we cannot relax all integer constraints because it may violate the structure of relaxed-CNF rules. Specifically, η_c and η_l (or $\eta_{l,i}$) must be integers in the construction of relaxed-CNF rules, and $\xi_{q,i}$ needs to be an integer to precisely calculate the noise variable ξ_q . However, we can relax feature variable B_j^i and noise variable ξ_q and solve the corresponding MILP problem. To construct the MILP problem, we replace Eq. 4.1b with $0 \leq B_j^i \leq 1$ and Eq. 4.1c with $0 \leq \xi_q \leq 1$, and the rest of the constraints in Q remain the same. If non-zero B_j^i is found in the solution, we set it to 1 and then construct the rule according to Construction 7.

4.2.3 Incremental Mini-batch Learning

In Chapter 4.2.2, we present an ILP formulation for learning relaxed-CNF rules and then discussed the relaxation to the integer constraints in the MILP formulation to make the approach computationally tractable. However, each integer constraints in the formulation cannot be relaxed, as discussed in Chapter 4.2.2. Thus we require an improved learning technique to achieve scalability. We now describe a mini-batch learning approach to CRR, that learns relaxed-CNF rule \mathcal{R} incrementally from a set of mini-batches while solving a modified MILP query for each mini-batch.

In incremental mini-batch learning, the learning process repeats for a fixed number of iterations. In each iteration, we randomly select an equal number of samples from the full training set and generate a mini-batch with samples. We then construct an MILP query on the current mini-batch with a modified objective

function. This objective function simultaneously penalizes the prediction errors on the current mini-batch and the change in the rules learned in consecutive batches. In the following, we discuss the modified objective function and the MILP formulation.

Let $\mathbf{D} = \{(\mathbf{x}^{(i)}, y^{(i)})\}_{i=1}^n$ be a training dataset with n samples and m binary features and τ be the number of iterations in the learning process. In the p^{th} iteration, we randomly construct a mini-batch from \mathbf{D} with equal number n_p of samples and $n_p \ll n$, for $p = 1, \dots, \tau$. Note that all mini-batches have the same binary features $\mathbf{X} = \{X_1, \dots, X_m\}$ as in the training set and thus share the same feature variables B_j^i in the MILP query. Therefore, we devise an objective function that prefers to keep the assignment of B_j^i learned in the $(p-1)^{\text{th}}$ iteration while minimizing the prediction error on the current mini-batch. To this end, each B_j^i is assigned 0 initially in the learning process. This technique enables us to update the learned rule in terms of the update in the assignment of feature variables B_j^i over mini-batches.

Let Q_p be the MILP query for the p^{th} mini-batch for learning a k -clause relaxed-CNF rule \mathcal{R}_p . Thus, \mathcal{R}_0 is an empty rule. We consider an indicator function $I(\cdot) : B_j^i \rightarrow \{1, -1\}$, that takes a feature variable B_j^i as input and outputs -1 if B_j^i is assigned 1 in the solution of Q_{p-1} (i.e., feature X_j is selected in the i^{th} clause of \mathcal{R}_{p-1}), otherwise outputs 1.

$$I(B_j^i) = \begin{cases} -1 & \text{if } X_j \in \text{clause}(\mathcal{R}_{p-1}, i) \\ 1 & \text{otherwise} \end{cases}$$

We now discuss the modified objective function where we multiply $I(B_j^i)$ with B_j^i differently from the objective function in Eq. 4.1a.

$$\min \frac{\lambda}{n} \sum_{q=1}^{n_p} \xi_q + \frac{1-\lambda}{k \cdot m} \sum_{i=1}^k \sum_{j=1}^m B_j^i \cdot I(B_j^i) \quad (4.2)$$

In the objective function, the first term penalizes the prediction error of samples in the current mini-batch and the second term penalizes when B_j^i is assigned differently than its previous assignment. Note that the total prediction error is normalized by dividing by n , which is the size of the full training dataset. This normalization is useful as it assists in updating \mathcal{R}_p while also considering the relative size of the

mini-batch. Intuitively, if the size n_p of the mini-batch is close to the size n of the training set, more priority is given to the prediction accuracy on the current batch and vice versa. The constraints in the query Q_p are similar to the constraints in Eq. 4.1. Finally, the prediction rule \mathcal{R} is \mathcal{R}_τ that is learned for the last mini-batch.

Proposition 8. At each iteration, the MILP query in the incremental mini-batch learning approach has $k \cdot m + n_p \cdot (k + 3)$ constraints, where n_p is the size of the mini-batch.

Learning thresholds η_l and η_c : In the incremental learning, the objective function in Eq 4.2 does not impose any constraint on the thresholds. In fact, the thresholds are learned in each iteration by solving the corresponding MILP query and we consider their final values in the last iteration.

4.2.4 Learning with Non-binary Features

Since our problem formulation requires input instances to have binary features, datasets with categorical and continuous features require a preprocessing stage. Initially, for all continuous features, we apply entropy-based discretization [53] to infer the most appropriate number of categories/intervals by recursively splitting the domain of each continuous feature to minimize the class-entropy of the given dataset.³ For example, let $X_c \in [a, b]$ be a continuous feature, and entropy-based discretization splits the domain $[a, b]$ into three intervals with two split points $\{a', b'\}$, where $a < a' < b' < b$. Therefore, the result intervals are $X_c < a'$, $a' \leq X_c < b'$, and $X_c \geq b'$.

After applying entropy-based discretization on continuous features, the dataset contains only categorical features, that can be converted to binary features using one-hot encoding as in [95]. In this encoding, a Boolean vector is introduced with cardinality equal to the number of distinct categories. Let a categorical feature have three categories ‘red’, ‘green’, and ‘yellow’. In one-hot encoding, samples with category-value ‘red’, ‘green’, and ‘yellow’ would be converted into binary features while taking values 100, 010, and 001, respectively.

³A simple quantile-based discretization also works, but it requires an extra parameter (i.e., the number of quantiles).

4.2.5 Learning Rules in Other Logical Forms

While CRR learns classification rules in relaxed-CNF form, we can leverage this framework for learning classification rules in other logical forms, for example, CNF and DNF. To learn a CNF rule, we set $\eta_l = 1$ and $\eta_c = k$, which converts a relaxed-CNF to a CNF formula. Moreover, to learn a DNF rule, we first complement the class label of all samples, learn a CNF rule by setting the parameters as described and finally negate the learned rule, which we have discussed elaborately in Chapter 3.

4.3 Empirical Performance Analysis

We implement a prototype of CRR based on the Python API for CPLEX and conduct an extensive empirical analysis to understand the behavior of CRR on real-world instances. The objective of our experimental evaluation is to answer the following questions:

1. How do the accuracy and training time for CRR behave vis-a-vis state-of-the-art classifiers on large datasets arising in machine learning problems in practice?
2. Can CRR generate sparse rules compared to that of other rule-based models?
3. How do the training time, accuracy, and rule size vary with model hyper-parameters?

In summary, relaxed-CNF rules generated by CRR achieves higher accuracy and more concise representation than CNF rules in most of the datasets. Moreover, relaxed-CNF rules are shown to be sparser than decision lists with competitive accuracy in large datasets. Finally, we show how to control the trade-off between rule-sparsity and accuracy using the hyper-parameter λ ; and between accuracy and training time using the hyper-parameter k and size n_p of each mini-batch. In the following, we give a detailed description of the experiments.

4.3.1 Experimental Setup

We perform experiments on a high-performance computer cluster, where each node consists of E5-2690 v3 CPU with 24 cores, 96 GB of RAM. Each experiment

is run on four cores of a node with 16 GB memory. We compare the performance of CRR with state-of-the-art classifiers, e.g. IMLI (Chapter 3), RIPPER [38], BRS [188], random forest (RF), support vector classifier (SVC), nearest neighbors classifiers (k -NN), and l_1 penalized logistic regression (LR). Among them, IMLI, BRS, and RIPPER are rule-based classifiers. In particular, IMLI generates classification rules in CNF using a MaxSAT-based formulation and we use Open-WBO [119] as the MaxSAT solver for IMLI. We compare with propositional rule learning algorithm RIPPER, which is implemented in WEKA [67] and generates classification rules in the form of decision lists. BRS is a Bayesian framework for generating rule sets expressed as DNF. For other classifiers, we use the Scikit-learn module of Python [138]. For all classifiers, we set the training cut-off time to 1500 seconds.

We consider a comparable number of hyper-parameter choices for each classifier. Specifically for CRR, we choose the data-fidelity parameter $\lambda \in \{0.5, 0.67, 0.84, 0.99\}$, the number of clauses $k \in \{1, 2, 3\}$, the relative size of mini-batch $\frac{n_p}{n} \in \{0.25, 0.50, 0.75\}$, and the number of iterations $\tau \in \{2, 4, 8, 16\}$. We learn the value of η_c and η_l from the dataset as described in Chapter. 4.2.2. In CPLEX, we set the maximum solving time of the LP solver to 1000 seconds ($\frac{1000}{\tau}$ seconds for each iteration) and the remaining 500 seconds is allotted to construct the MLIP instances, parse the solutions and execute other auxiliary tasks of the learning algorithm. We present the current best solution of CPLEX when the solver times out while finding the optimal solution.

We control the cut-off of the number of examples in the leaf node in the case of RF and RIPPER. For SVC, k -NN, and LR we discretize the regularization parameter on a logarithmic grid. For BRS, we vary the max clause-length $\in \{3, 4, 5\}$, support $\in \{5, 10, 15\}$, and two other parameters $s \in \{100, 1000, 10000\}$ and $\rho \in \{0.9, 0.95, 0.99\}$. For IMLI, we consider $\lambda \in \{1, 5, 10\}$ and $k \in \{1, 2, 3\}$ and vary the number of batches τ such that each batch has at least 32 samples and at most 512 samples.

4.3.2 Experimental Results

In the following, we first discuss empirical results of rule-based classifiers, then extend analysis to non-rule-based classifiers, and finally discuss the effect of different

Table 4.1: Comparisons of test accuracy, rule size and training time among different rule-based classifiers. Every cell in the last four columns contains the test accuracy in percentage (top value), rule size (middle value), and training time in seconds (bottom value). In the experiments, CRR shows higher test accuracy than IMLI and generates sparser rules than RIPPER. Number in bold denotes the best result, such as maximum test accuracy, minimum rule size, and minimum training time among competitive classifiers.

Dataset	Size	Features	RIPPER	BRS	IMLI	CRR
Heart	303	31	78.69	72.13	72.13	77.69
			7	19	13	4.5
			5.27s	25.07s	1.8s	122.5s
Ionosphere	351	144	88.65	91.43	89.29	91.43
			8	4	8.5	20
			5.87s	75.53s	2.09s	5.59s
WDBC	569	88	95.22	95.65	93.91	94.69
			7.5	12	7	34.5
			5.7s	630.23s	1.38s	316.32s
Magic	19020	79	84.04	74.15	71.97	81.31
			115	3	24	31
			15.86s	56.46s	141.2s	1012.6s
Tom’s HW	28179	910	97.4	—	95.88	97.34
			36	—	30	4
			42.73s	—	92.65s	1071.58s
Credit	30000	110	81.68	—	81.42	82.04
			38.5	—	10	32
			14.52s	—	17.66s	1021.35s
Adult	32561	144	84.31	—	82.08	84.86
			94	—	23	18
			27.61s	—	11.91s	1016.36s
Twitter	49999	1511	95.74	—	94.24	95.16
			179.5	—	57	12
			170.87s	—	238.29s	1144.66s
Weather-AUS	107696	141	84.57	—	82.83	83.34
			195	—	7	2
			121.02s	—	366.12s	1115.27s
Skin	245057	119	98.32	—	98.92	95.08
			725	—	201	29
			1313.19s	—	103.8s	825.6s

choices of hyper-parameters.

4.3.2.1 Performance Evaluation of CRR with Rule-based Classifiers

We conduct an assessment of performance using five-fold nested cross-validation as in [41] and report the median of test accuracy, rule size and training time of all rule-based classifiers in Table 4.1. Specifically, we show the dataset, the number of samples and the number of discretized features in the first three columns in Table 4.1. Inside each cell of column four to 11, we present the test accuracy (top value), rule size (middle value) and training time (bottom value) of each classifier for each dataset.

We first compare relaxed-CNF rules generated by CRR with CNF rules generated by IMLI. In Table 4.1, relaxed-CNF rules exhibit higher prediction accuracy than CNF rules in the majority of the datasets, showing the effectiveness of using a more expressive representation of classification rules in capturing the decision boundary. In addition, the generated relaxed-CNF rules are comparatively smaller than CNF rules in terms of rule size in most of the datasets. Therefore, relaxed-CNF rules improve upon CNF rules in terms of both prediction accuracy and rule size in the majority of the datasets. In this context, CRR provides a trade-off between accuracy and rule size depending on the choice of hyper-parameters and the experimental results are discussed later in Chapter 4.3.2.3. We then compare relaxed-CNF rules with DNF rules generated by BRS and find that relaxed-CNF rules outperform DNF rules with respect to prediction accuracy in several datasets. At this point, BRS fails to scale on larger datasets as shown in Table 4.1. We finally compare relaxed-CNF rules with decision lists generated by RIPPER. In the experiments, relaxed-CNF rules achieve comparable prediction accuracy with decision lists in most of the datasets. In contrast, RIPPER generates very large decision lists compared to relaxed-CNF rules in the majority of the datasets, more precisely in large datasets. To summarize the performance of CRR among different rule-based classifiers, CRR can generate smaller relaxed-CNF rules with better accuracy in numbers of the cases with a couple of exceptions.

Moving focus on the training time, the non-incremental version of CRR times out on larger instances in the experiments, potentially producing sub-optimal rules with reduced accuracy, thereby highlighting the need for the incremental approach.

Table 4.2: Comparisons of test accuracy among CRR and non-rule-based classifiers. In the experiments, CRR achieves competitive prediction accuracy in spite of being a rule-based classifier.

Dataset	LR	SVC	RF	k -NN	CRR
Heart	84.29	83.33	81.97	78.69	77.69
Ionosphere	94.29	91.43	92.96	91.43	91.43
WDBC	98.26	96.46	96.90	95.61	94.69
Magic	85.15	84.45	85.30	77.9	81.31
Tom’s HW	97.62	97.66	97.52	94.59	97.34
Credit	82.04	82.12	81.97	80.5	82.04
Adult	87.24	86.82	86.84	84.68	84.86
Twitter	96.28	96.34	96.37	—	95.16
Weather-AUS	85.71	—	85.63	—	83.34
Skin	97.21	—	99.81	—	95.08

On the other hand, the incremental version of CRR can handle most of the datasets within the allotted amount of time. In Table 4.1, CRR takes a comparatively longer time to generate relaxed-CNF rules in comparison with other rule-based classifiers, e.g., RIPPER, and IMLI because of the flexible combinatorial structure of relaxed-CNF rules. However, the testing time of CRR is insignificant (< 0.01 seconds) and thus can be deployed in practice.

4.3.2.2 Performance Evaluation of CRR with Non-rule-based Classifiers

We compare the test accuracy of CRR with non-rule-based classifiers: LR, SVC, RF, and k -NN and report the results in Table 4.2. In the experiments, we find that CRR, in spite of being a rule-based classifier, is able to achieve competitive prediction accuracy with non-rule-based classifiers. In this context, SVC, and k -NN can not complete training within the allotted time particularly in the datasets with more than 10^5 samples, while CRR can still generate relaxed-CNF rules with competitive accuracy. Therefore, CRR shows the promise of applying rule-based classifiers in practice with an added benefit of interpretability along with competitive accuracy.

4.3.2.3 Varying Model Parameters

In Figure 4.2, 4.3, 4.4, and 4.5, we demonstrate the effect of varying the hyper-parameters of CRR. To understand the effect of a single hyper-parameter, we fix the

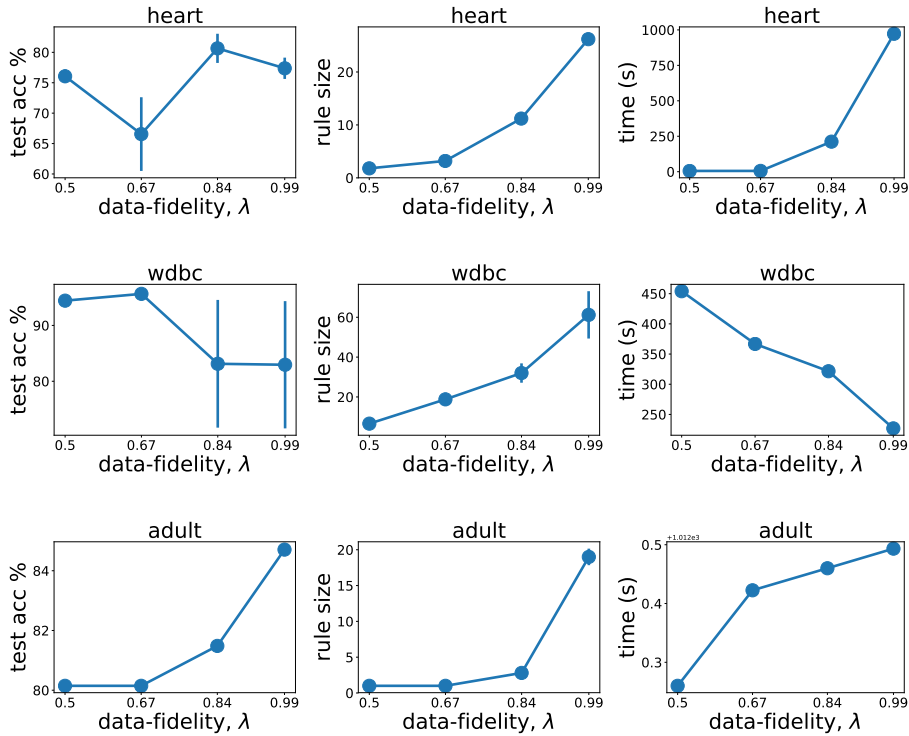


Figure 4.2: Effect of data-fidelity λ on test accuracy, rule size, and training time in CRR.

values of other hyper-parameters to a default choice where the default choice results in the most accurate rule.

Varying data-fidelity parameter (λ): In Figure 4.2, as we increase data-fidelity parameter λ in the objective function in Eq. 4.1a and Eq. 4.2, more priority is given to the prediction accuracy than the sparsity of the rules. In most of the datasets, we similarly observe an increase in accuracy and also an increase in the size of the rules when λ is higher. This suggests that improved interpretability can often come at a minor cost in accuracy. In addition, we find an increase in training time for most of the datasets indicating that the MILP query usually takes a longer time to find the solution when more priority is given on the prediction accuracy.

Varying the number of clauses (k): In Figure 4.3, as we increase k , CRR allows the generated rules to capture the variance in the given dataset more effectively, that results in higher accuracy in most of the datasets. The rule size also increases as we learn more clauses. In addition, the training time increases, that can be reasoned

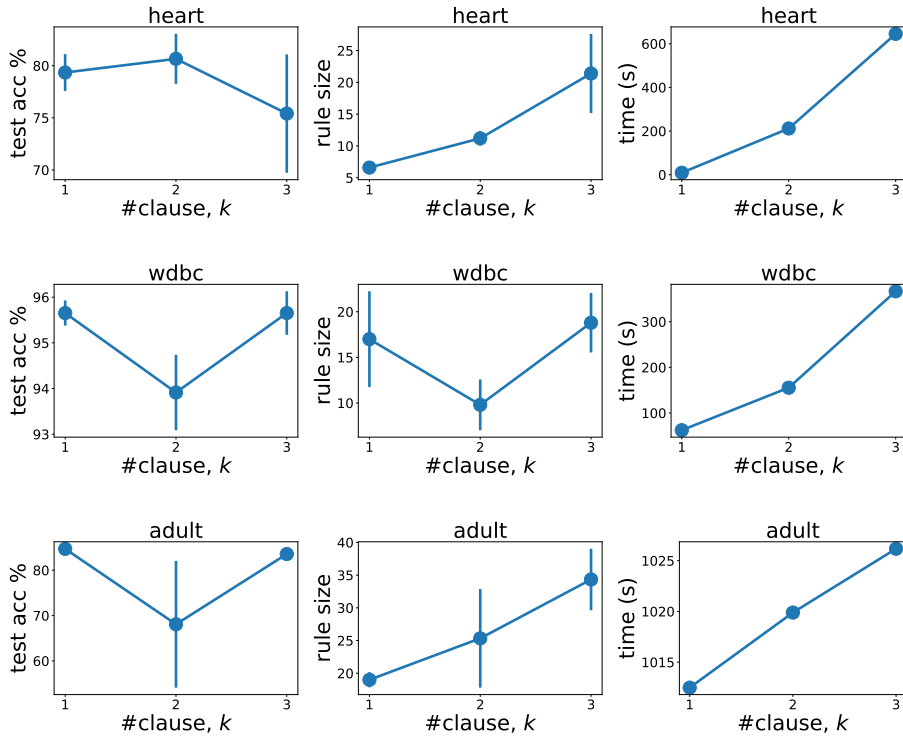


Figure 4.3: Effect of the number of clause k on test accuracy, rule size, and training time in CRR.

by the fact that the number of constraints in the MILP formulation is linear with k . Thereby, the number of clauses k provides a control over the accuracy of the generated rule and training time.

Relative size of the mini-batch: In Figure 4.4, we vary the relative size of the mini-batch $\frac{n_p}{n}$ to observe its effect on the accuracy and the size of the rules. In most datasets, the accuracy increases when more samples are considered in the mini-batch, costing higher training time. Moreover, the size of the generated rule increases as $\frac{n_p}{n}$ increases, that can be supported by the increase in the variance of the samples in the mini-batch.

Varying the number of iterations (τ): In Figure 4.5, as we allow more iterations in the learning process, we find an increase in accuracy in most datasets. The training time also increases with τ because CRR is required to solve in total τ queries. We also observe an increase in rule size in most datasets. The reason is that the objective function in the incremental mini-batch approach in Eq. 4.2 does not put a restriction

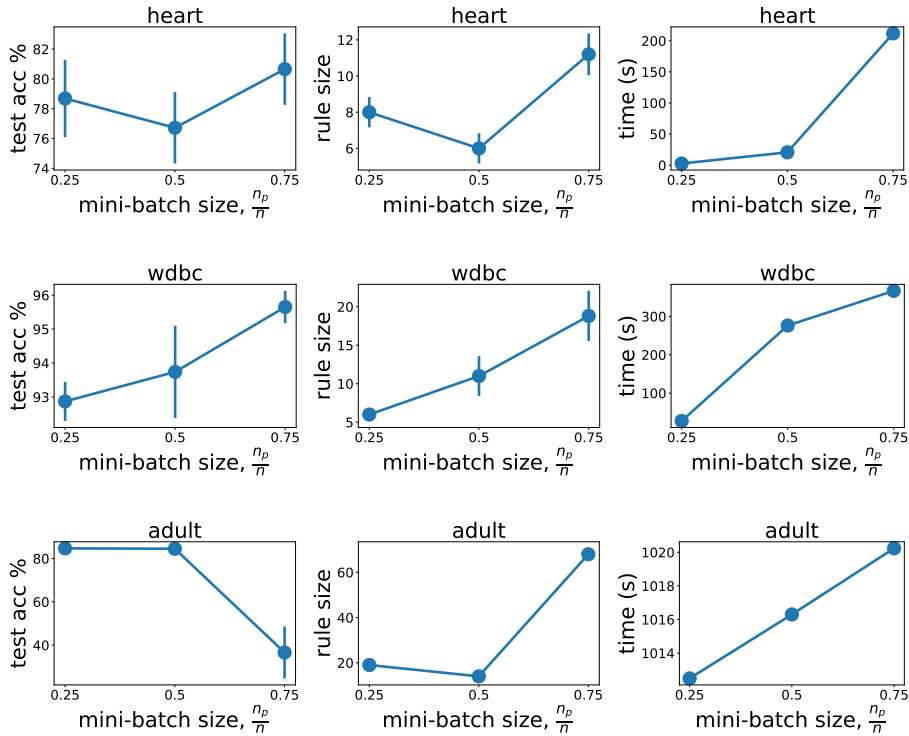


Figure 4.4: Effect of mini-batch size on test accuracy, rule size, and training time in CRR.

on the size of the rules, rather on the change of rules in consecutive iterations. In addition, the learned values of the thresholds η_c and η_l in one iteration are not carried to the MILP query in the next iteration, that may cause an increase of rule size.

4.4 Chapter Summary

We discuss an efficient combinatorial framework, called CRR, for learning relaxed-CNF classification rules. Relaxed-CNF rules are more expressive than CNF/DNF rules. CRR uses a novel integration of mini-batch learning procedure with the MILP framework to learn sparse relaxed-CNF rules. Our experimental results demonstrate that CRR is able to learn relaxed-CNF rules with higher accuracy and more concise representation than CNF rules. Moreover, the generated rules are sparser than decision lists in large datasets.

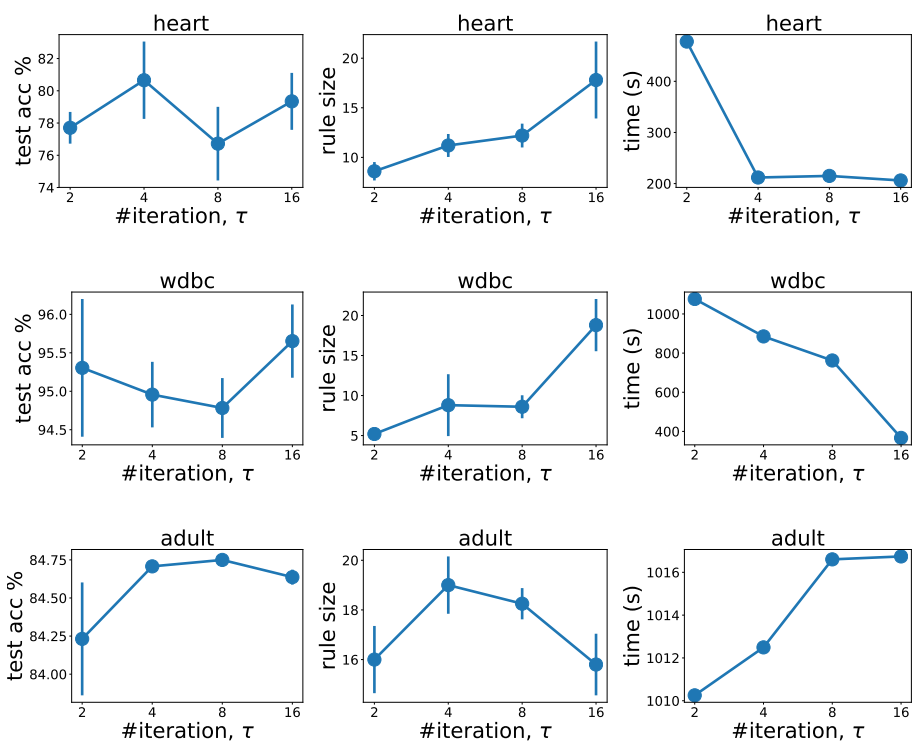


Figure 4.5: Effect of the number of iterations on test accuracy, rule size, and training time in CRR.

Part III

Fairness in Machine Learning

In Chapter 5, we discuss an SSAT-based framework to formally verify the fairness of finite classifiers encoded as Boolean formulas. In Chapter 6, we handle feature correlations in fairness verification and discuss a tractable fairness verification of linear classifiers.

Chapter 5

Fairness Verification using SSAT

We discuss formal fairness verification problem in machine learning where we verify the bias of a classifier given the probability distribution of features. To verify fairness as a model property, several probabilistic fairness verifiers such as FairSquare [4] and VeriFair [15] have been proposed. Though FairSquare and VeriFair are robust and have asymptotic convergence guarantees, we observe that they scale up poorly with the size of inputs and also do not generalize to non-Boolean and compound sensitive features. In contrast to the probabilistic verifiers, another line of work, referred to as sample-based verifiers, has focused on the design of testing methodologies on a given fixed data sample [59, 17]. Since sample-based verifiers are dataset-specific, they generally do not provide robustness over the distribution.

Thus, a *unified formal framework* to verify *different fairness metrics* of a classifier, which is *scalable*, capable of *handling compound sensitive groups*, *robust* with respect to the test data, and *operational on real-life* datasets and fairness-enhancing algorithms, is missing in the literature.

Contribution. We discuss model verifying different fairness metrics as a SSAT problem. We primarily focus on reductions to the exist-random quantified fragment of SSAT, which is also known as E-MAJSAT [106]. Our choice of SSAT as a target formulation is motivated by the recent algorithmic progress that has yielded efficient SSAT tools [98, 99].

Our contributions are summarised below:

- We discuss a unified SSAT-based approach, **Justicia**, to verify independence and separation metrics of group fairness metrics for different datasets and classifiers.

- Unlike earlier probabilistic verifiers, namely FairSquare and VeriFair, **Justicia** verifies fairness for compound and non-Boolean sensitive features.
- Our experiments validate that our method is more accurate and scalable than the probabilistic verifiers, such as FairSquare and VeriFair, and more robust than the sample-based empirical verifiers, such as AIF360.

We illustrate the contribution of this chapter using an example scenario.

Example 5.0.1. Let us consider a classification problem (Figure 5.1) of deciding the eligibility for health insurance depending on the fitness and income of individuals of different age groups (20-40 and 40-60). Typically, incomes of individuals increase as their ages increase while their fitness deteriorates (Figure 5.1a). We assume that the relation of income and fitness depends on ages as per the Normal distributions in Figure 5.1b. Now, if we train a decision tree [129] to decide the eligibility of an individual to get a health insurance given three features: fitness, income and age, we observe that the ‘optimal’ decision tree (ref. Figure 5.1c) does not predict based on the sensitive feature age. However, a fairness verifier, such as **Justicia**, would verify that the decision tree outputs positive prediction to an individual above and below 40 years with probabilities 0.18 and 0.72 respectively (Figure 5.1d). This simple example demonstrates that even if a classifier does not explicitly learn to differentiate on the basis of a sensitive feature, it discriminates different age groups due to the utilitarian sense of accuracy that it tries to optimize.

5.1 An SSAT-based Fairness Verifier

In this section, we present **Justicia**, which is an SSAT-based framework for verifying group and causal fairness metrics. Given a binary classifier \mathcal{M} , a probability distribution over features $(\mathbf{X}, \mathbf{A}, Y) \sim \mathcal{D}$, and a target fairness metric $f(\mathcal{M}, \mathcal{D})$, our goal is to estimate the fairness $f(\mathcal{M}, \mathcal{D})$ of the classifier \mathcal{M} given the distribution \mathcal{D} according to the fairness definition. Additionally, if a fairness threshold $\epsilon \in [0, 1]$ is provided, **Justicia** verifies whether the classifier is ϵ -fair by comparing f with ϵ (refer to Chapter 2). In **Justicia**, we focus on classifiers that can be represented as a CNF formula defined over a set of Boolean variables. Additionally, for each variable,

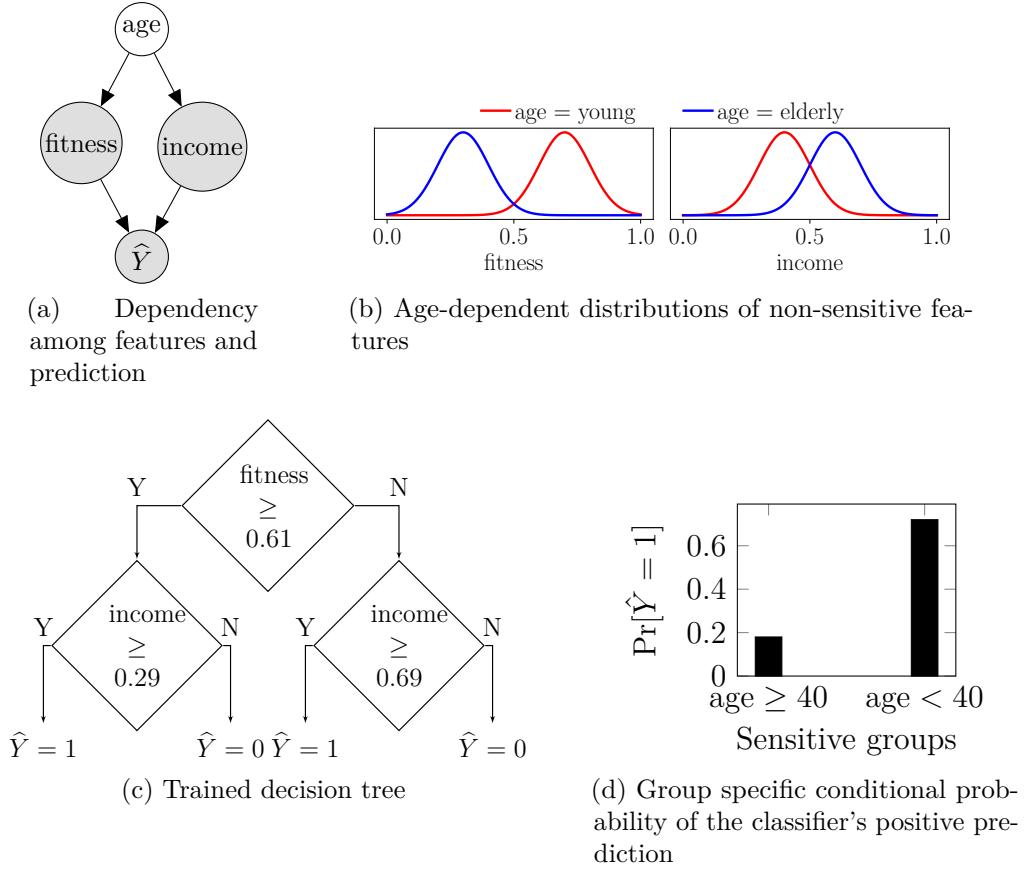


Figure 5.1: A trained decision tree to learn the eligibility for health insurance using age-dependent fitness and income indicators. This classifier makes unfair prediction to individuals with age above 40.

we query the distribution \mathcal{D} to derive the marginal probability of the variable to be assigned to 1. In this section, we discuss two equivalent approaches for fairness verification based on SSAT-based encodings: *enumeration* approach and *inference* approach. In both approaches, we verify fairness with the presence of compound sensitive groups. We then provide a theoretical analysis for a high-probability error bound on the fairness metric and conclude with an extension of *Justicia* in practical settings.

5.1.1 Enumeration Approach using RE-SSAT encoding

In order to estimate $f(\mathcal{M}, \mathcal{D})$ in the enumeration approach, the key idea is to compute the conditional probability of positive prediction of the classifier, $\Pr[\hat{Y} = 1 | \mathbf{A} = \mathbf{a}]$, for the compound sensitive group $\mathbf{A} = \mathbf{a}$ by solving an appropriately

designed SSAT formula. For simplicity, we initially make assumptions on the classifier \mathcal{M} and discuss practical relaxations later in this section. We first assume \mathcal{M} to be represented as a CNF formula, denoted by $\phi_{\hat{Y}}$, such that the prediction $\hat{Y} = 1$ when $\phi_{\hat{Y}}$ is satisfied and $\hat{Y} = 0$ otherwise. Additionally, all features $\mathbf{X} \cup \mathbf{A}$ are assumed to be Boolean variables. Finally, we consider independence probability assumption of non-sensitive features \mathbf{X} , where $p_i \triangleq \Pr[X_i = 1]$ is the marginal probability of X_i .

Now, we define an RE-SSAT formula $\Phi_{\mathbf{a}}$ to compute the conditional probability $\Pr[\hat{Y} = 1 | \mathbf{A} = \mathbf{a}]$ using the probability of satisfaction of $\Phi_{\mathbf{a}}$. In the prefix of $\Phi_{\mathbf{a}}$, all non-sensitive features \mathbf{X} are assigned randomized quantifiers and they are followed by sensitive features \mathbf{A} with existential quantifiers. In addition, the CNF formula ϕ in the SSAT formula $\Phi_{\mathbf{a}}$ is constructed such that ϕ encodes the event inside the target probability $\Pr[\hat{Y} = 1 | \mathbf{A} = \mathbf{a}]$. In order to specify the sensitive group $\mathbf{A} = \mathbf{a}$, we take the conjunction of the Boolean variables in \mathbf{A} that symbolically specifies the compound sensitive group $\mathbf{A} = \mathbf{a}$. For example, let us consider two sensitive features: $\text{race} \in \{\text{White}, \text{Colour}\}$ and $\text{sex} \in \{\text{male}, \text{female}\}$ by Boolean variables R and S , respectively. Hence, the compound groups $[\text{White}, \text{male}]$ and $[\text{Colour}, \text{female}]$ are represented by $R \wedge S$ and $\neg R \wedge \neg S$, respectively. Thus, the RE-SSAT formula for computing the probability $\Pr[\hat{Y} = 1 | \mathbf{A} = \mathbf{a}]$ is

$$\Phi_{\mathbf{a}} := \underbrace{\forall^{p_1} X_1, \dots, \forall^{p_{m_1}} X_{m_1}}_{\text{non-sensitive features}}, \underbrace{\exists A_1, \dots, \exists A_{m_2}}_{\text{sensitive features}}, \phi_{\hat{Y}} \wedge (\mathbf{A} = \mathbf{a}).$$

In the RE-SSAT formula $\Phi_{\mathbf{a}}$, existentially quantified variables $\{A_1, \dots, A_{m_2}\}$ are assigned Boolean values according to the constraint $\mathbf{A} = \mathbf{a}$.¹ Next, an SSAT solver computes the probability $\Pr[\Phi_{\mathbf{a}}]$ by considering the random values of $\{X_1, \dots, X_{m_1}\}$ while fixing the assignment of $\{A_1, \dots, A_{m_2}\}$. Therefore, $\Pr[\Phi_{\mathbf{a}}]$ equals the conditional probability of positive prediction of the classifier, $\Pr[\hat{Y} = 1 | \mathbf{A} = \mathbf{a}]$, for the sensitive group $\mathbf{A} = \mathbf{a}$.

For simplicity, we have described the computation of conditional probability $\Pr[\hat{Y} = 1 | \mathbf{A} = \mathbf{a}]$ without considering the correlation among sensitive and non-sensitive features. In reality, correlation exists among these features (for a detailed study on feature correlations in fairness verification, we refer to Chapter 6). As a result, non-sensitive features may have different conditional distributions for different

¹An RE-SSAT formula becomes an R-SSAT formula when the assignment to the existential variables are fixed.

sensitive groups. For a non-sensitive feature X_i , we incorporate its conditional probability in the RE-SSAT encoding by setting $p_i = \Pr[X_i = 1 | \mathbf{A} = \mathbf{a}]$ instead of the independent probability $\Pr[X_i = 1]$. Next, we illustrate this enumeration approach in Example 5.1.1.

Example 5.1.1 (RE-SSAT encoding). We illustrate the RE-SSAT encoding for calculating the probability of positive prediction for the sensitive group $\text{age} \geq 40$ in the decision tree of Figure 5.1. We assign three Boolean variables F, I, J for three nodes in the decision tree, where literal F, I, J denote $\text{fitness} \geq 0.61$, $\text{income} \geq 0.29$, and $\text{income} \geq 0.69$, respectively. We consider another Boolean variable A where the literal A represents the sensitive group $\text{age} \geq 40$ and $\neg A$ denotes $\text{age} < 40$. Thus, the CNF formula for the decision tree is $(\neg F \vee I) \wedge (F \vee J)$. From the distribution in Figure 5.1, we get $\Pr[F] = 0.41$, $\Pr[I] = 0.93$, and $\Pr[J] = 0.09$. Given this information, we calculate the probability of positive prediction for the sensitive group $\text{age} \geq 40$ by solving the following RE-SSAT formula:

$$\Phi_A := \mathfrak{P}^{0.41} F, \mathfrak{P}^{0.93} I, \mathfrak{P}^{0.09} J, \exists A, (\neg F \vee I) \wedge (F \vee J) \wedge A.$$

From the solution to this SSAT formula, we get $\Pr[\Phi_A] = 0.43$. Similarly, to calculate the probability of positive prediction for the group $\text{age} < 40$, we replace the unit clause² A with $\neg A$ in the CNF formula in Φ_A and construct another SSAT formula $\Phi_{\neg A}$.

$$\Phi_{\neg A} := \mathfrak{P}^{0.41} F, \mathfrak{P}^{0.93} I, \mathfrak{P}^{0.09} J, \exists A, (\neg F \vee I) \wedge (F \vee J) \wedge \neg A$$

For $\Phi_{\neg A}$, the solution $\Pr[\Phi_{\neg A}] = 0.43$ is similarly derived from an SSAT solver. Therefore, if $\Pr[F], \Pr[I], \Pr[J]$ are computed independently of the sensitive feature A , both age groups achieve an equal probability of positive prediction as the sensitive feature is not explicitly present in the classifier.

However, there is an implicit bias in the data distribution for different sensitive groups and the classifier unintentionally learns it. To capture this implicit bias, we calculate conditional probabilities $\Pr[F|A] = 0.01$, $\Pr[I|A] = 0.99$, and $\Pr[J|A] = 0.18$ from the distribution for group $\text{age} \geq 40$ in Figure 5.1. Providing the conditional

²A unit clause is a clause with a single literal.

probabilities, we construct a modified SSAT formula Φ'_A and compute $\Pr[\Phi'_A] = 0.18$ for $\text{age} \geq 40$.

$$\Phi'_A := \mathfrak{Y}^{0.01}F, \mathfrak{Y}^{0.99}I, \mathfrak{Y}^{0.18}J, \exists A, (\neg F \vee I) \wedge (F \vee J) \wedge A$$

For the sensitive group $\text{age} < 40$, we similarly obtain $\Pr[F|\neg A] = 0.82$, $\Pr[I|\neg A] = 0.88$, $\Pr[J|\neg A] = 0.01$, construct the modified formula $\Phi'_{\neg A}$ and get $\Pr[\Phi'_{\neg A}] = 0.72$.

$$\Phi'_{\neg A} := \mathfrak{Y}^{0.82}F, \mathfrak{Y}^{0.88}I, \mathfrak{Y}^{0.01}J, \exists A, (\neg F \vee I) \wedge (F \vee J) \wedge \neg A$$

In the later case with correlations among sensitive and non-sensitive features, the RE-SSAT encoding detects the discrimination of the classifier among different sensitive groups, where the classifier is more biased towards the younger group with $\text{age} < 40$ than the elderly group with $\text{age} \geq 40$.

5.1.1.1 Measuring Fairness Metrics

As we compute $\Pr[\Phi_{\mathbf{a}}] = \Pr[\widehat{Y} = 1 | \mathbf{A} = \mathbf{a}]$ by solving the SSAT formula $\Phi_{\mathbf{a}}$, we use $\Pr[\Phi_{\mathbf{a}}]$ to measure different fairness metrics. To this end, we compute $\Pr[\Phi_{\mathbf{a}}]$ for all compound groups $\mathbf{a} \in \mathbf{A}$ by solving an exponential number (with m_2) of SSAT formulas. We elaborate this enumeration approach, namely `Justicia_enum`, in Algorithm 5 (Line 1–8).

To measure the disparate impact of a classifier, we calculate the ratio between the minimum and the maximum conditional probability of positive prediction of the classifier, which are $\min_{\mathbf{a} \in \mathbf{A}} \Pr[\Phi_{\mathbf{a}}]$ and $\max_{\mathbf{a} \in \mathbf{A}} \Pr[\Phi_{\mathbf{a}}]$, respectively. We compute statistical parity by taking the difference between $\max_{\mathbf{a} \in \mathbf{A}} \Pr[\Phi_{\mathbf{a}}]$ and $\min_{\mathbf{a} \in \mathbf{A}} \Pr[\Phi_{\mathbf{a}}]$.

Moreover, to compute equalized odds, we call `Justicia` twice, one for the distribution \mathcal{D} conditioned on $Y = 1$ and another for $Y = 0$. In both calls, we compute $\max_{\mathbf{a}} \Pr[\widehat{Y} = 1 | \mathbf{A} = \mathbf{a}, Y = y] - \min_{\mathbf{a}} \Pr[\widehat{Y} = 1 | \mathbf{A} = \mathbf{a}, Y = y]$ for $y \in \{0, 1\}$ and take the maximum difference as the value of equalized odds. For measuring path-specific causal fairness, we compute $\max_{\mathbf{a}} \Pr[\widehat{Y} = 1 | \mathbf{A} = \mathbf{a}, \mathbf{Z}]$ and $\min_{\mathbf{a}} \Pr[\widehat{Y} = 1, \mathbf{Z} | \mathbf{A} = \mathbf{a}, \mathbf{Z}]$ by conditioning the distribution \mathcal{D} by mediator features \mathbf{Z} and take their difference. Thus, `Justicia_enum` allows us to compute different group and causal fairness metrics using a unified algorithmic framework.

Algorithm 5 Justicia: An SSAT-based Fairness Verifier

```
1: function Justicia_enum( $\mathbf{X}, \mathbf{A}, \hat{Y}$ )
2:    $\phi_{\hat{Y}} := \text{CNF}(\hat{Y} = 1)$ 
3:   for all  $\mathbf{a} \in \mathbf{A}$  do
4:      $p_i \leftarrow \text{Pr}[X_i = 1 | \mathbf{A} = \mathbf{a}], \forall X_i \in \mathbf{X}$ 
5:      $\phi := \phi_{\hat{Y}} \wedge (\mathbf{A} = \mathbf{a})$ 
6:      $\Phi_{\mathbf{a}} := \forall^{p_1} X_1, \dots, \forall^{p_{m_1}} X_{m_1}, \exists A_1, \dots, \exists A_{m_2}, \phi$ 
7:      $\text{Pr}[\Phi_{\mathbf{a}}] \leftarrow \text{SSAT}(\Phi_{\mathbf{a}})$  ▷ returns probability
8:   return  $\max_{\mathbf{a} \in \mathbf{A}} \text{Pr}[\Phi_{\mathbf{a}}], \min_{\mathbf{a} \in \mathbf{A}} \text{Pr}[\Phi_{\mathbf{a}}]$ 

9: function Justicia_infer( $\mathbf{X}, \mathbf{A}, \hat{Y}$ )
10:   $\phi_{\hat{Y}} := \text{CNF}(\hat{Y} = 1)$ 
11:   $p_i \leftarrow \text{Pr}[X_i = 1], \forall X_i \in \mathbf{X}$ 
12:   $\Phi_{\text{ER}} := \exists A_1, \dots, \exists A_{m_2}, \forall^{p_1} X_1, \dots, \forall^{p_{m_1}} X_{m_1}, \phi_{\hat{Y}}$ 
13:   $\Phi'_{\text{ER}} := \exists A_1, \dots, \exists A_{m_2}, \forall^{p_1} X_1, \dots, \forall^{p_{m_1}} X_{m_1}, \neg \phi_{\hat{Y}}$ 
14:  return  $\text{SSAT}(\Phi_{\text{ER}}), 1 - \text{SSAT}(\Phi'_{\text{ER}})$ 
```

5.1.2 Inference Approach using ER-SSAT Encoding

In most practical problems, there can be exponentially many compound sensitive groups due to the combination of categorical sensitive features. As a result, the enumeration approach may suffer from scalability issues due to the exponential number of calls to the SSAT solver. To this end, we discuss an efficient SSAT encoding, where we make two SSAT calls, one for inferring the *the most favored sensitive group* with the maximum conditional probability of positive prediction of the classifier and another for inferring the *the least favored sensitive group* with the minimum conditional probability of positive prediction of the same classifier. As discussed above, these two probabilities are sufficient to measure different group and causal fairness metrics.

5.1.2.1 Inferring the Most Favored Sensitive Group

In the prefix of an SSAT formula Φ , the order of quantified variables carries distinct interpretation of $\text{Pr}[\Phi]$. In an ER-SSAT formula, $\text{Pr}[\Phi]$ is the *maximum* satisfying probability of Φ over the optimal assignment of existentially quantified variables given the randomized quantified variables (by Semantic 2, Sec. 2.1.5). In this chapter, we leverage this property to compute the most favored sensitive group with the highest probability of positive prediction of the classifier. In particular, we

consider the following ER-SSAT formula:

$$\Phi_{\text{ER}} := \exists A_1, \dots, \exists A_{m_2}, \mathfrak{P}^{p_1} X_1, \dots, \mathfrak{P}^{p_{m_1}} X_{m_1}, \phi_{\hat{Y}}. \quad (5.1)$$

The CNF formula $\phi_{\hat{Y}}$ in Φ_{ER} is the CNF translation of the classifier $\hat{Y} = 1$ without any specification of the compound sensitive group. Therefore, as we solve Φ_{ER} , we find the optimal assignment to the existentially quantified variables $A_1 = a_1^{\max}, \dots, A_{m_2} = a_{m_2}^{\max}$ for which the probability of satisfaction of the ER-SSAT formula $\Pr[\Phi_{\text{ER}}]$ becomes maximum. Thus, we compute the most favored group $\mathbf{a}_{\max} \triangleq [a_1^{\max}, \dots, a_{m_2}^{\max}]$ achieving the highest probability of positive prediction of the classifier.

5.1.2.2 Inferring the Least Favored Sensitive Group

In order to infer the least favored sensitive group of the classifier, we compute the *minimum* conditional probability of positive prediction of the classifier with respect to all sensitive groups given the random values of the non-sensitive features. To this end, we solve a ‘universal-random’ (UR) SSAT formula with universal quantifiers over sensitive features and randomized quantification over non-sensitive features (by Semantic 3, Sec. 2.1.5).

$$\Phi_{\text{UR}} := \forall A_1, \dots, \forall A_{m_2}, \mathfrak{P}^{p_1} X_1, \dots, \mathfrak{P}^{p_{m_1}} X_{m_1}, \phi_{\hat{Y}} \quad (5.2)$$

Solving an UR-SSAT formula raises several practical issues and thus, there is an unavailability of an UR-SSAT solver. To resolve this problem, we leverage the *duality* between UR-SSAT and ER-SSAT formulas, where we solve an UR-SSAT formula on the CNF ϕ using the solution of an ER-SSAT formula on the complemented CNF $\neg\phi$ [106]. More specifically, we solve the following ER-SSAT formula for finding the least favored sensitive group.

$$\Phi'_{\text{ER}} := \exists A_1, \dots, \exists A_{m_2}, \mathfrak{P}^{p_1} X_1, \dots, \mathfrak{P}^{p_{m_1}} X_{m_1}, \neg\phi_{\hat{Y}} \quad (5.3)$$

In Lemma 9, we discuss the duality between UR-SSAT and ER-SSAT formulas.

Lemma 9. Given Eq. (5.2) and (5.3), $\Pr[\Phi_{\text{UR}}] = 1 - \Pr[\Phi'_{\text{ER}}]$.

Proof of Lemma 9. Both Φ_{UR} and Φ'_{ER} have random quantified variables in the identical order in the prefix. According to the definition of SSAT formulas,

$$\Pr[\Phi_{\text{UR}}] = \min_{a_1, \dots, a_{m_2}} \Pr[\phi_{\hat{Y}}] \text{ and } \Pr[\Phi'_{\text{ER}}] = \max_{a_1, \dots, a_{m_2}} \Pr[\neg\phi_{\hat{Y}}],$$

where $\Pr[\phi_{\hat{Y}}]$ and $\Pr[\neg\phi_{\hat{Y}}]$ are both computed for the random values of non-sensitive features \mathbf{X} .

Therefore, we derive the following duality between ER-SSAT and UR-SSAT,

$$\begin{aligned} \Pr[\Phi'_{\text{ER}}] &= \max_{a_1, \dots, a_{m_2}} \Pr[\neg\phi_{\hat{Y}}] \\ &= \min_{a_1, \dots, a_{m_2}} (1 - \Pr[\phi_{\hat{Y}}]) \\ &= 1 - \min_{a_1, \dots, a_{m_2}} \Pr[\phi_{\hat{Y}}] \\ &= 1 - \Pr[\Phi_{\text{UR}}]. \end{aligned}$$

□

As we solve Φ'_{ER} , we obtain the optimal assignment to the sensitive features $\mathbf{a}_{\min} \triangleq [a_1^{\min}, \dots, a_{m_2}^{\min}]$ that maximizes Φ'_{ER} . If p is the maximum satisfying probability of Φ'_{ER} , then according to Lemma 9, $1 - p$ is the minimum satisfying probability of Φ_{UR} ; which is also the minimum probability of positive prediction of the classifier. We present the algorithm for the inference approach, namely `Justicia_infer` in Algorithm 5 (Line 9–14).

In the ER-SSAT formula in Eq. (5.3), we need to negate the classifier $\phi_{\hat{Y}}$ to another CNF formula $\neg\phi_{\hat{Y}}$. The naïve approach of negating one CNF to another CNF generates an exponential number of new clauses. Here, we apply Tseitin transformation for the negation, which increases the number of clauses linearly while introducing a linear number of new variables [180]. As an alternative approach, we directly encode the binary classifier \mathcal{M} for the negative class label $\hat{Y} = 0$ as a CNF formula and pass it to Φ'_{ER} , whenever it is possible. The latter approach is generally more efficient than the former approach as the resulting CNF is often smaller.

Example 5.1.2 (ER-SSAT encoding). Here, we illustrate the ER-SSAT encoding for inferring the most favored and the least favored sensitive group of a classifier in the presence of compound sensitive groups. As the example in Figure 5.1 is degenerate for this purpose, we introduce another Boolean sensitive feature ‘sex’ $\in \{\text{male}, \text{female}\}$.

We consider a Boolean variable S for sex where the literal S denotes sex = male. With this new sensitive feature, let the classifier be $\mathcal{M} \triangleq (\neg F \vee I \vee S) \wedge (F \vee J)$, where variables corresponding to sensitive features F, I , and J have same distributions as discussed in Example 5.1.1. Hence, we obtain the following ER-SSAT formula of \mathcal{M} to infer the most favored sensitive group:

$$\Phi_{\text{ER}} = \exists S, \exists A, \mathfrak{P}^{0.41} F, \mathfrak{P}^{0.93} I, \mathfrak{P}^{0.09} J, (\neg F \vee I \vee S) \wedge (F \vee J).$$

As we solve Φ_{ER} , we infer that the optimal assignment to the existential variables $\sigma(S) = 1, \sigma(A) = 0$, which implies that ‘male individuals with age < 40’ is the most favored group with probability of positive prediction computed as $\Pr[\Phi_{\text{ER}}] = 0.46$. Similarly, to infer the least favored group, we negate the CNF translation of the classifier \mathcal{M} to obtain the following ER-SSAT formula:

$$\Phi'_{\text{ER}} = \exists S, \exists A, \mathfrak{P}^{0.41} F, \mathfrak{P}^{0.93} I, \mathfrak{P}^{0.09} J, \neg((\neg F \vee I \vee S) \wedge (F \vee J)).$$

Solving Φ'_{ER} , we learn the optimal assignment $\sigma(S) = 0, \sigma(A) = 0$ and $\Pr[\Phi'_{\text{ER}}] = 0.57$. Thus, ‘female individuals with age < 40’ constitute the least favored group with probability of positive prediction as $1 - 0.57 = 0.43$. Thus, `Justicia_infer` allows us to infer the most and least favored sensitive groups and the corresponding discrimination.

We next prove the equivalence of `Justicia_enum` and `Justicia_infer` in Lemma 10.

Lemma 10. Let $\Phi_{\mathbf{a}}$ be an RE-SSAT formula for computing the probability of positive prediction of a classifier corresponding to the sensitive group $\mathbf{A} = \mathbf{a}$. Additionally, for the same classifier, let Φ_{ER} be an ER-SSAT formula for inferring the most favored sensitive group and Φ_{UR} be a UR-SSAT formula for inferring the least favored sensitive group. Therefore, $\max_{\mathbf{a} \in \mathbf{A}} \Pr[\Phi_{\mathbf{a}}] = \Pr[\Phi_{\text{ER}}]$ and $\min_{\mathbf{a} \in \mathbf{A}} \Pr[\Phi_{\mathbf{a}}] = \Pr[\Phi_{\text{UR}}]$.

Proof of Lemma 10. It is trivial that the probability of positive prediction of the classifier for the most favored group \mathbf{a}_{max} is the maximum computed probability of all compound groups $\mathbf{a} \in \mathbf{A}$. Similar argument holds for the least favored group \mathbf{a}_{min} , which obtains the minimum probability of positive prediction of the classifier among all compound groups $\mathbf{a} \in \mathbf{A}$.

By construction of the SSAT formulas, $\Pr[\Phi_{\text{ER}}]$ and $\Pr[\Phi_{\text{UR}}]$ are the probabilities corresponding to the groups $\mathbf{A} = \mathbf{a}_{\text{max}}$ and $\mathbf{A} = \mathbf{a}_{\text{min}}$, respectively. Now, since $\Pr[\Phi_{\mathbf{a}}]$ is the probability for the group $\mathbf{A} = \mathbf{a}$, we derive the following.

$$\max_{\mathbf{a} \in \mathbf{A}} \Pr[\Phi_{\mathbf{a}}] = \Pr[\Phi_{\text{ER}}] \text{ and } \min_{\mathbf{a} \in \mathbf{A}} \Pr[\Phi_{\mathbf{a}}] = \Pr[\Phi_{\text{UR}}]$$

□

5.1.3 Practical Settings

We now relax the assumptions of **Justicia** on an access to Boolean classifiers and Boolean features, and extend **Justicia** to verify fairness metrics for more practical settings of decision trees, linear classifiers, and continuous features.

5.1.3.1 Extension to Decision Trees and Linear Classifiers

In the SSAT approach, we assume that the classifier \mathcal{M} is represented as a CNF formula. We extend **Justicia** beyond CNF classifiers to decision trees and linear classifiers, which are widely used in the fairness studies [196, 147, 199].

Binary decision trees are trivially encoded as CNF formulas. In the binary decision tree, each node in the tree is considered as a literal. A *path from the root to the leaf* is a conjunction of literals and thus, a *clause*. The *tree* itself is a disjunction of all paths and thus, a *DNF (Disjunctive Normal Form)*. In order to derive a CNF of a decision tree, we first construct a DNF by including all paths terminating at leaves with negative class label ($\hat{Y} = 0$) and then complement the DNF to CNF using De Morgan’s rule.

Linear classifiers on Boolean features are encoded into CNF formulas using pseudo-Boolean encoding [141]. We consider a linear classifier $\mathbf{W}\mathbf{X} + b \geq 0$ on Boolean features \mathbf{X} with weights $\mathbf{W} \in \mathbb{R}^{|\mathbf{X}|}$ and bias $b \in \mathbb{R}$. We first normalize \mathbf{W} and b in $[-1, 1]$ and then round to integers so that the decision boundary becomes a pseudo-Boolean constraint [156]. Then we apply pseudo-Boolean constraints to CNF translation [141] to encode the decision boundary to CNF. This encoding usually introduces additional Boolean variables and results in a large CNF. In order to generate a smaller CNF, we can trivially apply thresholding on the weights to

consider features with higher weights only. For instance, if the weight $|W_i| \leq \lambda$ for a threshold $\lambda \in \mathbb{R}^+$ and $W_i \in \mathbf{W}$, we can set $W_i = 0$. Thus, features with lower weights (less important) do not appear in the encoded CNF. Moreover, all introduced variables in this CNF translation are given existential (\exists) quantification and they appear in the inner-most position in the prefix of the SSAT formula. Thus, the presented ER-SSAT formulas become effectively ERE-SSAT formulas.

5.1.3.2 Extension to Continuous Features

In practical problems, features are generally real-valued or categorical but classifiers, which are naturally expressed as CNF (Chapter 3), are generally trained on a Boolean abstraction of input features. In order to perform the Boolean abstraction, each categorical feature is one-hot encoded and each real-valued feature is discretized into a set of Boolean features (Chapter 3).

For a binary decision tree, each feature, including the continuous ones, is compared against a constant at each node (except leaves) of the tree. We assign a Boolean variable to each internal node of the tree (except leaves), where the $\{0, 1\}$ assignment to the variable decides one of the two branches to choose from the current node.

Linear classifiers are generally trained on continuous features, where we apply discretization in the following way. Let us consider a continuous feature X_c , where W is its weight during training. We discretize X_c to a set \mathbf{B} of Boolean features and recalculate the weight of each variable in \mathbf{B} based on W . We consider the an interval-based approach for discretizing X_c . For each interval in the continuous space of X_c , we consider a Boolean variable $B_i \in \mathbf{B}$, such that B_i is assigned 1 when the feature-value of X_c lies within the i^{th} interval and B_i is assigned 0 otherwise. Following that, we assign the weight of B_i to be $\mu_i W$, where μ_i is the mean of feature values in the i^{th} interval. We can show that if we consider infinite number of intervals, $X_c \approx \sum_i \mu_i B_i$.

5.2 Empirical Performance Analysis

In this section, we discuss the empirical studies to evaluate the performance of *Justicia* in verifying different fairness metrics and algorithms. We first discuss

the experimental setup and the objective of the experiments and then evaluate the experimental results.

5.2.1 Experimental Setup

We have implemented a prototype of **Justicia** in Python (version 3.7.3). The core computation of **Justicia** relies on solving SSAT formulas using an off-the-shelf SSAT solver. To this end, we employ the state of the art RE-SSAT solver of [98] and the ER-SSAT solver of [99]. Both solvers output the exact satisfying probability of the SSAT formula.

For comparative evaluation of **Justicia**, we have experimented with two state-of-the-art probabilistic fairness verifiers FairSquare and VeriFair, and a sample-based fairness measuring tool: AIF360. In the experiments, we have studied three type of classifiers: decision tree, logistic regression classifier, and CNF learner. Decision tree and logistic regression are implemented using scikit-learn module of Python [138] and we use the MaxSAT-based CNF learner IMLI (Chapter 3). We have used the PySAT library [77] for encoding the decision function of the logistic regression classifier into a CNF formula. In our experiments, we have verified two fairness-enhancing algorithms: reweighing algorithm [85] and optimized pre-processing algorithm [28]. We have experimented on multiple datasets containing multiple sensitive features: the UCI³ Adult and German-credit dataset, ProPublica’s COMPAS recidivism dataset [7], Ricci dataset [121], and Titanic dataset⁴.

Our empirical studies have following objectives:

1. How accurate and scalable **Justicia** is with respect to existing fairness verifiers: FairSquare and VeriFair?
2. Can **Justicia** verify the effectiveness of different fairness-enhancing algorithms on different datasets?
3. Can **Justicia** verify fairness in the presence of compound sensitive groups?
4. How robust is **Justicia** in comparison to sample-based tools such as AIF360 for varying sample sizes?

³<http://archive.ics.uci.edu/ml>

⁴<https://www.kaggle.com/c/titanic>

Table 5.1: Results on synthetic benchmark. ‘—’ refers that the verifier cannot compute the metric. The number in bold denotes the best result, where the estimated fairness metric is closest to the exact value.

Metric	Exact	Justicia	FairSquare	VeriFair	AIF360
Disparate impact	0.26	0.25	0.99	0.99	0.25
Statistical parity	0.53	0.54	—	—	0.54

- How do the computational efficiencies of `Justicia_infer` and `Justicia_enum` compare?

Our experimental studies validate that `Justicia` is more accurate and scalable than the state-of-the-art verifiers: `FairSquare` and `VeriFair`. `Justicia` is able to verify the effectiveness of different fairness-enhancing algorithms for multiple fairness metrics and datasets. `Justicia` achieves scalable performance in the presence of compound sensitive groups that the existing verifiers cannot handle. `Justicia` is also more robust than the sample-based tools such as `AIF360`. Finally, `Justicia_infer` is significantly efficient in terms of runtime than `Justicia_enum`.

5.2.2 Experimental Analysis

5.2.2.1 Accuracy: Less Than 1%-error

In order to assess the accuracy of different verifiers, we have considered the decision tree in Figure 5.1 for which the fairness metrics are analytically computable. In Table 5.1, we show the computed fairness metrics by `Justicia`, `FairSquare`, `VeriFair`, and `AIF360`. We observe that `Justicia` and `AIF360` yield more accurate estimates of disparate impact and statistical compared against the ground truth values of fairness metrics with less than 1% error. In contrast, `FairSquare` and `VeriFair` estimate disparate impact to be 0.99 and thus, being unable to verify the fairness violation. Therefore, `Justicia` is significantly more accurate than the existing formal verifiers: `FairSquare` and `VeriFair`.

5.2.2.2 Scalability: 1 to 3 Orders of Magnitude Speed-up

We have tested the scalability of `Justicia`, `FairSquare`, and `VeriFair` on practical benchmarks with a timeout of 900 seconds and reported the execution time of

Table 5.2: Scalability of different verifiers in terms of execution time (in seconds). The number in bold refers to the best result incurring minimum execution time among competitive verifiers. ‘—’ refers to timeout.

Classifier	Dataset	FairSquare	VeriFair	Justicia
Decision Tree	Ricci	4.8	5.3	0.1
	Titanic	16	1.2	0.1
	COMPAS	36.9	15.9	0.1
	Adult	—	295.6	0.2
Logistic Regression	Ricci	—	2.2	0.2
	Titanic	—	0.8	0.9
	COMPAS	—	11.3	0.2
	Adult	—	61.1	1.0

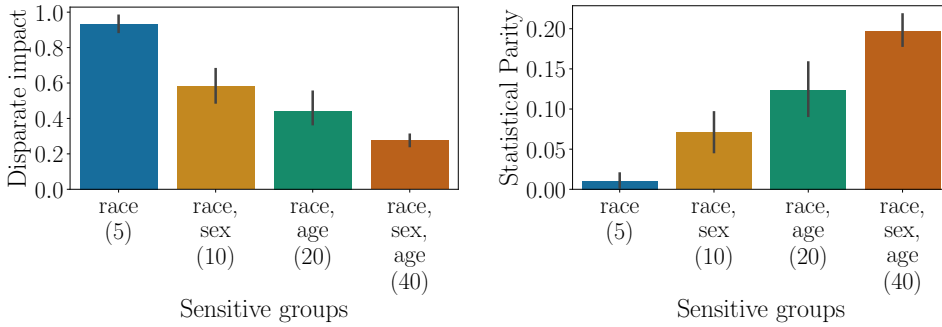


Figure 5.2: Fairness metrics measured by Justicia for different sensitive groups in the Adult dataset. The number within parenthesis in the xticks denotes total compound sensitive groups, which increases due to the increasing combination of sensitive features. For higher sensitive groups, fairness becomes worse.

these verifiers on decision tree and logistic regression in Table 5.2. We observe that Justicia shows impressive scalability than the competing verifiers. Particularly, among benchmarks where all three verifiers output results, Justicia is 1 to 2 orders of magnitude faster than FairSquare and 1 to 3 orders of magnitude faster than VeriFair. Additionally, FairSquare times out in most benchmarks. Thus, Justicia is not only accurate but also scalable than the existing verifiers.

5.2.2.3 Verification: Detecting Compounded Discrimination in Sensitive Groups

We have tested Justicia for datasets consisting of multiple sensitive features and reported results in Figure 5.2. Justicia operates on datasets with even 40

compound sensitive groups and can potentially scale more than that while the state-of-the-art fairness verifiers (e.g., FairSquare and VeriFair) consider a single sensitive feature with two sensitive groups. Thus, **Justicia** removes an important limitation in practical fairness verification, which was previously restricted to Boolean sensitive groups. Additionally, in most datasets, we observe that disparate impact decreases and thus, discrimination increases as more compound sensitive groups are considered. For instance, when we increase the total groups from 5 to 40 in the Adult dataset, disparate impact decreases from around 0.9 to 0.3, thereby detecting higher discrimination. Thus, **Justicia** detects that the marginalized individuals of a specific type (e.g., ‘race’) are even more discriminated and marginalized when they also belong to a marginalized group of another type (e.g., ‘sex’).

5.2.2.4 Verification: Fairness of Algorithms on Datasets

We have experimented with two fairness-enhancing algorithms: reweighing (RW) algorithm and optimized-preprocessing (OP) algorithm. Both of them pre-process to remove statistical bias from the dataset. We study the effectiveness of these algorithms using **Justicia** on different 5 datasets each with two different sensitive features. In Table 5.3, we report different fairness metrics on logistic regression and decision tree. We observe that **Justicia** verifies fairness improvement as the bias mitigating algorithms are applied. For example, for the Adult dataset with ‘race’ as the sensitive feature, disparate impact increases from 0.23 to 0.85 for applying the reweighing algorithm on logistic regression classifier. In addition, statistical parity decreases from 0.09 to 0.01, and equalized odds decreases from 0.13 to 0.03, thereby showing the effectiveness of reweighing algorithm in all three fairness metrics. **Justicia** also finds instances where the fairness algorithms fail, specially when considering the decision tree classifier. Thus, **Justicia** verifies the effectiveness of different fairness enhancing algorithms.

5.2.2.5 Robustness: Stability to Sample Size

We have empirically compared the robustness of our probabilistic fairness verifier **Justicia** with dataset-centric verifier AIF360 by varying the sample-size and reporting the standard deviation of different fairness metrics. In Figure 5.3, AIF360 shows higher standard deviation for lower sample-size and the value decreases as the

Table 5.3: Verification of different fairness enhancing algorithms for multiple datasets and classifiers using Justicia. Numbers in bold refer to fairness improvement compared against the unprocessed (orig.) dataset. RW and OP refer to reweighing and optimized-preprocessing algorithm respectively.

Classifier	Dataset →		Adult						COMPAS					
	Sensitive →		Race			Sex			Race			Sex		
	Algorithm →	orig.	RW	OP	orig.	RW	OP	orig.	RW	OP	orig.	RW	OP	
Logistic regression	Disparate impact	0.23	0.85	0.59	0.03	0.61	0.62	0.34	0.36	0.47	0.48	0.80	0.74	
	Statistical parity	0.09	0.01	0.05	0.16	0.04	0.03	0.39	0.33	0.21	0.23	0.09	0.10	
	Equalized odds	0.13	0.03	0.10	0.30	0.02	0.06	0.38	0.33	0.18	0.17	0.19	0.07	
Decision tree	Disparate impact	0.82	0.60	0.67	0.00	0.73	0.95	0.61	0.58	0.57	0.94	0.78	0.63	
	Statistical parity	0.02	0.05	0.04	0.14	0.05	0.01	0.18	0.17	0.17	0.02	0.09	0.18	
	Equalized odds	0.07	0.05	0.03	0.47	0.03	0.04	0.17	0.16	0.16	0.07	0.05	0.16	

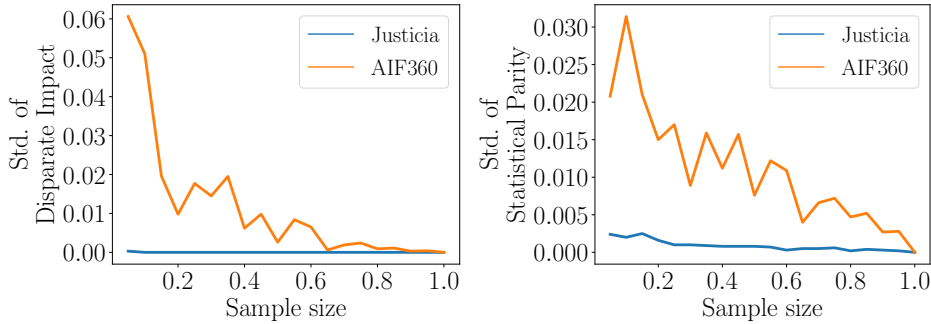


Figure 5.3: Standard deviation in estimation of disparate impact (DI) and stat. parity (SP) for different sample sizes (sample size = 1 refers to the entire dataset). **Justicia** is more robust with variation of sample size than **AIF360**. Sample size = 1 denotes the full dataset considering all samples.

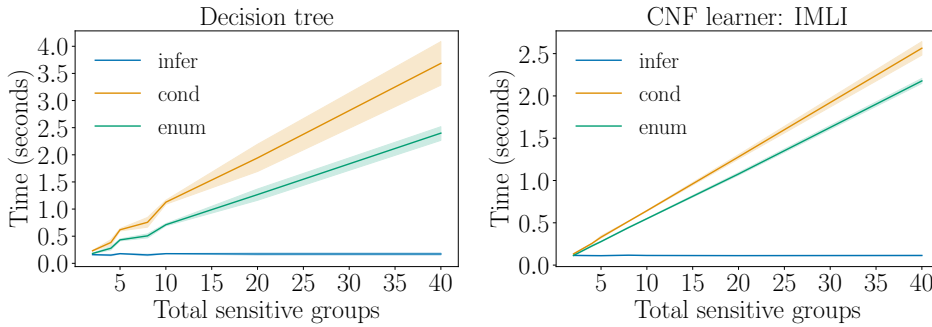


Figure 5.4: Runtime comparison of different encodings while varying total sensitive groups in the Adult dataset.

sample-size increases. In contrast, **Justicia** shows significantly lower ($\sim 10\times$ to $100\times$) standard deviation for different sample-sizes. The reason is that **AIF360** empirically measures on a fixed dataset whereas **Justicia** provides estimates over the distribution. Thus, **Justicia** is more robust than the sample-based verifier **AIF360**.

5.2.2.6 Comparative Evaluation of Different Encodings

Both **Justicia_enum** and **Justicia_infer** have the same output according to Lemma 10. However, **Justicia_infer** improves exponentially in runtime than **Justicia_enum** on both decision tree and Boolean CNF classifiers as we vary the total compound groups in Figure 5.4. **Justicia_cond** (**Justicia_enum** encoding where we consider conditional probabilities of non-sensitive features w.r.t. sensitive groups) also has an exponential trend in runtime similar to **Justicia_enum**. This analysis justifies that

the naïve enumeration-based approach cannot verify large-scale fairness problems containing multiple sensitive features, and `Justicia_infer` is a more efficient approach for practical use.

5.3 Chapter Summary

Formal verification of different fairness metrics of machine learning for different datasets is an important question. Existing fairness verifiers, however, are not scalable, accurate, and extendable to non-Boolean sensitive features. We discuss a stochastic SAT-based approach, `Justicia`, that formally verifies multiple group and causal fairness metrics for different classifiers and distributions for compound sensitive groups. Experimental evaluations demonstrate that `Justicia` achieves *higher accuracy* and *scalability* in comparison to the state-of-the-art verifiers, FairSquare and VeriFair, while yielding *higher robustness* than the sample-based tools, such as AIF360. A limitation of `Justicia` is the lack of consideration of feature correlations in the SSAT-based verifier, which we alleviate in the next chapter.

Chapter 6

Handling Feature Correlations in Fairness Verification

In this chapter, we extend formal fairness verification problem to a more practical scenario by accounting for the correlation of features, which is prevalent in most classification datasets. Existing fairness verifiers [4, 15], including Justicia in Chapter 5, suffer from limited accuracy due to considering specific input distribution. For example, they assume feature independence of non-sensitive features and consider correlated features within a limited scope, such as conditional probabilities of non-sensitive features with respect to sensitive features, and ignore correlations among non-sensitive features. Thus, it is desirable to design a fairness verification framework where the input is a probability distribution containing feature correlations.

Towards the goal of considering feature correlations in fairness verification, we particularly focus on the verification of *linear classifiers* because of the significant attention on linear classifiers in fair algorithms [143, 194, 45, 82]. In this context, existing approaches suffer from limited scalability while verifying linear classifiers. This is due to the encoding of linear classifiers into SSAT (Chapter 5) or SMT formulas [4]. For example, Justicia applies pseudo-Boolean to CNF translation of linear classifiers as a pre-processing step, and the encoding becomes large depending on the number of features and the precision of real-valued coefficients in linear classifiers.

Considering these two aspects, our goal in this chapter is to design a fairness verifier particularly tailored for linear classifiers that addresses both the scalability and accuracy challenges of existing verifiers.

Contributions. The contributions of this chapter are summarized below.

- *Framework:* We discuss a fairness verification framework, namely **FVGM** (**F**airness **V**erification with **G**raphical **M**odels), for accurately and efficiently verifying linear classifiers.
- *Scalability:* **FVGM** relies a novel *stochastic subset-sum* encoding for linear classifiers with an efficient pseudo-polynomial solution using dynamic programming.
- *Accuracy:* To address feature-correlations, **FVGM** considers a graphical model, particularly a Bayesian Network that represents conditional dependence (and independence) among features in the form of a Directed Acyclic Graph (DAG).
- *Experimental Results:* Experimentally, **FVGM** is more accurate and scalable than existing fairness verifiers; **FVGM** can verify group and causal fairness metrics for multiple fairness algorithms.

6.1 Fairness Verification with Graphical Models

In this section, we present **FVGM**, a fairness verification framework for linear classifiers that accounts for correlated features represented as a graphical model. The core idea of verifying fairness of a classifier is to compute the probability of positive prediction of the classifier with respect to all compound sensitive groups. To this end, **FVGM** solves a stochastic subset sum problem, **S3P**, that is equivalent to computing the probability of positive prediction of the classifier for the most and the least favored sensitive group¹. In this section, we first define **S3P** and present an efficient dynamic programming solution for **S3P**. We then extend **S3P** to consider correlated features as input. Finally, we conclude by discussing fairness verification based on the solution of **S3P**.

Problem Formulation. Given a linear classifier $\mathcal{M} : (\mathbf{X}, \mathbf{A}) \rightarrow \hat{Y}$ and a probability distribution \mathcal{D} of $\mathbf{X} \cup \mathbf{A}$, our objective is to compute $\max_{\mathbf{a}} \Pr[\hat{Y} = 1 | \mathbf{A} = \mathbf{a}]$ and $\min_{\mathbf{a}} \Pr[\hat{Y} = 1 | \mathbf{A} = \mathbf{a}]$ with respect to \mathcal{D} . In this study, we express a linear classifier \mathcal{M} as

¹The most (resp. least) favored sensitive group obtains the maximum (resp. minimum) probability of positive prediction of the classifier.

$$\hat{Y} = \mathbb{1} \left[\sum_i W_{X_i} X_i + \sum_j W_{A_j} A_j \geq \tau \right].$$

Here, W denotes the weight (or coefficients) of a feature, τ denotes the bias or the offset parameter of the classifier, and $\mathbb{1}$ is an indicator function. Hence, the prediction $\hat{Y} = 1$ if and only if the inner inequality holds. Thus, computing the maximum (resp. minimum) probability of positive prediction is equivalent to finding out the assignment of A_j 's for which the probability of satisfying the inner inequality is highest (resp. lowest). We reduce this computation into an instance of **S3P**. To perform this reduction, we assume weight W and bias τ as integers, and features $\mathbf{X} \cup \mathbf{A}$ as Boolean. In Sec. 6.1.5, we relax these assumptions and extend to the practical settings.

6.1.1 Stochastic Subset Sum Problem

Now, we formally describe the specification and semantics of **S3P**. **S3P** operates on a set of Boolean variables $\mathbf{B} = \{B_i\}_{i=1}^n \in \{0, 1\}^n$, where $W_i \in \mathbb{Z}$ is the weight of B_i , and $n \triangleq |\mathbf{B}|$. Given a constant threshold $\tau \in \mathbb{Z}$, **S3P** computes the *probability* of a subset of \mathbf{B} with sum of weights of non-zero variables to be at least τ . Formally,

$$S(\mathbf{B}, \tau) \triangleq \Pr \left[\sum_i W_i B_i \geq \tau \right].$$

Aligning with terminologies in stochastic satisfiability (SSAT) [106], we categorize the variables \mathbf{B} into two types: (i) *chance variables* that are stochastic and have an associated probability of being assigned to 1 and (ii) *choice variables* that we optimize while computing $S(\mathbf{B}, \tau)$. To specify the category of variables, we consider a *quantifier* $Q_i \in \{\mathfrak{P}^i, \exists, \forall\}$ for each B_i . Elaborately, \mathfrak{P}^p is a *random quantifier* corresponding to a chance variable $B \in \mathbf{B}$, where $p \triangleq \Pr[B = 1]$. In contrast, \exists is an *existential quantifier* corresponding to a choice variable B such that a Boolean assignment of B *maximizes* $S(\mathbf{B}, \tau)$. Finally, \forall is an *universal quantifier* for a choice variable B that fixes an assignment to B that *minimizes* $S(\mathbf{B}, \tau)$.

Now, we formally present the semantics of $S(\mathbf{B}, \tau)$ provided that each variable B_i has weight W_i and quantifier Q_i . Let $\mathbf{B}[2 : n] \triangleq \{B_j\}_{j=2}^n$ be the subset of \mathbf{B} without the first variable B_1 . Then $S(\mathbf{B}, \tau)$ is recursively defined as:

$$S(\mathbf{B}, \tau) = \begin{cases} \mathbb{1}[\tau \leq 0], & \text{if } \mathbf{B} = \emptyset \\ S(\mathbf{B}[2:n], \tau - \max\{W_1, 0\}), & \text{if } Q_1 = \exists \\ S(\mathbf{B}[2:n], \tau - \min\{W_1, 0\}), & \text{if } Q_1 = \forall \\ p_1 \times S(\mathbf{B}[2:n], \tau - W_1) + \\ (1 - p_1) \times S(\mathbf{B}[2:n], \tau), & \text{if } Q_1 = \mathfrak{P}^1 \end{cases} \quad (6.1)$$

Observe that when \mathbf{B} is empty, S is computed as 1 if $\tau \leq 0$, and $S = 0$ otherwise. For existential and universal quantifiers, we compute S based on the weight. Specifically, if $Q_1 = \exists$, we decrement the threshold τ by the maximum between W_1 and 0. For example, if $W_1 > 0$, B_1 is assigned 1, and assigned 0 otherwise. Therefore, by solving for an existential variable, we maximize S . In contrast, when if $Q_1 = \forall$, we fix an assignment of B_1 that minimizes S by choosing between the minimum of W_1 and 0. Finally, for random quantifiers, we decompose the computation of S into two sub-problems: one sub-problem where $B_1 = 1$ and the updated threshold becomes $\tau - W_1$ and another sub-problem where $B_1 = 0$ and the updated threshold remains the same. Herein, we compute S as the expected output of both sub-problems.

Remark. $S(\mathbf{B}, \tau)$ does not depend on the order of \mathbf{B} .

Computing Minimum and Maximum probability of positive prediction of Linear Classifiers Using S3P. For computing $\max_{\mathbf{a}} \Pr[\hat{Y} = 1 | \mathbf{A} = \mathbf{a}]$ of a linear classifier, we set existential quantifiers \exists to sensitive features A_j , randomized quantifiers \mathfrak{P} to non-sensitive features X_i and construct a set $\mathbf{B} = \mathbf{A} \cup \mathbf{X}$. The coefficients W_{A_j} and W_{X_i} of the classifier become weights of \mathbf{B} . Also, we get $n = m_1 + m_2$. For non-sensitive variables X_i , which are chance variables, we derive their marginal probability $p_i = \Pr[X_i = 1]$ from the distribution \mathcal{D} . According to semantic of S3P, setting \exists quantifiers on \mathbf{A} computes the maximum value of $S(\mathbf{B}, \tau)$ that equalizes the maximum probability of positive prediction of the classifier. In this case, the *inferred* assignment of \mathbf{A} implies the most favored group $\mathbf{a}_{\max} = \arg \max_{\mathbf{a}} \Pr[\hat{Y} = 1 | \mathbf{A} = \mathbf{a}]$. In contrast, to compute the minimum probability of positive prediction, we instead assign each variable A_j a universal

quantifier while keeping random quantifiers over X_i , and infer the least favored group $\mathbf{a}_{\min} = \arg \min_{\mathbf{a}} \Pr[\widehat{Y} = 1 | \mathbf{A} = \mathbf{a}]$.

6.1.2 A Dynamic Programming Solution

We discuss a dynamic programming approach [142, 189] to solve S3P as the problem has overlapping sub-problem properties. For example, $S(\mathbf{B}, \tau)$ can be solved by solving $S(\mathbf{B}[2 : n], \tau')$, where the updated threshold τ' , called the *residual threshold*, depends on the original threshold τ and the assignment of B_1 as shown in Eq. (6.1). Building on this observation, we discuss the recursion and terminating condition leading to our dynamic programming algorithm.

Recursion. We consider a function $\mathbf{dp}(i, \tau)$ that solves the sub-problem $S(\mathbf{B}[i : n], \tau)$, for $i \in \{1, \dots, n\}$. The semantics of $S(\mathbf{B}, \tau)$ in Eq. (6.1) induces the recursive definition of $\mathbf{dp}(i, \tau)$ as:

$$\mathbf{dp}(i, \tau) = \begin{cases} \mathbf{dp}(i + 1, \tau - \max\{W_i, 0\}), & \text{if } Q_i = \exists \\ \mathbf{dp}(i + 1, \tau - \min\{W_i, 0\}), & \text{if } Q_i = \forall \\ p_i \times \mathbf{dp}(i + 1, \tau - W_i) + \\ (1 - p_i) \times \mathbf{dp}(i + 1, \tau), & \text{if } Q_i = \mathfrak{F}^{p_i} \end{cases} \quad (6.2)$$

Eq. (6.2) shows that $S(\mathbf{B}, \tau)$ can be solved by instantiating $\mathbf{dp}(1, \tau)$, which includes all the variables in \mathbf{B} .

Terminating Condition. Let W_{neg} , W_{pos} , and W_{all} be the sum of negative, positive, and all weights of \mathbf{B} , respectively. We observe that $W_{neg} \leq W_{all} \leq W_{pos}$. Thus, for any i , if the residual threshold $\tau \leq W_{neg}$, there is always a subset of $\mathbf{B}[i : n]$ with sum of weights at least τ . Conversely, when $\tau > W_{pos}$, there is no subset of $\mathbf{B}[i : n]$ with sum of weights at least τ . We leverage this bound and tighten the terminating conditions of $\mathbf{dp}(i, \tau)$ in Eq. (6.3).

$$\mathbf{dp}(i, \tau) = \begin{cases} 1 & \text{if } \tau \leq W_{neg} \\ 0 & \text{if } \tau > W_{pos} \\ \mathbf{1}[\tau \leq 0] & \text{if } i = n + 1 \end{cases} \quad (6.3)$$

Eq. (6.2) and (6.3) together define our dynamic programming algorithm. While deploying the algorithm, we store $\text{dp}(i, \tau)$ in memory to avoid repetitive computations. This allows us to achieve a pseudo-polynomial algorithm (Lemma 11) instead of a naïve exponential algorithm enumerating all possible assignments. In particular, the time complexity is pseudo-polynomial for chance (random) variables and linear for choice (existential and universal) variables.

Lemma 11. Let n' be the number of existential and universal variables in \mathbf{B} . Let

$$W_{\exists} = \sum_{B_i \in \mathbf{B} | Q_i = \exists} \max\{W_i, 0\} \text{ and } W_{\forall} = \sum_{B_i \in \mathbf{B} | Q_i = \forall} \min\{W_i, 0\}$$

be the considered sum of weights of existential and universal variables, respectively. We can exactly solve S3P using dynamic programming with time complexity $\mathcal{O}((n - n')(\tau + |W_{neg}| - W_{\exists} - W_{\forall}) + n')$. The space complexity is $\mathcal{O}((n - n')(\tau + |W_{neg}| - W_{\exists} - W_{\forall}))$.

Proof. **Case 1: All n variables in \mathbf{B} have randomized quantifiers.**

At step i of the dynamic programming (Eq. (6.2)), we modify the residual threshold of that step, namely τ_i , either by subtracting W_i or by retaining it. Now, we observe that the residual threshold τ_i for any $i \in \{1, \dots, n\}$ will be in $[0, \tau + |W_{neg}|]$. This holds because if τ_i crosses these bounds, the dynamic programming is terminated as shown in Equation (6.3). Since all weights of $\{W_i\}_{i=1}^n$ are integers, the maximum number of values that the residual threshold can take, is $\tau + |W_{neg}|$. Thus, we need to store at most $n(\tau + |W_{neg}|)$ values in the memory for performing dynamic programming with n variables and $(\tau + |W_{neg}|)$ number of possible weights. Thus, the space complexity is $\mathcal{O}(n(\tau + |W_{neg}|))$.

In order to construct the dynamic programming table, we have to call the dp function $\mathcal{O}(n(\tau + |W_{neg}|))$ times, in the worst-case. Thus, the time complexity of our method is $\mathcal{O}(n(\tau + |W_{neg}|))$.

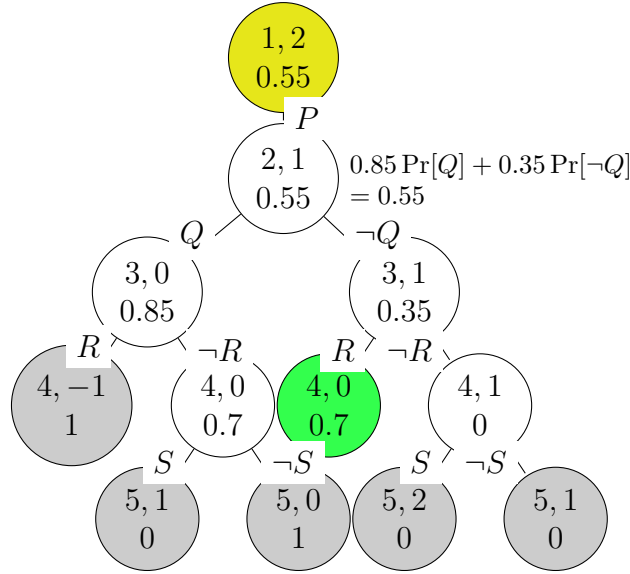
Case 2: n' variables have existential and universal quantifiers and $n - n'$ variables have randomized quantifiers in \mathbf{B} .

According to Eq. (6.2), W_{\exists} and W_{\forall} are the fixed weights of all existential and universal variables, respectively. Therefore, we need to consider at most $\tau + |W_{neg}| - W_{\exists} - W_{\forall}$ values of residual weights for random variables. By applying analysis in Case 1, the space and time complexity is derived as $\mathcal{O}((n - n')(\tau + |W_{neg}| - W_{\exists} - W_{\forall}))$.

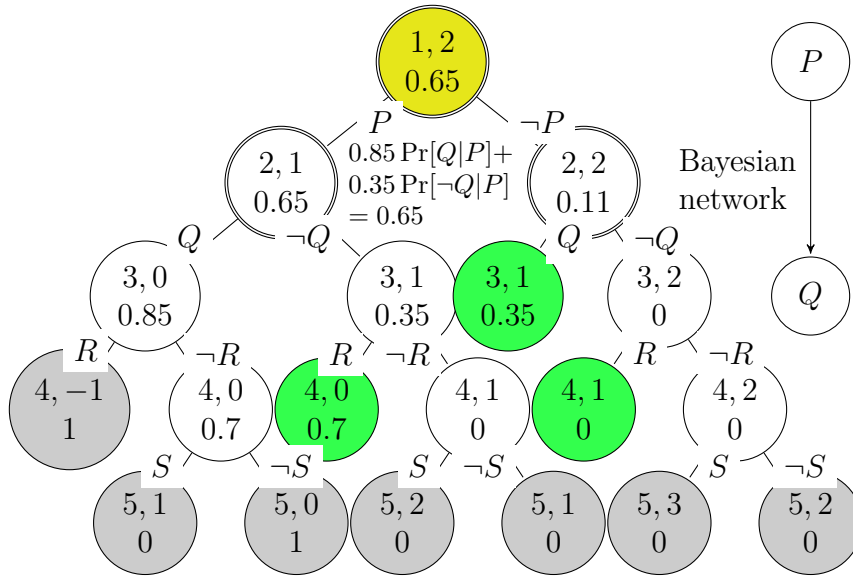
We note that there is an additional time complexity of $\mathcal{O}(n')$ for existential and universal variables in Eq. (6.2). Thus the time complexity becomes $\mathcal{O}((n - n')(\tau + |W_{neg}| - W_{\exists} - W_{\forall}) + n')$. We, however, do not require to store any entry for existential and universal variables in **dp** function and thus, the space complexity remains the same as $\mathcal{O}((n - n')(\tau + |W_{neg}| - W_{\exists} - W_{\forall}))$. \square

A Heuristic for Faster Computation. We discuss two improvements for a faster computation of the dynamic programming solution. Firstly, we observe that in Eq. (6.2), existential/universal variables are deterministically assigned based on their weights. Hence, we reorder **B** such that existential/universal variables appear earlier in **B** than random variables. This allows us to avoid unnecessary repeated exploration of existential/universal variables in **dp**. Moreover, according to the remark in Chapter 6.1.1, reordering **B** still produces the same exact solution of S3P. Secondly, to reach the terminating condition of $\mathbf{dp}(i, \tau)$ more frequently, we sort **B** based on their weights—more specifically, within each cluster of random, existential, and universal variables. In particular, if $\tau \leq 0.5(W_{pos} - W_{neg})$, τ is closer to W_{pos} than W_{neg} . Hence, we sort each cluster in descending order of weights. Otherwise, we sort in ascending order. We illustrate our dynamic programming approach in Example 6.1.1.

Example 6.1.1. We consider a linear classifier $P + Q + R - S \geq 2$. Herein, P is a Boolean sensitive feature, and Q, R, S are Boolean non-sensitive features with $\Pr[Q] = 0.4, \Pr[R] = 0.5$, and $\Pr[S] = 0.3$. To compute the maximum probability of positive prediction of the classifier, we impose an existential quantifier on P and randomized quantifiers on others. This leads us to the observation that $P = 1$ is the optimal assignment as $W_P = 1 > 0$. We now require to compute $\Pr[Q + R - S \geq 1]$, which by dynamic programming, is computed as 0.55. The solution is visualized as a search tree in Figure 6.1a, where we observe that storing the solution of sub-problems in the memory avoids repetitive computation, such as exploring the node $(4, 0)$. Similarly, the minimum probability of positive prediction of the classifier is 0.14 (not shown in Figure 6.1a) where we impose a universal quantifier on P to obtain $P = 0$ as the optimal assignment.



(a) Known marginal probabilities.



(b) Probabilities computed with a Bayesian network.

Figure 6.1: Search tree representation of S3P for computing the maximum probability of positive prediction of the classifier on variables $\mathbf{B} = \{P, Q, R, S\}$ with weights $\{1, 1, 1, -1\}$ and threshold $\tau = 2$. Each node is labeled by (i, τ') , where i is the index of \mathbf{B} and τ' is the residual threshold. The tree is explored using Depth-First Search (DFS) starting with left child. Within a node, the value in the bottom denotes $\text{dp}(i, \tau')$ that is solved recursively based on sub-problems $\text{dp}(i + 1, \cdot)$ in child nodes. Yellow nodes denote *existential* variables and all other nodes are *random* variables. Additionally, a green node denotes a collision, in which case a previously computed dp solution is returned. Leaf nodes (gray) are computed based on terminating conditions in Eq. (6.3). In Figure 6.1b, nodes with double circles, such as $\{(1, 2), (2, 1), (2, 2)\}$, are enumerated exponentially to compute conditional probabilities from the Bayesian network.

6.1.3 Stochastic Subset Sum Problem with Correlated Variables

In S3P presented in Chapter 6.1.1, we consider all Boolean variables to be probabilistically independent. This independence assumption often leads to an *inaccurate estimate* of the probability of positive prediction of the classifier because both sensitive and non-sensitive features can be correlated in practical fairness problems. Therefore, we extend S3P to include correlations among variables.

We consider a Bayesian network $\text{BN} = (G, \theta)$ to represent correlated variables, where $G \triangleq (\mathbf{V}, \mathbf{E})$, $\mathbf{V} \subseteq \mathbf{B}$, $\mathbf{E} \subseteq \mathbf{V} \times \mathbf{V}$, and θ is the parameter of the network. In BN, we constrain that there is no conditional probability of choice (i.e., existential and universal) variables as we optimize their assignment in S3P. Choice variables, however, can impose conditions on chance (i.e., random) variables. In practice, we achieve this by allowing no incoming edge on choice variables while learning BN (ref. Chapter 6.2).

For a chance variable $B_i \in \mathbf{V}$, let $\text{Pa}(B_i)$ denote its parents. According to Eq. (2.2), for an assignment \mathbf{u} of $\text{Pa}(B_i)$, BN ensures B_i to be independent of other non-descendant variables in \mathbf{V} . Hence, in the recursion of Eq. (6.2), we substitute p_i with $\Pr[B_i = 1 | \text{Pa}(B_i) = \mathbf{u}]$. In order to explicate the dependence on \mathbf{u} , we denote the expected solution of $S(\mathbf{B}[i : n], \tau)$ as $\text{dp}(i, \tau, \mathbf{u})$, which for $B_i \in \mathbf{V}$ is modified as follows:

$$\begin{aligned} \text{dp}(i, \tau, \mathbf{u}) &= \Pr[B_i = 0 | \text{Pa}(B_i) = \mathbf{u}] \text{dp}(i + 1, \tau, \mathbf{u} \cup \{0\}) \\ &\quad + \Pr[B_i = 1 | \text{Pa}(B_i) = \mathbf{u}] \text{dp}(i + 1, \tau - W_i, \mathbf{u} \cup \{1\}). \end{aligned}$$

Since $\text{dp}(i, \tau, \mathbf{u})$ involves \mathbf{u} , we initially perform a topological sort of \mathbf{V} to enumerate the assignment of parents before computing dp on the child. Moreover, there are $2^{|\text{Pa}(B_i)|}$ assignments of $\text{Pa}(B_i)$, and we compute $\text{dp}(i, \tau, \mathbf{u})$ for $\mathbf{u} \in \{0, 1\}^{|\text{Pa}(B_i)|}$ to incorporate all conditional probabilities into S3P. For this enumeration, we do not store $\text{dp}(i, \tau, \mathbf{u})$ in memory. However, for $B_i \notin \mathbf{V}$ that does not appear in the network, we instead compute $\text{dp}(i, \tau)$ and store it in memory as in Chapter 6.1.2, because B_i is not correlated with other variables. Lemma 12 presents the complexity of solving S3P with correlated variables, wherein unlike Lemma 11, the complexity differentiates based on variables in \mathbf{V} (exponential) and $\mathbf{B} \setminus \mathbf{V}$ (pseudo-polynomial).

Lemma 12. Let $\mathbf{V} \subseteq \mathbf{B}$ be the set of vertices in the Bayesian network and n'' be the number of existential and universal variables in $\mathbf{B} \setminus \mathbf{V}$. Let

$$w'_{\exists} = \sum_{B_i \in \mathbf{B} \setminus \mathbf{V} | Q_i = \exists} \max\{W_i, 0\} \text{ and } w'_{\forall} = \sum_{B_i \in \mathbf{B} \setminus \mathbf{V} | Q_i = \forall} \min\{W_i, 0\}$$

be the sum of considered weights of existential and universal variables, respectively that only appear in $\mathbf{B} \setminus \mathbf{V}$. To exactly compute S3P with correlated variables in the dynamic programming approach, time complexity is $\mathcal{O}(2^{|\mathbf{V}|} + (n - n'' - |\mathbf{V}|)(\tau + |W_{neg}| - w'_{\exists} - w'_{\forall}) + n'')$ and space complexity is $\mathcal{O}((n - n'' - |\mathbf{V}|)(\tau + |W_{neg}| - w'_{\exists} - w'_{\forall}))$.

Proof. We first separate analysis of space and time complexity for variables in \mathbf{V} and in $\mathbf{B} \setminus \mathbf{V}$. For each Boolean variable in \mathbf{V} , we enumerate all assignments, which has time complexity of $2^{|\mathbf{V}|}$ and there is no space complexity as discussed in Chapter 6.1.3.

For variables in $\mathbf{B} \setminus \mathbf{V}$, we apply analysis from Lemma 11, where we consider $(n - n'' - |\mathbf{V}|)$ random variables, n'' existential/universal variables, and residual weights can take at most $(\tau + |W_{neg}| - w'_{\exists} - w'_{\forall})$ values. Hence, time complexity is $\mathcal{O}((n - n'' - |\mathbf{V}|)(\tau + |W_{neg}| - w'_{\exists} - w'_{\forall}) + n'')$, and space complexity is $\mathcal{O}((n - n'' - |\mathbf{V}|)(\tau + |W_{neg}| - w'_{\exists} - w'_{\forall}))$

Combining two cases, overall time complexity is $\mathcal{O}(2^{|\mathbf{V}|} + (n - n'' - |\mathbf{V}|)(\tau + |W_{neg}| - w'_{\exists} - w'_{\forall}) + n'')$ and space complexity is $\mathcal{O}((n - n'' - |\mathbf{V}|)(\tau + |W_{neg}| - w'_{\exists} - w'_{\forall}))$. \square

A Heuristic for Faster Computation. We observe that to encode conditional probabilities, we enumerate all assignments of variables in \mathbf{V} that are in the Bayesian network. For computing the probability of positive prediction of a linear classifier with correlated features, we consider a heuristic to sort variables in $\mathbf{B} = \mathbf{A} \cup \mathbf{X}$. Let $\mathbf{V} \subseteq \mathbf{B}$ be the set of vertices in the network and $\mathbf{V}^c = \mathbf{B} \setminus \mathbf{V}$. In this heuristic, we sort sensitive variables \mathbf{A} by positioning $\mathbf{A} \cap \mathbf{V}$ in the beginning followed by $\mathbf{A} \cap \mathbf{V}^c$. Then we order the variables \mathbf{B} such that variables in \mathbf{X} precedes those in $\mathbf{X} \cap \mathbf{V}$, and the variables in $\mathbf{X} \cap \mathbf{V}^c$ follows the ones in $\mathbf{X} \cap \mathbf{V}$. This sorting allows us to avoid repetitive enumeration of variables in $\mathbf{V} \subseteq \mathbf{B}$ as they are placed earlier in \mathbf{B} .

Example 6.1.2. We extend Example 6.1.1 with a Bayesian Network (G, θ) with $\mathbf{V} = \{P, Q\}$ and $\mathbf{E} = \{(P, Q)\}$. Parameters θ imply conditional probabilities

$\Pr[Q|P] = 0.6$ and $\Pr[Q|\neg P] = 0.3$. In Figure 6.1b, we enumerate all assignment of P and Q to incorporate all conditional probabilities of Q given P . We, however, observe that the dynamic programming solution in Chapter 6.1.2 still prunes search space for variables that do not appear in \mathbf{V} , such as $\{R, S\}$. Hence following the calculation in Figure 6.1b, we obtain the maximum probability of positive prediction of the classifier as 0.65 for $P = 1$. The minimum probability of positive prediction (not shown) is similarly calculated as 0.11 for $P = 0$.

6.1.4 Fairness Verification using Probability of Positive Prediction

Given a classifier \mathcal{M} , a distribution \mathcal{D} , and a fairness metric f , verifying whether a classifier is ϵ -fair for $\epsilon \in [0, 1]$ is equivalent to computing $\mathbb{1}[f(\mathcal{M}|\mathcal{D}) \leq \epsilon]$. We now compute $f(\mathcal{M}|\mathcal{D})$ based on the maximum probability of positive prediction $\max_{\mathbf{a}} \Pr[\hat{Y} = 1|\mathbf{A} = \mathbf{a}]$ and the minimum probability of positive prediction $\min_{\mathbf{a}} \Pr[\hat{Y} = 1|\mathbf{A} = \mathbf{a}]$ of a classifier.

For measuring fairness metric SP, we compute the difference $\max_{\mathbf{a}} \Pr[\hat{Y} = 1|\mathbf{A} = \mathbf{a}] - \min_{\mathbf{a}} \Pr[\hat{Y} = 1|\mathbf{A} = \mathbf{a}]$. We, however, deploy FVGM twice while measuring EO, one for the distribution \mathcal{D} conditioned on $Y = 1$ and another for $Y = 0$. In each case, we compute $\max_{\mathbf{a}} \Pr[\hat{Y} = 1|\mathbf{A} = \mathbf{a}, Y = y] - \min_{\mathbf{a}} \Pr[\hat{Y} = 1|\mathbf{A} = \mathbf{a}, Y = y]$ for $y \in \{0, 1\}$ and take the maximum difference as the value of EO. For measuring causal metric PCF, we compute $\max_{\mathbf{a}} \Pr[\hat{Y} = 1|\mathbf{A} = \mathbf{a}, \mathbf{Z}]$ and $\min_{\mathbf{a}} \Pr[\hat{Y} = 1, \mathbf{Z}|\mathbf{A} = \mathbf{a}, \mathbf{Z}]$ conditioned on mediator features \mathbf{Z} and take their difference. To measure disparate impact DI, we compute the ratio $\max_{\mathbf{a}} \Pr[\hat{Y} = 1|\mathbf{A} = \mathbf{a}] / \min_{\mathbf{a}} \Pr[\hat{Y} = 1|\mathbf{A} = \mathbf{a}]$. In contrast to other fairness metrics, DI closer to 1 indicates higher fairness level. Thus, we verify whether a classifier achieves $(1 - \epsilon)$ -DI by checking $\mathbb{1}[f_{\text{DI}}(\mathcal{M}|\mathcal{D}) \geq 1 - \epsilon]$.

6.1.5 Extension to Practical Settings

For verifying linear classifiers with real-valued features and coefficients, we preprocess them so that FVGM can be invoked. Let $X \in \mathbb{R}$ be a continuous real-valued feature with coefficient $W \in \mathbb{R}$ in the classifier. We discretize X to a set \mathbf{B} of k Boolean variables using binning-based discretization and assign a Boolean variable to each bin. Hence, $B_i \in \mathbf{B}$ becomes 1, when X belongs to the i^{th} bin. Let

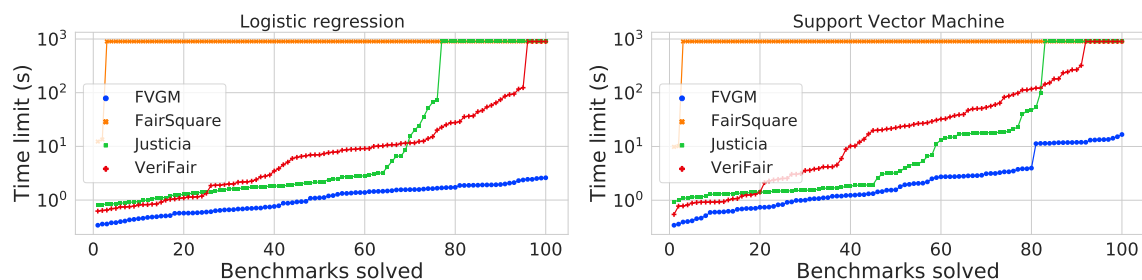


Figure 6.2: A cactus plot to present the scalability of different fairness verifiers. The number of solved benchmarks are on the X -axis and the required time is on the Y -axis; a point (x, y) implies that a verifier takes less than or equal to y seconds to compute fairness metrics of x many benchmarks. We consider 100 benchmarks generated from 5 real-world datasets using 5-fold cross-validation. In each fold, we consider $\{25, 50, 75, 100\}$ percent of non-sensitive features.

μ_i denote the mean of feature-values within i^{th} bin. We then set the coefficient of B_i as $\mu_i W$. By the law of large numbers, $X \approx \sum_i \mu_i B_i$ for infinitely many bins [64]. Finally, we multiply the coefficients of discretized variables by $l \in \mathbb{N} \setminus \{0\}$ and round to an integer. The accuracy of the preprocessing step relies on the number of bins k and the multiplier l . Therefore, we empirically fine-tune both k and l by comparing the processed classifier with the initial classifier on a validation dataset.

6.2 Empirical Performance Analysis

In this section, we empirically evaluate the performance of FVGM. We first present the experimental setup followed by experimental results.

Experimental Setup. We implement a prototype of FVGM in Python (version 3.8). We deploy the Scikit-learn library for learning linear classifiers such as Logistic Regression (LR) and Support Vector Machine (SVM) with linear kernels. We perform five-fold cross-validation on a dataset. While the classifier is trained on continuous features, we discretize them to Boolean features to be invoked by FVGM. During discretization, we apply a grid-search to estimate the best bin-size within a maximum bin of 10. To convert the coefficients of features into integers, we employ another grid-search to choose the best multiplier within $\{1, 2, \dots, 100\}$. For learning a Bayesian network on the converted Boolean data, we deploy the PGMPY

library [8]. For network learning, we apply a Hill-climbing search algorithm that learns a DAG structure by optimizing K2 score [88]. For estimating parameters of the network, we use Maximum Likelihood Estimation (MLE) algorithm.

We compare FVGM with three existing fairness verifiers: Justicia (Chapter 5), FairSquare [4], and VeriFair [15]. In the following, we discuss a comparative analysis among all verifiers based on scalability and accuracy, where FVGM yields superior performance than others.

6.2.1 Scalability Analysis

Benchmarks. We perform the scalability analysis on five real-world datasets studied in the literature of fairness in machine learning: UCI Adult, German-credit [44], COMPAS [7], Ricci [121], and Titanic (<https://www.kaggle.com/c/titanic>). We consider 100 benchmarks generated from 5 real-world datasets and report the computation times for disparate impact and statistical parity metrics of different verifiers.

Results. In Figure 6.2, we present the scalability results of different verifiers. First, we observe that FairSquare often times out (= 900 seconds) and can solve ≤ 5 benchmarks. This indicates that SMT-based reduction for linear classifiers cannot scale. Similarly, SSAT-based verifier Justicia that performs pseudo-Boolean to CNF translation for linear classifiers, times out for around 20 out of 100 benchmarks. Sampling-based framework, VeriFair, has comparatively better scalability than SMT/SSAT-based frameworks and can solve more than 90 benchmarks. Finally, FVGM achieves impressive scalability by solving all 100 benchmarks with 1 to 2 orders of magnitude runtime improvements than existing verifiers. Therefore, *S3P-based framework FVGM proves to be highly scalable in verifying fairness properties of linear classifiers than the state-of-the-art.*

6.2.2 Accuracy Analysis

Benchmark Generation. To perform accuracy analysis, we require the ground truth, which is not available for real-world instances. Therefore, we focus on

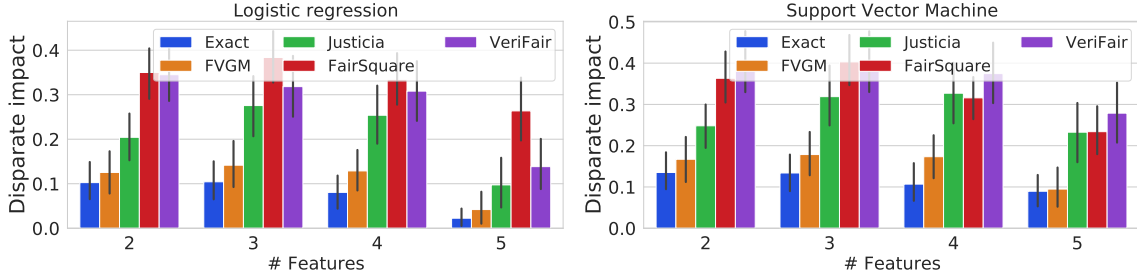


Figure 6.3: Comparing the average accuracy of different verifiers over 100 synthetic benchmarks while varying the number of features. **FVGM** yields the closest estimation of the analytically calculated *Exact* values of disparate impact for LR and SVM classifiers.

generating synthetic benchmarks for analytically computing the ground truth of different fairness metrics, such as disparate impact, from the known distribution of features. In each benchmark, we consider $n \in \{2, 3, 4, 5\}$ features including one Boolean sensitive feature, say A , generated from a Bernoulli distribution with mean 0.5. We generate non-sensitive features X_i from Gaussian distributions such that $\Pr[X_i|A = 1] \sim \mathcal{N}(\mu_i, \sigma^2)$ and $\Pr[X_i|A = 0] \sim \mathcal{N}(\mu'_i, \sigma^2)$, where $\mu_i, \mu'_i \in [0, 1]$, $\sigma = 0.1$, and μ_i, μ'_i are chosen from a uniform distribution in $[0, 1]$. Finally, we create label $Y = \mathbf{1}[\sum_{i=1}^{n-1} X_i \geq 0.5 \sum_{i=1}^{n-1} (\mu_i + \mu'_i)]$ such that Y does not directly depend on the sensitive feature. For each n , we generate 100 random benchmarks, learn LR and SVM classifiers on them, and compute disparate impact using different verifiers.

Analytic Computation of Disparate Impact. Let the coefficients of the classifier be w_i for X_i and w_A for A , and bias be τ . Since all non-sensitive features are from Gaussian distributions, we compute the probability of the predicted class $\Pr[\hat{Y}|A = 1] \sim \mathcal{N}(\sum_{i=1}^{n-1} w_i \mu_i, \sigma_{\hat{Y}}^2)$ and $\Pr[\hat{Y}|A = 0] \sim \mathcal{N}(\sum_{i=1}^{n-1} w_i \mu'_i, \sigma_{\hat{Y}}^2)$ with $\sigma_{\hat{Y}}^2 = (\sum_{i=1}^{n-1} w_i^2) \sigma^2$. Hence, the probability of positive prediction of the classifier is $1 - \text{CDF}_{\hat{Y}|A=1}(\tau - w_A)$ for $A = 1$ and $1 - \text{CDF}_{\hat{Y}|A=0}(\tau)$ for $A = 0$, where CDF is the cumulative distribution function. Finally, we compute disparate impact by taking the ratio of the minimum and the maximum of the probability of positive prediction of the classifier for $A = 1$ and $A = 0$.

Results. We assess the accuracy of the competing verifiers in estimating fairness metrics, specifically disparate impact with LR and SVM classifiers. In Figure 6.3, FVGM computes disparate impact closest to the *Exact* value for different number of features and both type of classifiers. In contrast, Justicia, FairSquare, and VeriFair measure disparate impact far from the *Exact* because of ignoring correlations among the features. For example, for SVM classifier with $n = 5$ (right plot in Figure 6.3), *Exact* disparate impact is 0.089 (average over 100 random benchmarks). Here, FVGM computes disparate impact as 0.094, while all other verifiers compute disparate impact as at least 0.233. Therefore, *FVGM is more accurate than existing verifiers as it explicitly considers correlations among features.*

6.3 Chapter Summary

We discuss FVGM, an efficient fairness verification framework for linear classifiers based on a novel stochastic subset-sum problem. FVGM encodes a graphical model of feature-correlations, represented as a Bayesian Network, and computes multiple group and causal fairness metrics accurately. We experimentally demonstrate that FVGM is more accurate and scalable than the existing verifiers.

Part IV

Epilogue

In Chapter 7, we envision towards combining two research themes in the thesis: interpretability and fairness, and discuss an algorithmic framework to interpret fairness in machine learning. In Chapter 8, we conclude the thesis and discuss future work.

Chapter 7

Interpreting Fairness: Identifying Sources of Bias

As demonstrated in Chapter 5 and 6, fairness metrics measure global bias, but do not detect or interpret its sources [16, 110, 133]. In order to diagnose the emergence of bias in the predictions of classifier, it is important to compute explanations, such as how different features attribute to the global bias. Motivated by the GDPR’s “right to explanation”, research on interpreting model predictions [151, 112, 111] has surged, but interpreting prediction bias has received less attention [16, 110]. In order to identify and interpret the sources of bias and also the impact of affirmative/punitive actions to alleviate/deteriorate bias, it is important to understand *which features contribute how much to the bias of a classifier* applied on a dataset. To this end, we follow a global feature-attribution approach to interpret the sources of bias, where we relate the *influences* of input features towards the resulting bias of the classifier. In this context, existing bias attributing methods [16, 110] are variants of local function approximation [171], whereas bias is a global statistical property of a classifier. Thus, *we aim to design a bias attribution method that is global by construction*. In addition, existing methods only attribute the individual influence of features on bias while neglecting the *intersectionality* among features. Quantifying intersectionality allows us to interpret bias induced by the higher-order interactions among features; hence accounting for intersectionality is important to understand bias as suggested by recent literature [27, 185]. In this chapter, *we aim to design a global bias attribution framework and a corresponding algorithm that can quantify both the individual and intersectional influences of features leading to granular and functional explanation of the sources of bias*.

Contributions. Our contributions are three-fold.

1. **Formalism:** We discuss how to measure the contribution of individual and intersectional features towards the bias of a classifier operating on a dataset by estimating their **F**airness **I**nfluence **F**unctions (FIFs) (Chapter 7.2). Our method is based on transforming existing fairness metrics into the difference of scaled conditional variances of classifier’s prediction, which we then decompose using Global Sensitivity Analysis (GSA)—a standard technique recommended by regulators to assess numerical models[52, 132]. FIFs have several desirable properties (Theorem 14), including the decomposability property [16, 110]. This property states that the sum of FIFs of all individual and intersectional features equals the bias of the classifier. With this formulation of FIFs, we can identify which features have the greatest influence on bias by looking at the disparity in their scaled decomposed variance between sensitive groups.
2. **Algorithmic:** We discuss a new algorithm, called **FairXplainer**, to estimate individual and intersectional FIFs of features given a dataset, a classifier, and a fairness metric. The algorithm is capable of working with any linear group fairness metric, including statistical parity, equalized odds, or predictive parity (Chapter 7.3). Building on GSA[161] techniques, **FairXplainer** solves a local regression problem [108] based on cubic splines [102] to decompose the variance of the classifier’s prediction among all the subsets of features.
3. **Experimental:** We evaluate **FairXplainer** on a variety of real-world datasets and machine learning classifiers to demonstrate its efficiency in estimating the individual and intersectional FIFs of features. Our results show that **FairXplainer** has a higher accuracy in approximating bias using estimated FIFs compared to existing methods (Chapter 7.4). Our estimation of FIFs also shows a strong correlation with fairness interventions. Furthermore, **FairXplainer** yields more granular explanation of the sources of bias by combining both individual and intersectional FIFs, and also detects patterns that existing fairness explainers cannot. Finally, **FairXplainer** enables us to observe changes in FIFs as a result of different fairness enhancing algorithms [28, 69, 86, 196,

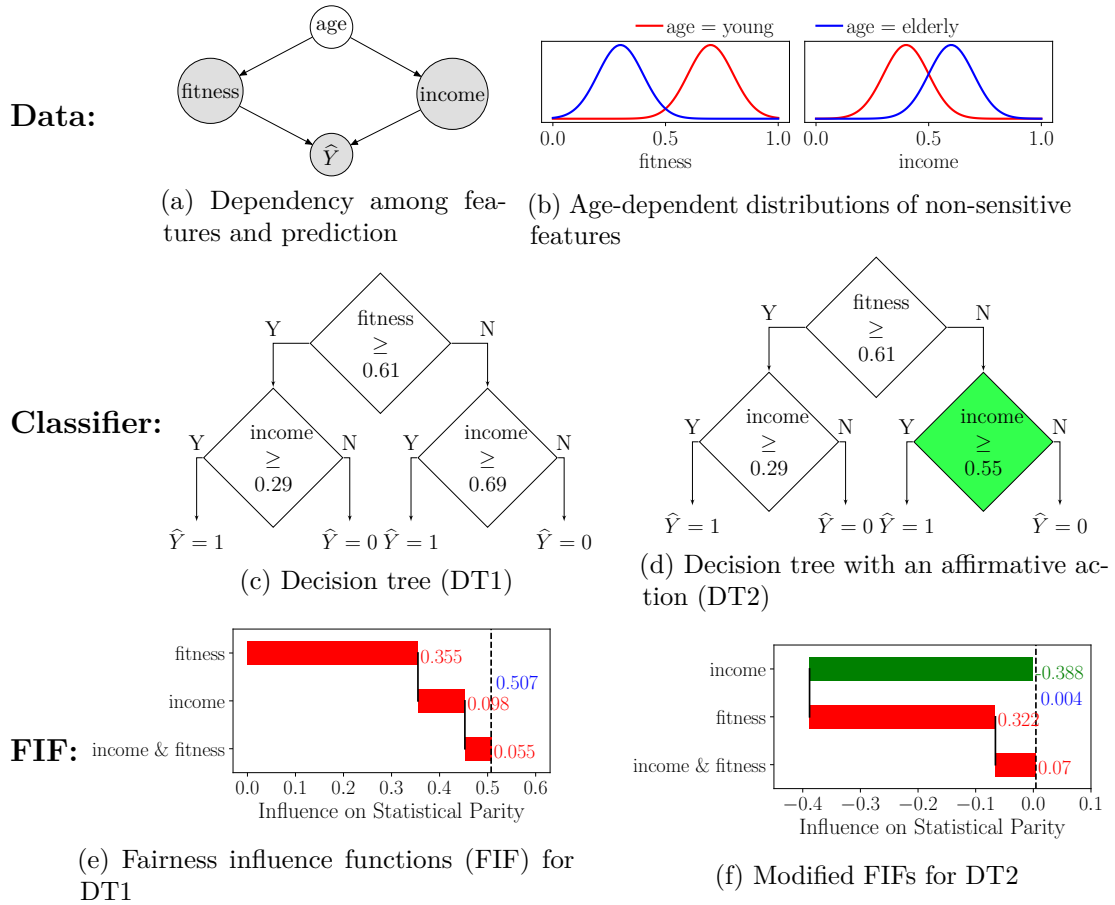


Figure 7.1: FIFs of input features to investigate the bias (statistical parity) of a decision tree predicting the eligibility for health insurance using age-dependent features ‘fitness’ and ‘income’. An affirmative action reduces bias as corresponding FIFs reflect it.

197, 198, 199] and fairness reducing attacks [72, 122, 174]. This creates opportunities to further examine the impact of these algorithms.

We illustrate the usefulness of our contributions via an example scenario presented in Example 5.0.1.

Example 7.0.1. We consider a classifier that decides an individual’s eligibility for health insurance based on non-sensitive features: fitness and income. Fitness and income depend on a sensitive feature $age \in \{\text{young}, \text{elderly}\}$ leading to two sensitive groups, as highlighted in (Figure 7.1a–7.1b).

Case study 1: For each sensitive group, we generate 1000 samples of (income, fitness) and train a decision tree (DT1), which predicts without explicitly using the

sensitive feature (Figure 7.1c). Using the 1000 samples and corresponding predictions, we estimate the statistical parity of DT1 as $\Pr[\hat{Y} = 1 \mid \text{age} = \text{young}] - \Pr[\hat{Y} = 1 \mid \text{age} = \text{elderly}] = 0.695 - 0.165 = 0.53$. Therefore, DT1 is unfair towards the elderly group.

Using the methods described in this chapter, we examine the sources of unfairness in DT1 by calculating the FIFs of each feature subset. Positive values represent a reduction in fairness due to increased statistical parity, while negative values indicate an improvement in fairness. The results, shown in the waterfall diagram in Figure 7.1e, indicate that fitness (FIF = 0.355), income (FIF = 0.098), and the combination of income and fitness (FIF = 0.055) contribute to higher statistical parity and bias. Fitness, being the root of DT1, has a greater impact on statistical parity than income, which is at the second level of DT1. Our method also reveals the joint effect of income and fitness on statistical parity, which prior methods do not account for (Chapter 7.1). The total of the FIFs of all features, $0.355 + 0.098 + 0.055 = 0.507 \approx 0.53$, approximately matches the statistical parity of the classifier, providing a way to break down the bias among all feature subsets. Note that we discuss the estimation error of FIFs in Chapter 7.3.

Case study 2: To address the unfairness of DT1 towards the elderly, we introduce DT2 which applies an affirmative action. Specifically, for lower fitness, which is typical for the elderly group (Figure 7.1b), we decrease the threshold on income from 0.69 to 0.55 (green node in Figure 7.1d). This allows more elderly individuals to receive insurance as they tend to have higher income, and the lower threshold accommodates their eligibility. The statistical parity of DT2 is calculated to be $\Pr[\hat{Y} = 1 \mid \text{age} = \text{young}] - \Pr[\hat{Y} = 1 \mid \text{age} = \text{elderly}] = 0.707 - 0.706 = 0.001$, which is negligible compared to the earlier statistical parity of 0.53 in DT1. We estimate the FIFs of features, with -0.388 for income, 0.322 for fitness, and 0.07 for both features combined. Hence, the negative influence of income confirms the affirmative action, and nullifies the disparity induced by fitness. Additionally, the sum of FIFs $-0.388 + 0.322 + 0.07 = 0.004$ coincides with the statistical parity of DT2.

7.1 Related Work

Recently, local explanation methods have been applied to black-box classifiers to explain sources of bias through feature-attribution[16, 110] and causal path decomposition[133]. Our work uses the feature-attribution approach and highlights three limitations of existing methods: (i) a failure to estimate intersectional FIFs, (ii) inaccuracies in approximating bias based on FIFs, and (iii) less correlation of FIFs to fairness intervention. Elaborately, to interpret group fairness—a global property of a classifier—existing local explanation approaches such as [16, 110] estimate FIFs based on a local black-box explainer SHAP [112]. They apply a global aggregation (i.e. expectation) of all local explanations corresponding to all data points in a dataset. Such a global aggregation of local explanations is often empirically justified and does not approximate bias accurately (Chapter 7.4). In addition, existing methods ignore the joint contribution of correlated features on bias. To address these limitations, *we develop a formal framework to interpret sources of group unfairness in a classifier and also a novel methodology to estimate FIFs. To the best of our knowledge, this is the first work to do both.*

Among other related works, [18] links GSA measures such as Sobol and Cramér-von-Mises indices to different fairness metrics. While their approach relates the GSA of sensitive features on bias, we focus on applying GSA to all features to estimate FIFs. *Their approach detects the presence or absence of bias, while we focus on decomposing bias as the sum of FIFs of all feature subsets.* In another line of work, [42] estimate feature-influence as the shifting of bias from its original value by randomly intervening features. Their work is different from the decomposability property of FIFs, where the sum of FIFs is equal to the bias. A separate line of work estimates the fairness influence of data points in a dataset [104, 187], while *our focus is on quantifying influences of input features.*

7.2 Fairness Influence Functions: Formulation and Properties

We formalize Fairness Influence Functions (FIF) as a quantifier of the contribution of a subset of features to the resultant bias of a classifier applied on a dataset. In

GSA, we observe that the variance of the output of a function can be attributed to the corresponding subset of input variables through variance decomposition (Eq. (2.5)). To leverage the power of GSA in fairness in machine learning, we first express the existing fairness metrics in terms of the variance of classifier’s prediction in Chapter 7.2.1. This allows us to formulate FIF by leveraging variance decomposition (Chapter 7.2.2).

7.2.1 Fairness Metrics as the Variance of Prediction

First we recall the definition of statistical parity in Chapter 2.3.2.

$$f_{\text{SP}}(\mathcal{M}, \mathbf{D}) \triangleq \max_{\mathbf{a}} \Pr[\hat{Y} = 1 | \mathbf{A} = \mathbf{a}] - \min_{\mathbf{a}} \Pr[\hat{Y} = 1 | \mathbf{A} = \mathbf{a}]$$

Therefore, the random variable central to computing statistical parity is $\mathbf{1}[\hat{Y} = 1 | \mathbf{A} = \mathbf{a}]$. We refer to this indicator function as *Conditional Positive Prediction (CPP)* of a classifier. Now, we express statistical parity as a functional of the probability of CPPs for different sensitive groups [18]. For brevity, we defer similar formulations for the other fairness metrics, i.e. equalized odds and predictive parity, to Appendix D.3.

Our key idea for computing FIFs of features is to represent fairness metrics using the variance of CPPs. Formally, we express statistical parity using the variance of CPPs in Lemma 13.

Lemma 13 (Statistical Parity as Difference of Variances of CPPs). Let $\mathbf{a}_{\max} = \arg \max_{\mathbf{a}} \Pr[\hat{Y} = 1 | \mathbf{A} = \mathbf{a}]$ and $\mathbf{a}_{\min} = \arg \min_{\mathbf{a}} \Pr[\hat{Y} = 1 | \mathbf{A} = \mathbf{a}]$ be the most and the least favored sensitive groups, respectively. The statistical parity of a binary¹ classifier is the difference in the scaled variance of CPPs. Formally, if $\Pr[\hat{Y} = 0 | \mathbf{A} = \mathbf{a}_{\max}] \neq 0$ and $\Pr[\hat{Y} = 0 | \mathbf{A} = \mathbf{a}_{\min}] \neq 0$,

$$f_{\text{SP}}(\mathcal{M}, \mathbf{D}) = \frac{\text{Var}[\hat{Y} = 1 | \mathbf{A} = \mathbf{a}_{\max}]}{\Pr[\hat{Y} = 0 | \mathbf{A} = \mathbf{a}_{\max}]} - \frac{\text{Var}[\hat{Y} = 1 | \mathbf{A} = \mathbf{a}_{\min}]}{\Pr[\hat{Y} = 0 | \mathbf{A} = \mathbf{a}_{\min}]}.$$

Proof. For a sensitive group \mathbf{a} , CPP is a Bernoulli random variable, where probability² $p_{\mathbf{a}} = \Pr[\hat{Y} = 1 | \mathbf{A} = \mathbf{a}]$ and variance $V_{\mathbf{a}} = \text{Var}[\hat{Y} = 1 | \mathbf{A} = \mathbf{a}] = p_{\mathbf{a}}(1 - p_{\mathbf{a}})$.

¹For a multi-class classifier, statistical parity of the target class $y \in \mathbb{N}$ is $\frac{\text{Var}[\hat{Y}=y|\mathbf{A}=\mathbf{a}_{\max}]}{1-\Pr[\hat{Y}=y|\mathbf{A}=\mathbf{a}_{\max}]} - \frac{\text{Var}[\hat{Y}=y|\mathbf{A}=\mathbf{a}_{\min}]}{1-\Pr[\hat{Y}=y|\mathbf{A}=\mathbf{a}_{\min}]}$.

²For any binary event E , expectation and probability are identical, $\mathbb{E}[\mathbf{1}(E)] = \Pr[E = 1]$.

Thus, for sensitive groups \mathbf{a}_{\max} and \mathbf{a}_{\min} , the statistical parity of the classifier is $p_{\mathbf{a}_{\max}} - p_{\mathbf{a}_{\min}} = \frac{V_{\mathbf{a}_{\max}}}{1-p_{\mathbf{a}_{\max}}} - \frac{V_{\mathbf{a}_{\min}}}{1-p_{\mathbf{a}_{\min}}}$. Replacing $1 - p_{\mathbf{a}} = \Pr[\hat{Y} = 0 \mid \mathbf{A} = \mathbf{a}]$ proves the lemma. \square

Example 7.0.1 (Revisited). From Figure 7.1c, the probability of CPPs of the decision tree for the most and least favored groups are $\Pr[\hat{Y} = 1 \mid \text{age} = \text{young}] = 0.695$ and $\Pr[\hat{Y} = 1 \mid \text{age} = \text{elderly}] = 0.165$, respectively. Thus, the statistical parity is $0.695 - 0.165 = 0.53$. Next, we compute variance of CPPs as $\text{Var}[\hat{Y} = 1 \mid \text{age} = \text{young}] = 0.212$ and $\text{Var}[\hat{Y} = 1 \mid \text{age} = \text{elderly}] = 0.138$. Thus, following Lemma 13, we compute the difference in the scaled variance of CPPs as $\frac{0.212}{1-0.695} - \frac{0.138}{1-0.165} = 0.529 \approx 0.53$, which coincides with the statistical parity reported earlier.

7.2.2 Formulation of FIF

We are given a binary classifier \mathcal{M} , a dataset \mathbf{D} , and a fairness metric $f(\mathcal{M}, \mathbf{D}) \in \mathbb{R}^{\geq 0}$. Our objective is to compute the influences of features on f . Particularly, we compute the influence of each subset of features $\mathbf{Z}_{\mathbf{S}}$, where $\mathbf{S} = \{S_i \mid 1 \leq |S_i| \leq m\} \subseteq [m]$ is a non-empty subset of indices of \mathbf{Z} .

Definition 1. Fairness Influence Function (FIF)³, denoted by $w_{\mathbf{S}} : (\mathcal{M}, \mathbf{Z}_{\mathbf{S}}) \rightarrow \mathbb{R}$, measures the quantitative contribution of features $\mathbf{Z}_{\mathbf{S}} \subseteq \mathbf{Z}$ on the incurred bias $f(\mathcal{M}, \mathbf{D})$. Leveraging the variance-difference representation of $f(\mathcal{M}, \mathbf{D})$ (Lemma 13) and variance decomposition (Eq. (2.5)), we particularly define $w_{\mathbf{S}}$ as

$$w_{\mathbf{S}} \triangleq \frac{V_{\mathbf{a}_{\max}, \mathbf{S}}}{\Pr[\hat{Y} = 0 \mid \mathbf{A} = \mathbf{a}_{\max}]} - \frac{V_{\mathbf{a}_{\min}, \mathbf{S}}}{\Pr[\hat{Y} = 0 \mid \mathbf{A} = \mathbf{a}_{\min}]}.$$
 (7.1)

Here, given a sensitive group \mathbf{a} , $V_{\mathbf{a}, \mathbf{S}} \triangleq \text{Var}_{\mathbf{Z}_{\mathbf{S}}}[\mathbb{E}_{\mathbf{Z} \setminus \mathbf{Z}_{\mathbf{S}}}[\hat{Y} = 1 \mid \mathbf{A} = \mathbf{a}, \mathbf{Z}_{\mathbf{S}}]] - \sum_{\mathbf{S}' \subset \mathbf{S}} V_{\mathbf{a}, \mathbf{S}'}$ is the contribution (decomposed variance) of features $\mathbf{Z}_{\mathbf{S}}$ in $\text{Var}[\hat{Y} = 1 \mid \mathbf{A} = \mathbf{a}]$.

Informally, the FIF $w_{\mathbf{S}}$ of $\mathbf{Z}_{\mathbf{S}}$ is the difference in the scaled decomposed variance of CPPs between sensitive groups \mathbf{a}_{\max} and \mathbf{a}_{\min} as induced by $\mathbf{Z}_{\mathbf{S}}$. Thus, FIF of features is non-zero when the scaled decomposed variance-difference of CPPs is non-zero for those features, and vice versa. We refer to $w_{\mathbf{S}}$ as an *individual influence*

³For equalized odds, a precise definition of FIF is $w_{\mathbf{S}} : (\mathcal{M}, Y, \mathbf{Z}_{\mathbf{S}}) \rightarrow \mathbb{R}$ taking the ground class Y as an additional input. For predictive parity, FIF is defined as $w_{\mathbf{S}} : (\mathcal{M}, \hat{Y}, \mathbf{Z}_{\mathbf{S}}) \rightarrow \mathbb{R}$ taking the predicted class \hat{Y} as an additional input.

when $|\mathbf{S}| = 1$, and as an *intersectional influence* when $|\mathbf{S}| > 1$. Being able to naturally quantify the higher-order influences allow FIFs to interpret the sources of bias in a more fine-grained manner. We experimentally validate this in Chapter 7.4.

Properties of FIF FIF as defined in Eq. (7.1) yields interesting properties, such as decomposability⁴, symmetry, and null properties, which we formally state in Theorem 14.

Theorem 14 (Properties of FIF). Let $f(\mathcal{M}, \mathbf{D})$ be the bias/unfairness of the classifier \mathcal{M} on dataset \mathbf{D} according to linear group fairness metrics such as statistical parity. Let $w_{\mathbf{S}}$ be the FIF of a subset of features $\mathbf{Z}_{\mathbf{S}}$ as defined in Eq. (7.1).

- (a) *The decomposability property* of FIF states that the sum of FIFs of all subset of features is equal to the bias of the classifier.

$$\sum_{\mathbf{S} \subseteq [m]} w_{\mathbf{S}} = f(\mathcal{M}, \mathbf{D}) \quad (7.2)$$

- (b) *The symmetry property* states that two features Z_i and Z_j are equivalent based on FIF if the sum of corresponding individual influences and the intersectional influences with all other features are the same. Mathematically,

$$\sum_{\mathbf{S}'' \subseteq [m] \setminus \{i, j\}} w_{\mathbf{S}'' \cup \{i\}} = \sum_{\mathbf{S}'' \subseteq [m] \setminus \{i, j\}} w_{\mathbf{S}'' \cup \{j\}} \quad (7.3)$$

if $\sum_{\mathbf{S}' \subseteq \mathbf{S} \cup \{i\}} w_{\mathbf{S}'} = \sum_{\mathbf{S}' \subseteq \mathbf{S} \cup \{j\}} w_{\mathbf{S}'}$ for every non-empty subset \mathbf{S} of $[m]$ containing neither i nor j .

- (c) *The null property* of FIF states that feature X_i is a dummy or neutral feature if sum of its individual influence and the intersectional influences with all other features is zero. Mathematically,

$$\sum_{\mathbf{S}'' \subseteq [m] \setminus \{i\}} w_{\mathbf{S}'' \cup \{i\}} = 0 \quad (7.4)$$

if $\sum_{\mathbf{S}' \subseteq \mathbf{S} \cup \{i\}} w_{\mathbf{S}'} = \sum_{\mathbf{S}' \subseteq \mathbf{S}} w_{\mathbf{S}'}$ for every non-empty subset \mathbf{S} of $[m]$ that does not contain i .

⁴Decomposability property is also known as the efficiency property in the context of Shapley values [155].

We emphasize that the decomposability property discussed here is global, i.e. it holds for a whole dataset, but the one used for Shapley-value based explanations (ref. Def. 1, [112]), or any local explanation method [68], is specific to a given data point [171]. Thus, they are fundamentally different.

The symmetry and null properties of FIFs also distinguish the FIF quantification discussed in Eq. (7.1) from the attribution methods considering only individual features, like SHAP. For example, a feature i has zero impact on bias if not only its individual influence but the sum of influences of all the subsets of features that includes i is zero. Thus, the symmetry and null properties stated here are by default global and intersectional, and these two aspects are absent in the existing bias explainers.

Bias Amplifying and Eliminating Features. The sign of $w_{\mathbf{S}}$ indicates whether features $\mathbf{Z}_{\mathbf{S}}$ amplify the bias of the classifier or eliminate it. When the scaled decomposed variance of CPPs w.r.t. features $\mathbf{Z}_{\mathbf{S}}$ for the sensitive group \mathbf{a}_{\max} is higher than the group \mathbf{a}_{\min} , $w_{\mathbf{S}} > 0$. As such, $\mathbf{Z}_{\mathbf{S}}$ increase bias. Conversely, when $w_{\mathbf{S}} < 0$, $\mathbf{Z}_{\mathbf{S}}$ eliminates bias, and improves fairness. Finally, features $\mathbf{Z}_{\mathbf{S}}$ are neutral in bias when $w_{\mathbf{S}} = 0$.

Now, we present the following two propositions that relate the sign of $w_{\mathbf{S}}$ with the decomposed variance of CPPs.

Proposition 15. When $w_{\mathbf{S}} < 0$, i.e. features $\mathbf{Z}_{\mathbf{S}}$ decrease bias, the decomposed variance of CPPs w.r.t. $\mathbf{Z}_{\mathbf{S}}$ follows $V_{\mathbf{a}_{\max}, \mathbf{S}} < V_{\mathbf{a}_{\min}, \mathbf{S}}$.

Proposition 15 implies that if a subset of features $\mathbf{Z}_{\mathbf{S}}$ is bias-eliminating, the conditional variance in positive outcomes induced by $\mathbf{Z}_{\mathbf{S}}$ is smaller for the most favoured group than that of the least favoured group.

Proposition 16. If the decomposed variance of CPPs w.r.t. $\mathbf{Z}_{\mathbf{S}}$ satisfies $V_{\mathbf{a}_{\max}, \mathbf{S}} > V_{\mathbf{a}_{\min}, \mathbf{S}}$, the corresponding FIF $w_{\mathbf{S}} > 0$, i.e. features $\mathbf{Z}_{\mathbf{S}}$ increase bias.

Proposition 16 implies that if the conditional variance in positive outcomes induced by $\mathbf{Z}_{\mathbf{S}}$ is larger for the most favoured group than that of the least favoured group, then this subset of features $\mathbf{Z}_{\mathbf{S}}$ is bias-inducing.

Special Cases. Since our FIF formulation is based on the variance of prediction, for (degenerate) cases when the conditional prediction of the classifier is always positive or always negative for any sensitive group, the variance of prediction becomes zero. This observation results in following two propositions.

Proposition 17 (Perfectly Unbiased Classifiers). When $\Pr[\hat{Y} = 1 \mid \mathbf{A} = \mathbf{a}_{\max}] = \Pr[\hat{Y} = 1 \mid \mathbf{A} = \mathbf{a}_{\min}]$ and both conditional probabilities are either 0 or 1, the FIF $w_{\mathbf{S}} = 0$ for all subsets of features $\mathbf{Z}_{\mathbf{S}}$.

When $\Pr[\hat{Y} = 1 \mid \mathbf{A} = \mathbf{a}_{\max}] = \Pr[\hat{Y} = 1 \mid \mathbf{A} = \mathbf{a}_{\min}]$ for a classifier, it means that the classifier equally yields positive predictions for each of the sensitive groups. Thus, there is no bias (in terms of statistical parity) in the classifier outcome. In that case, our formulation of FIF yields $w_{\mathbf{S}} = 0$ for all the subsets of features, and leads to a degenerate conclusion that all subsets of features are neutral or zero-bias inducing.

Proposition 18 (Perfectly Biased Classifier). When statistical parity is 1, i.e. $\Pr[\hat{Y} = 1 \mid \mathbf{A} = \mathbf{a}_{\max}] = 1$ and $\Pr[\hat{Y} = 1 \mid \mathbf{A} = \mathbf{a}_{\min}] = 0$, the sensitive features \mathbf{A} are solely responsible for bias. In this case, the FIF $w_{\mathbf{S}} = 0$ for all features.

When a classifier always yields positive predictions for the most favoured group and only negative predictions for the least favoured group, we obtain $\Pr[\hat{Y} = 1 \mid \mathbf{A} = \mathbf{a}_{\max}] = 1$ and $\Pr[\hat{Y} = 1 \mid \mathbf{A} = \mathbf{a}_{\min}] = 0$. This is a perfectly biased classifier, which can be expressed by the binary rule $\hat{Y} = 1$ if $\mathbf{A} = \mathbf{a}_{\max}$ and 0 otherwise. As the discrimination is only due to the sensitive features, our FIF formulation cannot attribute any bias to the any other subset of features, which leads to $w_{\mathbf{S}} = 0$ for all \mathbf{S} .

Remark. For detecting degenerate cases, we require to compute $\Pr[\hat{Y} = 1 \mid \mathbf{A} = \mathbf{a}_{\max}]$ and $\Pr[\hat{Y} = 1 \mid \mathbf{A} = \mathbf{a}_{\min}]$ on the dataset \mathbf{D} . Hence, the detection can be performed in a straightforward manner.

Expressing FIF in terms of the variance decomposition over a subset of features allows us to import and extend well-studied techniques of GSA to perform FIF estimation, which we elaborate on Chapter 7.3.

7.3 An Algorithm to Estimate Fairness Influence Functions

We discuss an algorithm, **FairXplainer**, that leverages the variance decomposition of CPPs to estimate the FIFs of all subsets of features. **FairXplainer** has two algorithmic blocks: (i) local regression to decompose the classifier into component functions taking distinct subsets of features as input and (ii) computing the variance (or covariance) of each component function. We describe the schematic of **FairXplainer** in Algorithm 6.

A Set-additive Representation of the Classifier. To apply variance decomposition (Eq. (2.5)), we learn a set-additive representation of the classifier (Eq. (2.4)) with input $\mathbf{Z} \equiv (\mathbf{X}, \mathbf{A})$. Let us denote the classifier \mathcal{M} conditioned on a sensitive group \mathbf{a} as $g_{\mathbf{a}}(\mathbf{Z}) \triangleq \mathcal{M}(\mathbf{X}, \mathbf{A} = \mathbf{a})$. We express $g_{\mathbf{a}}$ as a set-additive model:

$$g_{\mathbf{a}}(\mathbf{Z}) = g_{\mathbf{a},0} + \sum_{\mathbf{S} \subseteq [m], |\mathbf{S}| \leq \lambda} g_{\mathbf{a},\mathbf{S}}(\mathbf{Z}_{\mathbf{S}}) + \delta \quad (7.5)$$

Here, $g_{\mathbf{a},0}$ is a constant, $g_{\mathbf{a},\mathbf{S}}$ is a *component function* of $g_{\mathbf{a}}$ taking a non-empty subset of features $\mathbf{Z}_{\mathbf{S}}$ as input, and δ is the approximation error. For computational tractability, we consider only components of *maximum order* λ , denoting the maximum order of intersectionality. **FairXplainer** deploys backfitting algorithm for learning component functions in Eq. (7.5), as discussed in the following.

Local Regression with Backfitting. We perform local regression with backfitting algorithm to learn the component functions up to a given order λ (Line 6–13). Backfitting algorithm is an iterative algorithm, where in each iteration one component function, say $g_{\mathbf{a},\mathbf{S}}$, is learned while keeping other component functions fixed. Specifically, $g_{\mathbf{a},\mathbf{S}}$ is learned as a smoothed function of g and rest of the components $g_{\mathbf{a},\mathbf{S}'}$, where $\mathbf{S}' \neq \mathbf{S}$ is a non-empty subset of $[m]$. To keep every component function mean centered, backfitting requires to impose two constraints: (i) $g_{\mathbf{a},0} = \text{MEAN}(\{g(\mathbf{z}^{(i)})\}_{i=1, \mathbf{a}^{(i)}=\mathbf{a}}^n)$ (Line 7), which is the mean of $g_{\mathbf{a}}$ evaluated on data points belonging to the sensitive group \mathbf{a} ; and (ii) $\sum_{i=1, \mathbf{a}^{(i)}=\mathbf{a}}^n g_{\mathbf{a},\mathbf{S}}(\mathbf{z}_{\mathbf{S}}^{(i)}) = 0$ (Line 11), where $\mathbf{z}_{\mathbf{S}}^{(i)}$ is the subset of feature values associated with feature indices \mathbf{S} for the i -th data point $\mathbf{z}^{(i)}$. These constraints assign the expectation of $g_{\mathbf{a}}$ on the constant term $g_{\mathbf{a},0}$ and the variance of $g_{\mathbf{a}}$ to the component functions.

Algorithm 6 FairXplainer: An algorithm for estimating FIFs

Input: Classifier $\mathcal{M} : (\mathbf{X}, \mathbf{A}) \rightarrow \hat{Y}$, dataset $\mathbf{D} = \{(\mathbf{z}^{(i)}, y^{(i)})\}_{i=1}^n$, fairness metric $f(\mathcal{M}, \mathbf{D}) \in \mathbb{R}^{\geq 0}$, and maximum order of intersectional influence λ

Output: FIF $w_{\mathbf{S}}$ for the subsets of features $\{\mathbf{Z}_{\mathbf{S}}\}$

```

1:  $\mathbf{a}_{\max} = \arg \max_{\mathbf{a}} \Pr[\hat{Y} = 1 | \mathbf{A} = \mathbf{a}]$ ,  $\mathbf{a}_{\min} = \arg \min_{\mathbf{a}} \Pr[\hat{Y} = 1 | \mathbf{A} = \mathbf{a}]$ ,  $m \leftarrow |\mathbf{Z}|$ ,  $\mathbf{Z} \equiv (\mathbf{X}, \mathbf{A})$ 
2: for  $\mathbf{a} \in \{\mathbf{a}_{\max}, \mathbf{a}_{\min}\}$  do ▷ Enumerate for specific sensitive groups
3:    $g_{\mathbf{a}, \mathbf{S}}, g_{\mathbf{a}, 0} \leftarrow \text{LOCALREGRESSION}(\mathcal{M}(\mathbf{X}, \mathbf{A} = \mathbf{a}), \{\mathbf{z}^{(i)}\}_{i=1}^n, \lambda, m)$ 
4:    $V_{\mathbf{a}, \mathbf{S}} \leftarrow \text{COVARIANCE}(g_{\mathbf{a}}, \{\mathbf{z}^{(i)}\}_{i=1}^n, g_{\mathbf{a}, \mathbf{S}}, g_{\mathbf{a}, 0})$ 
5: Compute  $w_{\mathbf{S}}$  using  $V_{\mathbf{a}_{\max}, \mathbf{S}}$  and  $V_{\mathbf{a}_{\min}, \mathbf{S}}$  as in Equation (7.1)

6: function LOCALREGRESSION( $g_{\mathbf{a}}, \{\mathbf{z}^{(i)}\}_{i=1}^n, \lambda, m$ )
7:   Initialize:  $g_{\mathbf{a}, 0} \leftarrow \text{MEAN}(\{g(\mathbf{z}^{(i)})\}_{i=1, \mathbf{a}^{(i)}=\mathbf{a}}^n)$ ,  $\hat{g}_{\mathbf{a}, \mathbf{S}} \leftarrow 0, \forall \mathbf{S} \in [m], \mathbf{S} \neq \emptyset, |\mathbf{S}| \leq \lambda$ 
8:   while each  $\hat{g}_{\mathbf{a}, \mathbf{S}}$  does not converge do
9:     for each  $\mathbf{S}$  do
10:       $\hat{g}_{\mathbf{a}, \mathbf{S}} \leftarrow \text{SMOOTH}(\{g_{\mathbf{a}}(\mathbf{z}^{(i)}) - g_{\mathbf{a}, 0} - \sum_{\mathbf{S}' \neq \mathbf{S}} \hat{g}_{\mathbf{a}, \mathbf{S}'}(\mathbf{z}_{\mathbf{S}}^{(i)})\}_{i=1, \mathbf{a}^{(i)}=\mathbf{a}}^n)$ 
11:       $\hat{g}_{\mathbf{a}, \mathbf{S}} \leftarrow \hat{g}_{\mathbf{a}, \mathbf{S}} - \text{MEAN}(\{\hat{g}_{\mathbf{a}, \mathbf{S}}(\mathbf{z}_{\mathbf{S}}^{(i)})\}_{i=1, \mathbf{a}^{(i)}=\mathbf{a}}^n)$  ▷ Mean centering
12:
13:   return  $g_{\mathbf{a}, \mathbf{S}}, g_{\mathbf{a}, 0}$ 
14: function COVARIANCE( $g_{\mathbf{a}}, \{\mathbf{z}^{(i)}\}_{i=1}^n, g_{\mathbf{a}, \mathbf{S}}, g_{\mathbf{a}, 0}$ )
15:
16:   return  $\sum_{i=1, \mathbf{a}^{(i)}=\mathbf{a}}^n g_{\mathbf{a}, \mathbf{S}}(\mathbf{z}_{\mathbf{S}}^{(i)})(g_{\mathbf{a}}(\mathbf{z}^{(i)}) - g_{\mathbf{a}, 0})$ 

```

While performing local regression, backfitting uses a smoothing operator [107] over the set of data points (Line 10). A smoothing operator, referred as SMOOTH, allows us to learn a global representation of a component function by smoothly interpolating $\tau + 2$ local points obtained by local regression [107]. In this chapter, we apply cubic spline smoothing [102] to learn each component function. Cubic spline is a piecewise polynomial of degree 3 with C^2 continuity interpolating local points in τ intervals. Hence, the first and second derivatives of each piecewise term are zero at the endpoints of intervals. We refer to Appendix D.2 for details of implementation. An ablation study demonstrating the impacts of the hyperparameters τ and λ on the performance of FairXplainer is in Appendix D.4.

Variance and Covariance Computation. Once each component function $g_{\mathbf{a}, \mathbf{S}}$ is learned with LOCALREGRESSION (Line 6–13), we compute variances of the component functions and their covariances using $g_{\mathbf{a}}(\cdot)$. Since each component

function is mean centered (Line 11), we compute the variance of $g_{\mathbf{a},\mathbf{S}}$ for the dataset \mathbf{D} as $\text{Var}[g_{\mathbf{a},\mathbf{S}}] = \sum_{i=1, \mathbf{a}^{(i)}=\mathbf{a}}^n (g_{\mathbf{a},\mathbf{S}}(\mathbf{z}_{\mathbf{S}}^{(i)}))^2$. Hence, variance captures the independent effect of $g_{\mathbf{a},\mathbf{S}}$. Covariance is computed to account for the correlation among features \mathbf{Z} . We compute the covariance of $g_{\mathbf{a},\mathbf{S}}$ with $g_{\mathbf{a}}$ on the dataset as

$$\text{Cov}[g_{\mathbf{a},\mathbf{S}}, g_{\mathbf{a}}] = \sum_{i=1, \mathbf{a}^{(i)}=\mathbf{a}}^n g_{\mathbf{a},\mathbf{S}}(\mathbf{z}_{\mathbf{S}}^{(i)}) (g_{\mathbf{a}}(\mathbf{z}^{(i)}) - g_{\mathbf{a},0}).$$

Here, $g_{\mathbf{a}}(\cdot) - g_{\mathbf{a},0}$ is the mean centered form of $g_{\mathbf{a}}$. Covariance of $g_{\mathbf{a},\mathbf{S}}$ can be both positive and negative depending on whether the features $\mathbf{Z}_{\mathbf{S}}$ are positively or negatively correlated with $g_{\mathbf{a}}$. Specifically, under the set additive model, we obtain $\text{Cov}[g_{\mathbf{a},\mathbf{S}}, g_{\mathbf{a}}] = \text{Var}[g_{\mathbf{a},\mathbf{S}}] + \text{Cov}[g_{\mathbf{a},\mathbf{S}}, \sum_{\mathbf{S}' \neq \mathbf{S}} g_{\mathbf{a},\mathbf{S}}']$. Now, we use $V_{\mathbf{a},\mathbf{S}} = \text{Cov}[g_{\mathbf{a},\mathbf{S}}, g_{\mathbf{a}}]$ as the effective variance of $\mathbf{Z}_{\mathbf{S}}$ for a given sensitive group \mathbf{a} (Line 14–16). In Line 1–5, we compute $V_{\mathbf{a},\mathbf{S}}$ for the most and the least favored groups, and plug them in Eq. (7.1) to yield an estimate of FIF of $\mathbf{Z}_{\mathbf{S}}$.

Proposition 19 (Time Complexity of FairXplainer). Let t be the number of iterations of the backfitting algorithm, m be the number of features, λ be the maximum order of intersectional features, and s be the runtime complexity of the smoothing oracle⁵. Then, the runtime complexity of Algorithm 6 is $\mathcal{O}\left(ts \sum_{i=1}^{\lambda} \binom{m}{i}\right)$. For example, if we are interested in up to first and second order intersectional features, the runtime complexities are $\mathcal{O}(tsm)$ and $\mathcal{O}(tsm^2)$, respectively.

7.4 Empirical Performance Analysis

In this section, we perform an empirical evaluation of FairXplainer. Particularly, we discuss the experimental setup, the objectives of experiments, and experimental results.

Experimental Setup. We implement a prototype of FairXplainer in Python (version 3.7.6). To estimate FIFs, we leverage and modify the ‘HDMR’ module in SALib library [70] based on global sensitivity analysis. In experiments, we consider four widely studied datasets from fairness literature, namely German-credit [46], Titanic (<https://www.kaggle.com/c/titanic>), COMPAS [7], and Adult dataset [46].

⁵Typically, the runtime complexity of smoothing oracles, particularly of cubic splines, is linear with respect to n , i.e. the number of samples [179].

We deploy Scikit-learn [138] to learn different classifiers: logistic regression classifier, support vector machine (SVM), neural network, and decision tree with 5-fold cross-validation. In experiments, we specify FairXplainer to compute intersectional influences up to the second order ($\lambda = 2$). While applying cubic-spline based local regression in FairXplainer, we set τ , the number of spline intervals to 6. We compare FairXplainer with the existing Shapley-valued based FIF computational framework (<https://shorturl.at/iqtuX>), referred as SHAP [110]. For both FairXplainer and SHAP, we set a timeout of 300 seconds for estimating FIFs. In addition, we deploy FairXplainer along with a fairness-enhancing algorithm [85] and a fairness attack [174] algorithm, and analyze the effect of these algorithms on the FIFs and the resultant fairness metric. In the following, we discuss the objectives of our empirical study.

1. *Performance*: How **accurate and computationally efficient** FairXplainer and SHAP are in approximating the bias of a classifier based on estimated FIFs?
2. *Functionality*: How do FIFs estimated by FairXplainer and SHAP **correlate with the impact a fairness intervention** strategy on features?
3. *Granularity of explanation*: How effective are the **intersectional FIFs** in comparison with the **individual FIFs** while tracing the sources of bias?
4. *Application*: How do FIFs quantify the impact of **applying** different fairness enhancing algorithms, i.e. **affirmative actions**, and fairness attacks, i.e. **punitive actions**?

In summary, (1) we observe that FairXplainer yields *less estimation error* than SHAP while approximating statistical parity using FIFs. FairXplainer incurs lower execution time, i.e. *better efficiency in computing individual FIFs* than SHAP while also enabling computation of intersectional FIFs for real-world datasets and classifiers. (2) While considering a fairness intervention, i.e. change in bias due to omission of a feature, FIFs estimated by FairXplainer have *higher correlation with increase/decrease in bias due to the intervention than SHAP*. Thus, FairXplainer demonstrates to be a *better choice for identifying the features influencing the group fairness metrics* than SHAP. (3) *By quantifying both the individual and intersectional influences of features,*

Table 7.1: Median error (over 5-fold cross validation and all combinations of sensitive features) of estimating statistical parity, $|\text{SP} - \widehat{\text{SP}}|$, using FIFs computed by different methods (columns 5 to 7). Best results (lowest error) are in bold color. ‘—’ denotes timeout.

Dataset	Dimension (n, m)	Max $ \mathbf{A} $	Classifier	SHAP	FairXplainer	
					$\lambda = 1$	$\lambda = 2$
Titanic	(834, 11)	3	Logistic Regression	2.018	0.218	0.003
			SVM	1.000	0.137	0.000
			Neural Network	—	0.215	0.003
			Decision Tree	0.018	0.396	0.079
German	(417, 23)	2	Logistic Regression	0.361	0.205	—
			SVM	0.676	0.218	—
			Neural Network	—	0.181	0.001
			Decision Tree	0.000	0.262	0.001
COMPAS	(5771, 8)	3	Logistic Regression	0.468	0.118	0.056
			SVM	0.360	0.037	0.020
			Neural Network	—	0.108	0.053
			Decision Tree	0.041	0.087	0.055
Adult	(26048, 11)	3	Logistic Regression	2.751	0.109	0.011
			SVM	0.963	0.095	0.001
			Neural Network	—	0.067	0.000
			Decision Tree	0.027	0.146	0.081

FairXplainer *leads to a more accurate and granular interpretation of the sources of bias*, which is absent in earlier bias explaining methods like SHAP. (4) Finally, as an application of the FIF formulation, FairXplainer also detects the effects of the affirmative and punitive actions on the bias of a classifier and the corresponding tensions between different subsets of features. Here, we elaborate on experimental results, and defer additional experiments such as applying FairXplainer on other fairness metrics: equalized odds and predictive parity, and an ablation study of hyper-parameters: maximum order of intersectionality λ and spline intervals τ to Appendix D.4.

7.4.1 Performance and Functionality in Estimating FIFs

Accurate Approximation of Bias with FIFs. We compare FairXplainer with SHAP in estimating statistical parity by summing all FIFs, as dictated by the decomposability property (Theorem 14). To our best knowledge, the ground truth

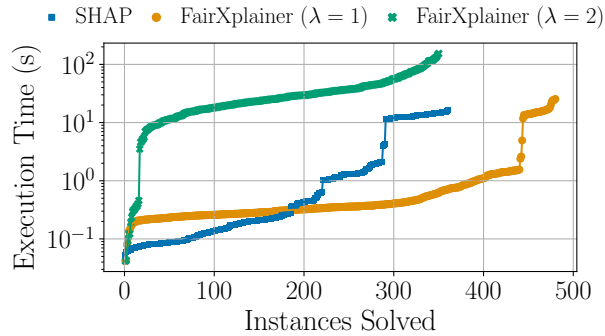


Figure 7.2: Execution time of different methods for estimating FIFs. **FairXplainer** with $\lambda = 1$ is more efficient than SHAP, while **FairXplainer** ($\lambda = 2$) requires more computational effort.

of FIF is not known for real-world datasets and classifiers. As such, we cannot compare accuracy of **FairXplainer** and SHAP directly on the estimated FIFs. Since both methods follow the decomposability property, one way to compare them is to test accuracy of the sum of estimated FIFs yielding bias/unfairness, as the ground truth of bias of a classifier can be exactly calculated for a given dataset [17]. We compute estimation error by taking the absolute difference between the exact and estimated values of statistical parity, and present median results in Table 7.1.

In general, **FairXplainer** achieves less estimation with $\lambda = 2$ than with $\lambda = 1$ in all datasets and classifiers. This implies that combining intersectional FIFs with individual FIFs captures bias more accurately than the individual FIFs alone. In each dataset, **FairXplainer** ($\lambda = 2$) demonstrates less estimation error than SHAP in all classifiers except in decision trees, denoting that GSA based approach **FairXplainer** is more accurate in approximating group fairness metrics through FIFs than the local explainer SHAP. In decision trees, **FairXplainer**—which is model-agnostic in methodology—with $\lambda = 2$ often demonstrates a comparable accuracy with SHAP, especially the optimized tree-based explanation counterpart of SHAP [111]. In the context of neural networks, SHAP, particularly Kernel-SHAP, often fails to estimate FIFs within the provided time-limit, while **FairXplainer** with $\lambda = 2$ yields highly accurate estimates (median estimation error between 0 to 0.053). Therefore, we conclude that *FairXplainer is more accurate in estimating statistical parity using FIFs than SHAP.*

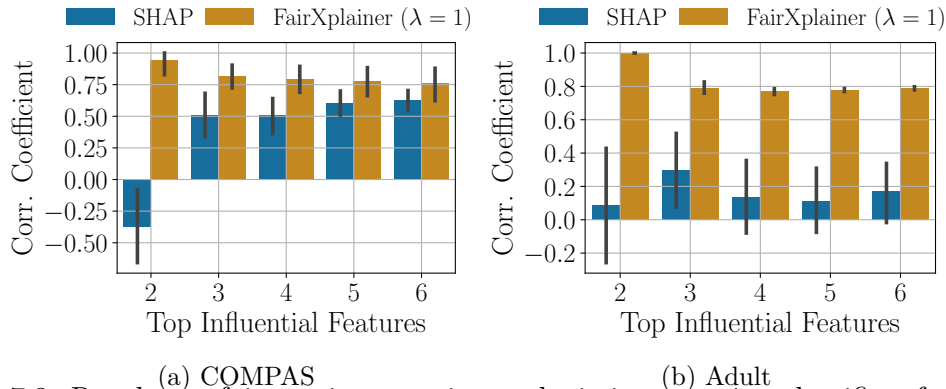


Figure 7.3: Results on fairness intervention on logistic regression classifiers for COMPAS and Adult datasets. Pearson’s correlation coefficient between bias-difference due to the intervention and FIFs is higher for top ranked influential features by FairXplainer compared to SHAP.

Execution Time: FairXplainer vs. SHAP We compare the execution time of FairXplainer vs. SHAP in a cactus plot in Figure 7.2, where a point (x, y) denotes that a method computes FIFs of x many fairness instances within y seconds. We consider 480 fairness instances from 4 datasets constituting 24 distinct combinations of sensitive features, 4 classifiers, and 5 cross-validation folds. In Figure 7.2, FairXplainer with $\lambda = 1$ is faster than $\lambda = 2$. For example, within 10 seconds, FairXplainer with $\lambda = 1$ solves 443 instances vs. 41 instances with $\lambda = 2$. In addition, FairXplainer with $\lambda = 1$ solves all 480 instances compared to 360 instances solved by SHAP. Thus, FairXplainer with $\lambda = 1$ demonstrates its higher efficiency in estimating individual FIFs compared to SHAP. While estimating intersectional FIFs, FairXplainer also demonstrates its practical applicability by solving 350 instances within 160 seconds. *Therefore, FairXplainer demonstrates computational efficiency in interpreting group fairness metrics of real-world datasets and classifiers.*

FIFs under Fairness Intervention We consider a fairness intervention strategy to hide the impact of an individual feature on a classifier and record the correlation between fairness improvement/reduction of the intervened classifier with the FIF of the feature. Our intervention strategy of modifying the classifier is different than [42], where the dataset is modified by replacing features with random values. In particular, we intervene a logistic regression classifier by setting the coefficient to zero for the corresponding feature. Intuitively, when the coefficient becomes zero for a feature,

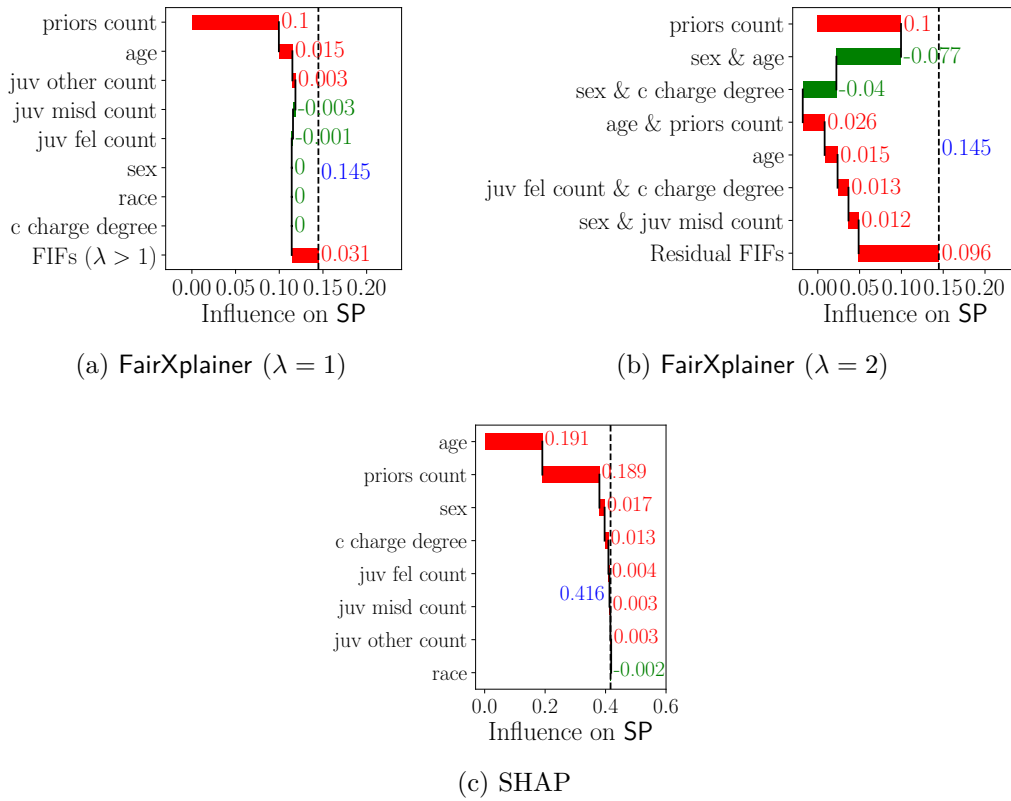


Figure 7.4: FIFs for COMPAS dataset on interpreting statistical parity. Both individual and intersectional FIFs in Figure 7.4b depict sources of bias in detail than individual FIFs alone in Figure 7.4a. In Figure 7.4c, individual FIFs estimated by SHAP are far from correctly approximating statistical parity (exact value 0.174).

the prediction of the classifier may become independent on the feature; thereby, the bias of the classifier may also be independent on the conditional variances of the feature for different sensitive groups. As a result, a feature with a positive FIF value (i.e. increases bias) is likely to decrease bias under the intervention, and vice versa. In Figure 7.3, we report Pearson’s correlation coefficient between the difference in bias (statistical parity) due to intervention and the FIFs of features in COMPAS and Adult datasets, where features are sorted in descending order of their absolute FIFs estimated by FairXplainer and SHAP. In FairXplainer, the correlation coefficient generally decreases with an increase of top influential features, denoting that features with higher absolute FIFs highly correlate with bias-differences. SHAP, in contrast, demonstrates less correlation, specially for the top most influential features. *Therefore, FIFs estimated by FairXplainer shows the potential of being deployed to design improved fairness algorithms in future.*

7.4.2 Explainability and Applicability of FIFs

Individual vs. Intersectional FIFs. Now, we aim to understand the importance of intersectional FIFs over individual FIFs in Figure 7.4. We consider COMPAS dataset with $\text{race} \in \{\text{Caucasian}, \text{non-Caucasian}\}$ as the sensitive feature, and a logistic regression classifier to predict whether a person will re-offend crimes within the next two years. Since the classifier only optimizes training error, it demonstrates statistical parity of 0.174, i.e. it suggests that a non-Caucasian has 0.174 higher probability of re-offending crimes than a Caucasian. Next, we investigate the sources of bias and present individual FIFs in Figure 7.4a, and both individual and intersectional FIFs in Figure 7.4b. In both figures, we present influential features and their FIFs in the descending order of absolute values. According to FairXplainer, the priors count (FIF = 0.1) dominates in increasing statistical parity—between Caucasian and non-Caucasian, their prior count demonstrates the maximum difference in the scaled variance of positive prediction. Other non-sensitive features have almost zero FIFs. However, in Figure 7.4a, higher-order FIFs ($\lambda > 1$) increases statistical parity by 0.031, denoting that the data is correlated and presenting only individual FIFs is not sufficient for understanding the sources of bias. For example, while both sex and age individually demonstrate almost zero influence on bias (Figure 7.4a), their combined effect and intersectional effects with c-charge degree, priors count, and juvenile miscellaneous count contribute highly on statistical parity. In contrast to FairXplainer, SHAP only estimates individual FIFs (Figure 7.4c) and approximates statistical parity with higher error than FairXplainer. Interestingly, FairXplainer yields FIF estimates of the classifier trained on COMPAS dataset that significantly matches with the rule-based classifier extracted from the COMPAS dataset using Certifiably Optimal Rule Lists (CORELS) algorithm [157, Figure 3]. From Figure 3 in [157], we observe that prior count is the only feature used individually to predict arrests, while age is paired with sex and prior counts respectively. While considering second-order intersectionality, FairXplainer ($\lambda = 2$) yields priors count, (sex, age), and (age, priors count) as *three of the top four features* that explains the observation of [157] better than SHAP and FairXplainer ($\lambda = 1$) considering only individual features. *Therefore, FairXplainer demonstrates a clearer*

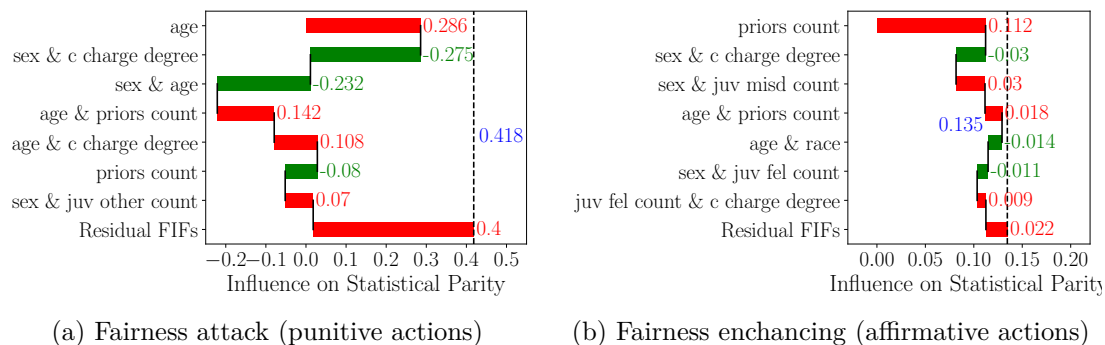


Figure 7.5: Effects of a fairness attack [174] and a fairness enhancing [85] algorithms on FIFs.

understanding on the sources of bias of a classifier by simultaneously quantifying on intersectional influences and individual influences .

Quantifying Impacts of Affirmative/Punitive Actions. Continuing on the experiment in Figure 7.4, we evaluate the effect of fairness attack and enhancing algorithms on FIFs on COMPAS dataset in Figure 7.5. Without applying any fairness algorithm, the statistical parity of the classifier is 0.174. Applying a data poisoning fairness attack [174] increases statistical parity to 0.502 (approximated as 0.418 in Figure 7.5a), whereas a fairness-enhancing algorithm based on data reweighing [85] decreases statistical parity to 0.151 (approximated as 0.135 in Figure 7.5b). In Figure 7.5a, the attack algorithm would be more successful if it could hide the influence of features with positive FIFs, such as priors count and the intersectional effects of age and c-charge degree with sex. In contrast, in Figure 7.5b, the fairness enhancing algorithm can improve by further ameliorating the effect features with negative FIFs, such as priors count. Thus, FairXplainer *demonstrates the potential as a dissecting tool to undertake necessary steps to improve or worsen fairness of a classifier.*

7.5 Chapter Summary

We discuss fairness influence function (FIF) to measure the effect of input features on the bias of classifiers on a given dataset. Our approach combines global sensitivity analysis and group-based fairness metrics in machine learning.

Thereby, it is natural in our approach to formulate FIF of intersectional features, which together with individual FIFs interprets bias with higher granularity. We theoretically analyze the properties of FIFs and provide an algorithm, **FairXplainer**, for estimating FIFs using global variance decomposition and local regression. In experiments, **FairXplainer** estimates individual and intersectional FIFs in real-world datasets and classifiers, approximates bias using FIFs with less estimation error than earlier methods, demonstrates a high correlation between FIFs and fairness interventions, and analyzes the impact of fairness enhancing and attack algorithms on FIFs. The results instantiate **FairXplainer** as a global, granular, and more accurate explanation method to understand the sources of bias. Additionally, the resonance between the rules extracted by CORELS [157] and the most influential features detected by **FairXplainer** indicates that FIFs can be exploited in future to create an explainable proxy of a biased/unbiased classifier. Also, we aim to extend **FairXplainer** to compute FIFs for complex data, such as image and text, and design algorithms leveraging FIFs to yield unbiased decisions.

Chapter 8

Conclusion And Future Work

Over the past decade, machine learning has been applied to various safety-critical domains, and it's crucial for classifiers to be interpretable, fair, robust, and private to ensure trustworthy and responsible AI. In this thesis, we focus on the interpretability and fairness aspects of machine learning and aim to improve the scalability and accuracy of the underlying problems. We utilize formal methods to make the following contributions: (i) In interpretable machine learning, we design an incremental learning technique for interpretable rule-based classifiers of varied expressiveness. (ii) In fairness in machine learning, we develop a formal probabilistic fairness verification framework that can verify multiple fairness definitions of classifiers. Additionally, we develop techniques to interpret fairness metrics by identifying feature combinations responsible for the bias of the classifier.

To demonstrate the efficacy of our methods, we have constructed open-source tools and conducted experiments on real-world datasets in machine learning. In the context of interpretable rule-based machine learning, we have developed an incremental learning framework, known as **IMLI**, that scales classification to million-size datasets while maintaining competitive prediction accuracy and rule size compared to existing rule-based classifiers. Additionally, in our pursuit of more expressive yet interpretable classifiers, we have introduced another learning framework, called **CRR**, for logical relaxed classification rules that are based on incremental learning. Experimental results show that **CRR** is capable of learning more concise and accurate rule-based classifiers.

Our work on fairness in machine learning introduces two novel probabilistic fairness verifiers, **Justicia** and **FVGM**, which exhibit superior performance in accuracy and scalability compared to state-of-the-art verifiers. **Justicia** is a stochastic-SAT-based verifier that enables scalable verification of fairness for compound sensitive

groups of Boolean classifiers, such as decision trees, which was previously infeasible with existing methods. On the other hand, FVGM takes correlated features into account and is capable of verifying the fairness of linear classifiers with higher scalability and accuracy than previous verifiers. Additionally, we discuss a global sensitivity analysis-based method, FairXplainer, that interprets group fairness metrics by computing fairness influences of individual and intersectional features. Notably, FairXplainer approximates bias more accurately using fairness influence functions (FIFs) and demonstrates a higher correlation of FIFs with fairness intervention than the local interpretability-based approach.

Our future research is dedicated to developing practical and scalable algorithms for trustworthy machine learning. Machine learning and artificial intelligence have been compared to the new electricity, with the potential to transform various aspects of human life, evident from the overwhelming response to generative AI. Ensuring fairness and interpretability in deployed machine learning is now more necessary than ever. To accomplish this, we aim to work in a collaborative environment, gaining insights into real-world challenges and leveraging advances in the field, alongside formal methods, to make significant progress. We have identified key research themes that will guide our work towards this vision.

Fairness and Interpretability As a Service. The goal of modern machine learning extends beyond learning patterns from large-scale historical data to ensuring responsible decision-making through careful regulation to establish trustworthiness. For instance, in a job application scenario, a machine learning algorithm must be fair across different demographic groups, resilient to non-actionable changes in candidate profiles, and interpretable to allow candidates to understand the decision-making process. The long-term research goal of this thesis is to offer fairness and interpretability as a service with machine learning-based decision-making.

- **Interpretability with Guarantees.** Our research in interpretable machine learning spans **two-fold directions**. (i) *Interpretability by design*: There is a growing interest for interpretable machine learning in safety-critical domains [157]. Building upon our interpretable rule-based classifier IMLI, we aim to enhance learning algorithms for interpretable models in large-scale datasets

across supervised, semi-supervised, and unsupervised settings. (ii) *Post-hoc interpretability*: To explain black-box predictions, we focus on explanations with formal guarantees [78, 152, 65]. For example, an explanation model must be robust, learned in a privacy-preserving manner, and provide the confidence level of explanations to increase transparency and trust in the decision-making process.

- **Fairness Auditing.** Any technology that is publicly used presently undergoes an audit mechanism, where we understand the impacts and limitations of using that technology, and why are they caused. Machine learning is becoming the pervasive technology of our time and the discourse on bias induced by machine learning systems is attracting attention, e.g. the demonstration of bias in popular generative machine learning and large language models [1, 128, 183]. As a result, there has been significant research interest in auditing classifiers for bias, from standard supervised learning to deep neural networks, computer vision, large language models and so on. Thus, we aim to design a fairness auditing framework [158, 191] with formal guarantees. There are three key questions that we aim to investigate in fairness auditing.

1. **Which fairness metrics to choose?** Fairness in machine learning is bestowed with multiple notions of fairness. Our first line of investigation is to categorize different fairness metrics and suggest the best metric based on application, data, and prevailing policy, similar to “Fairness Compass” [158]. This would help stakeholders pick the right definition of fairness for their application.
2. **How to quantify bias?** Accurate quantification of bias is an important step towards designing algorithms to mitigate bias. As discussed in the thesis, fairness verification allows us to formally quantify the bias of a classifier. To this end, we aim to extend formal fairness verification to broader classes of fairness metrics, classifiers, and data.

Fairness Metrics. We aim to extend fairness verification of beyond group fairness, such as individual fairness [82], causal fairness [133, 198], and counterfactual fairness [190, 33]. Each category of fairness metrics

poses distinct challenges in formal verification. For example, verifying individual fairness is related to verifying robustness of a model. As such, statistical methods from robustness verification has been applied to individual fairness [82]. Formal methods, such as SMT-based encoding is also proposed in this regard [24]. In our research endeavor, we aim to leverage SAT or quantified Boolean formula (QBF) based verification, which may improve the scalability of verification.

Broader Classifiers. We aim to extend fairness verification to broader machine learning classifiers, such as random forests and deep neural networks. For random forests, we can leverage CNF-based translation of the ensemble of trees by converting each tree as a CNF and a cardinality constraint to implement the ranking function of the prediction of multiple trees. For a special case of binarized neural networks (BNNs) [74], we can leverage existing CNF encoding and deploy SSAT-based verifier. However, for general neural networks with continuous parameters, MILP-based encoding can possibly be explored [123]. In addition, for neural networks, other surrogate representation beyond CNF or MILP can also be studied in future. In all cases, fairness verification, particularly for group-based metrics, relies on an access to efficient counter of CNF/MILP encoding; thus a dedicated effort to design better counter is a challenging, yet important research direction to explore.

Complex data. We have explored fairness verification of tabular data; an important research question is to formally verify the fairness of classifiers with complex data such as images [131] and languages [1, 128, 183]. For such data, one way to adapt existing verification methods, such as *Justicia*, is to apply them on the learned feature representation by the neural network and propagate verification results back to the input layer with images or text. In future, we aim to explore this possibility.

3. **How to explain bias?** We aim to design fair and interpretable algorithms for machine learning. We are interested in how these two goals relate to each other. This is inline with GDPR’s emphasis on making models transparent and trustworthy, which is deployed in public. To-

wards bridging the gap between fairness and interpretability in predictive systems, we explore following research questions:

- a) How fair are interpretable machine learning models?
- b) How can we improve the fairness of interpretable models?
- c) How can we apply interpretability to enhance fairness?
- d) How can we jointly optimize a classifier for fairness and interpretability?

A New Paradigm for Scalability: Trustworthy Machine Learning with Formal Methods and Beyond. The SAT and SMT revolution has accelerated the field of formal methods and automated reasoning with powerful solvers for various problem domains such as SAT/SMT for decision problems, MaxSAT/MaxSMT for optimization problems, and SSAT for hybrid optimization and counting problems. By leveraging the clear distinction between the modeling and solving aspects of SAT, MaxSAT, or SSAT, our goal is to enhance fairness and explainability in machine learning through an efficient translation into formal methods. Furthermore, my aim is to explore alternative formulations within formal methods, including functional analysis, abstract interpretation, and solvers with expressive theories. These explorations seek to further improve the verification process of machine learning models. Concurrently, the outcomes of our research have a broader impact, potentially inspiring advancements in the field of formal methods by benchmarking trustworthy machine learning.

Bibliography

- [1] A. Abid, M. Farooqi, and J. Zou, “Persistent anti-muslim bias in large language models”, in *Proceedings of the 2021 AAAI/ACM Conference on AI, Ethics, and Society*, 2021, pp. 298–306.
- [2] A. F. M. Agarap, “On breast cancer detection: An application of machine learning algorithms on the wisconsin diagnostic dataset”, in *Proceedings of the 2nd international conference on machine learning and soft computing*, 2018, pp. 5–9.
- [3] I. Ajunwa, S. Friedler, C. E. Scheidegger, and S. Venkatasubramanian, “Hiring by algorithm: Predicting and preventing disparate impact”, *Available at SSRN*, 2016, URL: <http://sorelle.friedler.net/papers/SSRN-id2746078.pdf>.
- [4] A. Albarghouthi, L. D’Antoni, S. Drews, and A. V. Nori, “FairSquare: Probabilistic verification of program fairness”, *Proceedings of the ACM on Programming Languages*, vol. 1, pp. 1–30, 2017.
- [5] J. Alos, C. Ansotegui, and E. Torres, “Learning optimal decision trees using MaxSAT”, 2021.
- [6] E. Angelino, N. Larus-Stone, D. Alabi, M. Seltzer, and C. Rudin, “Learning certifiably optimal rule lists for categorical data”, *The Journal of Machine Learning Research*, vol. 18, pp. 8753–8830, 2017.
- [7] J. Angwin, J. Larson, S. Mattu, and L. Kirchner, “Machine bias risk assessments in criminal sentencing”, *ProPublica, May*, vol. 23, 2016.
- [8] A. Ankan and A. Panda, “Pgmpy: Probabilistic graphical models using python”, in *Proceedings of the 14th Python in Science Conference (SCIPY 2015)*, Citeseer, 2015.
- [9] J. Argelich, C.-M. Li, F. Manyá, and J. Planes, “The first and second Max-SAT evaluations”, vol. 4, IOS Press, 2008, pp. 251–278.

- [10] M. G. Augasta and T. Kathirvalavakumar, “Rule extraction from neural networks—a comparative study”, in *International Conference on Pattern Recognition, Informatics and Medical Engineering (PRIME-2012)*, IEEE, 2012, pp. 404–408.
- [11] T. Balyo, M. Heule, and M. Jarvisalo, “SAT competition 2016: Recent developments”, in *Proceedings of the AAAI Conference on Artificial Intelligence*, vol. 31, 2017.
- [12] N. Barakat and J. Diederich, “Learning-based rule-extraction from support vector machines”, , not found, 2004.
- [13] N. Barakat and J. Diederich, “Eclectic rule-extraction from support vector machines”, , vol. 2, Citeseer, 2005, pp. 59–62.
- [14] S. Barocas, M. Hardt, and A. Narayanan, “Fairness in machine learning”, *NIPS Tutorial*, vol. 1, 2017.
- [15] O. Bastani, X. Zhang, and A. Solar-Lezama, “Probabilistic verification of fairness properties via concentration”, *Proceedings of the ACM on Programming Languages*, vol. 3, pp. 1–27, 2019.
- [16] T. Begley, T. Schwedes, C. Frye, and I. Feige, “Explainability for fair machine learning”, *arXiv preprint arXiv:2010.07389*, 2020.
- [17] R. K. E. Bellamy, K. Dey, M. Hind, S. C. Hoffman, S. Houde, K. Kannan, P. Lohia, J. Martino, S. Mehta, A. Mojsilovic, S. Nagar, K. N. Ramamurthy, J. Richards, D. Saha, P. Sattigeri, M. Singh, K. R. Varshney, and Y. Zhang, “AI Fairness 360: An extensible toolkit for detecting, understanding, and mitigating unwanted algorithmic bias”, Oct. 2018. [Online]. Available: <https://arxiv.org/abs/1810.01943>.
- [18] C. Bénése, F. Gamboa, J.-M. Loubes, and T. Boissin, “Fairness seen as global sensitivity analysis”, *arXiv preprint arXiv:2103.04613*, 2021.
- [19] B. Benhamou, L. Sais, and P. Siegel, “Two proof procedures for a cardinality based language in propositional calculus”, in *Annual Symposium on Theoretical Aspects of Computer Science*, Springer, 1994, pp. 71–82.
- [20] O. J. Berg, A. J. Hyttinen, and M. J. Jarvisalo, “Applications of MaxSAT in data analysis”, , EasyChair Publications, 2019.

- [21] R. Berk, “Accuracy and fairness for juvenile justice risk assessments”, *Journal of Empirical Legal Studies*, vol. 16, pp. 175–194, 2019.
- [22] P. Besse, E. del Barrio, P. Gordaliza, J.-M. Loubes, and L. Risser, “A survey of bias in machine learning through the prism of statistical parity”, *The American Statistician*, pp. 1–11, 2021.
- [23] C. Bessiere, E. Hebrard, and B. O’Sullivan, “Minimising decision tree size as combinatorial optimisation”, in *International Conference on Principles and Practice of Constraint Programming*, Springer, 2009, pp. 173–187.
- [24] S. Biswas and H. Rajan, “Fairify: Fairness verification of neural networks”, *arXiv preprint arXiv:2212.06140*, 2022.
- [25] C. de Boor, “Subroutine package for calculating with b-splines.” Los Alamos National Lab.(LANL), Los Alamos, NM (United States), Tech. Rep., 1971.
- [26] K. C. Briggs, “Myers-Briggs type indicator”, Consulting Psychologists Press Palo Alto, CA, 1976.
- [27] J. Buolamwini and T. Gebru, “Gender shades: Intersectional accuracy disparities in commercial gender classification”, in *Conference on fairness, accountability and transparency*, PMLR, 2018, pp. 77–91.
- [28] F. Calmon, D. Wei, B. Vinzamuri, K. N. Ramamurthy, and K. R. Varshney, “Optimized pre-processing for discrimination prevention”, in *Advances in Neural Information Processing Systems*, 2017, pp. 3992–4001.
- [29] G. Cauwenberghs and T. Poggio, “Incremental and decremental support vector machine learning”, in *Proc. of NIPS*, 2001.
- [30] S. Chakraborty, D. J. Fremont, K. S. Meel, S. A. Seshia, and M. Y. Vardi, “Distribution-aware sampling and weighted model counting for sat”, *arXiv preprint arXiv:1404.2984*, 2014.
- [31] S. Chakraborty, K. S. Meel, and M. Y. Vardi, “A scalable approximate model counter”, in *International Conference on Principles and Practice of Constraint Programming*, Springer, 2013, pp. 200–216.
- [32] M. Chavira and A. Darwiche, “On probabilistic inference by weighted model counting”, *Artificial Intelligence*, vol. 172, pp. 772–799, 2008.

- [33] S. Chiappa, “Path-specific counterfactual fairness”, in *Proceedings of the AAAI Conference on Artificial Intelligence*, vol. 33, 2019, pp. 7801–7808.
- [34] A. Chouldechova and A. Roth, “A snapshot of the frontiers of fairness in machine learning”, *Communications of the ACM*, vol. 63, pp. 82–89, 2020.
- [35] L. Ciampiconi, B. Ghosh, J. Scarlett, and K. S. Meel, “A MaxSAT-based framework for group testing”, in *Proceedings of AAAI*, 2020.
- [36] P. Clark and T. Niblett, “The CN2 induction algorithm”, 1989.
- [37] W. W. Cohen and Y. Singer, “A simple, fast, and effective rule learner”, in *Proc. of AAAI*, Orlando, FL, 1999.
- [38] W. W. Cohen, “Fast effective rule induction”, in *Machine learning proceedings 1995*, Elsevier, 1995, pp. 115–123.
- [39] M. Craven and J. W. Shavlik, “Extracting tree-structured representations of trained networks”, in *Advances in neural information processing systems*, 1996, pp. 24–30.
- [40] S. Dash and J. Goncalves, “LPRules: Rule induction in knowledge graphs using linear programming”, 2021.
- [41] S. Dash, O. Gunluk, and D. Wei, “Boolean decision rules via column generation”, in *Advances in Neural Information Processing Systems*, 2018, pp. 4655–4665.
- [42] A. Datta, S. Sen, and Y. Zick, “Algorithmic transparency via quantitative input influence: Theory and experiments with learning systems”, in *2016 IEEE symposium on security and privacy (SP)*, IEEE, 2016, pp. 598–617.
- [43] J. Diederich, “Rule extraction from support vector machines: An introduction”, in *Rule extraction from support vector machines*, Springer, 2008, pp. 3–31.
- [44] F. Doshi-Velez and B. Kim, “Towards a rigorous science of interpretable machine learning”, *arXiv preprint arXiv:1702.08608*, 2017.
- [45] J. Dressel and H. Farid, “The accuracy, fairness, and limits of predicting recidivism”, *Science advances*, vol. 4, eaao5580, 2018.

- [46] D. Dua and C. Graff, “UCI machine learning repository”, 2017. [Online]. Available: <http://archive.ics.uci.edu/ml>.
- [47] C. Dwork, M. Hardt, T. Pitassi, O. Reingold, and R. Zemel, “Fairness through awareness”, in *Proceedings of the 3rd innovations in theoretical computer science conference*, 2012, pp. 214–226.
- [48] M. Dyer, “Approximate counting by dynamic programming”, in *Proceedings of the thirty-fifth annual ACM symposium on Theory of computing*, 2003, pp. 693–699.
- [49] A. Emad, K. R. Varshney, and D. M. Malioutov, “A semiquantitative group testing approach for learning interpretable clinical prediction rules”, in *Proc. Signal Process. Adapt. Sparse Struct. Repr. Workshop, Cambridge, UK*, 2015.
- [50] B. J. Erickson, P. Korfiatis, Z. Akkus, and T. L. Kline, “Machine learning for medical imaging”, vol. 37, Radiological Society of North America, 2017, pp. 505–515.
- [51] B. Eshete, “Making machine learning trustworthy”, *Science*, vol. 373, no. 6556, pp. 743–744, 2021.
- [52] European Commission, “Better regulation toolbox”, Brussels, Belgium, 2021.
- [53] U. Fayyad and K. Irani, “Multi-interval discretization of continuous-valued attributes for classification learning”, 1993.
- [54] M. Feldman, S. A. Friedler, J. Moeller, C. Scheidegger, and S. Venkatasubramanian, “Certifying and removing disparate impact”, in *proceedings of the 21th ACM SIGKDD international conference on knowledge discovery and data mining*, 2015, pp. 259–268.
- [55] M. L. Fisher, “The lagrangian relaxation method for solving integer programming problems”, vol. 27, INFORMS, 1981, pp. 1–18.
- [56] D. J. Fremont, M. N. Rabe, and S. A. Seshia, “Maximum model counting.” In *AAAI*, 2017, pp. 3885–3892.
- [57] J. Fürnkranz, “Separate-and-conquer rule learning”, vol. 13, Springer, 1999, pp. 3–54.

- [58] B. F. Gage, A. D. Waterman, W. Shannon, M. Boechler, M. W. Rich, and M. J. Radford, “Validation of clinical classification schemes for predicting stroke: Results from the national registry of atrial fibrillation”, *Jama*, vol. 285, pp. 2864–2870, 2001.
- [59] S. Galhotra, Y. Brun, and A. Meliou, “Fairness testing: Testing software for discrimination”, in *Proceedings of the 2017 11th Joint Meeting on Foundations of Software Engineering*, 2017, pp. 498–510.
- [60] P. Garg, J. Villasenor, and V. Foggo, “Fairness metrics: A comparative analysis”, in *2020 IEEE International Conference on Big Data (Big Data)*, IEEE, 2020, pp. 3662–3666.
- [61] A. Gawande, “Checklist manifesto, the (HB)”, Penguin Books India, 2010.
- [62] B. Ghosh and K. S. Meel, “IMLI: An incremental framework for MaxSAT-based learning of interpretable classification rules”, in *Proceedings of AAAI/ACM Conference on AI, Ethics, and Society(AIES)*, 2019.
- [63] N. Gill, P. Hall, K. Montgomery, and N. Schmidt, “A responsible machine learning workflow with focus on interpretable models, post-hoc explanation, and discrimination testing”, vol. 11, Multidisciplinary Digital Publishing Institute, 2020, p. 137.
- [64] G. Grimmett and D. Stirzaker, “Probability and random processes”, Oxford university press, 2020.
- [65] R. Guidotti, A. Monreale, S. Ruggieri, D. Pedreschi, F. Turini, and F. Giannotti, “Local rule-based explanations of black box decision systems”, 2018.
- [66] T. Hailesilassie, “Rule extraction algorithm for deep neural networks: A review”, 2016.
- [67] M. Hall, E. Frank, G. Holmes, B. Pfahringer, P. Reutemann, and I. H. Witten, “The weka data mining software: An update”, *ACM SIGKDD explorations newsletter*, vol. 11, pp. 10–18, 2009.
- [68] T. Han, S. Srinivas, and H. Lakkaraju, “Which explanation should i choose? a function approximation perspective to characterizing post hoc explanations”, *arXiv preprint arXiv:2206.01254*, 2022.

- [69] M. Hardt, E. Price, and N. Srebro, “Equality of opportunity in supervised learning”, in *Advances in neural information processing systems*, 2016, pp. 3315–3323.
- [70] J. Herman and W. Usher, “SALib: An open-source python library for sensitivity analysis”, *The Journal of Open Source Software*, vol. 2, no. 9, 2017. [Online]. Available: <https://doi.org/10.21105/joss.00097>.
- [71] G. Hinton, N. Srivastava, and K. Swersky, “Neural networks for machine learning lecture 6a overview of mini-batch gradient descent”, vol. 14, 2012, p. 2.
- [72] X. Hua, H. Xu, J. Blanchet, and V. Nguyen, “Human imperceptible attacks and applications to improve fairness”, *arXiv preprint arXiv:2111.15603*, 2021.
- [73] J. Huang *et al.*, “Combining knowledge compilation and search for conformant probabilistic planning.” In *ICAPS*, 2006, pp. 253–262.
- [74] I. Hubara, M. Courbariaux, D. Soudry, R. El-Yaniv, and Y. Bengio, “Binarized neural networks”, *Advances in neural information processing systems*, vol. 29, 2016.
- [75] A. Ignatiev, E. Lam, P. J. Stuckey, and J. Marques-Silva, “A scalable two stage approach to computing optimal decision sets”, 2021.
- [76] A. Ignatiev, J. Marques-Silva, N. Narodytska, and P. J. Stuckey, “Reasoning-based learning of interpretable ML models”, in *International Joint Conference on Artificial Intelligence (IJCAI)*, 2021.
- [77] A. Ignatiev, A. Morgado, and J. Marques-Silva, “PySAT: A Python toolkit for prototyping with SAT oracles”, in *SAT*, 2018, pp. 428–437. [Online]. Available: https://doi.org/10.1007/978-3-319-94144-8_26.
- [78] A. Ignatiev, N. Narodytska, and J. Marques-Silva, “Abduction-based explanations for machine learning models”, in *Proceedings of the AAAI Conference on Artificial Intelligence*, vol. 33, 2019, pp. 1511–1519.
- [79] A. Ignatiev, F. Pereira, N. Narodytska, and J. Marques-Silva, “A sat-based approach to learn explainable decision sets”, in *International Joint Conference on Automated Reasoning*, Springer, 2018, pp. 627–645.

- [80] Y. Izza, A. Ignatiev, and J. Marques-Silva, “On explaining decision trees”, 2020.
- [81] M. Janota and A. Morgado, “SAT-based encodings for optimal decision trees with explicit paths”, in *International Conference on Theory and Applications of Satisfiability Testing*, Springer, 2020, pp. 501–518.
- [82] P. G. John, D. Vijaykeerthy, and D. Saha, “Verifying individual fairness in machine learning models”, *arXiv preprint arXiv:2006.11737*, 2020.
- [83] J. K. Johnson, D. M. Malioutov, and A. S. Willsky, “Lagrangian relaxation for MAP estimation in graphical models”, 2007.
- [84] G. A. Kaissis, M. R. Makowski, D. Rückert, and R. F. Braren, “Secure, privacy-preserving and federated machine learning in medical imaging”, vol. 2, Nature Publishing Group, 2020, pp. 305–311.
- [85] F. Kamiran and T. Calders, “Data preprocessing techniques for classification without discrimination”, *Knowledge and Information Systems*, vol. 33, pp. 1–33, 2012.
- [86] F. Kamiran, A. Karim, and X. Zhang, “Decision theory for discrimination-aware classification”, in *2012 IEEE 12th International Conference on Data Mining*, IEEE, 2012, pp. 924–929.
- [87] J. Kleinberg and E. Tardos, “Algorithm design”, 2006.
- [88] D. Koller and N. Friedman, “Probabilistic graphical models: principles and techniques”, MIT press, 2009.
- [89] J. Konečný, B. McMahan, and D. Ramage, “Federated optimization: Distributed optimization beyond the datacenter”, 2015.
- [90] J. Konečný, H. B. McMahan, D. Ramage, and P. Richtárik, “Federated optimization: Distributed machine learning for on-device intelligence”, 2016.
- [91] I. Kononenko, “Machine learning for medical diagnosis: History, state of the art and perspective”, vol. 23, Elsevier, 2001, pp. 89–109.
- [92] R. S. S. Kumar, D. R. O’Brien, K. Albert, and S. Vilojen, “Law and adversarial machine learning”, 2018.

- [93] H. Lakkaraju, S. H. Bach, and J. Leskovec, “Interpretable decision sets: A joint framework for description and prediction”, in *Proceedings of the 22nd ACM SIGKDD international conference on knowledge discovery and data mining*, 2016, pp. 1675–1684.
- [94] H. Lakkaraju, E. Kamar, R. Caruana, and J. Leskovec, “Interpretable & explorable approximations of black box models”, 2017.
- [95] H. Lakkaraju, E. Kamar, R. Caruana, and J. Leskovec, “Faithful and customizable explanations of black box models”, in *Proc. of AIES*, 2019.
- [96] F. J. Landy, J. L. Barnes, and K. R. Murphy, “Correlates of perceived fairness and accuracy of performance evaluation.” *Journal of Applied psychology*, vol. 63, p. 751, 1978.
- [97] N.-Z. Lee and J.-H. R. Jiang, “Towards formal evaluation and verification of probabilistic design”, *IEEE Transactions on Computers*, vol. 67, pp. 1202–1216, 2018.
- [98] N.-Z. Lee, Y.-S. Wang, and J.-H. R. Jiang, “Solving stochastic boolean satisfiability under random-exist quantification.” In *IJCAI*, 2017, pp. 688–694.
- [99] N.-Z. Lee, Y.-S. Wang, and J.-H. R. Jiang, “Solving exist-random quantified stochastic boolean satisfiability via clause selection.” In *IJCAI*, 2018, pp. 1339–1345.
- [100] C. Lemaréchal, “Lagrangian relaxation”, in *Computational combinatorial optimization*, Springer, 2001, pp. 112–156.
- [101] B. Letham, C. Rudin, T. H. McCormick, and D. Madigan, “Interpretable classifiers using rules and Bayesian analysis: Building a better stroke prediction model”, vol. 9, Institute of Mathematical Statistics, 2015, pp. 1350–1371.
- [102] G. Li, H. Rabitz, P. E. Yelvington, O. O. Oluwole, F. Bacon, C. E. Kolb, and J. Schoendorf, “Global sensitivity analysis for systems with independent and/or correlated inputs”, *The journal of physical chemistry A*, vol. 114, no. 19, pp. 6022–6032, 2010.

- [103] M. Li, T. Zhang, Y. Chen, and A. J. Smola, “Efficient mini-batch training for stochastic optimization”, in *Proceedings of the 20th ACM SIGKDD international conference on Knowledge discovery and data mining*, 2014, pp. 661–670.
- [104] P. Li and H. Liu, “Achieving fairness at no utility cost via data reweighing with influence”, in *International Conference on Machine Learning*, PMLR, 2022, pp. 12 917–12 930.
- [105] P.-C. K. Lin and S. P. Khatri, “Application of Max-SAT-based ATPG to optimal cancer therapy design”, vol. 13, Springer, 2012, pp. 1–10.
- [106] M. L. Littman, S. M. Majercik, and T. Pitassi, “Stochastic boolean satisfiability”, *Journal of Automated Reasoning*, vol. 27, pp. 251–296, 2001.
- [107] C. Loader, “Smoothing: Local regression techniques”, in *Handbook of computational statistics*, Springer, 2012, pp. 571–596.
- [108] C. Loader, “Local regression and likelihood”, Springer Science & Business Media, 2006.
- [109] R. Luckin, “Machine Learning and Human Intelligence: The future of education for the 21st century.” ERIC, 2018.
- [110] S. M. Lundberg, “Explaining quantitative measures of fairness”, in *Fair & Responsible AI Workshop@ CHI2020*, 2020.
- [111] S. M. Lundberg, G. Erion, H. Chen, A. DeGrave, J. M. Prutkin, B. Nair, R. Katz, J. Himmelfarb, N. Bansal, and S.-I. Lee, “From local explanations to global understanding with explainable ai for trees”, *Nature Machine Intelligence*, vol. 2, no. 1, pp. 2522–5839, 2020.
- [112] S. M. Lundberg and S.-I. Lee, “A unified approach to interpreting model predictions”, in *Proceedings of the 31st international conference on neural information processing systems*, 2017, pp. 4768–4777.
- [113] S. M. Majercik, “Appssat: Approximate probabilistic planning using stochastic satisfiability”, *International Journal of Approximate Reasoning*, vol. 45, pp. 402–419, 2007.

- [114] S. M. Majercik and B. Boots, “Dc-ssat: A divide-and-conquer approach to solving stochastic satisfiability problems efficiently”, in *AAAI*, 2005, pp. 416–422.
- [115] D. Malioutov and K. S. Meel, “MLIC: A MaxSAT-based framework for learning interpretable classification rules”, in *International Conference on Principles and Practice of Constraint Programming*, Springer, 2018, pp. 312–327.
- [116] D. Malioutov and K. Varshney, “Exact rule learning via boolean compressed sensing”, in *International Conference on Machine Learning*, PMLR, 2013, pp. 765–773.
- [117] D. Martens, J. Huysmans, R. Setiono, J. Vanthienen, and B. Baesens, “Rule extraction from support vector machines: An overview of issues and application in credit scoring”, Springer, 2008, pp. 33–63.
- [118] B. Martinez Neda, Y. Zeng, and S. Gago-Masague, “Using machine learning in admissions: Reducing human and algorithmic bias in the selection process”, in *Proceedings of the 52nd ACM Technical Symposium on Computer Science Education*, 2021, pp. 1323–1323.
- [119] R. Martins, V. Manquinho, and I. Lynce, “Open-WBO: A modular MaxSAT solver”, in *International Conference on Theory and Applications of Satisfiability Testing*, Springer, 2014, pp. 438–445.
- [120] D. Masters and C. Luschi, “Revisiting small batch training for deep neural networks”, 2018.
- [121] A. C. McGinley, “Ricci v. destefano: A masculinities theory analysis”, *Harv. JL & Gender*, vol. 33, p. 581, 2010.
- [122] N. Mehrabi, M. Naveed, F. Morstatter, and A. Galstyan, “Exacerbating algorithmic bias through fairness attacks”, *arXiv preprint arXiv:2012.08723*, 2020.
- [123] S. Mistry, I. Saha, and S. Biswas, “An milp encoding for efficient verification of quantized deep neural networks”, *IEEE Transactions on Computer-Aided Design of Integrated Circuits and Systems*, vol. 41, no. 11, pp. 4445–4456, 2022.

- [124] M. Moradi and M. Samwald, “Post-hoc explanation of black-box classifiers using confident itemsets”, vol. 165, Elsevier, 2021, p. 113941.
- [125] S. K. Murakonda, R. Shokri, and G. Theodorakopoulos, “Quantifying the privacy risks of learning high-dimensional graphical models”, in *International Conference on Artificial Intelligence and Statistics*, PMLR, 2021, pp. 2287–2295.
- [126] I. B. Myers, “The Myers-Briggs type indicator: Manual (1962).”, Consulting Psychologists Press, 1962.
- [127] R. Nabi and I. Shpitser, “Fair inference on outcomes”, in *Proceedings of the AAAI Conference on Artificial Intelligence*, vol. 32, 2018.
- [128] M. Nadeem, A. Bethke, and S. Reddy, “Stereoset: Measuring stereotypical bias in pretrained language models”, *arXiv preprint arXiv:2004.09456*, 2020.
- [129] N. Narodytska, A. Ignatiev, F. Pereira, J. Marques-Silva, and I. RAS, “Learning optimal decision trees with sat.” In *IJCAI*, 2018, pp. 1362–1368.
- [130] H. Núñez, C. Angulo, and A. Català, “Rule extraction from support vector machines.” In *Esann*, 2002, pp. 107–112.
- [131] O. Nuriel, S. Benaïm, and L. Wolf, “Permuted adain: Reducing the bias towards global statistics in image classification”, in *Proceedings of the IEEE/CVF Conference on Computer Vision and Pattern Recognition*, 2021, pp. 9482–9491.
- [132] Office of the Science Advisor, Council for Regulatory Environmental Modeling, “Guidance on the development, evaluation, and application of environmental models”, U.S. Environmental Protection Agency, Washington, USA, 2009, https://web.archive.org/web/20110426180258/http://www.epa.gov/CREM/library/cred_guidance_0309.pdf.
- [133] W. Pan, S. Cui, J. Bian, C. Zhang, and F. Wang, “Explaining algorithmic fairness through fairness-aware causal path decomposition”, in *Proceedings of the 27th ACM SIGKDD Conference on Knowledge Discovery & Data Mining*, 2021, pp. 1287–1297.
- [134] C. H. Papadimitriou, “Games against nature”, *Journal of Computer and System Sciences*, vol. 31, pp. 288–301, 1985.

- [135] N. Papernot, P. McDaniel, A. Sinha, and M. Wellman, “Towards the science of security and privacy in machine learning”, *arXiv preprint arXiv:1611.03814*, 2016.
- [136] E. Pastor and E. Baralis, “Explaining black box models by means of local rules”, in *Proceedings of the 34th ACM/SIGAPP symposium on applied computing*, 2019, pp. 510–517.
- [137] J. Pearl, “Bayesian networks: A model of self-activated memory for evidential reasoning”, in *Proceedings of the 7th conference of the Cognitive Science Society, University of California, Irvine, CA, USA*, 1985, pp. 15–17.
- [138] F. Pedregosa, G. Varoquaux, A. Gramfort, V. Michel, B. Thirion, O. Grisel, M. Blondel, P. Prettenhofer, R. Weiss, V. Dubourg, J. Vanderplas, A. Passos, D. Cournapeau, M. Brucher, M. Perrot, and E. Duchesnay, “Scikit-learn: Machine learning in Python”, *Journal of Machine Learning Research*, vol. 12, pp. 2825–2830, 2011.
- [139] I. Peled, F. Rodrigues, and F. C. Pereira, “Model-based machine learning for transportation”, in *Mobility patterns, big data and transport analytics*, Elsevier, 2019, pp. 145–171.
- [140] W. W. Peterson and E. J. Weldon, “Error-correcting codes”, MIT press, 1972.
- [141] T. Philipp and P. Steinke, “Pbilib—a library for encoding pseudo-boolean constraints into cnf”, in *International Conference on Theory and Applications of Satisfiability Testing*, Springer, 2015, pp. 9–16.
- [142] D. Pisinger, “Linear time algorithms for knapsack problems with bounded weights”, *Journal of Algorithms*, vol. 33, no. 1, pp. 1–14, 1999.
- [143] G. Pleiss, M. Raghavan, F. Wu, J. Kleinberg, and K. Q. Weinberger, “On fairness and calibration”, *arXiv preprint arXiv:1709.02012*, 2017.
- [144] J. R. Quinlan, “Induction of decision trees”, vol. 1, Springer, 1986, pp. 81–106.
- [145] J. R. Quinlan, “Simplifying decision trees”, vol. 27, Elsevier, 1987, pp. 221–234.
- [146] J. R. Quinlan, “C4. 5: Programming for machine learning”, 1993.

- [147] E. Raff, J. Sylvester, and S. Mills, “Fair forests: Regularized tree induction to minimize model bias”, in *Proceedings of the 2018 AAAI/ACM Conference on AI, Ethics, and Society*, 2018, pp. 243–250.
- [148] D. Rajapaksha, C. Bergmeir, and W. Buntine, “LoRMikA: Local rule-based model interpretability with K-optimal associations”, vol. 540, Elsevier, 2020, pp. 221–241.
- [149] L. Ralaivola and F. d’Alché Buc, “Incremental support vector machine learning: A local approach”, in *Proc. of ICANN*, 2001.
- [150] J. Rauber, W. Brendel, and M. Bethge, “Foolbox: A python toolbox to benchmark the robustness of machine learning models”, *arXiv preprint arXiv:1707.04131*, 2017.
- [151] M. T. Ribeiro, S. Singh, and C. Guestrin, “Why should i trust you? explaining the predictions of any classifier”, in *Proceedings of the 22nd ACM SIGKDD international conference on knowledge discovery and data mining*, 2016, pp. 1135–1144.
- [152] M. T. Ribeiro, S. Singh, and C. Guestrin, “Anchors: High-precision model-agnostic explanations”, in *Proceedings of the AAAI conference on artificial intelligence*, vol. 32, 2018.
- [153] R. L. Rivest, “Learning decision lists”, vol. 2, Springer, 1987, pp. 229–246.
- [154] N. Robinson, C. Gretton, D. N. Pham, and A. Sattar, “Partial weighted MaxSAT for optimal planning”, in *Pacific rim international conference on artificial intelligence*, Springer, 2010, pp. 231–243.
- [155] A. E. Roth, “The Shapley value: essays in honor of Lloyd S. Shapley”, Cambridge University Press, 1988.
- [156] O. Roussel and V. M. Manquinho, “Pseudo-boolean and cardinality constraints.” *Handbook of satisfiability*, vol. 185, pp. 695–733, 2009.
- [157] C. Rudin, “Stop explaining black box machine learning models for high stakes decisions and use interpretable models instead”, vol. 1, Nature Publishing Group, 2019, pp. 206–215.

- [158] B. Ruf and M. Detyniecki, “Towards the right kind of fairness in ai”, *arXiv preprint arXiv:2102.08453*, 2021.
- [159] S. Ruping, “Incremental learning with support vector machines”, in *Proc. of ICDM*, 2001.
- [160] A. Saltelli, G. Bammer, I. Bruno, E. Charters, M. Di Fiore, E. Didier, W. Nelson Espeland, J. Kay, S. Lo Piano, D. Mayo, *et al.*, “Five ways to ensure that models serve society: A manifesto”, 2020.
- [161] A. Saltelli, M. Ratto, T. Andres, F. Campolongo, J. Cariboni, D. Gatelli, M. Saisana, and S. Tarantola, “Global sensitivity analysis: the primer”, John Wiley & Sons, 2008.
- [162] T. Sang, F. Bacchus, P. Beame, H. A. Kautz, and T. Pitassi, “Combining component caching and clause learning for effective model counting.” *SAT*, vol. 4, 7th, 2004.
- [163] M. Sato and H. Tsukimoto, “Rule extraction from neural networks via decision tree induction”, in *IJCNN’01. International Joint Conference on Neural Networks. Proceedings (Cat. No. 01CH37222)*, IEEE, vol. 3, 2001, pp. 1870–1875.
- [164] A. Schidler and S. Szeider, “SAT-based decision tree learning for large data sets”, in *Proceedings of AAAI*, vol. 21, 2021.
- [165] L. Schumaker, “Spline functions: basic theory”, Cambridge University Press, 2007.
- [166] R. Setiono and H. Liu, “Understanding neural networks via rule extraction”, in *IJCAI*, Citeseer, vol. 1, 1995, pp. 480–485.
- [167] P. Shati, E. Cohen, and S. McIlraith, “SAT-based approach for learning optimal decision trees with non-binary features”, in *27th International Conference on Principles and Practice of Constraint Programming (CP 2021)*, Schloss Dagstuhl-Leibniz-Zentrum für Informatik, 2021.
- [168] J. P. M. Silva and K. A. Sakallah, “GRASP—a new search algorithm for satisfiability”, in *The Best of ICCAD*, Springer, 2003, pp. 73–89.

- [169] C. Sinz, “Towards an optimal cnf encoding of boolean cardinality constraints”, in *International conference on principles and practice of constraint programming*, Springer, 2005, pp. 827–831.
- [170] D. Slack, S. Hilgard, E. Jia, S. Singh, and H. Lakkaraju, “Fooling LIME and SHAP: Adversarial attacks on post hoc explanation methods”, in *Proceedings of the AAAI/ACM Conference on AI, Ethics, and Society*, 2020, pp. 180–186.
- [171] J. Sliwinski, M. Strobel, and Y. Zick, “Axiomatic characterization of data-driven influence measures for classification”, in *Proceedings of the AAAI Conference on Artificial Intelligence*, vol. 33, 2019, pp. 718–725.
- [172] I. M. Sobol’, “On sensitivity estimation for nonlinear mathematical models”, *Matematicheskoe modelirovanie*, vol. 2, no. 1, pp. 112–118, 1990.
- [173] I. M. Sobol’, “Global sensitivity indices for nonlinear mathematical models and their Monte Carlo estimates”, *Mathematics and computers in simulation*, vol. 55, no. 1-3, pp. 271–280, 2001.
- [174] D. Solans, B. Biggio, and C. Castillo, “Poisoning attacks on algorithmic fairness”, *arXiv preprint arXiv:2004.07401*, 2020.
- [175] G. Su, D. Wei, K. R. Varshney, and D. M. Malioutov, “Learning sparse two-level Boolean rules”, in *2016 IEEE 26th International Workshop on Machine Learning for Signal Processing (MLSP)*, IEEE, 2016, pp. 1–6.
- [176] H. Surden, “Machine learning and law”, vol. 89, HeinOnline, 2014, p. 87.
- [177] N. A. Syed, S. Huan, L. Kah, and K. Sung, “Incremental learning with support vector machines”, Citeseer, 1999.
- [178] N. Tollenaar and P. Van der Heijden, “Which method predicts recidivism best?: A comparison of statistical, machine learning and data mining predictive models”, *Journal of the Royal Statistical Society: Series A (Statistics in Society)*, vol. 176, pp. 565–584, 2013.
- [179] K. Toraichi, K. Katagishi, I. Sekita, and R. Mori, “Computational complexity of spline interpolation”, *International journal of systems science*, vol. 18, no. 5, pp. 945–954, 1987.

- [180] G. S. Tseitin, “On the complexity of derivation in propositional calculus”, in *Automation of reasoning*, Springer, 1983, pp. 466–483.
- [181] J. Vanschoren, J. N. van Rijn, B. Bischl, and L. Torgo, “OpenML: Networked science in machine learning”, vol. 15, New York, NY, USA: ACM, 2013, pp. 49–60. [Online]. Available: <http://doi.acm.org/10.1145/2641190.2641198>.
- [182] S. Verma and J. Rubin, “Fairness definitions explained”, in *2018 IEEE/ACM International Workshop on Software Fairness (FairWare)*, IEEE, 2018, pp. 1–7.
- [183] J. Vig, S. Gehrmann, Y. Belinkov, S. Qian, D. Nevo, Y. Singer, and S. Shieber, “Investigating gender bias in language models using causal mediation analysis”, *Advances in neural information processing systems*, vol. 33, pp. 12 388–12 401, 2020.
- [184] R. Walter, C. Zengler, and W. Küchlin, “Applications of MaxSAT in automotive configuration.” In *Configuration Workshop*, Citeseer, vol. 1, 2013, p. 21.
- [185] A. Wang, V. V. Ramaswamy, and O. Russakovsky, “Towards intersectionality in machine learning: Including more identities, handling underrepresentation, and performing evaluation”, in *2022 ACM Conference on Fairness, Accountability, and Transparency*, 2022, pp. 336–349.
- [186] F. Wang and C. Rudin, “Falling rule lists”, in *Artificial Intelligence and Statistics*, PMLR, 2015, pp. 1013–1022.
- [187] J. Wang, X. E. Wang, and Y. Liu, “Understanding instance-level impact of fairness constraints”, in *International Conference on Machine Learning*, PMLR, 2022, pp. 23 114–23 130.
- [188] T. Wang, C. Rudin, F. Doshi-Velez, Y. Liu, E. Klampfl, and P. MacNeille, “A Bayesian framework for learning rule sets for interpretable classification”, vol. 18, JMLR. org, 2017, pp. 2357–2393.
- [189] G. J. Woeginger and Z. Yu, “On the equal-subset-sum problem”, *Information Processing Letters*, vol. 42, pp. 299–302, 1992.

- [190] Y. Wu, L. Zhang, and X. Wu, “Counterfactual fairness: Unidentification, bound and algorithm.” In *IJCAI*, 2019, pp. 1438–1444.
- [191] T. Yan and C. Zhang, “Active fairness auditing”, in *International Conference on Machine Learning*, PMLR, 2022, pp. 24 929–24 962.
- [192] J. Yu, A. Ignatiev, P. L. Bodic, and P. J. Stuckey, “Optimal decision lists using SAT” ,, 2020.
- [193] J. Yu, A. Ignatiev, P. J. Stuckey, and P. L. Bodic, “Computing optimal decision sets with sat”, *arXiv preprint arXiv:2007.15140*, 2020.
- [194] M. B. Zafar, I. Valera, M. G. Rogriguez, and K. P. Gummadi, “Fairness constraints: Mechanisms for fair classification”, in *Artificial Intelligence and Statistics*, 2017, pp. 962–970.
- [195] F. Zantalis, G. Koulouras, S. Karabetsos, and D. Kandris, “A review of machine learning and IoT in smart transportation” ,, vol. 11, Multidisciplinary Digital Publishing Institute, 2019, p. 94.
- [196] R. Zemel, Y. Wu, K. Swersky, T. Pitassi, and C. Dwork, “Learning fair representations”, in *International Conference on Machine Learning*, 2013, pp. 325–333.
- [197] B. H. Zhang, B. Lemoine, and M. Mitchell, “Mitigating unwanted biases with adversarial learning”, in *Proceedings of the 2018 AAAI/ACM Conference on AI, Ethics, and Society*, 2018, pp. 335–340.
- [198] J. Zhang and E. Bareinboim, “Fairness in decision-making—the causal explanation formula”, in *Proceedings of the AAAI Conference on Artificial Intelligence*, vol. 32, 2018.
- [199] W. Zhang and E. Ntoutsi, “Faht: An adaptive fairness-aware decision tree classifier”, *arXiv preprint arXiv:1907.07237*, 2019.
- [200] Z.-H. Zhou, “Rule extraction: Using neural networks or for neural networks?”, vol. 19, Springer, 2004, pp. 249–253.
- [201] J. R. Zilke, E. L. Mencía, and F. Janssen, “Deepred–rule extraction from deep neural networks”, in *International Conference on Discovery Science*, Springer, 2016, pp. 457–473.

- [202] I. Zliobaite, “On the relation between accuracy and fairness in binary classification”, *arXiv preprint arXiv:1505.05723*, 2015.

Appendix A

Interpretable Classification Rules

A.1 Performance Comparison: Incremental vs. Non-incremental Encoding

We compare the performance of two encoding techniques, naïve non-incremental encoding and efficient incremental encoding in IMLI, for learning interpretable CNF classification rules in datasets of various sizes. We demonstrate the scalability results using a cactus plot in Figure A.1. Each point (x, y) represents the ability to solve x classification instances within y seconds. We test both incremental and non-incremental encoding using 360 instances for each dataset with varying hyper-parameters. As the dataset size increases, the non-incremental encoding times out, failing to solve all 360 instances within 1000 seconds in the Credit and Adult datasets. In contrast, the incremental encoding in IMLI demonstrates higher scalability, solving all 360 instances in less than 10 seconds in the Titanic dataset, and efficiently solving all 360 instances within the timeout in the Credit and Adult datasets. Hence, the incremental encoding is superior in terms of scalability compared to the non-incremental encoding.

In Figure A.2, we compare both non-incremental and incremental encoding in terms of median training time, rule size, test accuracy, and train accuracy over ten cross validation folds. In all datasets, the incremental encoding demonstrates higher efficiency than the non-incremental encoding by requiring less training time. In large datasets, such as Magic, Credit, and Adult, the non-incremental encoding always times out, thereby producing zero-size rules because of failing to solve the MaxSAT query. As a result, the accuracy of the non-incremental encoding is also less than the incremental encoding in large datasets. In small datasets, the incremental

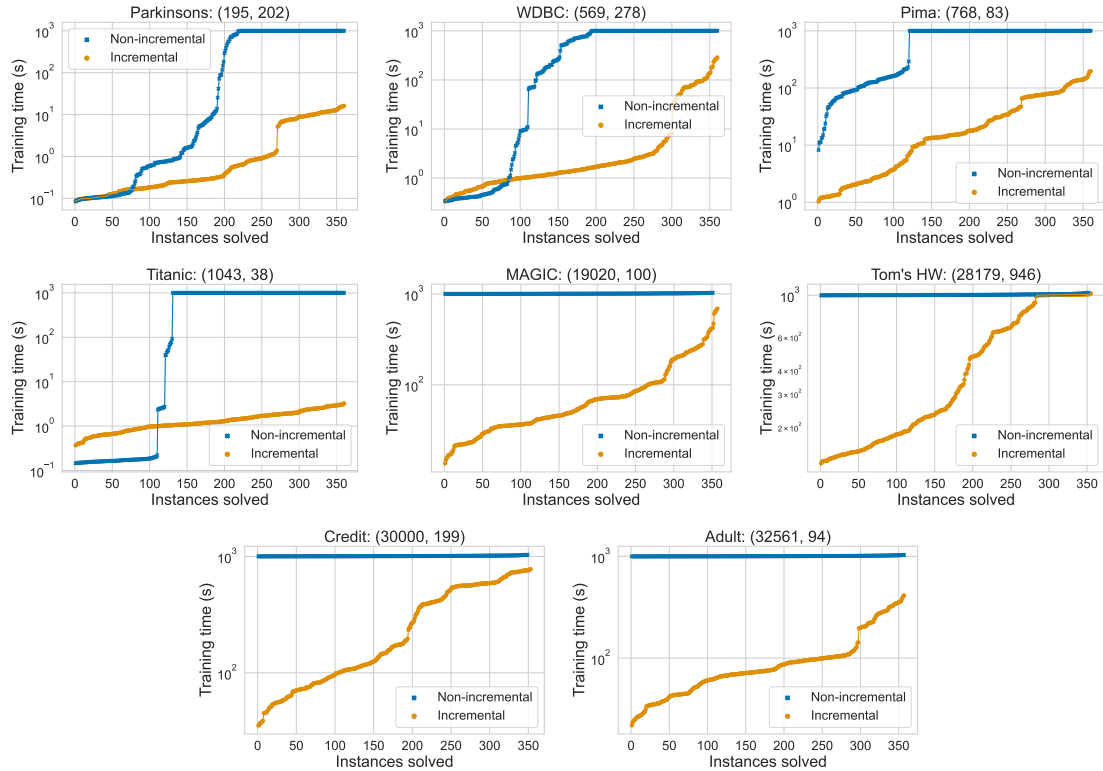


Figure A.1: Detailed scalability results of incremental vs. non-incremental encoding in IMLI, presented as a cactus plot. As datasets become large, the non-incremental encoding suffers from poor scalability by witnessing time-outs more frequently than the incremental encoding IMLI.

encoding demonstrates a competitive accuracy and rule size with the non-incremental encoding. Therefore, the incremental encoding in IMLI demonstrates its effectiveness in training time, accuracy, and rule size over the non-incremental encoding.

A.2 Representative Interpretable Classifiers

In the following, we present representative CNF classifiers learned in different datasets. In each dataset, if an input satisfies the CNF formula, it is predicted class 1 and vice-versa.

Parkinsons:

$0.3 \leq \text{Average vocal fundamental frequency} < 0.4$ **OR** $0.5 \leq \text{Average vocal fundamental frequency} < 0.6$ **OR** $0.1 \leq \text{Maximum vocal fundamental frequency} < 0.2$ **OR** $0.5 \leq \text{Minimum vocal fundamental frequency} < 0.6$ **OR** $0.1 \leq \text{Shimmer:APQ5}$

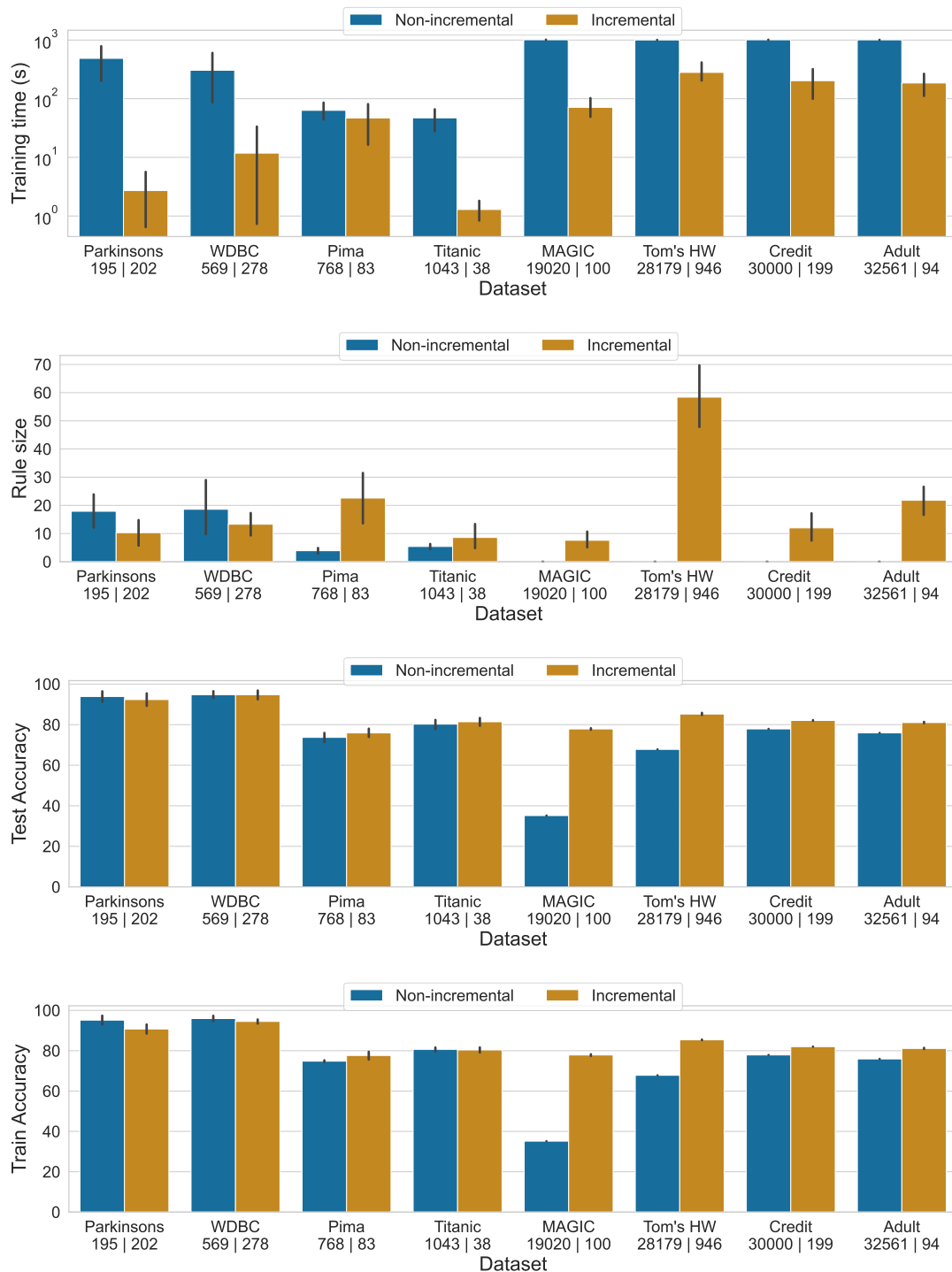


Figure A.2: Comparison of training time, rule size, and test and train accuracy between non-incremental vs. incremental encoding in IMLI. In X-axis, the dimension of the dataset (#samples | #features) is shown below dataset name. In large datasets, non-incremental encoding often times out and learns zero-size classification rules yielding less test and train accuracy than the incremental encoding.

< 0.2 **OR** $0.5 \leq \text{DFA} < 0.6$ **OR** $0.3 \leq \text{spread1} < 0.4$ **OR** $0.8 \leq \text{spread2} < 0.9$ **OR**
 $0.3 \leq \text{PPE} < 0.4$ **OR NOT** $-\infty \leq \text{MDVP:APQ} < 0.1$ **AND**

NOT $0.8 \leq \text{Average vocal fundamental frequency} < 0.9$

WDBC:

$0.4 \leq \text{perimeter} < 0.5$ **OR** $0.8 \leq \text{symmetry} < 0.9$ **OR** $0.5 \leq \text{largest concave points} < 0.6$ **OR** $0.6 \leq \text{largest concave points} < 0.7$ **OR** $0.7 \leq \text{largest concave points} < 0.8$ **OR** $0.6 \leq \text{largest symmetry} < 0.7$ **OR NOT** $-\infty \leq \text{area SE} < 0.1$ **AND**

$0.4 \leq \text{texture} < 0.5$ **OR** $0.5 \leq \text{texture} < 0.6$ **OR** $0.5 \leq \text{perimeter} < 0.6$ **OR**
 $0.5 \leq \text{smoothness} < 0.6$ **OR** $0.4 \leq \text{concave points} < 0.5$ **OR** $0.5 \leq \text{concave points} < 0.6$ **OR** $0.2 \leq \text{largest concavity} < 0.3$ **OR** $0.6 \leq \text{largest concave points} < 0.7$ **OR** $0.7 \leq \text{largest concave points} < 0.8$ **OR** $0.4 \leq \text{largest symmetry} < 0.5$ **OR** $0.6 \leq \text{largest symmetry} < 0.7$

Pima:

$x1 = 11$ **OR** $x1 = 14$ **OR** $x1 = 15$ **OR** $0.7 \leq x2 < 0.8$ **OR** $0.8 \leq x2 < 0.9$ **OR** $0.9 \leq x2 < \infty$ **OR** $0.9 \leq x3 < \infty$ **OR** $0.4 \leq x5 < 0.5$ **OR** $0.7 \leq x5 < 0.8$ **OR** $0.7 \leq x6 < 0.8$ **OR** $0.4 \leq x7 < 0.5$ **OR** $0.5 \leq x7 < 0.6$ **OR** $0.9 \leq x7 < \infty$ **AND**

$x1 = 7$ **OR** $x1 = 8$ **OR** $0.6 \leq x2 < 0.7$ **OR** $0.8 \leq x2 < 0.9$ **OR** $0.9 \leq x2 < \infty$ **OR** $-\infty \leq x3 < 0.1$ **OR** $0.7 \leq x3 < 0.8$ **OR** $0.9 \leq x3 < \infty$ **OR** $0.2 \leq x5 < 0.3$ **OR** $0.7 \leq x6 < 0.8$ **OR** $0.1 \leq x7 < 0.2$ **OR** $0.3 \leq x7 < 0.4$ **OR** $0.4 \leq x8 < 0.5$ **OR** $0.8 \leq x8 < 0.9$ **AND**

$x1 = 2$ **OR** $x1 = 6$ **OR** $x1 = 7$ **OR** $x1 = 9$ **OR** $-\infty \leq x3 < 0.1$ **OR** $0.8 \leq x3 < 0.9$ **OR** $0.1 \leq x5 < 0.2$ **OR** $0.2 \leq x5 < 0.3$ **OR** $0.7 \leq x5 < 0.8$ **OR** $0.5 \leq x6 < 0.6$ **OR** $0.6 \leq x6 < 0.7$ **OR** $0.4 \leq x7 < 0.5$ **OR** $0.9 \leq x7 < \infty$ **OR** $0.1 \leq x8 < 0.2$ **OR** $0.3 \leq x8 < 0.4$ **OR** $0.6 \leq x8 < 0.7$ **OR** $0.8 \leq x8 < 0.9$ **AND**

$x_1 = 8$ **OR** $0.5 \leq x_2 < 0.6$ **OR** $0.8 \leq x_2 < 0.9$ **OR** $0.9 \leq x_2 < \infty$ **OR** $0.7 \leq x_3 < 0.8$ **OR** $-\infty \leq x_4 < 0.1$ **OR** $0.1 \leq x_5 < 0.2$ **OR** $0.3 \leq x_5 < 0.4$ **OR** $0.5 \leq x_7 < 0.6$ **OR** $0.1 \leq x_8 < 0.2$ **OR** $0.4 \leq x_8 < 0.5$ **OR** $0.8 \leq x_8 < 0.9$

Titanic:

$-\infty \leq \text{age} < 0.1$ **OR** $0.9 \leq \text{age} < \infty$ **OR** $0.9 \leq \text{fare} < \infty$ **OR NOT** sex **AND**

passenger-class = 2 **OR** $0.4 \leq \text{age} < 0.5$ **OR** $0.6 \leq \text{age} < 0.7$ **OR** siblings-or-spouces-aboard = 0 **OR** $0.1 \leq \text{fare} < 0.2$ **OR** $0.5 \leq \text{fare} < 0.6$ **OR** embarked = C **AND**

$-\infty \leq \text{age} < 0.1$ **OR** $0.1 \leq \text{age} < 0.2$ **OR** $0.7 \leq \text{age} < 0.8$ **OR** siblings-or-spouces-aboard = 1 **OR** parents-or-childred-aboard = 1 **OR** embarked = C **OR NOT** passenger-class = 3 **AND**

$-\infty \leq \text{age} < 0.1$ **OR** $0.2 \leq \text{age} < 0.3$ **OR** $0.3 \leq \text{age} < 0.4$ **OR** parents-or-childred-aboard = 0 **OR NOT** passenger-class = 3 **OR NOT** siblings-or-spouces-aboard = 0 **AND**

NOT passenger-class = 2 **OR NOT** $0.7 \leq \text{age} < 0.8$

MAGIC:

$-\infty \leq \text{length} < 0.1$ **OR** $-\infty \leq \text{size} < 0.1$ **OR** $0.8 \leq \text{conc} < 0.9$ **OR** $-\infty \leq \text{alpha} < 0.1$ **OR** $0.1 \leq \text{alpha} < 0.2$ **OR** $0.2 \leq \text{dist} < 0.3$

Tom's HW:

$0.4 \leq x_{10} < 0.5$ **OR** $0.1 \leq x_{11} < 0.2$ **OR** $0.4 \leq x_{11} < 0.5$ **OR** $0.4 \leq x_{12} < 0.5$ **OR** $0.3 \leq x_{13} < 0.4$ **OR** $0.6 \leq x_{13} < 0.7$ **OR** $0.3 \leq x_{15} < 0.4$ **OR** $0.6 \leq x_{15} < 0.7$ **OR** $0.4 \leq x_{16} < 0.5$ **OR** $0.1 \leq x_{57} < 0.2$ **OR** $0.5 \leq x_{59} < 0.6$ **OR** $0.3 \leq x_{60} < 0.4$ **OR** $0.2 \leq x_{62} < 0.3$ **OR** $0.2 \leq x_{73} < 0.3$ **OR** $0.1 \leq x_{74} < 0.2$ **OR NOT**

$-\infty \leq x_{74} < 0.1$ **OR NOT** $-\infty \leq x_{96} < 0.1$ **AND**

$0.4 \leq x_9 < 0.5$ **OR** $0.8 \leq x_9 < 0.9$ **OR** $0.2 \leq x_{12} < 0.3$ **OR** $0.3 \leq x_{12} < 0.4$ **OR** $0.3 \leq x_{15} < 0.4$ **OR** $0.6 \leq x_{15} < 0.7$ **OR** $0.1 \leq x_{60} < 0.2$ **OR** $0.1 \leq x_{61} < 0.2$ **OR** $0.6 \leq x_{78} < 0.7$ **OR NOT** $-\infty \leq x_{11} < 0.1$ **OR NOT** $-\infty \leq x_{13} < 0.1$ **OR NOT** $-\infty \leq x_{46} < 0.1$ **OR NOT** $-\infty \leq x_{64} < 0.1$ **OR NOT** $-\infty \leq x_{72} < 0.1$ **OR NOT** $-\infty \leq x_{77} < 0.1$ **AND**

$-\infty \leq x_{50} < 0.1$ **OR** $0.1 \leq x_{57} < 0.2$ **AND**

$-\infty \leq x_{49} < 0.1$ **OR NOT** $-\infty \leq x_{17} < 0.1$ **AND**

$0.3 \leq x_{14} < 0.4$ **OR** $0.6 \leq x_{74} < 0.7$ **OR** $0.9 \leq x_{79} < \infty$ **OR NOT** $-\infty \leq x_9 < 0.1$ **OR NOT** $-\infty \leq x_{15} < 0.1$ **OR NOT** $-\infty \leq x_{73} < 0.1$ **OR NOT** $-\infty \leq x_{80} < 0.1$

Credit:

Repayment-status-in-September = 2 **OR** Repayment-status-in-September = 3 **OR** Repayment-status-in-August = 3 **OR** Repayment-status-in-May = 3 **OR** Repayment-status-in-May = 5 **OR** Repayment-status-in-April = 3 **AND**

$0.4 \leq \text{Age} < 0.5$ **OR** Repayment-status-in-September = 1 **OR** Repayment-status-in-August = 0 **OR** Repayment-status-in-July = 2 **OR** Repayment-status-in-May = 2 **OR** Repayment-status-in-April = 7 **OR** $0.3 \leq \text{Amount-of-bill-statement-in-April} < 0.4$ **OR NOT** Repayment-status-in-May = -1 **OR NOT** $-\infty \leq \text{Amount-of-bill-statement-in-May} < 0.1$ **AND**

Gender **OR** $-\infty \leq \text{Age} < 0.1$ **OR** $0.3 \leq \text{Age} < 0.4$ **OR** Repayment-status-in-September = 1 **OR** $0.1 \leq \text{Amount-of-bill-statement-in-August} < 0.2$ **OR NOT** Education = 3 **OR NOT** $0.2 \leq \text{Amount-of-bill-statement-in-September} < 0.3$

Adult:

education = Doctorate **OR** education = Prof-school **OR** $0.1 \leq \text{capital-gain} < 0.2$
OR $0.2 \leq \text{capital-gain} < 0.3$ **OR** $0.9 \leq \text{capital-gain} < \infty$ **OR** $0.4 \leq \text{capital-loss} <$
 0.5 **OR** $0.5 \leq \text{capital-loss} < 0.6$ **AND**

relationship = Husband **OR** relationship = Wife **OR** $0.5 \leq \text{capital-loss} < 0.6$
OR $0.6 \leq \text{capital-loss} < 0.7$ **OR** $0.8 \leq \text{capital-loss} < 0.9$ **OR NOT** $-\infty \leq \text{capital-}$
 $\text{gain} < 0.1$ **AND**

$0.1 \leq \text{age} < 0.2$ **OR** $0.7 \leq \text{age} < 0.8$ **OR** workclass = State-gov **OR** education =
Bachelors **OR** marital-status = Separated **OR** occupation = Exec-managerial **OR**
occupation = Farming-fishing **OR** occupation = Prof-specialty **OR** occupation =
Protective-serv **OR** occupation = Tech-support **OR** relationship = Unmarried **OR**
 $0.4 \leq \text{capital-loss} < 0.5$ **OR** $0.6 \leq \text{capital-loss} < 0.7$ **OR** $0.2 \leq \text{hours-per-week} <$
 0.3 **OR** $0.4 \leq \text{hours-per-week} < 0.5$ **OR** $0.7 \leq \text{hours-per-week} < 0.8$ **OR** $0.9 \leq$
 $\text{hours-per-week} < \infty$ **OR NOT** $-\infty \leq \text{capital-gain} < 0.1$

Bank Marketing:

$0.7 \leq \text{age} < 0.8$ **OR** $0.2 \leq \text{duration} < 0.3$ **OR** $0.3 \leq \text{duration} < 0.4$ **OR** $0.4 \leq$
 $\text{duration} < 0.5$ **OR** $0.5 \leq \text{duration} < 0.6$ **OR** poutcome = success **AND**

housing **OR** $0.8 \leq \text{age} < 0.9$ **OR** job = admin. **OR** job = management **OR**
job = self-employed **OR** job = services **OR** job = unemployed **OR** $0.2 \leq \text{duration}$
 < 0.3 **OR** $0.1 \leq \text{campaign} < 0.2$ **OR** poutcome = success **AND**

job = services **OR** $0.2 \leq \text{balance} < 0.3$ **OR** contact = cellular **OR** $0.1 \leq \text{du-}$
 $\text{ration} < 0.2$ **OR** $0.2 \leq \text{duration} < 0.3$ **OR** $0.2 \leq \text{pdays} < 0.3$ **OR** poutcome =
unknown **OR NOT** $-\infty \leq \text{balance} < 0.1$ **OR NOT** $-\infty \leq \text{previous} < 0.1$ **AND**

$0.2 \leq \text{age} < 0.3$ **OR** $0.3 \leq \text{age} < 0.4$ **OR** $0.8 \leq \text{age} < 0.9$ **OR** job = man-
agement **OR** job = student **OR** job = unemployed **OR** education = secondary **OR**
 $0.1 \leq \text{balance} < 0.2$ **OR** $0.1 \leq \text{duration} < 0.2$ **OR** $-\infty \leq \text{pdays} < 0.1$ **OR** $0.2 \leq$

$pdays < 0.3$ **OR** $poutcome = unknown$

Connect-4:

$b2 = 1$ **OR** $c2 = 1$ **OR** $d2 = 1$ **OR** $d4 = 1$ **OR** $d5 = 0$ **OR** $e2 = 1$ **OR** $f3 = 0$ **OR**
NOT $d1 = 0$ **AND**

$b2 = 1$ **OR** $b3 = 1$ **OR** $b4 = 1$ **OR** $d4 = 1$ **OR** $f2 = 1$ **OR** **NOT** $d3 = 0$
OR **NOT** $f3 = 2$ **AND**

$c1 = 2$ **OR** $c2 = 2$ **OR** $c3 = 1$ **OR** $c3 = 2$ **OR** $c4 = 1$ **OR** $c6 = 0$ **OR** $d2 = 1$ **OR**
 $d4 = 1$ **OR** $e2 = 1$ **OR** $e3 = 1$ **OR** $f4 = 1$ **OR** **NOT** $a3 = 2$ **OR** **NOT** $b6 = 2$ **AND**

$a1 = 0$ **OR** $a2 = 0$ **OR** $a6 = 0$ **OR** $b2 = 1$ **OR** $b4 = 1$ **OR** $b5 = 0$ **OR** $c2$
 $= 1$ **OR** $c4 = 1$ **OR** $c5 = 0$ **OR** $d1 = 1$ **OR** $d2 = 1$ **OR** $e2 = 1$ **OR** $g1 = 0$ **OR** $g2$
 $= 0$ **OR** **NOT** $d5 = 2$ **OR** **NOT** $d6 = 2$ **AND**

$b2 = 1$ **OR** $b4 = 1$ **OR** $c3 = 1$ **OR** $d3 = 1$ **OR** $e2 = 1$ **OR** $f2 = 1$ **OR** $f3$
 $= 1$ **OR** $g3 = 0$ **OR** $g5 = 0$ **OR** **NOT** $c2 = 0$ **OR** **NOT** $c4 = 2$ **OR** **NOT** $d2 = 2$

Weather AUS:

$0.7 \leq Rainfall < 0.8$ **OR** $0.8 \leq Humidity3pm < 0.9$ **OR** $0.9 \leq Humidity3pm < \infty$
AND

$RainToday$ **OR** $0.5 \leq WindGustSpeed < 0.6$ **OR** $0.7 \leq Humidity9am < 0.8$ **OR** 0.9
 $\leq Humidity3pm < \infty$ **OR** $0.4 \leq Pressure3pm < 0.5$ **OR** **NOT** $0.9 \leq Humidity9am$
 $< \infty$ **AND**

$0.1 \leq MinTemp < 0.2$ **OR** $0.8 \leq MinTemp < 0.9$ **OR** $0.9 \leq WindSpeed9am$
 $< \infty$ **OR** $0.9 \leq Humidity9am < \infty$ **OR** $0.8 \leq Humidity3pm < 0.9$ **OR** $0.9 \leq$
 $Humidity3pm < \infty$ **OR** $0.5 \leq Temp3pm < 0.6$ **OR** **NOT** $0.7 \leq Rainfall < 0.8$ **AND**

WindGustDir = NNW **OR** WindDir3pm = W **OR NOT** $0.8 \leq \text{Temp3pm} < 0.9$ **AND**

WindGustDir = NNW **OR** WindGustDir = NW **OR** $0.1 \leq \text{Pressure9am} < 0.2$ **OR NOT** $0.7 \leq \text{Temp3pm} < 0.8$

Vote:

NOT physician-fee-freeze **AND**

NOT adoption-of-the-budget-resolution **OR NOT** anti-satellite-test-ban **OR NOT** synfuels-corporation-cutback **AND**

adoption-of-the-budget-resolution **OR** el-salvador-aid **OR NOT** duty-free-exports **AND**

mx-missile **OR NOT** adoption-of-the-budget-resolution **OR NOT** el-salvador-aid **OR NOT** anti-satellite-test-ban **AND**

adoption-of-the-budget-resolution **OR** mx-missile **OR NOT** synfuels-corporation-cutback **OR NOT** education-spending

Skin Seg:

$0.2 \leq \text{Red} < 0.3$ **OR** $0.3 \leq \text{Red} < 0.4$ **OR** $0.4 \leq \text{Red} < 0.5$ **OR** $0.9 \leq \text{Red} < \infty$ **OR** $0.9 \leq \text{Green} < \infty$ **OR** $0.4 \leq \text{Blue} < 0.5$ **OR NOT** $0.9 \leq \text{Blue} < \infty$ **AND**

$0.2 \leq \text{Red} < 0.3$ **OR** $0.7 \leq \text{Red} < 0.8$ **OR** $0.8 \leq \text{Red} < 0.9$ **OR** $0.9 \leq \text{Red} < \infty$ **OR NOT** $0.8 \leq \text{Blue} < 0.9$ **AND**

$0.7 \leq \text{Red} < 0.8$ **OR** $0.8 \leq \text{Red} < 0.9$ **OR** $0.9 \leq \text{Red} < \infty$ **OR** $-\infty \leq \text{Green} < 0.1$ **OR NOT** $0.7 \leq \text{Blue} < 0.8$

BNG(labor):

$0.5 \leq \text{wage-increase-first-year} < 0.6$ **OR** $\text{pension} = \text{empl-contr}$ **OR** $\text{contribution-to-dental-plan} = \text{full}$ **AND**

$0.6 \leq \text{wage-increase-first-year} < 0.7$ **OR** $0.7 \leq \text{wage-increase-second-year} < 0.8$ **OR**
 $0.5 \leq \text{shift-differential} < 0.6$ **OR NOT** $\text{longterm-disability-assistance}$ **AND**

$0.2 \leq \text{wage-increase-first-year} < 0.3$ **OR** $0.3 \leq \text{wage-increase-first-year} < 0.4$ **OR** 0.4
 $\leq \text{wage-increase-first-year} < 0.5$ **OR** $0.5 \leq \text{wage-increase-first-year} < 0.6$ **OR** 0.6
 $\leq \text{wage-increase-first-year} < 0.7$ **OR** $0.7 \leq \text{wage-increase-first-year} < 0.8$ **OR** 0.6
 $\leq \text{wage-increase-second-year} < 0.7$ **OR** $\text{cost-of-living-adjustment} = \text{tcf}$ **OR** $0.3 \leq$
 $\text{working-hours} < 0.4$ **OR** $0.4 \leq \text{working-hours} < 0.5$ **OR** $0.5 \leq \text{working-hours} < 0.6$
OR $\text{pension} = \text{ret-allw}$ **OR** $0.7 \leq \text{standby-pay} < 0.8$ **OR** $\text{contribution-to-dental-plan}$
 $= \text{full}$ **OR** $\text{contribution-to-health-plan} = \text{half}$ **OR NOT** $\text{education-allowance}$ **AND**

$0.5 \leq \text{shift-differential} < 0.6$ **OR** $\text{contribution-to-dental-plan} = \text{full}$ **OR** $\text{contribution-to-dental-plan} = \text{half}$ **OR**
 $\text{contribution-to-health-plan} = \text{half}$ **OR** $\text{contribution-to-health-plan} = \text{none}$ **AND**

$0.3 \leq \text{wage-increase-first-year} < 0.4$ **OR** $0.6 \leq \text{wage-increase-first-year} < 0.7$ **OR**
 $0.7 \leq \text{wage-increase-second-year} < 0.8$ **OR** $0.4 \leq \text{working-hours} < 0.5$ **OR** $\text{pension} = \text{empl-contr}$ **OR**
 $\text{pension} = \text{ret-allw}$ **OR** $0.9 \leq \text{statutory-holidays} < \text{inf}$

BNG(credit-g):

foreign-worker **OR** $\text{checking-status} = \text{'no checking'}$ **OR** $\text{checking-status} = \geq 200$
OR $-\infty \leq \text{duration} < 0.1$ **OR** $0.1 \leq \text{duration} < 0.2$ **OR** $\text{credit-history} = \text{'critical/other existing credit'}$ **OR**
 $\text{purpose} = \text{'used car'}$ **OR** $\text{savings-status} = \text{'no known savings'}$ **OR** $\text{savings-status} = \geq 1000$ **OR** $\text{other-parties} = \text{guarantor}$ **AND**

foreign-worker **OR** $\text{checking-status} = \text{'no checking'}$ **OR** $\text{checking-status} = \geq 200$
OR $\text{credit-history} = \text{'delayed previously'}$ **OR** $\text{purpose} = \text{'used car'}$ **OR** purpose

= radio/tv **OR** other-parties = guarantor **OR** $0.4 \leq \text{age} < 0.5$ **OR NOT** other-payment-plans = bank **AND**

checking-status = 'no checking' **OR** credit-history = 'critical/other existing credit' **OR** purpose = 'used car' **OR** purpose = radio/tv **OR** purpose = retraining **OR** employment = $4 \leq X < 7$ **OR** property-magnitude = 'real estate' **OR NOT** checking-status = < 0

Appendix B

Fairness Verification with Feature Correlation

In this chapter, we discuss the extended experimental results as a continuation of Chapter 6.

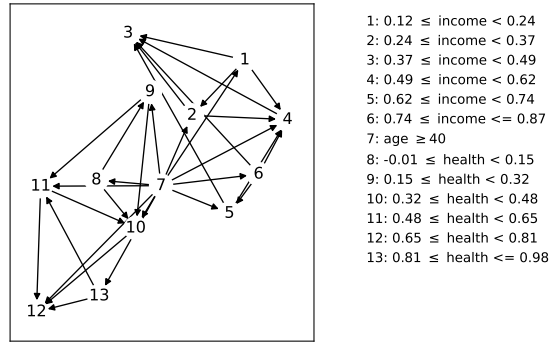
B.1 Extended Experimental Results

Each experiment is performed on Intel Xeon E7 – 8857 v2 CPUs with 16GB memory, 64bit Linux distribution based on Debian OS and clock speed 3 GHz.

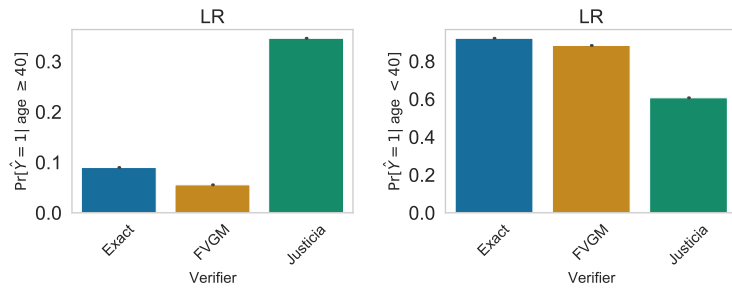
B.1.1 Accuracy Comparison Among Different Verifiers

We have considered a synthetic problem for comparing accuracy among different verifiers. For Example 5.0.1, we consider ‘age ≥ 40 ’ as a Bernoulli random variable with probability 0.5. For ‘income’ feature (I), we consider two Gaussian distributions $\Pr[I|\text{age} \geq 40] \sim \mathcal{N}(0.6, 0.1)$ and $\Pr[I|\text{age} < 40] \sim \mathcal{N}(0.4, 0.1)$ separated by two age groups. Moreover, for ‘fitness’ feature (F), we consider two Gaussian distributions $\Pr[F|\text{age} \geq 40] \sim \mathcal{N}(0.7, 0.1)$ and $\Pr[F|\text{age} < 40] \sim \mathcal{N}(0.3, 0.1)$. On this data, the trained LR and SVM classifier has decision boundary as $7.26I + 7.4F - 1.34A \geq 6.62$ and $9.37I + 9.75F - 0.34A \geq 9.4$, respectively.

In Figure B.1a we show the Bayesian Network on discretized features, in particular for income and fitness features. In Figure B.1b and Figure B.1c, we show PPVs of logistic regression classifier computed by different verifiers, where FVGM outputs closest to exactly computed values, in comparison with Justicia. In Figure B.1d and Figure B.1e, we show the effect of sample size on FVGM in measuring fairness metrics: disparate impact and statistical parity, where with increasing sample size,

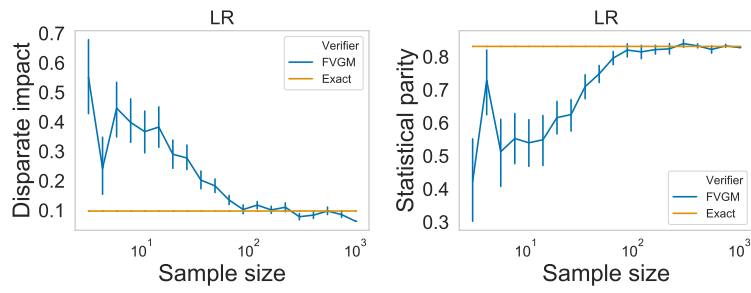


(a)



(b)

(c)



(d)

(e)

Figure B.1: Measuring accuracy of different fairness verifiers for Example 5.0.1 on logistic regression classifier.

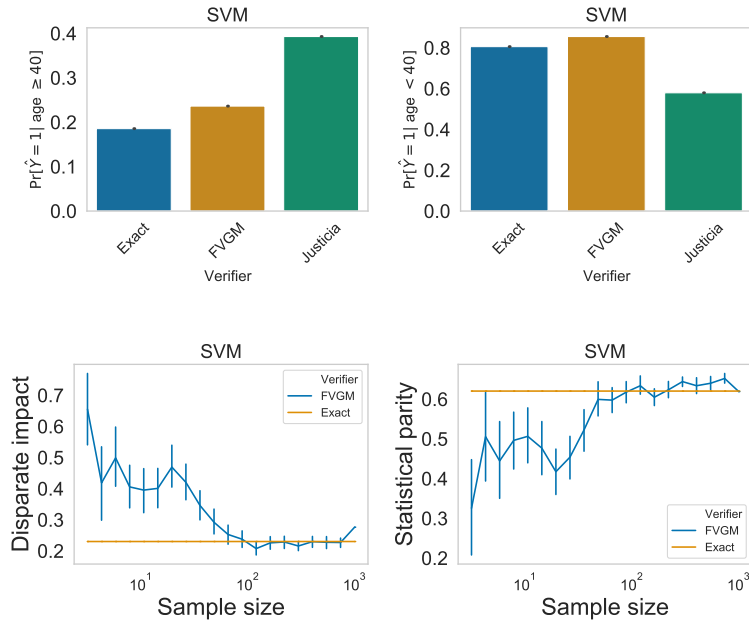


Figure B.2: Measuring accuracy of different fairness verifiers for Example 5.0.1 on SVM classifier.

the estimate becomes more accurate. Similar observations are recorded for SVM classifier in Figure B.2.

B.1.2 Scalability Comparison Among Different Verifiers

In Figure B.3, we present the runtime of different fairness verifiers while varying the number of features in different datasets. We observe that with an increase of features, the runtime increases in general.

B.1.3 Verifying Fairness Algorithms on Multiple Fairness Metrics

We show extended results on verifying fairness attack in Figure B.4 for two fairness metrics: disparate impact (DI) and statistical parity (SP). We observe that FVGM can detect poisoning attack for both metrics. In Figure B.5 we show verification results on compound sensitive groups with respect to multiple fairness metrics. In this figure, we observe that with an increase in the number of groups, fairness metrics worsens—disparate impact decreases and other three metrics increases.

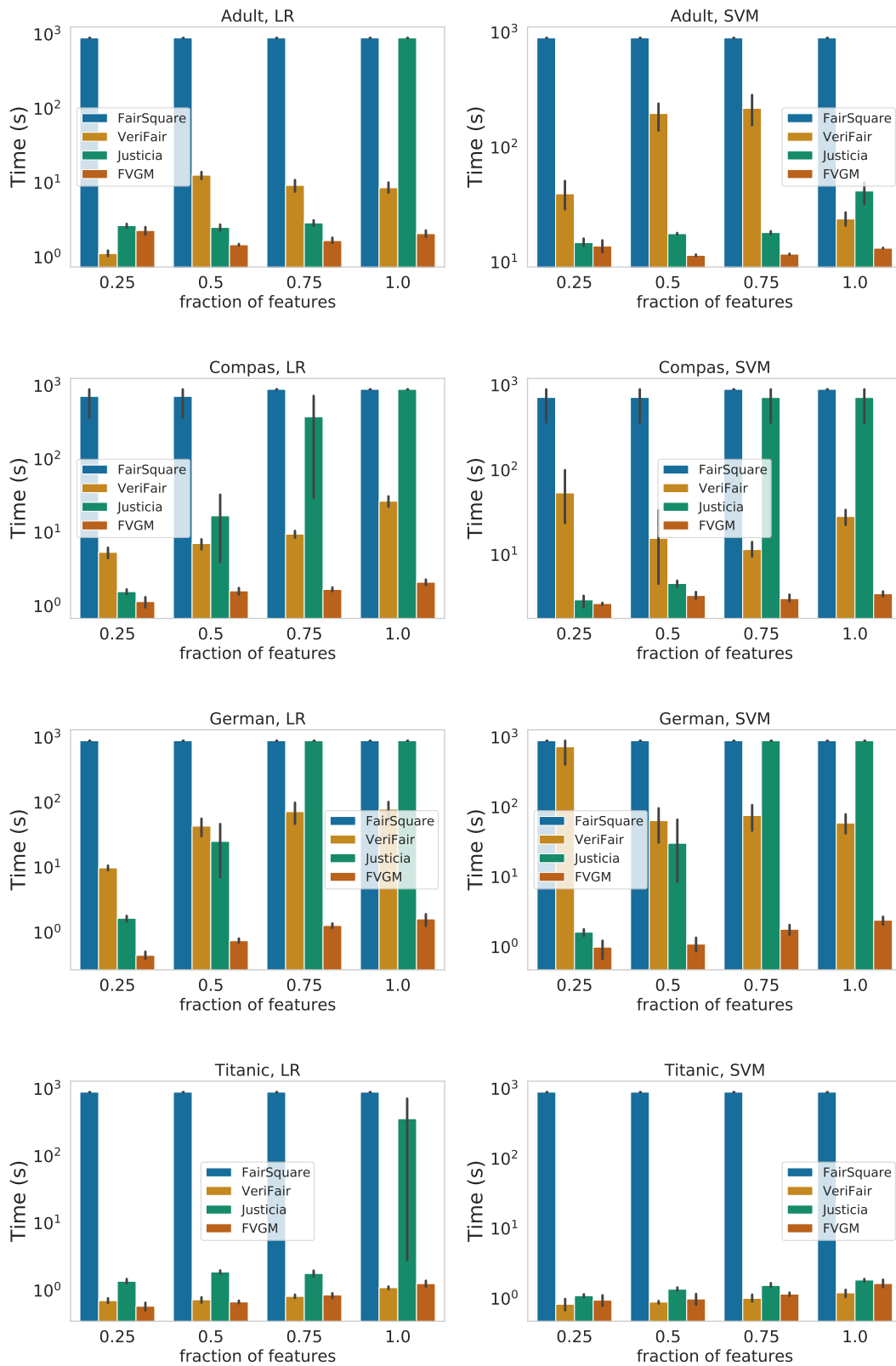


Figure B.3: Effect of number of features on the runtime of different datasets for LR and SVM classifiers.

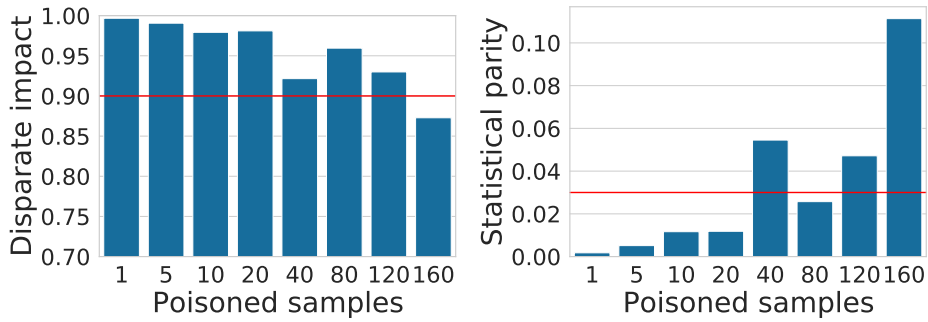


Figure B.4: Verifying fairness poisoning attack using FVGM. The red line denotes safety margin, which being exceeded denotes system-vulnerability by the attack algorithm. As the number of poisoned samples increase, disparate impact (DI) decreases and statistical parity (SP) increases.

B.1.4 Performance Analysis of Bayesian Network

In Figure B.6, we analyze the performance of encoding Bayesian Networks of differing complexity. We define the complexity of the network as $\frac{|V|}{|XUA|}$, which is the ratio between the number of features appearing in the network and total features. In this figure, as the ratio increases, both computation time of FVGM and learning time of Bayesian Network increase.

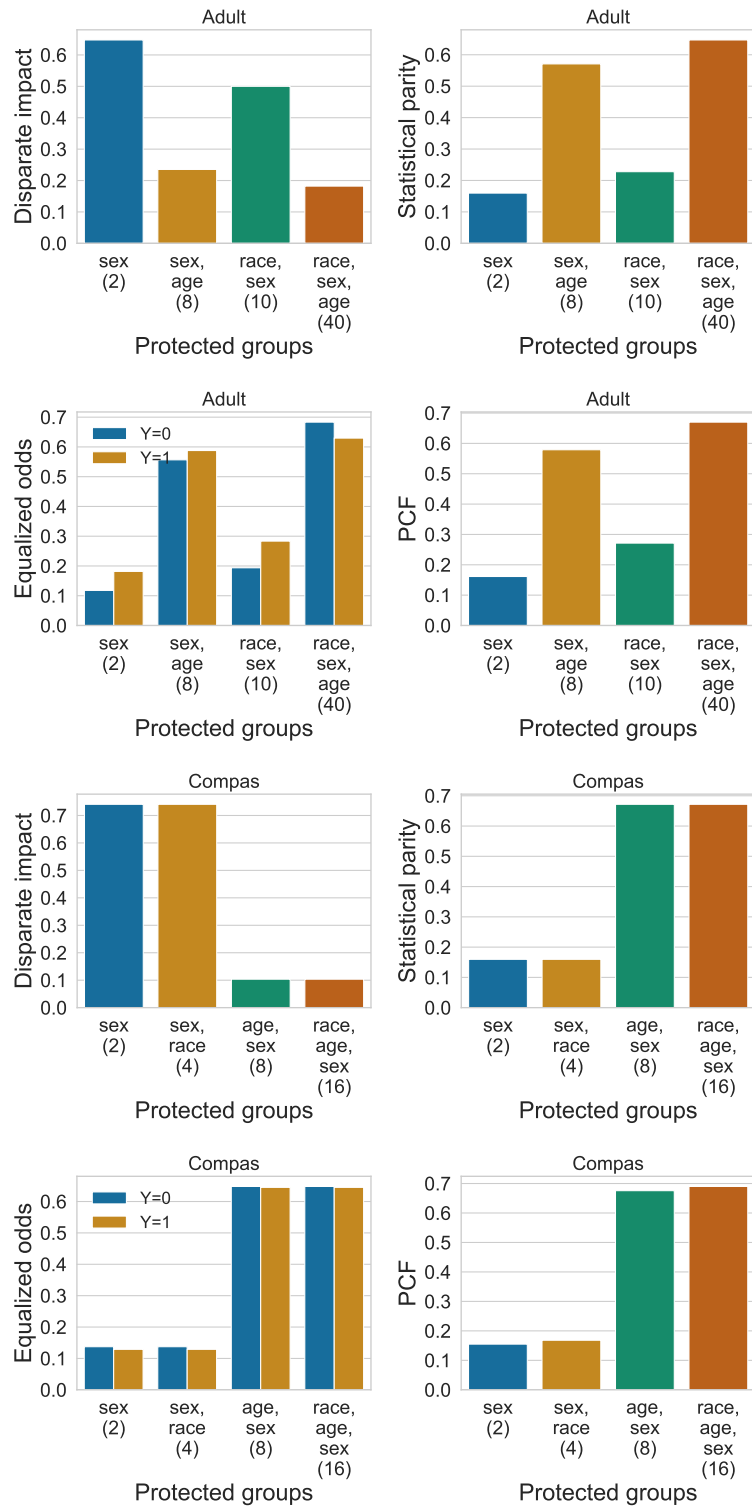


Figure B.5: Verifying compound sensitive groups with respect to multiple fairness metrics. In each plot, the X -axis shows sensitive features with the number of compound groups (within parenthesis) and Y -axis shows computed group and causal fairness metrics.

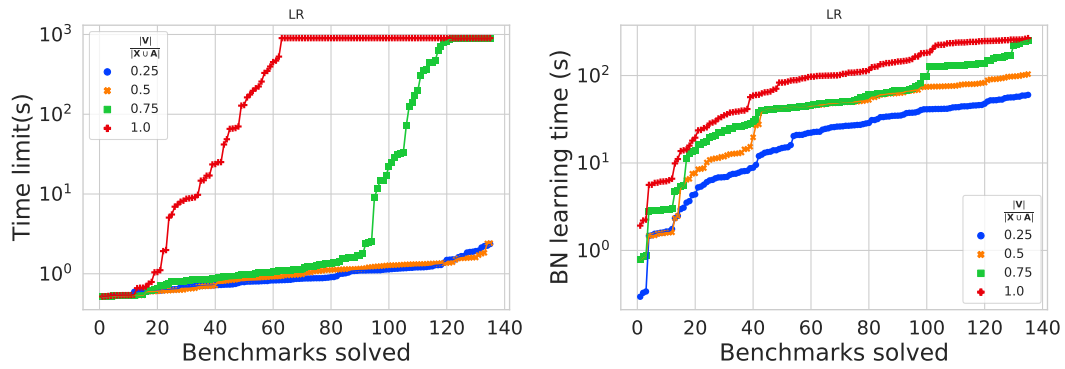


Figure B.6: Effect of number of variables in the learned Bayesian Network on computation time of FVGM. In both plots, we vary $\frac{|V|}{|X \cup A|}$, that is the ratio between the number of variables in the Bayesian Network to the number of features. We observe that as this ratio increases to 1, both runtime of FVGM (left plot) and network learning time (right plot) increase.

Appendix C

Feature Correlations in SSAT-based Fairness Verifier

In Chapter 5, *Justicia* verifies the fairness of CNF classifiers without considering correlation among features. Now, we address fairness verification of CNF classifiers with correlated features. In particular, we present the encoding of conditional probabilities from a Bayesian network into the SSAT formulation in *Justicia*.

Methodology

For CNF classifiers, SSAT is a natural choice as it computes the probability of satisfaction of a CNF formula given quantified Boolean variables, where quantifiers distinguish between (random) non-sensitive variables and (existential or universal) sensitive variables. Let $\phi_{\hat{Y}}$ be a CNF classifier such that a satisfying assignment of $\phi_{\hat{Y}}$ denotes the positive prediction of the classifier $\hat{Y} = 1$. We consider another CNF formula ϕ_{BN} to encode the conditional dependencies among variables in the Bayesian Network BN , which is given as the input distribution. ϕ_{BN} contains auxiliary variables to encode the conditional dependencies, which we discuss shortly. The outline of our methodology is to construct a conjoined CNF formula $\phi_{\hat{Y}} \wedge \phi_{\text{BN}}$, assign appropriate quantifiers to the variables, and solve an SSAT problem on quantified formula $\phi_{\hat{Y}} \wedge \phi_{\text{BN}}$ to answer queries such as $\max_{\mathbf{a}} \Pr[\hat{Y} = 1 | \mathbf{A} = \mathbf{a}]$ and $\min_{\mathbf{a}} \Pr[\hat{Y} = 1 | \mathbf{A} = \mathbf{a}]$ —the maximum and minimum conditional positive prediction of the classifiers with correlated features, respectively.

Encoding a Bayesian Network as a CNF Formula. Our goal is to encode the Bayesian network $\text{BN} = (G, \theta)$ into a CNF formula ϕ_{BN} such that *the weighted model count* of ϕ_{BN} exactly computes the joint probability distribution in BN [32].

In this context, an SSAT formula trivially does not allow conditional probabilities of randomized quantified variables. Hence, ϕ_{BN} contains additional *auxiliary variables* to capture the conditional probabilities, as discussed next.

Let $G = (\mathbf{V}, \mathbf{E})$ where $\mathbf{V} \subseteq \mathbf{X} \cup \mathbf{A}$, $\mathbf{E} \subseteq \mathbf{V} \times \mathbf{V}$, and each variable $V_i \in \mathbf{V}$ is Boolean. For each network variable $V_i \in \mathbf{V}$, we define a Boolean *indicator* variable λ_{V_i} such that $\Pr[\lambda_{V_i}] \triangleq \Pr[V_i]$. We add following constraint in ϕ_{BN} to establish the relation between λ_{V_i} and V_i .

$$\lambda_{V_i} \leftrightarrow V_i, \quad (\text{C.1})$$

Intuitively, both λ_{V_i} and V_i are either true or false. This constraint can be trivially translated to clauses in CNF using the equivalence rule $A \leftrightarrow B \equiv (\neg A \vee B) \wedge (A \vee \neg B)$ for Boolean variables A, B .

We now present the encoding of conditional probabilities induced by parameters in the network θ . Let $V_i \in \mathbf{V}$ be a vertex in G where $\text{Pa}(V_i) \neq \emptyset$ be V_i 's parents and $|\text{Pa}(V_i)| = k$. Additionally, let v and $\mathbf{u} \triangleq [u_1, \dots, u_k]$ be an assignment of V_i and $\text{Pa}(V_i)$, respectively. To encode $\Pr[V_i = v | \text{Pa}(V_i) = \mathbf{u}]$, we introduce auxiliary variable $\lambda_{v, \mathbf{u}}$ and add following constraints in ϕ_{BN} .

$$\lambda_{v, \mathbf{u}} \wedge \bigwedge_{j=1}^k \lambda_{u_j} \rightarrow \lambda_v \quad (\text{C.2})$$

$$\neg \lambda_{v, \mathbf{u}} \wedge \bigwedge_{j=1}^k \lambda_{u_j} \rightarrow \neg \lambda_v \quad (\text{C.3})$$

where $\lambda_v \equiv \lambda_{V_i}$. Moreover, λ_{u_j} is the indicator variable corresponding to the j^{th} parent in $\text{Pa}(V_i)$. In the above two constraints, for a fixed assignment \mathbf{u} of parents $\text{Pa}(V_i)$, both λ_v and $\lambda_{v, \mathbf{u}}$ are either true or false. Hence, these two constraints encode the conditional probability of $V_i = v$ given $\text{Pa}(V_i) = \mathbf{u}$ using $\Pr[\lambda_{v, \mathbf{u}}] = \Pr[V_i = v | \text{Pa}(V_i) = \mathbf{u}]$. Both constraints can be translated to CNF clauses trivially. For example, Eq. C.2 is translated as $\neg \lambda_{v, \mathbf{u}} \vee \bigvee_{j=1}^k \neg \lambda_{u_j} \vee \lambda_v$. We next analyze the complexity of ϕ_{BN} in terms of the number of variables and clauses.

Lemma 20. For a Bayesian network $\text{BN} = (G, \theta)$ defined over n Boolean variables and $C(G)$ network complexity, the encoded CNF formula ϕ_{BN} has $n + C(G)$ variables and $2(n + C(G))$ clauses.

Proof. Since the DAG in the Bayesian network has n vertices, we consider n indicator variables. Moreover, for encoding conditional probabilities, we consider $C(G)$ auxiliary variables where $C(G)$ denotes the the number of independent parameters in the network (ref. Chapter 2.4). Hence, total variables in ϕ_{BN} is $n + C(G)$.

According to Eq. (C.1), (C.2), (C.3), there are $2(n + C(G))$ clauses in ϕ_{BN} . □

Quantifiers in $\phi_{\widehat{\mathcal{Y}}} \wedge \phi_{\text{BN}}$. We now discuss the quantifiers in $\phi_{\widehat{\mathcal{Y}}} \wedge \phi_{\text{BN}}$, the SSAT solution of which constitutes the maximum (minimum) probability of positive prediction of a CNF classifier. $\phi_{\widehat{\mathcal{Y}}} \wedge \phi_{\text{BN}}$ contains four categories of variables: (i) sensitive variables \mathbf{A} , (ii) non-sensitive variables \mathbf{X} , (iii) indicator variables λ_{V_i} , and (iv) auxiliary variables $\lambda_{v,\mathbf{u}}$. Among them, (iii) and (iv) are associated with ϕ_{BN} and the rest for $\phi_{\widehat{\mathcal{Y}}}$. For computing the maximum probability of positive prediction of the classifier, we construct an exists-random-exists (ERE) SSAT formula with following quantifiers: we set sensitive features \mathbf{A} with existential quantifiers in the beginning of the prefix of the SSAT formula followed by $\lambda_{V_i}, \lambda_{v,\mathbf{u}}$, and $X_j \in \mathbf{X} \setminus \mathbf{V}$ with randomized quantifiers. The remaining variables $X_i \in \mathbf{V}$ are existentially quantified as their assignment is fixed by indicator variables λ_{V_i} . In contrast, for computing the minimum probability of positive prediction of the classifier, we consider an universal-random-exists (URE) SSAT formula where we set sensitive features \mathbf{A} as universal quantifiers with all other quantifiers remaining same.

Appendix D

Fairness Influence Functions

D.1 Proofs of Properties and Implications of FIF

Theorem 14. Let $f(\mathcal{M}, \mathbf{D})$ be the bias/unfairness of the classifier \mathcal{M} on dataset \mathbf{D} according to linear group fairness metrics such as statistical parity. Let $w_{\mathbf{S}}$ be the FIF of a subset of features $\mathbf{Z}_{\mathbf{S}}$ as defined in Eq. (7.1).

- (a) *The decomposability property* of FIF states that the sum of FIFs of all subset of features is equal to the bias of the classifier.

$$\sum_{\mathbf{S} \subseteq [m]} w_{\mathbf{S}} = f(\mathcal{M}, \mathbf{D}) \quad (\text{D.1})$$

- (b) *The symmetry property* states that two features Z_i and Z_j are equivalent based on FIF if the sum of corresponding individual influences and the intersectional influences with all other features are the same. Mathematically,

$$\sum_{\mathbf{S}'' \subseteq [m] \setminus \{i, j\}} w_{\mathbf{S}'' \cup \{i\}} = \sum_{\mathbf{S}'' \subseteq [m] \setminus \{i, j\}} w_{\mathbf{S}'' \cup \{j\}} \quad (\text{D.2})$$

if $\sum_{\mathbf{S}' \subseteq \mathbf{S} \cup \{i\}} w_{\mathbf{S}'} = \sum_{\mathbf{S}' \subseteq \mathbf{S} \cup \{j\}} w_{\mathbf{S}'}$ for every non-empty subset \mathbf{S} of $[m]$ containing neither i nor j .

- (c) *The null property* of FIF states that feature X_i is a dummy or neutral feature if sum of its individual influence and the intersectional influences with all other features is zero. Mathematically,

$$\sum_{\mathbf{S}'' \subseteq [m] \setminus \{i\}} w_{\mathbf{S}'' \cup \{i\}} = 0 \quad (\text{D.3})$$

if $\sum_{\mathbf{S}' \subseteq \mathbf{S} \cup \{i\}} w_{\mathbf{S}'} = \sum_{\mathbf{S}' \subseteq \mathbf{S}} w_{\mathbf{S}'}$ for every non-empty subset \mathbf{S} of $[m]$ that does not contain i .

Proof. (a) The decomposability property of FIF is based on GSA, where the total variance is decomposed to the variances of individual and intersectional inputs.

$$\begin{aligned}
\sum_{\mathbf{S} \subseteq [m]} w_{\mathbf{S}} &= \sum_{\mathbf{S} \subseteq [m]} \frac{V_{\mathbf{a}_{\max}, \mathbf{S}}}{\Pr[\widehat{Y} = 0 \mid \mathbf{A} = \mathbf{a}_{\max}]} - \frac{V_{\mathbf{a}_{\min}, \mathbf{S}}}{\Pr[\widehat{Y} = 0 \mid \mathbf{A} = \mathbf{a}_{\min}]} \\
&= \frac{\sum_{\mathbf{S} \subseteq [m]} V_{\mathbf{a}_{\max}, \mathbf{S}}}{\Pr[\widehat{Y} = 0 \mid \mathbf{A} = \mathbf{a}_{\max}]} - \frac{\sum_{\mathbf{S} \subseteq [m]} V_{\mathbf{a}_{\min}, \mathbf{S}}}{\Pr[\widehat{Y} = 0 \mid \mathbf{A} = \mathbf{a}_{\min}]} \\
&= \frac{V_{\mathbf{a}_{\max}}}{\Pr[\widehat{Y} = 0 \mid \mathbf{A} = \mathbf{a}_{\max}]} - \frac{V_{\mathbf{a}_{\min}}}{\Pr[\widehat{Y} = 0 \mid \mathbf{A} = \mathbf{a}_{\min}]} \\
&= \frac{\text{Var}[\widehat{Y} = 1 \mid \mathbf{A} = \mathbf{a}_{\max}]}{\Pr[\widehat{Y} = 0 \mid \mathbf{A} = \mathbf{a}_{\max}]} - \frac{\text{Var}[\widehat{Y} = 1 \mid \mathbf{A} = \mathbf{a}_{\min}]}{\Pr[\widehat{Y} = 0 \mid \mathbf{A} = \mathbf{a}_{\min}]} \\
&= f_{\text{SP}}(\mathcal{M}, \mathbf{D})
\end{aligned}$$

Thus, applying Lemma 13, we prove the decomposability property of FIF for statistical parity.

(c) We observe that

$$\sum_{\mathbf{S}' \subseteq \mathbf{S} \cup \{i\}} w_{\mathbf{S}'} = \sum_{\mathbf{S}' \subseteq \mathbf{S}} w_{\mathbf{S}'} + \sum_{\mathbf{S}'' \subseteq \mathbf{S}} w_{\mathbf{S}'' \cup \{i\}}. \quad (\text{D.4})$$

This means that we can decompose the sum of FIFs of all the subsets of $\mathbf{S} \cup \{i\}$ into two non-overlapping sums: the subsets that include i and the subsets that do not include.

Since we assume that for i , $\sum_{\mathbf{S}' \subseteq \mathbf{S} \cup \{i\}} w_{\mathbf{S}'} = \sum_{\mathbf{S}' \subseteq \mathbf{S}} w_{\mathbf{S}'}$ holds true, it implies

$$\sum_{\mathbf{S}'' \subseteq \mathbf{S}} w_{\mathbf{S}'' \cup \{i\}} = 0.$$

Now, considering $\mathbf{S} = [m] \setminus \{i\}$, i.e. the set of all features except i , concludes the proof.

(b) Proof of the symmetry property follows similar decomposition of the sum of FIFs as Equation (D.4). \square

Proposition 15. When $w_{\mathbf{S}} < 0$, i.e. features $\mathbf{Z}_{\mathbf{S}}$ decrease bias, the decomposed variance of CPPs w.r.t. $\mathbf{Z}_{\mathbf{S}}$ follows $V_{\mathbf{a}_{\max}, \mathbf{S}} < V_{\mathbf{a}_{\min}, \mathbf{S}}$.

Proof. When $w_{\mathbf{S}} < 0$,

$$\begin{aligned}
& \frac{V_{\mathbf{a}_{\max}, \mathbf{S}}}{\Pr[\hat{Y} = 0 \mid \mathbf{A} = \mathbf{a}_{\max}]} - \frac{V_{\mathbf{a}_{\min}, \mathbf{S}}}{\Pr[\hat{Y} = 0 \mid \mathbf{A} = \mathbf{a}_{\min}]} < 0 \\
\implies & \frac{V_{\mathbf{a}_{\max}, \mathbf{S}}}{\Pr[\hat{Y} = 0 \mid \mathbf{A} = \mathbf{a}_{\max}]} < \frac{V_{\mathbf{a}_{\min}, \mathbf{S}}}{\Pr[\hat{Y} = 0 \mid \mathbf{A} = \mathbf{a}_{\min}]} \\
\implies & \frac{V_{\mathbf{a}_{\max}, \mathbf{S}}}{V_{\mathbf{a}_{\min}, \mathbf{S}}} < \frac{\Pr[\hat{Y} = 0 \mid \mathbf{A} = \mathbf{a}_{\max}]}{\Pr[\hat{Y} = 0 \mid \mathbf{A} = \mathbf{a}_{\min}]} \leq 1 \\
\implies & \frac{V_{\mathbf{a}_{\max}, \mathbf{S}}}{V_{\mathbf{a}_{\min}, \mathbf{S}}} < 1 \\
\implies & V_{\mathbf{a}_{\max}, \mathbf{S}} < V_{\mathbf{a}_{\min}, \mathbf{S}}
\end{aligned}$$

□

Proposition 16. If the decomposed variance of CPPs w.r.t. $\mathbf{Z}_{\mathbf{S}}$ satisfies $V_{\mathbf{a}_{\max}, \mathbf{S}} > V_{\mathbf{a}_{\min}, \mathbf{S}}$, the corresponding FIF $w_{\mathbf{S}} > 0$, i.e. features $\mathbf{Z}_{\mathbf{S}}$ increase bias.

Proof. Since $V_{\mathbf{a}_{\max}, \mathbf{S}} > V_{\mathbf{a}_{\min}, \mathbf{S}}$, we obtain $\frac{V_{\mathbf{a}_{\max}, \mathbf{S}}}{V_{\mathbf{a}_{\min}, \mathbf{S}}} > 1$. Since \mathbf{a}_{\max} and \mathbf{a}_{\min} are the most and least favored groups respectively, the probability of yielding a positive prediction is greater or equal for \mathbf{a}_{\max} than \mathbf{a}_{\min} . Thus, $\Pr[\hat{Y} = 0 \mid \mathbf{A} = \mathbf{a}_{\max}] \leq \Pr[\hat{Y} = 0 \mid \mathbf{A} = \mathbf{a}_{\min}]$, which implies that $\frac{\Pr[\hat{Y}=0 \mid \mathbf{A}=\mathbf{a}_{\max}]}{\Pr[\hat{Y}=0 \mid \mathbf{A}=\mathbf{a}_{\min}]} \leq 1$.

Combining both the observations, we obtain

$$\begin{aligned}
& \frac{V_{\mathbf{a}_{\max}, \mathbf{S}}}{V_{\mathbf{a}_{\min}, \mathbf{S}}} > \frac{\Pr[\hat{Y} = 0 \mid \mathbf{A} = \mathbf{a}_{\max}]}{\Pr[\hat{Y} = 0 \mid \mathbf{A} = \mathbf{a}_{\min}]} \\
\implies & \frac{V_{\mathbf{a}_{\max}, \mathbf{S}}}{\Pr[\hat{Y} = 0 \mid \mathbf{A} = \mathbf{a}_{\max}]} > \frac{V_{\mathbf{a}_{\min}, \mathbf{S}}}{\Pr[\hat{Y} = 0 \mid \mathbf{A} = \mathbf{a}_{\min}]} \\
\implies & \frac{V_{\mathbf{a}_{\max}, \mathbf{S}}}{\Pr[\hat{Y} = 0 \mid \mathbf{A} = \mathbf{a}_{\max}]} - \frac{V_{\mathbf{a}_{\min}, \mathbf{S}}}{\Pr[\hat{Y} = 0 \mid \mathbf{A} = \mathbf{a}_{\min}]} > 0 \\
\implies & w_{\mathbf{S}} > 0.
\end{aligned}$$

□

D.2 A Smoothing Operator: Cubic Splines

In the LOCALREGRESSION module of FairXplainer (Line 6–13, Algorithm 6), we use a smoothing operator SMOOTH (Line 10). In our experiments, *we use cubic*

splines as the smoothing operator. Here, we elucidate the technical details of cubic splines.

In interpolation problems, a B-spline of order n is traditionally used to smoothen the intersection of piecewise interpolators [165]. A B-spline of degree n is a piecewise polynomial of degree $n - 1$ defined over a variable Z . Each piece-wise term is computed on local points and is aggregated as a global curve smoothly fitting the data. The values of Z where the polynomial pieces meet together are called knots, and are denoted by $\{\dots, t_0, t_1, t_2, \dots\}$.

Let $B_{r,n}(Z)$ denote the basis function for a B-spline of order n , and r is the index of the knot vector. According to Carl de Boor [25], $B_{r,1}(Z)$, for $n = 1$, is defined as

$$B_{r,1}(Z) = \begin{cases} 0 & \text{if } Z < t_r \text{ or } Z \geq t_{r+1}, \\ 1 & \text{otherwise} \end{cases}$$

This definition satisfies $\sum_i B_{r,1}(Z) = 1$. The higher order basis functions are defined recursively as

$$B_{r,n+1}(Z) = p_{r,n}(Z)B_{r,n}(Z) + (1 - p_{r+1,n}(Z))B_{r+1,n}(Z),$$

where

$$p_{r,n}(Z) = \begin{cases} \frac{Z-t_r}{t_{r+n}-t_r} & \text{if } t_{r+n} \neq t_r, \\ 0 & \text{otherwise.} \end{cases}$$

In this chapter, we consider cubic splines with the basis function $B_{r,4}(Z)$ that constitutes a B-spline of degree 3. This polynomial has C^2 continuity, i.e. for each piecewise term, derivatives up to the second order are zero at the endpoints of each interval in the knot vector. We estimate component functions $g_{\mathbf{a},\mathbf{s}}$'s with the basis function $B_{r,4}(\mathbf{Z})$ of cubic splines [102], as shown in Equation (D.5).

$$\begin{aligned} g_{\mathbf{a},\{i\}}(\mathbf{Z}_{\{i\}}) &\approx \sum_{r=-1}^{\tau+1} \alpha_r^i B_{r,n}(\mathbf{Z}_{\{i\}}) \\ g_{\mathbf{a},\{i,j\}}(\mathbf{Z}_{\{i,j\}}) &\approx \sum_{p=-1}^{\tau+1} \sum_{q=-1}^{\tau+1} \beta_{pq}^{ij} B_p(\mathbf{Z}_{\{i\}}) B_q(\mathbf{Z}_{\{j\}}) \\ g_{\mathbf{a},\{i,j,k\}}(\mathbf{Z}_{\{i,j,k\}}) &\approx \sum_{p=-1}^{\tau+1} \sum_{q=-1}^{\tau+1} \sum_{r=-1}^{\tau+1} \gamma_{pqr}^{ijk} B_p(\mathbf{Z}_{\{i\}}) B_q(\mathbf{Z}_{\{j\}}) B_r(\mathbf{Z}_{\{k\}}) \end{aligned} \quad (\text{D.5})$$

Here, τ is the number of knots, also called spline intervals. We learn the coefficients α, β, γ using the backfitting algorithm (Line 6–13, Algorithm 6).

τ is a hyper-parameter that influences the accuracy of the local regression and thus, the FIFs. We perform an ablation study to explicate the impact of τ on the performance of FairXplainer in Appendix D.4.

D.3 Computing FIFs for Equalized Odds and Predictive Parity

Due to brevity of space, we elaborate definition of statistical parity and corresponding methodology to compute FIFs in the main text. Here, we provide definition of other group-based fairness metrics [182]: equalized odds and predictive parity. We also explain the methodology to use FairXplainer in order to compute FIFs corresponding to these metrics.

Following the classification setting and notations described in Chapter 2, here we consider a binary classifier trained on dataset $\mathbf{D} \triangleq \{(\mathbf{x}^{(i)}, \mathbf{a}^{(i)}, y^{(i)})\}_{i=1}^n$ as $\mathcal{M} : (\mathbf{X}, \mathbf{A}) \rightarrow \hat{Y}$. $\hat{Y} \in \{0, 1\}$ and $Y \in \{0, 1\}$ represents the predicted class and the true class for a data point (\mathbf{X}, \mathbf{A}) with sensitive features \mathbf{A} and non-sensitive features \mathbf{X} .

D.3.1 FIFs of Equalized Odds

For equalized odds, we deploy FairXplainer twice, one for computing FIFs on a subset of data points in the dataset where $Y = 1$ and another on data points with $Y = 0$. Since, the maximum of the sum of FIFs between $Y = 1$ and $Y = 0$ is the equalized odds of the classifier, we finally report FIFs of features corresponding to the maximum sum of FIFs between $Y \in \{0, 1\}$.

D.3.2 FIFs of Predictive Parity

To compute FIFs for predictive parity, we condition the dataset by the predicted class \hat{Y} and separate into two sub-datasets: $\hat{Y} = 1$ and $\hat{Y} = 0$. For each sub-dataset, we deploy FairXplainer by setting the ground-truth class Y as label. This contrasts the computation for statistical parity and equalized odds, where the predicted class \hat{Y} is considered as label. Finally, the maximum of the sum of FIFs between two

sub-datasets for $\hat{Y} = 1$ and $\hat{Y} = 0$ measures the predictive parity. Similar to equalized odds, FIFs achieving the greatest sum of FIFs for $\hat{Y} \in \{0, 1\}$ are the reported FIFs for the predictive parity of the classifier.

D.4 Experimental Evaluations

D.4.1 Experimental Setup

We perform experiments on a Red Hat Enterprise Linux Server release 6.10 (Santiago) that has an E5 – 2690 v3 CPU and 16GB of RAM. With the aim of computing FIFs for any classifier, we do not adjust the classifier’s hyper-parameters during training. Instead, we utilize the default hyper-parameters provided by Scikit-learn [138]. For equalized odds and predictive parity, FairXplainer (similarly SHAP) is deployed twice. Hence, we double the time limit, $2 * 300 = 600$ seconds.

D.4.2 Accuracy: Equalized Odds & Predictive Parity via FIFs.

The accuracy of approximating equalized odds and predictive parity for FairXplainer and SHAP is compared in Table D.1. FairXplainer shows lower estimation error compared to SHAP, especially when $\lambda = 2$. SHAP is unable to explain predictive parity as predictive parity relies on the ground label Y , which is not available for randomly generated data points by SHAP for estimating local explanations.

D.4.3 Execution Time: Equalized Odds & Predictive Parity via FIFs

In Figure D.1, we demonstrate the execution time of different methods in estimating FIFs of equalized odds and predictive parity in cactus plots. FairXplainer with $\lambda = 1$ is more efficient than $\lambda = 2$ and solves all 480 fairness instances with at least one order of magnitude less execution time. Compared to FairXplainer ($\lambda = 1$), SHAP demonstrates less computational efficiency.

Table D.1: Median estimation error (over 5-fold cross validation and all combinations of sensitive features) of equalized odds (columns 5 to 7) and predictive parity (columns 8 and 9) in terms of estimated FIFs by different methods. Best results (lowest error) are in bold color. ‘—’ denotes timeout. SHAP cannot estimate FIFs for predictive parity due to limited methodology.

Dataset	Dimension (n, m)	Max Sensitive Features, $ \mathbf{A} $	Classifier	Equalized Odds		Predictive Parity		
				SHAP	FairXplainer $\lambda = 1 \quad \lambda = 2$	FairXplainer $\lambda = 1 \quad \lambda = 2$	FairXplainer $\lambda = 1 \quad \lambda = 2$	
Titanic	(834, 11)	3	Logistic Regression	1.697	0.000	0.000	0.251	0.148
			SVM	1.000	0.000	0.000	0.092	0.045
			Neural Network	—	0.000	0.000	0.349	0.171
			Decision Tree	0.074	0.185	0.059	0.097	0.097
German	(417, 23)	2	Logistic Regression	0.382	0.109	0.001	0.075	0.001
			SVM	0.435	0.082	—	0.060	0.001
			Neural Network	—	0.149	0.000	0.184	0.000
			Decision Tree	0.000	0.000	0.000	0.000	0.000
COMPAS	(5771, 8)	3	Logistic Regression	0.380	0.167	0.071	0.201	0.214
			SVM	0.481	0.043	0.024	0.124	0.117
			Neural Network	—	0.143	0.055	0.078	0.129
			Decision Tree	0.071	0.069	0.031	0.348	0.340
Adult	(26048, 11)	3	Logistic Regression	1.647	0.186	0.013	0.090	0.002
			SVM	0.703	0.081	0.001	0.109	0.002
			Neural Network	—	0.077	0.000	0.091	0.002
			Decision Tree	0.062	0.263	0.190	0.216	0.203

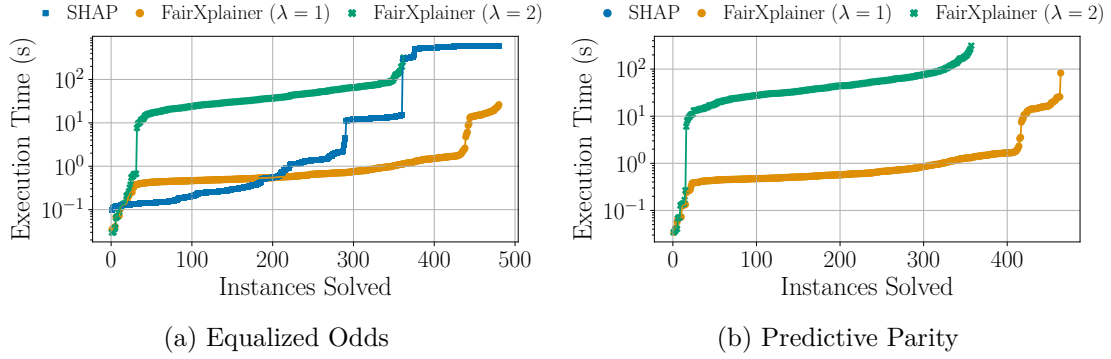


Figure D.1: Execution time of different methods for estimating FIFs for equalized odds and predictive parity. FairXplainer with $\lambda = 1$ is more efficient than SHAP, while FairXplainer ($\lambda = 2$) requires more computational effort. SHAP cannot explain predictive parity.

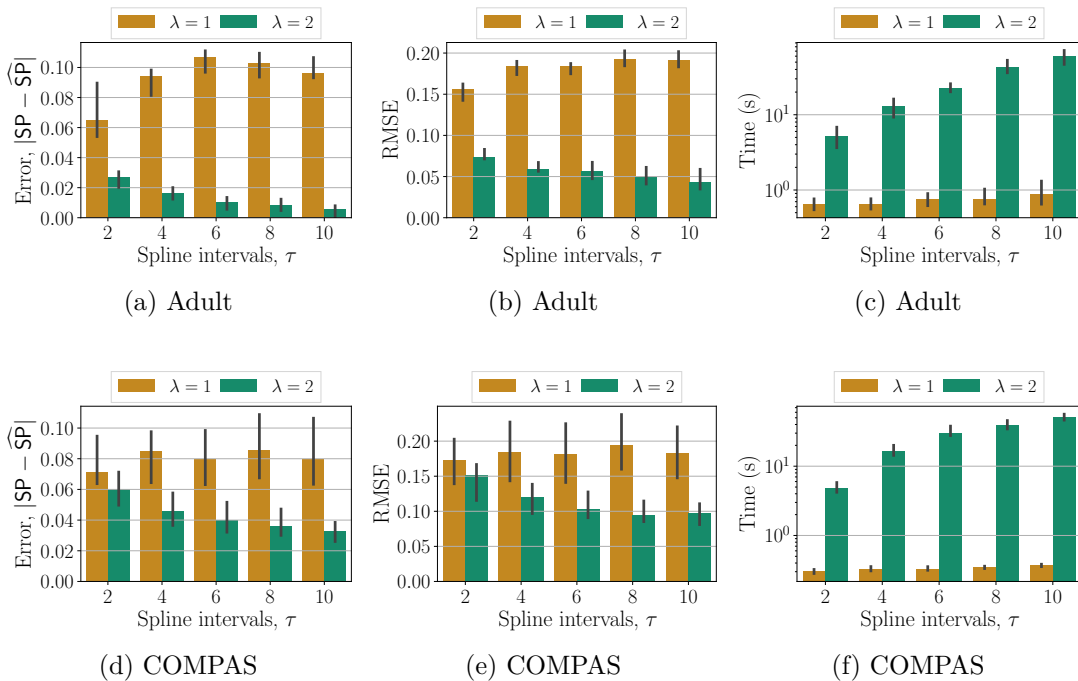


Figure D.2: Effect of spline intervals on the approximation error of statistical parity, root-mean square error (RMSE), and execution time of FairXplainer.

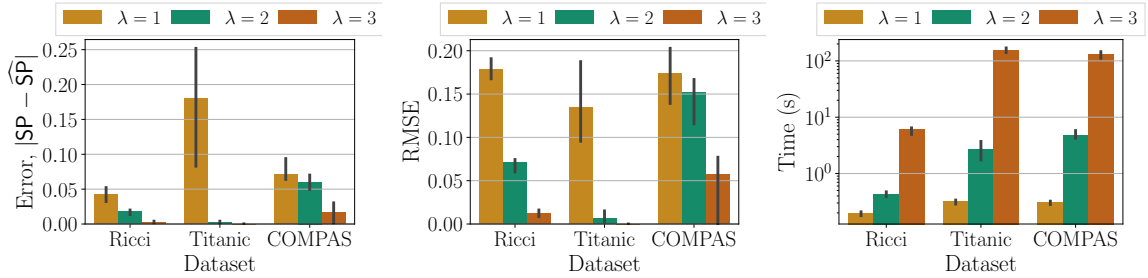


Figure D.3: Effect of maximum order λ on the approximation error of statistical parity, root-mean square error (RMSE) and execution time of FairXplainer.

D.4.4 Ablation Study: Effect of Spline Intervals

To understand the impact of spline intervals τ on FairXplainer, we conduct an experiment. τ determines the number of local points to include in the cubic-spline based smoothing, with higher values providing better approximation of the component functions in the set-additive decomposition of the classifier (ref. Eq. (7.5)). As shown in Figure D.2, as τ increases, the approximation error of statistical parity based on FIFs decreases as well as the root mean square error of the set-additive approximation of the classifier. On the other hand, with higher τ , the execution time of FairXplainer increases. Therefore, τ exhibits a trade-off between the estimation accuracy and execution time of FairXplainer.

D.4.5 Ablation Study: Effect of Maximum Order of Intersectionality

Figure D.3 examines the impact of the maximum order of intersectionality (λ) on FairXplainer in terms of accuracy and execution time on Ricci [121], Titanic, and COMPAS datasets. As λ increases, we see a decrease in approximation error for statistical parity based on FIFs, a decrease in the root mean squared error of the classifier’s set additive decomposition, and an increase in execution time across different datasets. This means λ provides a trade-off between accuracy and efficiency in FairXplainer.

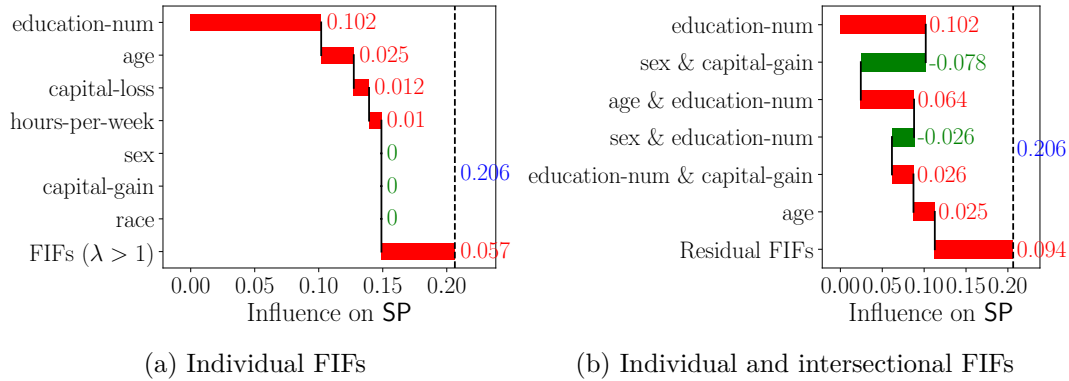


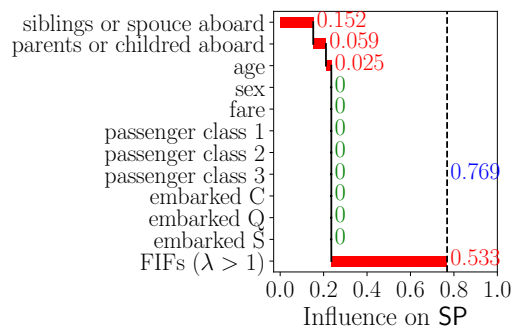
Figure D.4: FIFs for Adult dataset on explaining statistical parity.

D.4.6 FIF of Different Datasets

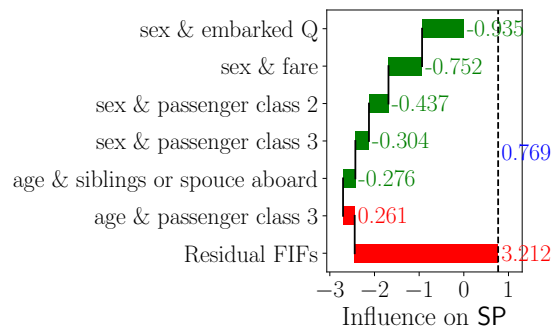
We deploy a neural network (3 hidden layers, each with 2 neurons, L2 penalty regularization term as 10^{-5} , a constant learning rate as 0.001) on different datasets, namely Adult and Titanic, and demonstrate the corresponding FIFs in Figures D.4 and D.5, respectively. In all the figures, both individual and intersectional FIFs depict the sources of bias more clearly than individual FIFs alone, as argued in Chapter 7.4.

In Adult dataset, the classifier predicts whether an individual earns more than \$50k per year or not, where race and sex are sensitive features. We observe that the trained network is unfair and it demonstrates statistical parity as 0.23. As we analyze FIFs, education number, age, and capital gain/loss are key features responsible for the bias.

In Titanic dataset, the neural network predicts whether a person survives the Titanic shipwreck or not. In this experiment, we consider the sex of a person as a sensitive feature and observe that the classifier is highly unfair achieving statistical parity as 0.83. Our FIF analysis reveals high correlation in Titanic, where individual FIFs are mostly zero while intersectional FIFs achieve high absolute values.



(a) Individual FIFs



(b) Individual and intersectional FIFs

Figure D.5: FIFs for Titanic dataset on explaining statistical parity.